Investigation of the molecular effects of cooling human burns

Mr Edmund Hugh Wright

Green Templeton College

University of Oxford

Thesis submitted for degree of Doctor of Philosophy

to the Department of Oncology, University of Oxford

Michaelmas Term 2017

Supervisors: Prof AL Harris and Prof D Furniss

Declaration of Authenticity

The work presented in this thesis is my own, except for instances where it is specifically stated otherwise. The work was performed under the supervision of Professor Adrian Harris of the Department of Oncology, Division of Medical Sciences, University of Oxford, and Professor Dominic Furniss of the Botnar Research Centre, Nuffield Department of Orthopaedics, Rheumatology and Musculoskeletal Sciences, University of Oxford.

Hugh Wright

March 2018

Dedication

I am dedicating this thesis to my wife Helen, and my family.

Acknowledgements

I would like to thank my supervisors Prof Adrian Harris and Prof Dominic Furniss for their help and guidance in the planning and execution of this project, and my college advisor Prof Sarah Darby. I also thank Mr Michael Tyler, Consultant Plastic Surgeon at Stoke Mandeville Hospital, Aylesbury, Buckinghamshire for his invaluable support in study design, patient recruitment, assistance with the clinical experiments and his encouragement throughout.

I thank the Restore Burn and Wound Research Charity for their funding of this project, the Director of Research Mr Jonathan Pleat, and the Trustees of the Charity for their support and guidance. I also thank the Royal College of Surgeons of England for their support of this work through the Enid Linder 1-Year Research Fellowship 2014-15, and the British Association of Plastic, Reconstructive and Aesthetic Surgeons for their support through the Paton Masser prize in 2016.

I thank Prof B Vojnovic and Dr I Tullis of the Gray Institute and the Advanced Technology Development Group at the Oxford Institute for Radiation Oncology and Biology for the design and manufacture of the apparatus that made the project possible.

I am extremely grateful to all those in the Weatherall Institute of Molecular Medicine in Oxford, particularly Dr Helen Sheldon, Dr Simon Wigfield, Dr Kathryn Robson, Dr Esther Bridges, Dr Russell Leek, Mr Graham Steers, Dr Helen Turley, Dr Bryony Graham, Dr Syed Haider and Dr Ana Cuervo for their help with laboratory techniques and protocols, and to Stephen Taylor and Nicki Gray of the Computational Biology Research Group (CBRG) for their help with bioinformatics training and analysis.

I must also thank Prof Benedikt Kessler and Dr Roman Fischer of the Target Discovery Institute of the Nuffield Department of Medicine of the University of Oxford for their help with proteomic analysis of samples and interpretation of data.

The staff in the Pathology Department of Buckinghamshire Healthcare NHS Trust were indispensable in their help with the safe transport of my precious specimens back to Oxford on hospital transport, and the use of cold storage facilities on both hospital sites. The Research and Development Department at Buckinghamshire Healthcare NHS Trust were also very helpful in getting the project set up.

I must thank Carol Cornelius and Sarah Kelly of the Clinical Trials Research Governance Department for their help with the preparation of the documents for review by the Regional Ethics Committee and its smooth passage through this process.

I acknowledge the help from Mr Paul Critchley and Mr Anthony Heywood, and the Oxford Deanery, in facilitating my time out of training to carry out this work. Green Templeton College, particularly Prof D Denise Lievesley, Dr Chris Sauer, Dr Mary McMenamin and Alison Franklin have been a huge source of support throughout.

Last, and by no means least, I must thank Helen Richards- now my wife- who has been with me from the very beginning of this project, and my family for their support.

1 Abstract ..... - 15 -

2 Glossary of terms ..... - 17 -

3 Introduction ..... - 22 -

3.1 The question: why does cooling a burn make a difference, and why does it matter? ..... - 22 -

3.2 The basic model of a cutaneous thermal injury: three zones ..... - 22 -

3.3 Cooling of burns: traditional medicine, basic science and first principles - 24 -

3.4 Measurements of burn injury severity and the effects of cooling .... - 27 -

3.4.1 Kinetics of dermal burning and cooling ..... - 27 -

3.4.2 Oedema and cooling ..... - 28 -

3.4.3 Cooling, dermal perfusion and microvasculature ..... - 31 -

3.4.4 Anticoagulant therapy ..... - 33 -

3.4.5 Cooling and healing ..... - 34 -

3.5 Mechanisms of burn injury pathophysiology ..... - 36 -

3.5.1 Cellular and humoural mediators ..... - 36 -

3.5.2 The interaction between cellular and humoural factors ..... - 37 -

3.5.3 Complement and coagulation activation ..... - 37 -

3.5.4 Substance P ..... - 38 -

3.6 Burns and gene expression ..... - 40 -

3.6.1 In animals ..... - 40 -

3.6.2 In humans ..... - 41 -

3.6.3 Protein expression and proteomics ..... - 43 -

3.7 Discussion ..... - 46 -

3.8 Conclusions and future directions of research ..... - 47 -

3.9 The aims of this project are as follows ..... - 49 -

3.9.1 Creation of a safe, robust, validated human model for burning and cooling - 49 -

3.9.2 Extract, purify and analyse RNA extracted from cooled and uncooled burns and controls using RNA sequencing ..... - 49 -

3.9.3 Extract protein samples from the same set of specimens and submit these for proteomic analysis ..... - 50 -

3.9.4 Immunohistochemical validation of these findings ..... - 50 -

4 Patients, materials and methods ..... - 51 -

4.1 Principles of the model ..... - 51 -

4.1.1 The suitability of the deep inferior epigastric perforator (DIEP) flap as the source of skin for the model ..... - 52 -

4.1.2 Patient selection ..... - 54 -

4.2 Apparatus ..... - 55 -

4.2.1 Burn creation device ..... - 56 -

4.2.2 Cooling ..... - 57 -

4.2.3 Measurement of time-points during burn-creation experiments ..... - 58 -

4.3 Ethical approval of the study and patient recruitment ..... - 59 -

4.3.1 Ethical approval ..... - 59 -

4.3.2 Patient recruitment ..... - 59 -

4.4 Burn creation and cooling ..... - 60 -

4.4.1 Burn creation ..... - 60 -

4.4.2 Cooling ..... - 61 -

4.5 Harvest, processing and storage of samples ..... - 62 -

4.6 Histological analysis of samples ..... - 64 -

4.6.1 Sectioning of skin samples ..... - 64 -

4.6.2 De-waxing and rehydration of sections ..... - 65 -

4.7 Staining of sections ..... - 65 -

4.7.1 Masson's trichrome stain ..... - 65 -

4.8 Immunohistochemistry ..... - 67 -

4.9 Measurement of burn-depth ..... - 70 -

4.10 RNA extraction and purification ..... - 72 -

4.10.1 RNA extraction protocol ..... - 72 -

4.10.2 RNA purification ..... - 74 -

4.10.3 RNA quality-control and quantification ..... - 76 -

4.11 Avoiding RNA degradation ..... - 78 -

4.12 Sequencing of the RNA ..... - 81 -

4.12.1 Preparation of cDNA libraries for sequencing ..... - 81 -

4.12.2 Analysis of the mRNA sequencing data ..... - 81 -

4.13 Validation with quantitative polymerase chain reaction (qPCR) ..... - 82 -

4.13.1 cDNA library preparation ..... - 82 -

4.13.2 qPCR analysis of the cDNA libraries ..... - 82 -

4.14 Pre-fractionated tandem mass-tagged (TMT) proteomics ..... - 84 -

4.14.1 Sample preparation ..... - 84 -

4.15 Summary of methodology chapter ..... - 88 -

5 Results Chapter 1: Creation and validation of standardised human burns ..... - 90 -

5.1 Establishing the relationship between contact-time and standardised burn-depth ..... - 90 -

5.2 Initial calibration phase ..... - 91 -

5.2.1 The clinical appearance of burns created with different contact-times - 92 -

5.3 The histological appearances of burns created with 5-60 seconds of contact-time ..... - 99 -

5.3.1 Haematoxylin and eosin stain of normal skin ..... - 99 -

5.3.2 Masson's trichrome staining of normal skin ..... - 102 -

5.3.3 Masson's trichrome staining of burns ..... - 102 -

5.4 Quantification of burn-depth ..... - 107 -

5.4.1 Measurement of standardised burn depth ..... - 107 -

5.4.2 The relationship between contact-time and standardised burn-depth ..... - 108 -

5.5 Selection of the duration of contact-time ..... - 111 -

5.6 Cooling of standardised burns ..... - 112 -

5.6.1 The effect of cooling on the clinical appearances of burns created with a 7.5 second contact time ..... - 113 -

5.6.2 The effect of cooling upon the standardised burn-depth of experimental burns three hours after injury ..... - 115 -

5.6.3 Analysis of all untreated standardised burn-depth data ..... - 118 -

5.7 Summary of the model ..... - 120 -

6 Results Chapter 2: RNA sequencing and qPCR validation of findings ..... - 123 -

6.1 RNA extraction from the samples ..... - 123 -

6.1.1 The yield and quality of RNA extracted from human skin ..... - 123 -

6.1.2 The effect of thermal injury on the integrity of RNA ..... - 124 -

6.1.3 The effect of cooling on the yield and quality of RNA extracted from thermally-injured human skin ..... - 126 -

6.2 Sequencing of the RNA extracted from the samples ..... - 127 -

6.2.1 The quality and consistency of the sequencing data ..... - 127 -

6.3 The transcriptome of human skin ..... - 130 -

6.3.1 The effect of thermal injury on the transcriptome of normal human skin .. - 130 -

6.4 Examination of gene ontologies affected by thermal injury ..... - 130 -

6.4.1 Ontological analysis with GOPlot 1.0.2 ..... - 131 -

6.4.2 Gene ontologies upregulated by burning ..... - 133 -

6.4.3 Metacore analysis of the data .....- 136 -

6.4.4 Summary of the effects of thermal injury on the transcriptome of human skin - 149 -

6.4.5 The effect of cooling on the transcriptome of thermally-injured human skin - 149 -

6.5 Validation of findings with qPCR .....- 160 -

6.5.1 Primer sequences .....- 162 -

6.5.2 Primer validation.....- 162 -

6.5.3 Validation of the genes altered by cooling in burns.....- 162 -

6.5.4 Confirmation of qPCR with samples from a further 5 patients .....- 169 -

6.6 Conclusions from the RNAseq and qPCR validation experiments.- 173 -

6.6.1 The RNA extraction, purification, yield and quality.....- 173 -

6.6.2 The RNAseq data quality .....- 173 -

6.6.3 The transcriptomic effects of burning .....- 174 -

6.7 Conclusions from transcriptomics .....- 175 -

7 Results chapter 3: Proteomics of thermally-injured skin, and the effects of cooling ..... - 177 -

7.1 Introduction .....- 177 -

7.2 Proteomic analysis of protein pellets from Trizol extraction process.....- 177 -

7.3 The effect of burning on the proteome of normal skin .....- 178 -

7.4 Overview of the effect of cooling on the proteome of burned skin - 181 -

7.5 Detailed analysis of the effect of burning on the proteome of human skin - 183 -

7.5.1 Enrichment in the proteome of thermally-injured human skin .....- 183 -

7.6 The effects of burning upon the clotting cascade .....- 186 -

7.7 The effects of thermal injury on the complement system .....- 190 -

7.8 Immunoglobulin deposition in thermally-injured skin .....- 195 -

7.8.1 Possible antigens in burns .....- 199 -

7.9 The interaction of complement and coagulation cascades within the experimental data .....- 201 -

7.10 The validation of the proteomics data .....- 204 -

7.10.1 The localisation of C4a within the burn injury .....- 204 -

7.10.2 The localisation of C5b-9 in the burn injury .....- 207 -

7.10.3 Staining normal skin for C5b-9 .....- 208 -

7.10.4 Staining an untreated burn for C5b-9 .....- 208 -

7.10.5 Neutrophil adhesion and migration within burned tissues .....- 210 -

7.10.6 The effect of de-roofing of the blister on the proteome of the burn .- 212 -

7.10.7 The clinical context of the proteomic findings.....- 213 -

7.11 The localisation of fibrinogen within the burn injury .....- 215 -

7.12 Platelet aggregation within the injured microvasculature .....- 218 -

7.12.1 Summary of the coagulation proteomics and immunohistochemistry- 219 -

7.13 Summary of the proteomics data ..... - 221 -

8 Discussion ..... - 224 -

8.1 Summary of the conception of the project ..... - 224 -

8.1.1 Establishment of a human burn model for cooling of a partial-thickness burn - 225 -

8.1.2 Optimisation of mRNA extraction from burns ..... - 226 -

8.1.3 Analysis of mRNA extracted from cooled and untreated burns and controls - 227 -

8.1.4 Immunohistochemical validation of key transcriptomic findings ..... - 233 -

8.1.5 Proteomic analysis of paired samples from the same specimens ... - 236 -

8.2 Integration of the results ..... - 242 -

8.3 Proposed mechanism of thermal injury, the role of cooling, and the supporting experimental evidence from this work ..... - 243 -

8.4 Summary ..... - 245 -

9 Future directions ..... - 246 -

9.1 Laboratory phase ..... - 246 -

9.1.1 Stain existing sections for IgM and IgG Fc ..... - 246 -

9.1.2 Identification of burn-induced neoantigen binding the IgM ..... - 246 -

9.1.3 Mathematical model of burn based on data from initial calibration of thermal injury depth ..... - 247 -

9.1.4 Cell culture, heat-shock, and cooling, and the effects on the transcriptome and the proteome ..... - 248 -

9.1.5 Small-molecule inhibitors .....- 248 -

9.2 Animal model .....- 249 -

10 Bibliography ..... - 251 -

11 Appendices ..... - 264 -

11.1 Appendix 1: The initial ethical approval for the study .....- 264 -

11.2 Appendix 2: First substantial amendment .....- 265 -

11.3 Appendix 3: Second substantial amendment .....- 266 -

11.4 Appendix 4: Patient information sheet .....- 267 -

11.5 Appendix 5: Patient consent form.....- 275 -

1 Abstract

Cooling of burns is key to acute burn management, and is a widely accepted practice in modern medicine. Cooled burns are less painful, heal more quickly, require fewer skin grafts, and leave less scarring. The vast majority of research in this area has used animal models, and focussed on optimising cooling, rather than investigating its mechanism. Cooling is not without risks and limitations, and understanding the mechanism might lead to pharmacological alternatives.

We aimed to develop a standardised human model for burning and cooling, and used this to investigate the transcriptional and proteomic effects of burning and cooling. This model used redundant skin discarded during surgery, and purpose-built apparatus for burn creation and cooling. Microvascular and other histological changes were demonstrated in response to burning, and modified by cooling. RNA and protein extracts from cooled and uncooled samples of burned and unburned skin were analysed with RNAseq and LC/MS3 techniques, respectively. Findings were validated with immunohistochemistry and qPCR.

We demonstrated that there was a significant change in 22% of the transcriptome of the skin, with gene ontologies related to wounding, angiogenesis, inflammation, haemostasis, innate immune response, degranulation and chemotaxis among those significantly upregulated. Downregulated ontologies included keratinisation, epidermal differentiation, hair follicle development and cornified envelope. Cooling of burns significantly increased the transcription of genes related to hair follicle differentiation while reducing the transcription of heat-shock proteins.

Burning caused significant activation of the complement and coagulation cascades, while cooling reduced the scale of these changes. Immunohistochemistry confirmed

complement proteins, including the membrane-attack complex (MAC) localised to the immediate area of the blistered epidermis, as were fibrinogen and platelets, with evidence of early neutrophil migration.

We have demonstrated the role of complement and coagulation activation as a damage-amplifying agent following thermal injury, and the role of cooling in attenuating this effect. The preservation of transcription of follicle-related genes indicates preservation of epidermal appendages as sites of re-epithelialisation.

Complement blockade is already utilised in the management of autoimmune conditions, and transplant rejection, and could modify the complement activation in burns, reducing injury-progression, and the associated systemic effects, and improving patient outcomes.

2 Glossary of terms

Abbreviation	Full term
17-DMAG	17-dimethylaminoethylamino-17-demethoxygeldanamycin
5HT	5-hydroxy tryptophan
BAL	Bronchoalveolar lavage
BC	Cooled burn
BCL-2	B-cell lymphoma 2
BCV	Biological coefficient of variability
BNC	Uncooled burn
cAMP	Cyclic adenosine monophosphate
CAT	Catalase
CC	Cooled control
CCL	Chemokine family with 2 cysteines in the N-terminal region
CD31	Cluster of differentiation 31(endothelial antigen)
CD61	Cluster of differentiation 61 (platelet antigen)
CD68	Cluster of differentiation 68 (macrophage antigen)
cDNA	Complementary deoxyribonucleic acid
cGMP	Cyclic guanosine monophosphate

Abbreviation	Full term
CNC	Uncooled control
CWT	Cold water treatment
CXCL	Chemokine family with 2 cysteines separated by other amino acid residues
DAB	Diaminobenzedine
DE	Differentially expressed
DEPC	Diethyl pyrocarbon
DIC	Disseminated intravascular coagulation
DMSO	Dimethyl sulphoxide
DMTU	Dimethylthiourea
DNA	Deoxyribonucleic acid
DPX	Distyrene, plasticiser (tricresyl phosphate), xylene
EDTA	Ethylenediaminetetraacetic acid
FAB	Antigen-binding fragment of Ig
Fc	Constant fragment of Ig
FDR	False discovery rate
FFPE	Formalin-fixed, paraffin embedded
FS	Frozen section
H&E	Haematoxylin and eosin

Abbreviation	Full term
HRP	Horseradish peroxidase
HSP	Heat shock protein
IgA	Immunoglobulin alpha
IgE	Immunoglobulin epsilon
IgG	Immunoglobulin gamma
IgM	Immunoglobulin μ
IHC	Immunohistochemistry
IMS	Industrial methylated spirit
KRT	Keratin
LC/MS/MS	Liquid chromatograph, mass spectrometry, mass spectrometry
LDH	Lactate dehydrogenase
Log2 FC	Log base 2 fold-change
MAC	Membrane attack complex
MCT	Mast cell tryptase (Mast cell antigen)
MDS	Multidimensional scaling
miRNA	Micro ribonucleic acid
MMP	Matrix metalloprotease
mRNA	Messenger ribonucleic acid

Abbreviation	Full term
NADPH	Nicotinamide adenine dinucleotide phosphate
NE	Neutrophil elastase (neutrophil antigen)
NF-kB	Nuclear factor kappa B
NGS	Next-generation sequencing
NK1R	Neurokinase 1 receptor
PCR	Polymerase chain reaction
PRKA	Protein kinase A
PRKC	Protein kinase C
qPCR	Quantitative polymerase chain reaction
RIN	Ribosomal integrity number
RINe	Ribosomal integrity number equivalent
RNAseq	RNA sequencing
ROS	Reactive oxygen species
RT	Room temperature
RTQPCR	Reverse transcriptase quantitative polymerase chain reaction
SD	Standard deviation
SOD	Superoxide dismutase
SP	Substance P

Abbreviation	Full term
SPRR2G	Small proline-rich protein 2G
TBSA	Total body surface area
TCHH	Trichohyalin
TCHHL1	Trichohyalin-like 1
TEAB	Tetraethylammonium bromide
TFA	Trifluoroacetic acid
TGF	Tissue growth factor
VEGF	Vascular endothelial growth factor
VWF	Von Willebrand factor

3 Introduction

3.1 The question: why does cooling a burn make a difference, and why does it matter?

Burns are extremely common injuries, with most people experiencing some sort of thermal injury during their lives. There is probably considerable underreporting of burns, but the British Burns Association estimates that 250,000 people in the UK sustain a burn each year, with 175,000 attending hospital with their injuries, with 13000 requiring admission, 1000 needing fluid resuscitation, and 300 dying from burns. Cooling of burns with water remains the mainstay of burns management, but its mechanism is not fully understood.

3.2 The basic model of a cutaneous thermal injury: three zones

The classical model for a burn injury was proposed by Jackson in 1953[1], and comprises three concentric zones of injury: a central zone of necrosis, a surrounding zone of stasis, and then a further zone of hyperaemia surrounding the zone of stasis.

The model was derived from observations of human burn injuries and their progression to healing. The necrotic area was coagulated tissue that progressed to form an eschar. The hyperaemic zone always healed rapidly. The zone of stasis between these two zones derived its name from the lack of circulation within the dermal capillaries. This was shown pathologically by erythrocytes packed in the superficial plexus, whilst clinically the skin blanched on pressure. Furthermore, there was reduced tissue oxygen consumption, shown clinically by the lack of cyanosis of

the tissue if the limb had a tourniquet applied. This area could progress to full thickness necrosis, or re-reepithelialise from the skin appendages.

In humans, this progression takes place over 24-48 hours post burn. Longitudinal histological studies have demonstrated progressive deepening of the level of the zone of stasis as evidenced by the deepest occluded capillary over the first 48 hours following a burn injury[2]. As this is after the dermal temperature has returned to normal as shown in the following graphs (Figure 1, Figure 2) plotting intradermal temperature against time in animal burn models, it indicates that the ongoing damage is mediated by other mechanisms that have been set in motion by the thermal injury, but continue long after the thermal energy has dissipated.

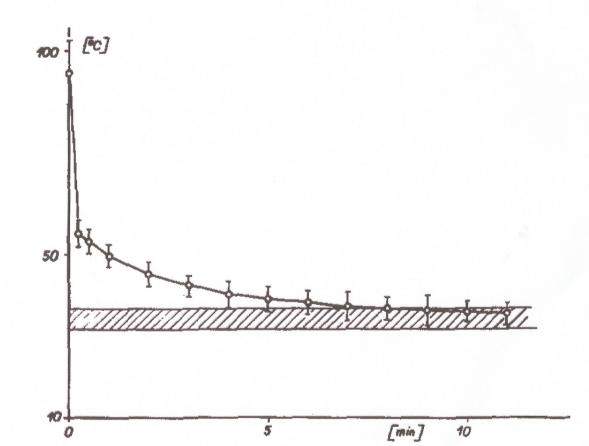


Fig. 1.—Subcutaneous temperatures in the central area of the burn.

Figure 1 Intradermal temperature from Moserova[3]

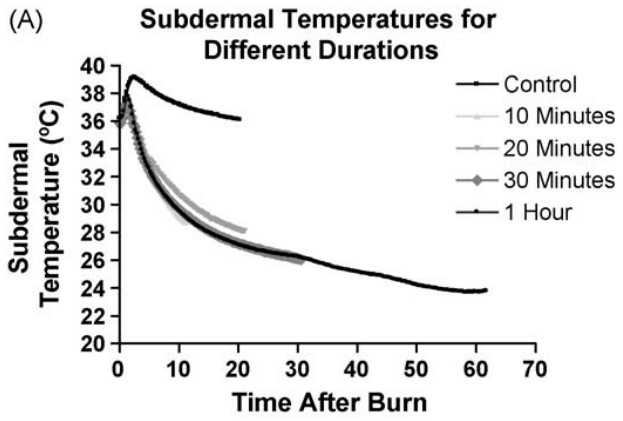


Figure 2 Intradermal temperature measurements from Cuttle et al[4]

Salvage of the zone of stasis is an area of great interest in the management of burns as this represents an element of the burn injury where intervention by the Burn Surgeon may influence the outcome in terms of healing and scarring. A productive approach is to identify interventions that empirically improve survival of the zone of stasis within the burn, validate these improvements with objective, quantifiable assays, and then seek ways to mimic or augment these interventions' effects in the management of burn injuries.

3.3 Cooling of burns: traditional medicine, basic science and first principles

Conventional first aid treatment of burns involves irrigation of the affected area with cool water, and this has been advocated since Galen (AD129-199), Rhazes (AD 852-923) and Earle (1799). As long as the temperature remains above 44 degrees centigrade, the burning continues[5]. There are numerous anecdotal accounts of prompt cooling of the burn resulting in reduced scarring or reduced mortality[6]. Such accounts are cited in the introduction of one of the first published cooling experimental models[7]. A case is cited in which a scald to the upper limb in a young girl sustained by immersion in boiling milk was immediately cooled to the elbow in icy

water in accordance with Scandinavian traditional medicine. The scarring was much reduced below the elbow compared to above[7]. It was postulated that the cooling had a beneficial effect by reducing the amount of thermal energy imparted to the tissues and so reduced tissue damage to the cooled areas.

Work with eggs found that cooling eggs previously immersed in boiling water in cool water resulted in less coagulation of the contents compared to those cooled in air, an effect exaggerated by the application of cloth wrappings to simulate clothing[7]. This supported the theory that the amount of heat delivered, and the rate of dissipation to a temperature below the critical threshold for tissue damage determined the severity of the burn. However, when the same study created scalds to the tails and backs of rats, topical cooling with ice-water resulted in high mortality, even with tail scalds only representing a few percent total body surface area (TBSA), but better results in terms of histological necrosis and oedema. It was concluded that a balance was required between hypothermia and cooling the burn. This study elegantly demonstrates the difference between a model based upon protein denaturing- an egg- and a model based upon a complex organism with interactions between different cellular and humoural systems. While cooling a thermally “injured” egg protected the egg’s contents from becoming denatured, the same degree of cooling had fatal consequences for the rat.

The primary concern of a burns surgeon is the management of human burns, and yet the accidental burns that are sustained in the general population are heterogenous in terms of mechanism, temperature and duration of injury, delay in presentation, and it is ethically difficult to thermally injure healthy people to study the mechanisms and effects of interventions. A retrospective cohort study in humans demonstrated the tendency for accidental scalds caused by more viscous liquids and

with more delay to cooling – therefore with more prolonged contact and more sustained energy delivery - to be more likely to cause a burn requiring skin grafting, a marker of increased burn depth[8], however this study does not examine the effects of cooling.

A human model for Cold Water Treatment (CWT) of burns attempted to create standardised thermal injuries on the medial arm with a heated brass block at 65˚C for 15 seconds under its own weight. These burns were then immersed in a water bath as first aid, but it showed only analgesic benefit[9] with cooled and uncooled burns healing within the same timeframe. It may be that the choice of burning at 65 degrees centigrade for 15 seconds would probably create full-thickness burns not responsive to cooling, as shown by the graph (Figure 3) of burn depth against contact time and temperature produced by Bull in 1963[10] based on work from Moritz[11] and Sevitt, and retrospective case series have shown that CWT reduces the need for grafting[6,12–14].

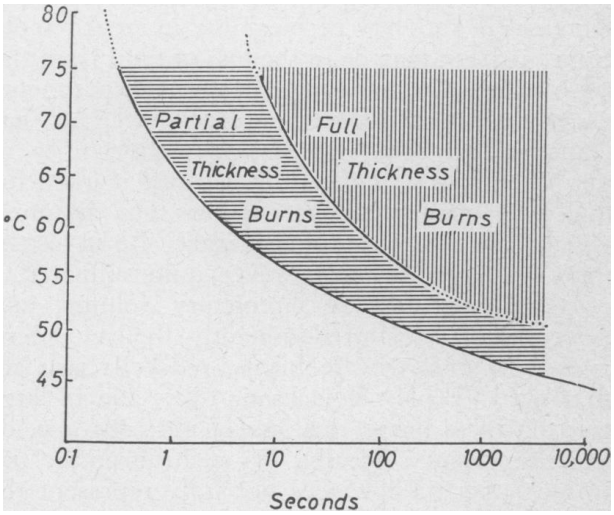


Figure 3 The effect of temperature and duration of contact on burn-depth, Bull 1963[10]

3.4 Measurements of burn injury severity and the effects of cooling

3.4.1 Kinetics of dermal burning and cooling

The effectiveness of cooling of a burn has been measured by the rate at which the dermal temperature returns to physiological or sub-physiological levels, indicating that the heat energy has been dissipated and is no longer damaging the tissues. This has been achieved by the placement of thermocouples within the dermis of the experimental animals' skin directly under the area where the burn is to be created allowing serial real-time temperature readings to be recorded.

In a rat model where a plasma-burner was used to create a full-thickness dorsal burn, dermal temperature returned to 40 degrees from a peak of 100 degrees centigrade within four minutes without cooling, while those burns cooled with ice until "at near-normal temperature" achieved the same temperature reduction within two minutes[3]. In a porcine scald model that utilised water at 85 degrees centigrade to produce a partial thickness burn, Jandera *et al* found dermal temperature fell to below 40 degrees centigrade in both non-cooled and in immediately water-cooled burns within two minutes of burning[15]. In another porcine scald model, again with water at 85 degrees centigrade, all scalds had returned to below 40 degrees centigrade within ten minutes, whether cooled or not[16], while others reported intradermal temperatures returning to below 40 degrees centigrade within two minutes regardless of cooling, or the modality in which it was delivered[17–20]. A guinea pig model found the dermal temperature returned to normal at 30 minutes post burn. A limited, single cohort study reported benefit in terms of analgesia and healing with CWT administered to burns in hospital- by definition delayed[12].

A key point underlined by these studies is the variability in the intradermal temperature and cooling achieved under similar experimental parameters, and the inconsistencies this must impart upon the subsequent results.

Thermodynamic calculations of the reduction of Arrhenius tissue damage have shown in a standardised burn that the improved removal of thermal energy by water compared to air cannot account for the benefit of CWT[21], and CWT experiments listed above point towards a change in cell behaviour, and hence changes in gene transcription and translation. One and two dimensional modelling of a contact burn and subsequent water cooling support this finding[22], as do empirical models discussed previously.

Taken together, these data demonstrate that intradermal temperature returns rapidly to normal in a variety of experimentally produced burns. This period of time has elapsed before many patients can initiate cooling of their own burns, suggesting that the benefit of cooling is not purely heat dissipation. It also highlights the difficulty in producing a comparable burn model when using similar, and more so when using different animals

3.4.2 Oedema and cooling

Oedema is an early feature of thermal injuries, and was thought to be responsible for tissue injury through the increase in interstitial volume increasing the distance between cells and capillaries, resulting in tissue hypoxia. In animal models, oedema became an accepted indicator of tissue damage from a thermal injury in the acute phase. Animal models have utilised either the hind paws for volume measurement using the mercury displacement technique[23], or the ears for wet-dry tissue mass ratio to calculate total water content of the tissues[24]. The former method had the

advantage of allowing serial measurements over time, while the latter required sacrifice of the animal. These models also suffered the restriction that the burn had to be created in such a way as to avoid blistering, as this interferes with the measurement of oedema.

In 1979 it was demonstrated in a sheep model that immediate cooling reduced acute oedema, but cooling delayed by two minutes increased oedema compared to no cooling[25], supporting the thermal energy removal mechanism hypothesis, as temperatures rapidly return to normal after a thermal injury. Blomgren *et al* found that application of water at 8 degrees centigrade for 30 minutes immediately following the scald was the most effective in oedema reduction when compared to other durations[26]. A scalded rat paw model showed that best reduction in oedema was achieved with 0 degrees centigrade Ringer's solution for 120 minutes, with 20 degree Ringer's solution worsening oedema compared to controls, possibly from a hyperaemic response[27].

Overall, these data, with improved results from the lowest temperatures of cooling, support the removal of heat from the tissues as the responsible mechanism for oedema reduction. However, this does not correlate with the findings of the studies that examined different modalities of and delays to cooling that found there was still benefit to healing with delayed cooling[20], and that ice was detrimental to healing compared to no cooling at all[16].

In order to validate the role of increased capillary leak, leading to oedema and burn progression, studies have attempted to pharmacologically mimic cooling. Boykin *et al*, utilising the hairless mouse ear model, showed reduced burn oedema at two hours with cold water treatment (CWT), and that CWT reduced histamine loss from

the burned tissues, with a subsequent reduction of peripheral oedema. This effect was recapitulated by administration of cimetidine, and to some extent indomethacin. There was no histological difference between CWT and control ears at 2 hours. Interestingly, a mouse ear is only 7%TBSA and yet a scald to this area had an appreciable effect on oedema distant to the burn injury[28], and the systemic effects of burns need to be carefully considered when selecting control areas.

A study of much larger TBSA burns (40-50%) in guinea pigs found a reduced level of circulating histamine and improved physiological parameters in CWT animals compared to controls, in a manner similar to pre and post-burn treatment with cimetidine[29]. Burn oedema in the rat paw was shown to be reduced by cimetidine, superoxide dismutase (SOD), catalase (CAT), and hydrocortisone, but worsened by albumen administration, indicating the involvement of reactive oxygen species as well as histamine in the pathophysiology of burns, and demonstrating a role for increased capillary leak in the generation of burn wound oedema[30]. However, another study found no benefit to cimetidine treatment in terms of oedema formation in all tissues, and that high doses were harmful[31]. The harmful effects of high-dose cimetidine were attributed to its cardio-depressive effects, and the larger TBSA compared to the other studies. A human study found no benefit from antihistamines in the healing of experimental burns[32].

In all, these findings show that histamine release from burned tissue has a role in the pathophysiology of burn wound oedema, but do not support a pivotal role for histamine suppression in mediating the effects of CWT, as the use of cimetidine did not reproduce the effect of cooling.

3.4.3 Cooling, dermal perfusion and microvasculature

Oedema can be thought of as a surrogate marker for tissue injury, but in fact oedema has been shown to have a poor correlation to histological signs of tissue damage[26], and reduction in oedema does not explain the benefit of cooling, as discussed above. Thus, further studies have assessed the effects of burning and cooling on the histology of the burnt tissue. Histological changes can be seen in the tissues: capillary damage as evidenced by the intercellular junctions forming gaps in the capillary walls; distinct spaces in the extracellular matrix; and neural destruction as evidenced by necrosis can be seen at 15 minutes following a deep burn. Furthermore, cytoplasmic damage with evidence of the venular endothelial cytoplasm becoming increasingly granular, organelle disruption and absence of micropinocytotic vesicles can be seen within four hours of a deep burn[33].

Video microscopy of bat-wing microvasculature demonstrated vascular dilatation and stasis within the zone of thermal injury and leukocyte extravasation with platelet and erythrocyte clumping, suggesting that the vascular endothelium was the site at the pathological changes were initiated. The administration of CWT reduced stasis, oedema, and haemorrhage seen at 24 hours post injury when compared to controls[34]. In a mouse ear model, the three zones of the burn injury described by Jackson were demonstrated using real-time video microscopy and the progressive occlusion of 10-12 micrometre vessels leading to a ten-fold increase in the zone of necrosis[35]. Erythrocyte aggregation was seen immediately, followed at 8-12 hours by leukocyte adhesion, with platelets forming occlusive plugs between 90 minutes and 48 hours[36]. In a mesenteric microvascular model for systemic burn oedema in rats, leukocyte adhesion was found to be significantly increased at 30-60 minutes after a 20% TBSA cutaneous burn and still above baseline at 6 hours, underlining the

difficulty in obtaining within-animal controls with large TBSA burns. Furthermore, an increase in vascular resistance combined with increased capillary permeability, mediated by circulating chemokines such as histamine, increased capillary leak[37]. A study in guinea pigs identified immediate cooling with ice water as improving hair follicle retention and dermal perfusion at 16 hours as measured by India ink perfusion[38].

A variable delay prior to cooling thermal injuries in guinea pigs has also been investigated. Raine *et al* found that the benefit of cooling to the preservation of dermal perfusion, as measured with India ink perfusion and Xenon washout, was significant with delays of up to 30 minutes before CWT commenced. Guinea pigs with up to 30 minutes delay to cooling healed with less scarring and more hairs than either untreated controls, or those waiting 60 minutes for cooling[39]. At 30 minutes the dermal temperature has returned to normal, and the benefit of cooling cannot be explained by the normalisation of tissue temperature. While the benefit of faster cooling, as would be achieved by a lower-temperature coolant holds for a model of heat energy removal from tissues, given that delaying cooling until tissues are normothermic is still beneficial, and cooling with ice has a detrimental effect on burn healing, the empirical evidence is that heat removal is not responsible for the beneficial effect of cooling a burn.

The effect of hypothermia on coagulation and clotting is well-documented, and presents a significant problem in trauma situations where large volumes of cold crystalloid and blood products are administered in a short period of time. A study investigating the effect of cooling on the prothrombin time (PT) and partial thromboplastin time (PTT) found that blood from healthy volunteers showed significant prolongation of both these values at 34˚C, 31˚C and 28˚C compared to

37˚C[40]. Cooling with water at 16˚C, as recommended from some experimental work might lower the temperature of the skin and circulating blood within it considerably further, and have a far more powerful anticoagulant effect and hence preserve the microvasculature. It is also worth noting that under conditions of profound hypothermia (4˚C or lower), platelets show a tendency to marginalise and clump more readily, and express higher levels of P-selectin at lower temperatures, as observed in patients during cardiac surgery[41]. Platelets also show increased shear-induced platelet-activation at lower temperatures[42]. These findings may explain the detrimental effects of applying ice to a burn[19], as the increased platelet activation would result in greater microvascular occlusion.

3.4.4 Anticoagulant therapy

This evidence of microvascular occlusion has lead researchers to investigate the effects of anti-thrombotic agents. The effect of heparin on this progressive dermal ischaemia was investigated by Robson *et al* using a guinea pig model and India ink perfusion, with no improvement of dermal perfusion between treatment and control groups[43]. Similar work using guinea pigs and the antithromboxane agents imidazole, dipyradamole, and methimazole found improved dermal perfusion in vivo and with India ink injection studies when compared to controls, and suggested a beneficial role in the reduction of Thromboxane A2 activity. This was confirmed with immunohistochemistry in the same specimens[44]. However, the effect of a highly selective thromboxane synthase inhibitor Dazmegrel did not improve dermal perfusion when administered either systemically or topically in guinea pigs, but in low doses did improve healing at 22 days[45]. This could indicate that Dazmegrel is acting directly on the burned tissues, rather than improving healing by maintaining

microvascular patency, by reducing progressive necrosis, and preserving epidermal appendages from which re-epithelialisation can begin.

3.4.5 Cooling and healing

Ultimately, the key outcome in treatment of burns is healing of the burn with minimal scarring. Therefore, the effects of timing, temperature, and modality of cooling have been investigated with healing as an endpoint. In a rat model previously discussed, immediate cooling using ice reduced the area of unhealed wound at 43 days compared to untreated controls [3].

A porcine model compared immediate cooling to cooling initiated after 30-minutes. Cooling was administered with abdominal swabs soaked in water at 14-16 degrees centigrade or gel treatment each applied for one hour. Here, it was found that the temperature of all burns, including the untreated control, were below 40 degrees centigrade within two minutes, yet cooling after a 30 minute delay was still beneficial. Burns treated with CWT healed better than those subjected to cooling by gel treatment[15]. Another porcine study of different modalities of cooling found running water at 22 degrees centigrade was superior to water sprayed onto the burn every 30 seconds, or wet towels changed every 3 minutes in terms of burn propagation, and healing[17].

When different temperatures of CWT, delivered as wet towels at predetermined temperatures changed every 3 minutes were compared in a porcine model, it was found that iced water at 1-8 degrees centigrade was more detrimental than non-treatment, CWT at 12-18 degrees lead to intermediate healing results, and the best healing was demonstrated when there was a 30 minute delay before three hours CWT at 16-18 degrees centigrade, again not in keeping with simple removal of

thermal energy[16]. A further porcine study of optimal duration of CWT at 22.4 degrees centigrade found 20 minutes most beneficial in terms of histological burn depth, with 5, 10, and 30 minutes less effective. There was no difference in healing time, possibly because the burns were all superficial partial thickness[18]. In another porcine study of temperature of CWT, burns treated for 20 minutes with CWT running across the wound at 1.6 litres/minute at 15 degrees centigrade healed with less scar contracture than burns treated with either ice granules applied directly to the skin, or CWT with water running at 1.6 litres/ minute at 2 degrees centigrade, although there were problems creating a consistent, reproducible burn[19]. Another porcine model found no difference in histological appearance of the tissue at 9 days between burns cooled immediately, and at 5, 20 and 60 minutes delay for 20 minutes with tap-water at 22.4 degrees centigrade[20].

Taken together, these studies demonstrate the importance of cooling when using an outcome relevant to patients. Furthermore, they emphasise that normalisation of dermal temperature is not the sole mechanism mediating the effects of CWT, and further investigation of this mechanism might yield therapeutic targets for novel burns treatments. Finally, the studies demonstrate that developing a model of consistent burn depth, consistent cooling temperature, delay and duration, will be important in future experimental work. The burn depth in such a model should be mid-dermal, representing the depth of burn most likely to benefit from intervention in humans.

3.5 Mechanisms of burn injury pathophysiology

The above literature point to mechanisms not related to thermal energy dissipation mediating the effects of CWT. It is therefore important to understand the cellular pathophysiology of burns at the gene, protein and cellular level, in order to facilitate the identification of potential therapeutic targets.

3.5.1 Cellular and humoural mediators

3.5.1.1 Cellular mediators

The role of leukocytes in the pathophysiology of burn injury has already been alluded to above[36,37]. These cell populations respond to inflammatory mediators and chemotactic factors that have been investigated in animal models. When the hind paws of irradiated rats were scalded there was no reduction in the volume of oedema compared to rats with normal numbers of neutrophils, implying the neutrophils do not have pivotal role in burn oedema[46].In a rabbit model, anti-ICAM and anti-CDw18 monoclonal antibodies were used to block neutrophil adhesion to the vascular endothelium, and resulted in improved perfusion of the zone of stasis, and less progression of the zone of stasis to necrosis[47]. Taken together, these results again dissociated burn oedema from tissue damage, but implicated neutrophil adhesion to vascular endothelium in the progression of the zone of stasis.

One of the main modes of action of the neutrophil is to produce reactive oxygen species via the NADPH pathway, and this was investigated in guinea-pigs treated with allopurinol, DMSO, and SOD prior to creation of a 5% TBSA burn. No difference was found in the rates of healing, hair retention, or de-differentiation of skin appendages, suggesting that the reactive oxygen species do not play a major role in burn injury[48].

3.5.2 The interaction between cellular and humoural factors

In 1988 a rat model was used to study complement activation through the formation of C5a, and neutrophil chemotaxis following a burn to the hindquarters. It was shown that neutrophil chemotaxis was significantly reduced by SOD and CAT, DMSO and DMTU, allopurinol, lodoxamine, and deferoxamine- an iron chelating agent, but neutrophil depletion had no effect on C5a levels, indicating that reactive oxygen species originating from the xanthine oxidase pathway are responsible for the activation of C5 to C5a[49], but that neutrophils were not their source, but rather were chemotactically attracted by C5a. A more recent study using knock-out mice deficient in Mast cell proteases (MCPs) 4 and 5 found that these MCPs are essential in burn-wound evolution and MCP 4 and 5 deficient mice are protected from post-scald ulceration[50].

3.5.3 Complement and coagulation activation

More recent studies have examined the complement system in greater detail as it has become clear that there is interaction between the complement and clotting cascades, and that there is a role for the activation of complement in many post-traumatic ischaemia-reperfusion injury models[51–54]. In particular, it has been shown that complement can be activated by thrombin in the absence of C3[55], and produce a functioning MAC. Rats lacking C4 have been shown to heal with less by way of scarring following thermal injury[56] compared to wild-type rats and blockade of IgM-non-muscle myosin binding and hence activation of the classical complement activation pathway has been shown to reduce burn progression and improve healing in a porcine model[57]. Human studies have demonstrated a decrease in IgM in the plasma of burns patients proportional to the size of the burn, suggesting sequestration of the IgM to the injury[58–60].

3.5.4 Substance P

The neuropeptide Substance P (SP) is a member of the tachykinin family, and is released from both the central and peripheral nervous system in response to depolarisation. It exerts its effects through binding the neurokinin receptors (NKRs), of which NK1 has the highest affinity for SP. NKRs are membrane-bound G-protein receptors that mediate their effects through cAMP, IP3, DAG, and increases in intracellular Ca^{++} as shown in Figure 4.

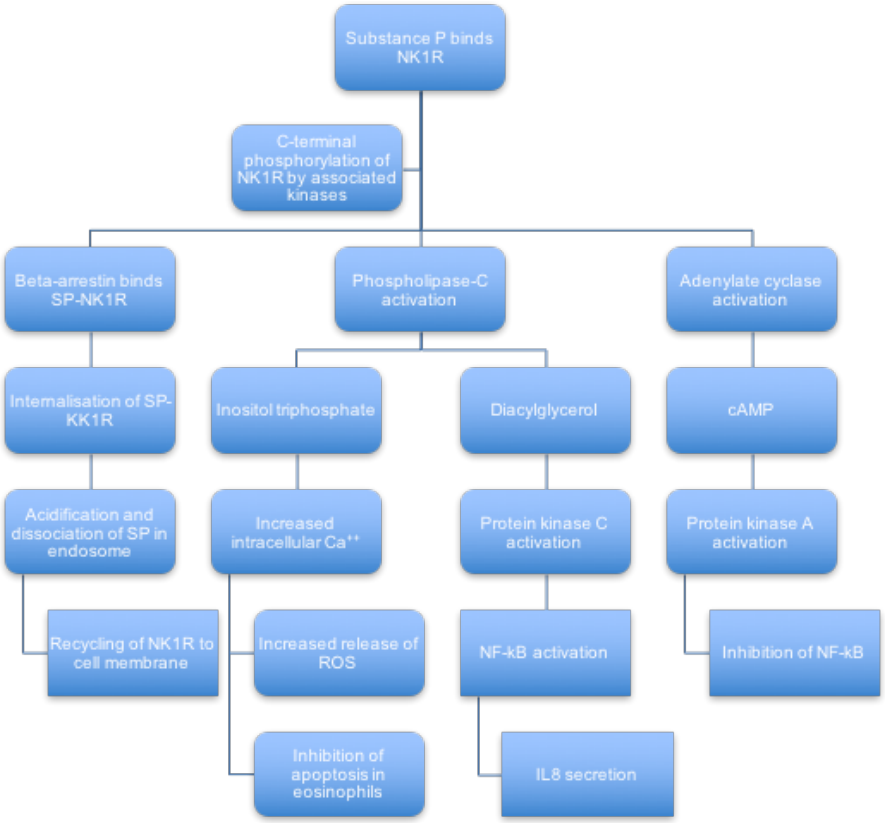


Figure 4: The effects of Substance P binding the NK1 receptor

The NKRs are expressed throughout the body, including within the cardiovascular system and on vascular endothelium, but particularly on immune cells, including Mast cells, eosinophils, macrophages, and neutrophils. The effects of SP binding NK1R is summarised in the diagram below:

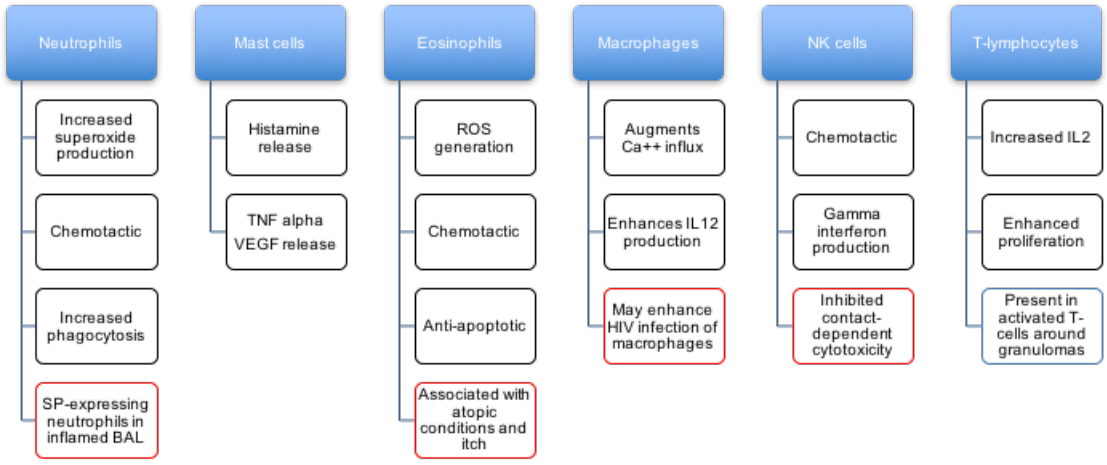


Figure 5: The effects of Substance P on white blood cell populations

In a rat model, NK1 receptor antagonist SR140333 inhibited thermal oedema formation, but had no effect on neutrophil accumulation in the tissues[61]. More recent work with NK1R-deficient rats showed that lack of NK1R, and the blockade of NK1R with SR140333 in wild-type mice prior to burning resulted in a significant initial reduction in the volume of oedema forming in burned ears at 10 and 30 minutes after injury. The blockade of Kinin B1 and B2 receptors caused a similar reduction in oedema at 10 and 30 minutes after injury. These differences were not maintained at 1 hour, when the knockout and treated groups converged with the controls. Neutrophil accumulation within burned tissues was unaffected by NK1R knock-out or pharmacological blockade[62].

Overall, it would seem that free radicals play an important role in burn pathology, and may have a role in complement activation, but do not originate from neutrophils, which in turn play an important role in burn progression, implying the parallel actions of different humoural and cellular pathways, which synergise in burn pathology. Simply blocking one pathway does not halt the progression of burns.

None of the studies above compared the various interventions directly to CWT within the same experiment. Similar experimental designs in terms of burning mechanism

and choice of animal, but investigating cooling were able to reproduce the clinical benefit of cooling. The fact that the vast majority of the studies did not replicate the benefits of CWT in different studies, but using similar animals would indicate that CWT does not deliver its benefits by blocking the single cellular or humoural event in question. The only exception to this is the blockade of non-muscle myosin IgG interaction[57], that reduced the progression of burns in the treated animals in parallel to the progression seen in C4-/- animals[56]. This implies a pivotal role for complement in burn pathophysiology.

3.6 Burns and gene expression

3.6.1 In animals

There exist in the literature some pilot studies of gene expression in burn injuries in both humans and animal models. A rat model has shown that modest systemic hypothermia of 31-33 degrees centigrade core temperature reduced the progression of “second degree” burns as measured histologically, even when delayed by 2 hours, and had a consistent and reproducible down-regulatory effect on the expression of matrixmetalloproteinase 9 (MMP9) mRNA, while up-regulating the expression of CXCL13, lipopolysaccharide binding protein, CCL6, and CCL24. These molecules have important functions in B-cell maturation, reduction of endotoxin load and improved bacterial opsonisation; keratinocyte proliferation; and collagen synthesis and deposition by fibroblasts [63]. This model used within-animal control areas, but from an unspecified site and it is worth noting that previous studies found small %TBSA burns had a systemic effect on tissue oedema, which could confound their conclusions[28] as a relatively large TBSA burn would have some systemic effect on the control sample and there is the potential for skin from a different anatomical

site to the burn samples to have a different basal transcriptome. The systemic hypothermic treatment also prevents direct comparison of cooled and untreated burns, and unburned, uncooled skin from the same animal.

3.6.2 In humans

3.6.2.1 RNA expression

As we are concerned with the management of human burns, human burn tissue is of the greatest interest in terms of genetic expression. In a comparison between normal skin excised from unburned patients in the course of cosmetic procedures, and debrided deep partial and full thickness burns at up to 17 days post injury, burned tissues showed expression of genes related to apoptosis, differentiation, and proliferation and healing were up-regulated, with temporal differences when the burns were grouped in 0-3, 4-7 and >7 days[64]. This study pooled patients' samples to neutralise individual responses, and the burn group was extremely heterogeneous with burns of 2-80%, and variable thickness. It is also unclear which parts of the burn were sampled. Nonetheless, it demonstrated proof of concept that it is feasible to perform genomic analysis on burned human skin, and that there are changes in gene expression over time.

3.6.2.2 MicroRNA expression

A further study of microRNA in three human burns showed significant differences in microRNA in denatured dermis from the extremities and normal skin left over from split skin grafts taken from the trunk, with possible effects on Wnt, VEGF and MAPK. These burns were traumatic, and the samples were collected at four days post injury, with possible confounding variables in the site of the burns and the control skin, mechanism of injury, and anatomical sites of the burn, but may nonetheless point to

the role of gene expression and post-transcription modification in burns pathophysiology[65].

Species	Control skin	Uncooled burn	Cooled burn
Human[64]	Upregulated 1136 genes, ontologies: apoptosis 6, cell adhesion 14, collagen 6, epidermal differentiation 10, inflammation 89, regulation of transcription 13		
	Downregulated 1003 genes		
Human[65]	Upregulated 32 miRNA species		
	Downregulated 34 miRNA species		
	Functional ontologies include: apoptosis, cell adhesion, Notch, wnt, TGFß, VEGF, p53 and MAPK signalling (fold-changes not stated)		
Rat[66]	HSP47 and HSP70 mRNA upregulated by burning		
		HSP47 and HSP70 mRNA downregulated by cooling	

Species	Control skin	Uncooled burn	Cooled burn
Rat[63]	Genes associated with skin-specific functions downregulated in burn		
	Inflammation, apoptosis and tissue structure (MMPs) upregulated in burn		
		CXCL13, CCL6&24, LPBP upregulated by cooling	
		MMP9 and type II keratin downregulated by cooling	

Table 1: Summary of mRNA and miRNA changes in burns, and between cooled and uncooled burns

3.6.3 Protein expression and proteomics

3.6.3.1 Animal models

Longitudinal burn studies in rats have shown an increase in staining for markers of autophagy (Beclin 1) in hair follicles and apoptosis (tunel) within the epidermis respectively, and corresponding loss of antiapoptotic BCl2 and increase in apoptotic BAX proteins[63]. The role of HSPs in the burn wound were also investigated in a rat model where the HSP90 alpha mRNA and protein were shown to increase significantly in skin after burning, within a matter of hours. The changes were localised to the burned area of the skin biopsy. Topical application of HSP90 alpha inhibited apoptosis in an *in vitro* human cultured keratinocyte heat shock scratch model, and improved gap-closure, and improved burn wound healing in rats, while

17-DMAG- an HSP90 alpha inhibitor- increased the rate of apoptosis, and impaired healing in both the in vitro and rat models[67].

3.6.3.2 Human models

A human study of skin excised from burn patients in the course of their normal surgical treatment examined protein expression with mass-spectrometry and 2D-difference gel electrophoresis. Normal skin from breast reduction surgery was used as a control, and the burns were again grouped as 0-3, 4-7 and >7 days. Again, these data show that there is a definable change in protein expression in burns, with a temporal pattern fitting to the known pathophysiology of burns wounds. HSPs, those genes associated with anaerobic metabolism LDHB has role in autophagy (LDH), and protease inhibitors - known to be essential in wound healing- are all altered in burns[68]. The importance of protease inhibitors in wound healing has been demonstrated in mice deficient in secretory leukocyte protease inhibitor (SLPI) that display delayed wound healing, and indeed deterioration of wounds compared to controls[69].

None of these studies investigated the effects of cooling. Burns that are excised are by definition deep, have not benefitted from CWT, even if it was administered, and conclusions as to gene-expression modification in human burns mediated by CWT cannot be reached from these studies alone.

Species	Control	Uncooled burn	Cooled burn
Human[69]	LDH, HSP90, fibrinogen, serpins SCCA1 and 2, SLPI, TCTP, laminin receptor, KRT 5, 6, 16, 17 all upregulated by burning		
	KRT1 downregulated by burning		
Rat[66]	HSP47 and HSP70 upregulated by burning		
		HSP47 and HSP70 downregulated by cooling of burn	
Rat[70]	Beclin 1 and Tunel staining increased after burning, BCl2 decreased and BAX increased after burning		

Table 2: Summary of proteomic changes in burns compared to controls, and between cooled and uncooled burns

3.7 Discussion

The studies reviewed have established that there is a clinical benefit in terms of healing[12] and reducing the need for surgery[13,71] from the administration of CWT to superficial burns, and that these benefits have been reproduced in some animal studies, when the correct burn depth and modality of CWT has been selected[4,15–17,63]. The mechanism by which the benefit is delivered is not thermal energy removal, or oedema reduction, and pharmacological antagonism of histamine release has been ineffective in both animals[28,30,31] and humans[32]. Many of the other interventions discussed above have not been compared directly to CWT, and with the exception of complement-activation blockade[56,57] have not reproduced the benefits of CWT in other studies of the same animal types. The small-animal models suffer from contamination of the control areas by the systemic effects of the burns that represent a significant %TBSA[24,26,37].

Human models have all used deep burns, either through the methodology of the experiment[9,32], or the fact that the patients were undergoing debridement of deep burns prior to skin grafting[65,69]. This limits what can be learned from the results in terms of how CWT improves outcome of partial-thickness burn injuries. However, these studies have demonstrated proof of concept that it is possible to extract RNA and proteins from burns, and that there are consistent temporal changes seen in these tissues. Further characterisation of these changes through the study of controlled burns in normal human skin may reveal therapeutic targets for the management of burns. This will need careful ethical consideration, study design and patient recruitment, but the scientific feasibility of such work has been demonstrated in previous works cited in this review.

3.8 Conclusions and future directions of research

In summary, the above work has established some important principles. Firstly, the benefit of CWT has been established in clinical experience, and proven in animal models. Secondly, the benefit of CWT cannot be explained purely on the basis of removal of thermal energy from the damaged tissues. Thirdly, there are important cellular and humoral mediators involved in burn injury pathophysiology, but modifying these individually does not affect burn progression in animal models, with the singular exception of modification of complement activation. Finally, there are changes in gene and protein expression in response to thermal injury, and the pattern of expression changes over time from burn injury. The events in these systems that have been elucidated from various human and animal models are summarised in relationship to one another in Figure 6. Integration of these findings in further experimental work in healthy human volunteers could yield valuable therapeutic targets for future burn treatment.

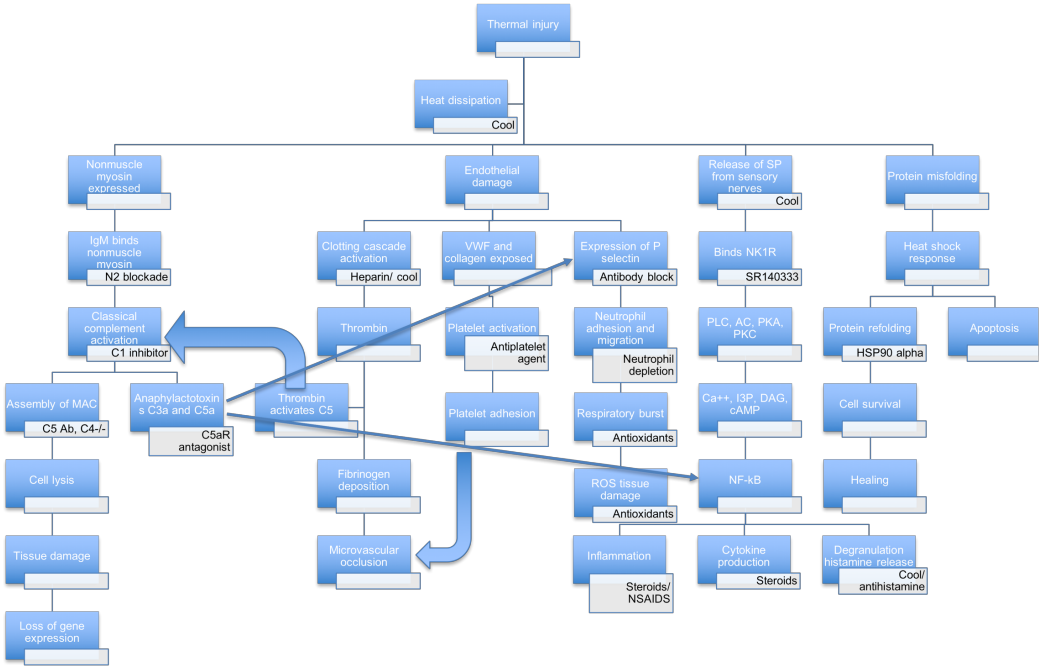


Figure 6: The integration of cellular, humoural, and transcriptomic events in burn pathophysiology, and experimental antagonists

Currently, all the work done on human burns has used tissue excised following injury in the course of wound debridement with a view to skin grafting. These are areas of skin that have, by definition, failed to survive the injury, and are now being excised. Whether they have been cooled or not, the intervention has been unsuccessful, so these burns cannot tell us how cooling actually works. It is difficult to justify excising parts of burns that do not need debridement in order to compare them to burns from the same patient that do warrant excision, so this direct comparison of cooled and untreated burns, where the cooling has actually been effective cannot be done ethically. A human model for burning and cooling of burns, using normal, consistent areas of skin and creating consistent burns, as have been demonstrated to be possible in animal models would allow a major knowledge-gap to be addressed.

There is already a thriving business supplying researchers with normal human skin excised during cosmetic procedures, particularly following weight-loss, and it might be possible to design a study whereby burns could be created on areas of skin during these operations, while they were still attached and perfused, but after anaesthesia, and then use these standardised burns to investigate the effects of burning and cooling on the proteome and transcriptome of normal human skin, with within-individual controls. This would have the added benefit of enabling burns to be studied in humans, rather than having to extrapolate findings in other species to humans, as has to be done with animal models.

3.9 The aims of this project are as follows

3.9.1 Creation of a safe, robust, validated human model for burning and cooling

The first, and key step in this project is identification of the parameters that will allow the creation of partial-thickness burns and administer cooling in a safe, consistent and predictable way. This will require the design and manufacture of specific apparatus. There is also the need to develop an objective measure of burn severity such that any significant reduction in burn-depth from cooling can be demonstrated. Without meeting these conditions, it will be impossible to correlate subsequent findings to actual burn pathology.

3.9.2 Extract, purify and analyse RNA extracted from cooled and uncooled burns and controls using RNA sequencing

The extraction of RNA from skin samples must be optimised to the conditions of the experiment, namely that there is relatively little RNA in skin, the samples will be small, skin has a high RNase activity, that it is mechanically hard to work with, and that burning may cause degradation of the samples. Once extracted and purified of

contaminating DNA, the RNA samples will be submitted for RNA sequencing to allow genome-wide sequencing and to allow for sample degradation, and also to examine non-coding RNA species. The effects of burning on the transcriptome of human skin and the effects of cooling on these changes will be analysed through pair-wise comparisons.

3.9.3 Extract protein samples from the same set of specimens and submit these for proteomic analysis

Protein samples from the same specimens will be submitted for proteomic analysis with the aims of firstly validating any changes identified at an RNA level, and secondly identifying changes in the proteome of thermally-injured skin resulting from the deposition of proteins synthesised elsewhere e.g. coagulation factors, complement proteins, immunoglobulins.

3.9.4 Immunohistochemical validation of these findings

The findings from the abovementioned experiments will be validated with immunohistochemical staining of sections from the respective halves of the samples submitted for RNAseq and proteomic analysis, as shown in Figure 16, and from samples representing the four conditions of cooled and uncooled burns and controls taken from other patients. This will allow validation and localisation of any changes to a particular site within the burn injury, and compensate for any variability between specimens and individuals.

4 Patients, materials and methods

4.1 Principles of the model

The successful establishment of the burn model required a number of conditions to be met:

Burns and control areas must be created in symmetrical, consistent anatomical areas within and between volunteers

It must be safe, with all possible risks to the volunteer and staff minimised

The volunteers must be healthy at the time of the experiment

The burns must be created in a consistent and reproducible manner

There must be a minimal use of local or topical agents applied to the area in which the burns are to be created

The cooling of one set of burn and control areas must be as standardised and as consistent as possible

Harvest of the specimens must be at consistent time-points after injury and atraumatic to the specimens

4.1.1 The suitability of the deep inferior epigastric perforator (DIEP) flap as the source of skin for the model

In keeping with the above conditions, the deep inferior epigastric perforator (DIEP) flap was identified as a good basis for a human burn model. The DIEP flap consists of fat and skin from the lower abdomen, and is a commonly-used option for breast reconstruction following mastectomy. During the operation, areas of skin in the lateral portions of the flap are discarded as they do not fit into the chest defect, and have tenuous perfusion via the deep inferior epigastric perforator vessels, making them unsuitable for inclusion in the reconstruction, but likely to result in a poor cosmetic outcome if not excised from the donor site where they will form “dog-ears”- standing cones of skin. The marking of the DIEP flap is shown in Figure 7, while closer detail is shown in Figure 8.

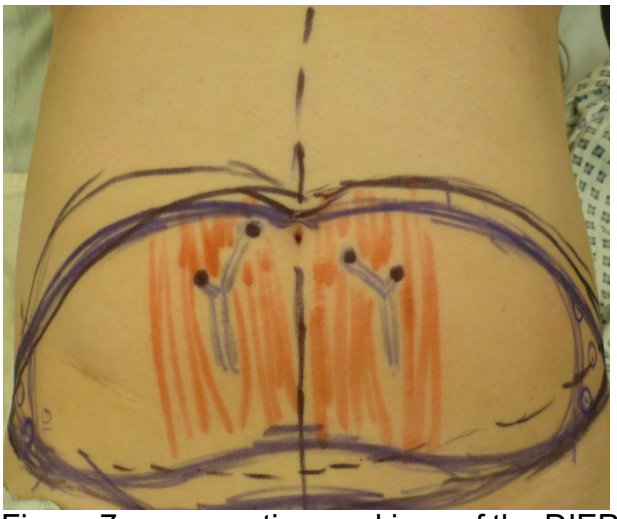


Figure 7: preoperative markings of the DIEP flap, showing the surface-markings of the vessels and the lateral areas forming the basis for the burn model

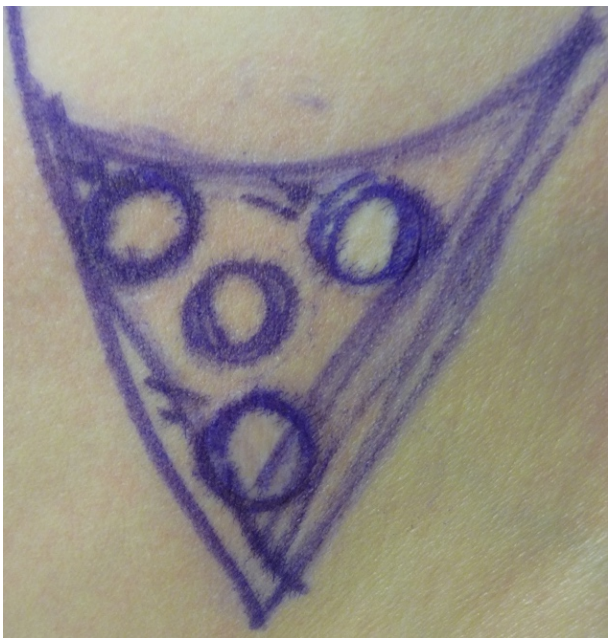


Figure 8: Close-up of the lateral corner of the flap, and the template markings of the 3 burns peripherally, and the control area centrally

The advantages of the DIEP flap as a basis for the model are the predictable, symmetrical areas of abdominal skin, and the operation having a predictable time-course.

The preoperative care of the patient prior to surgery begins with induction of anaesthesia in the anaesthetic room, followed by an interval of at least 20 minutes during which the anaesthetist establishes extra intravenous access, inserts an arterial line and urinary catheter, and ensures the patient is fully stabilised for surgery. This interval is sufficient for us to create the experimental burns using our purpose-built apparatus, administer 20 minutes of standardised cooling in line with best evidence regarding the duration of CWT first aid, and not impact upon the patient's surgery. The general anaesthesia of the patient obviated the need for topical anaesthesia that could have confounding effects on the samples.

The burns and their respective control areas could then be harvested with a 12mm diameter (the largest commercially available) biopsy punch after the patient had been

prepped and draped for surgery. The biopsies must be harvested before the pedicle of the DIEP flap was divided- rendering it temporarily ischaemic- and transferred to the chest for anastomosis onto the internal mammary vessels and inset to form the new breast-mound. It was established that a minimum of three hours would elapse between induction of anaesthesia in the anaesthetic room and excision of the excess triangles of skin from the lateral parts of the DIEP flap on the operating table. It was also established that it would be possible to excise burns and controls under sterile surgical conditions within 1 hour of creation, allowing the potential for the study of the time-course of burn pathophysiology.

4.1.2 Patient selection

Patients were selected on the basis of being aged under 65 years old, free of chronic inflammatory conditions such as rheumatoid arthritis, Crohn's disease, and ulcerative colitis, not suffering from any dermatological conditions such as psoriasis or adverse scarring, not diabetic, or taking any steroids, anti-inflammatory medications, disease-modifying agents, or immunotherapy, and in remission from their breast cancer, and not being treated with Herceptin. Following discussion with the anaesthetists, it was agreed to withhold antihistamine, steroid and NSAIDS until the samples were all harvested, in light of previously published work that had examined the effects of these classes of agents on burn pathology[30–32,44,72].

4.2 Apparatus

Apparatus was specifically designed by medical engineers in the Gray Institute of Radiation Biology, and formed part of the application for ethical approval. The design had to be safe for the volunteer, those using the apparatus, and other staff to avoid creating a burn to an unintended area. It needed to be compact and unobtrusive in the anaesthetic room or operating theatre, and be simple to use and control.

One major issue to resolve was that of the creation of a consistent, reproducible, predictable thermal injury in human skin, in terms of temperature, and duration[73] and pressure of contact[5]. For obvious ethical reasons, there is very little published concerning this[9,74]. The relationship between time and temperature burn-depth is summarised in Figure 9.

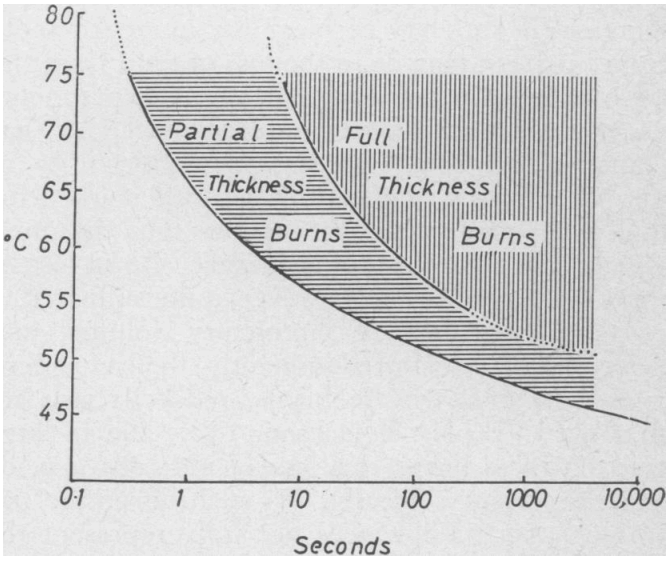


Figure 9: graph plotting temperature and contact-time against burn depth from article "Burns" by Bull, 1963[10]

Figure 9 uses a log 10 scale to plot time, and shows that an increase in temperature results in a more-than-linear reduction in time required to create a burn of any given depth. Time-points from Figure 9 are set out in Table 3.

Temperature/˚C	Onset of partial- thickness injury	Onset of full-thickness injury
55	23sec	6min 9sec
60	4.0sec	1min 8sec
65	1.3sec	25sec
70	0.5sec	10.8sec
75	0.3sec	6.8sec

Table 3: time-points extracted from Figure 9

It was decided that 70˚C would be adopted as the temperature for burn creation as a balance between the duration of contact over which a consistent pressure could be maintained by a human operator, and the inevitable human variation of actual contact time around the intended duration as a proportion of that intended. The aim was to create a mid-dermal injury, so 70˚C would provide a starting range of contact-time durations of 0.5 to just under 11 seconds, which could be adequately covered in 2.5-second intervals from 5 seconds upwards. Durations >10 seconds would also be explored to assess correlation of clinical and histological findings to the data set out in Figure 9.

4.2.1 Burn creation device

The device designed and built for the creation of the burns consists of an integrally-heated and thermostatically-controlled, spring-mounted copper rod 15mm in diameter, in an insulated hand-piece, and attached to the control console by the power-cable. Pressure of application is controlled by the consistent displacement of a spring within the hand-piece, and duration of contact is the remaining variable in depth of burn-

creation with this piece of apparatus. A template of circular holes was cut in a clear 6mm thick silicone sheet to allow the burns and control areas to be created with a consistent relationship to one another, and to prevent the inadvertent burning of the patient outside the intended area, as shown in the photograph in Figure 10.



Figure 10: Burn creation apparatus, showing thermostatic control unit, hand-piece, and silicone template with holes corresponding to the central control and 3 peripheral burn areas

4.2.2 Cooling

Cooling was administered using a second piece of apparatus, again purpose-built, that uses thermo-electric coolers to move heat from the base-plate of the device to the cooling fins on the upper surface, and controlled from a unit identical to the burn-creation device. Sterile water-based lubricating jelly was used as the thermal coupling agent to ensure good thermal contact with the skin, and to mimic as closely as possible the effect of being cooled with water. The baseplate of the device was large enough

to place over the entire triangular area forming the basis of the model, allowing the burns and corresponding control areas to both be subjected to identical, standardised cooling. The cooling device is shown in below in Figure 11, and Figure 12.



Figure 11: cooling block, viewed from under-surface where it contacts the patient's skin

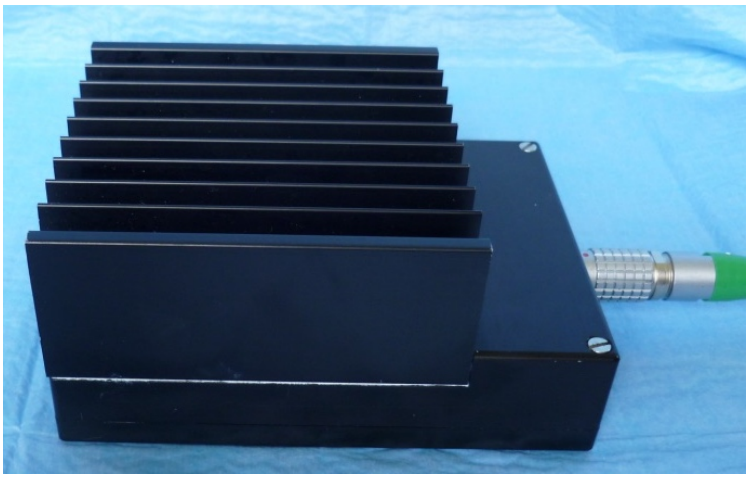


Figure 12: cooling block, showing cooling-fins on upper surface

4.2.3 Measurement of time-points during burn-creation experiments

The duration of contact-time during burn-creation was measured with an athletic interval timer set to “beep” at intervals of which the intended contact time(s) were all multiples. The same timer was used for all burn-creation experiments. The interval

between burn-creation and commencement of cooling, and the duration of cooling itself was measured with a standard stopwatch.

4.3 Ethical approval of the study and patient recruitment

4.3.1 Ethical approval

Ethical approval was obtained from the South Central (Berkshire) Regional Ethics Committee (REC) and from the Buckinghamshire Healthcare NHS Trust Research and Development department to recruit patients into the study. The Study was sponsored by the University of Oxford via the Clinical Trials Research Governance department. Initial approval was granted for the recruitment of patients undergoing DIEP flap reconstructions of a single breast, as a delayed procedure. Subsequent substantial amendments were made to allow the recruitment of patients undergoing bilateral and immediate breast reconstructions, and for the use of the cooling device once it had been fully developed.

All patient information sheets, consent forms and elements of the study were approved by the REC (approval number 13/SC/0518). The letters of approval from the REC and the information sheet and consent form can be found in 11 Appendices 1-5.

4.3.2 Patient recruitment

Suitable patients were identified and a patient information leaflet was sent to them before their preoperative assessment. The researcher only approached patients to discuss participation in the study after an interest in doing so had been established by the consultant in charge of their surgical care. Patients signed the consent form at least 24 hours before their surgery, having had several days in which to read the patient information leaflet at their leisure, and any questions answered.

4.4 Burn creation and cooling

Consenting patients were anaesthetised as normal, with steroids, antihistamines and NSAIDS withheld until all samples had been harvested, as stated above. Once the patient had been anaesthetised and airway was secured with a cuffed endotracheal tube, the patient could be judged not to be at risk of any discomfort from the burn creation.

4.4.1 Burn creation

The template was used to mark out the control areas and burns on each triangular area of skin that was to form the basis of the model, as shown in Figure 8. The unheated burn creation device was then used to press onto each control area with the same pressure as wound subsequently be used for burn-creation. The burn creation device was then switched on, and allowed to equilibrate at 70˚C, selected on the basis of previous work that had found that this temperature would produce a thermal injury, but not so rapidly as to be difficult to modulate its effects or use safely. The heated probe was then applied for 5, 7.5, 10, 15, 30, or 60 seconds with a consistent pressure. The use of the burn-creation device and template are shown in Figure 13.

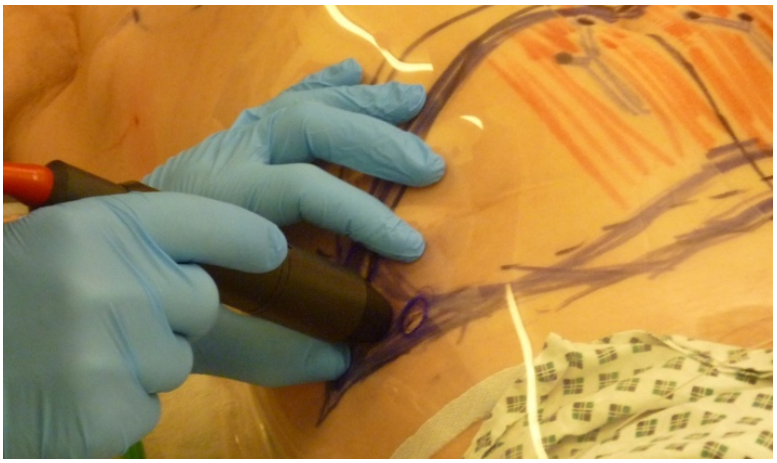


Figure 13: The safe creation of a burn using the hand-piece and the silicone template

Initially, the full range of application-times was used across several different individuals with the aim of establishing, for this particular piece of apparatus, what duration of contact would produce a reliable mid-dermal injury that would be most likely to show significant benefit from cooling.

Once the duration of contact that created a predictable, mid-dermal thermal injury had been established, that duration was adopted for all future experiments in all individuals, and cooling was administered.

4.4.2 Cooling

The cooling device was set to 16˚C, as this had previously been found to be the optimal temperature for first aid[19]. Optilube®- a sterile, water-based lubricating jelly- was used as the thermal coupling agent to ensure good contact with the skin and consistent cooling. The device was placed over one entire set of burned and control areas of skin, applied with only the force of its own weight, and kept in place for 20 minutes, as per the best evidence available for first aid[18], as shown in Figure 14. Once the cooling was completed, and the anaesthetist had completed their interventions, the patient was transferred to the operating table, and the surgery commenced as normal.

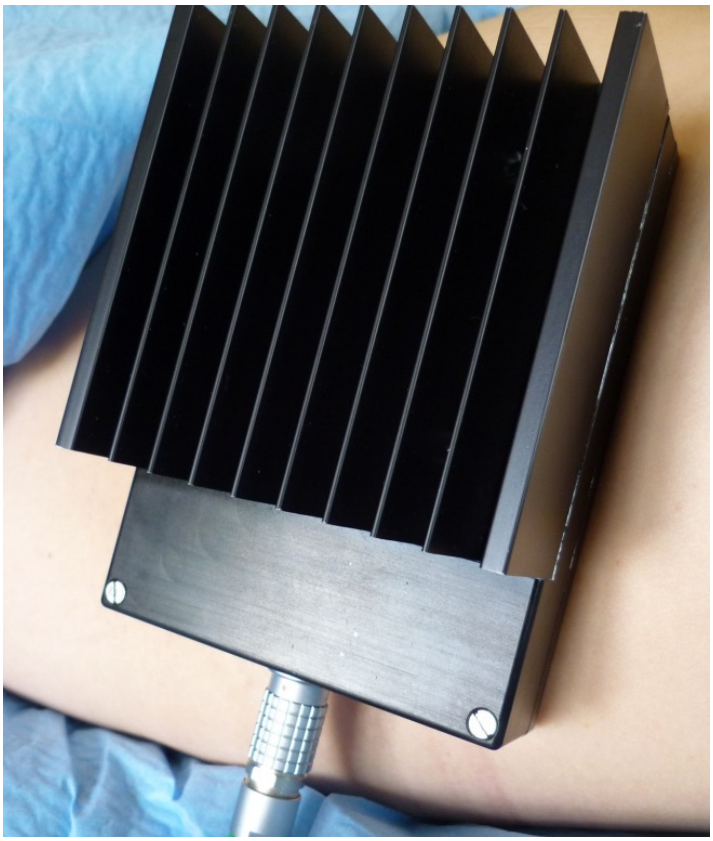


Figure 14: application of the cooling device to one side of the burn model

4.5 Harvest, processing and storage of samples

In the initial calibration phase of the study, all burns were harvested at 3 hours with a 12mm diameter biopsy punch (Schuco,) as shown in Figure 15. When that phase was completed, complete sets of cooled and untreated burns and their respective control areas- 4 samples in total) were harvested at 1, 2, or 3 hours after burning. To allow a respective control sample for each burn, the template was modified to have 3 central control areas to match the 3 peripheral burn areas.

Each sample was hemisected across its equator with a fresh scalpel. One half had the subcutaneous fat excised from its deep surface, as shown in Figure 16, and was placed into a labelled Cryovial and immediately frozen in liquid nitrogen to preserve RNA species from degradation by the skin's RNAse. The other half was left with the subcutaneous fat attached as an orientation marker and was placed in a cassette and

fixed in pathology-grade 10% formalin, and subsequently embedded in paraffin using an automated tissue processor on an overnight cycle.

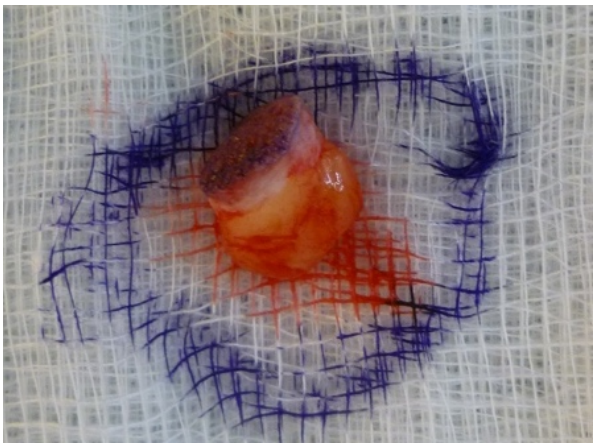


Figure 15: harvested skin sample

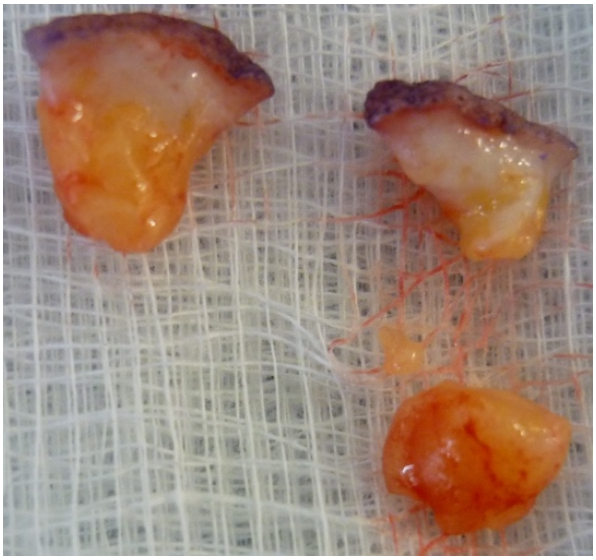


Figure 16: hemisected skin specimen, the left half will undergo FFPE, and the right half has been defatted and will be snap-frozen

4.6 Histological analysis of samples

4.6.1 Sectioning of skin samples

Formalin-fixed paraffin-embedded (FFPE) skin samples were sectioned as follows using a Leica microtome:

Each semi-circular skin sample was embedded in a block of paraffin, with the epidermal surface perpendicular to the face of the block, and the straight edge facing the face to be cut

The block was “faced” to fully expose the specimen for sectioning

The block was placed cut face down-most in a shallow tray containing “Cellsoft” (CellPath, EAA-1500-25A)- a proprietary solution that facilitates the cutting of hard or tough tissues such as skin, nail, or bone- for 30 minutes

The block was rinsed and placed face-down onto a cold-plate at 0˚C for 30 minutes

The block was mounted onto the microtome, and cut at 4μm sections. Ribbons of consecutive sections which were floated on the surface of a warm water-bath (37˚C) to allow them to flatten and be inspected for macroscopic damage, and then mounted on charged glass microscope slides and incubated overnight at 37˚C to ensure adhesion

4.6.2 De-waxing and rehydration of sections

Prior to staining, sections were de-waxed and rehydrated in racks through reagent troughs as follows:

5 minutes in each of 2 troughs containing Histoclear® (National Diagnostics, HS200)- a xylene-free solvent derived from oranges for the de-waxing and dehydration of sections

5 minutes in each of 2 troughs containing 100% industrial methylated spirit (IMS) to remove the Histoclear®

5 minutes in 75% IMS

5 minutes in 50% IMS

5 minutes in running tap-water

After these rehydration steps, the sections were ready for staining.

4.7 Staining of sections

4.7.1 Masson's trichrome stain

Masson's Trichrome stain (Sigma-Aldrich) was used to stain sections of burned and normal skin in the initial phase of the study, as it stains epidermal keratin red, dermal collagen blue, and also stains occluded dermal vessels red, contrasting with the surrounding blue collagen, and is well-published in burns literature[2,63,75,76]. The method used was a modification of the Sigma-Aldrich protocol and was as follows:

Mourdant in Bouin's solution for 15 minutes at room temperature (RT) to reduce subsequent leaching of the stain from sections

Rinse in running tap water until yellow tinge is gone

Rinse in deionised water

Dip in Gill's Number 3 haematoxylin solution for 10 seconds

Rinsed in running tap water for 5 minutes, then in deionised water

Incubated at RT for 5 minutes in Biebrich Acid-Fuschin, and then rinsed with deionised water

Incubated in 50:50 phosphotungstic-phosphomolybdic acid solution

Incubated at RT in Aniline blue stain for 5 minutes

Incubated for 2 minutes in 1% acetic acid at RT

Rinsed in running tap water

Either air-dried overnight or dehydrated through an identical sequence of reagents to dewaxing and rehydration, but in reverse order

Mounted under cover-slips with DPX mounting media (Sigma-Aldrich)

4.8 Immunohistochemistry

Sections undergoing immunohistochemical analysis were dewaxed and rehydrated as normal, and then underwent heat-induced antigen retrieval as dictated by the antibody and antigen using the Dako Autostainer 48 system and proprietary reagents, or manual staining if requiring less than one minute or more than 3 hours of incubation, low temperature, or if using very expensive, scarce antibodies.

The protocol followed is as set out in Figure 17.

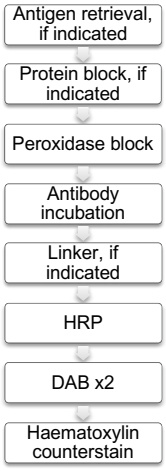


Figure 17: sequence followed in manual or automated immunohistochemical staining

Antibody concentrations, incubation times, and choice of blocking agents, visualisation, and amplification systems were optimised for individual antibodies and the tissue to minimise background staining, starting from the data sheets supplied with the antibody. A summary of the protocols is set out in Table 4. Antigen retrieval was performed using the Dako PT link automated device and either the Dako high or low pH target-retrieval solution (Dako 1699, or 1700) and 20 minutes at 97˚C.

Antibody	Target retrieval	Dako protein block used	Incubation time	Visualisation
BCl2 (Dako M0887) MM	High pH	Yes	20 minutes	DAB
C4a (Abcam ab172730)† RM	Low pH	Yes	20 minutes	DAB
C5b-9 (Abcam ab55811)† RP	Low pH	Yes	20 minutes	DAB
CD31 (Dako M0823) MM	High pH	No	30 minutes	DAB
CD61 (Dako M0753) MM	Low pH	No	30 minutes	DAB
CD68 (Dako M0876) MM	High pH	No	20 minutes	DAB
Fibrinogen (Dako F0111)† RP	Low pH	Yes	5 minutes	DAB
HSP90 alpha (Abcam ab79849) † MM	Low pH	Yes	30 minutes	DAB
HSPA6 (Sigma HPA028549) RP	Low pH	No	1 hour	Linker/ DAB
KRT82 (Sigma SAB1301581) RP	Low pH	No	1 hour	Linker/ DAB

Antibody	Target retrieval	Dako protein block used	Incubation time	Visualisation
Mast cell tryptase (Dako M7052)† MM	Low pH	Yes	5 minutes	DAB
Neutrophil elastase (Dako M0752) MM	Nil	No	30 minutes	DAB
TCHH (Abcam ab58755)† MM	Low pH	Yes	12 hrs 4˚C	Linker/ DAB

Table 4: experimental protocols for immunohistochemical staining of specimens, manufacturer of antibody in parentheses, † indicates Dako background-reducing antibody diluent used, MM- mouse monoclonal, MP- mouse polyclonal, RM-rabbit monoclonal, RP- rabbit polyclonal

Slides were examined with standard light microscopy, and photographed with an Olympus BX51 microscope with a DP70 camera.

4.9 Measurement of burn-depth

Masson's trichrome-stained sections were examined with the microscope, using an eyepiece reticule to measure the proportion of the dermal thickness showing vascular occlusion at 1mm intervals across the section, as shown in Figure 18, and will be referred to as "standardised burn depth" henceforth.

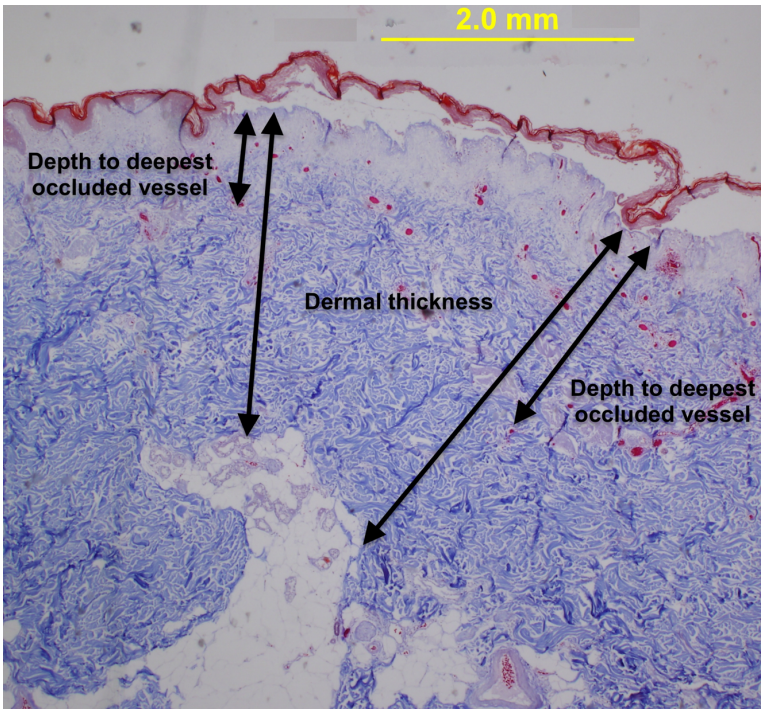


Figure 18: section of burn, Masson's Trichrome stain, occluded vessels and epidermis staining red, dermal collagen staining blue

"Standardised burn depth" was calculated as shown in Equation 1:

Equation 1: calculation of Standardised Burn Depth

$$\frac{\text{Distance to deepest occluded dermal vessel}}{\text{Dermal thickness at that point}} \times 100$$

These measurements were averaged across the entire sample at 1mm intervals, allowing for the variability in dermal thickness within and between samples within the same individual. Comparisons were made to determine the following:

The relationship between standardised burn-depth and contact-time between and within individuals

The effect of cooling on standardised burn-depth within individuals

The time-course of burn progression from 1-2, 1-3, and 2-3 hour time-points post injury, and the effects of cooling on burn progression

Analysis was performed with Prism 7 software, and differences were tested for with 1-way Anova testing for unpaired data and paired t-testing for paired data within the same individual. Significance was taken as $p<0.05$.

4.10 RNA extraction and purification

4.10.1 RNA extraction protocol

The extraction of the RNA followed the steps of homogenisation, lysis, partitioning and precipitation.

4.10.1.1 Sample homogenisation

All burn and control samples were stored in Cryovials in liquid nitrogen prior to processing. When required, they were removed and placed on dry ice to prevent thawing. Each Cryovial was weighed and the mass of the vial and tissue recorded.

All metallic apparatus that would be in contact with the specimens- Biopulveisers, homogeniser heads, spatulas- were stripped down and cleaned thoroughly with RNAzap and rinsed thoroughly before being individually wrapped in aluminium foil and baked at 180° centigrade Celcius for 4 hours to eliminate all RNase activity. Apparatus was cleaned in this manner between each contact with specimens to eliminate carry-over between samples. All plastic items- Falcon and Eppendorf tubes, pipette tips, and pipettes- were from freshly-opened containers and certified nuclease and pyrogen-free. All reagents were drawn from freshly-opened containers, and certified nuclease and pyrogen-free.

A cleaned Biopulveriser was chilled in liquid nitrogen until bubbling of the liquid nitrogen stopped, indicating that the Biopulveriser had equilibrated with the liquid nitrogen. One sample of skin was then placed in the Biopulveriser chamber and the pestle part inserted. The hammer supplied with the Biopulveriser was then used to deliver a series of blows to the pestle, that was rotated between each blow. The contents were then carefully scraped out of the mortar part of the Buopulveriser into a

50ml Falcon tube buried in dry ice using a chilled, RNase-free metal spatula. The empty Cryovial and its cap were then weighed to determine the sample mass.

4.10.1.2 Lysis of the homogenate

The 50ml Falcon tube was then transferred to an ice bucket and 2ml of Trizol was added to the crushed tissue. A Turax homogeniser was then used at maximum setting to homogenise the tissue, using 5-second pulses, and while the Falcon tube was embedded in the ice to prevent heating of the RNA. As many pulses were used to fully homogenise the skin, leaving no visible larger fragments in the bottom of the tube. The Falcon tube and its homogenised contents were then left at room temperature for 15 minutes.

4.10.1.3 Partitioning of the homogenate

The homogenate was then transferred in 1ml aliquots to 1.5ml nuclease-free Eppendorf tubes, and 0.2ml of chloroform was added to each. The contents of each Eppendorf were thoroughly mixed by vortexing and allowed to stand for 10 minutes at room temperature, before being centrifuged at 21000g for 15 minutes at 4°C.

4.10.1.4 RNA precipitation

The upper, RNA-containing fraction was then transferred to a fresh 1.5ml Eppendorf tube, and 0.5ml of Isopropanol added, mixed by vortexing, and then allowed to stand at room temperature for 5 minutes. The Eppendorf was then centrifuged at 21000g for 10 minutes at 4°C, and the supernatant removed from the precipitated RNA pellet, that was then washed with 1ml of 75% ethanol, and then centrifuged at 21000g for 5 minutes at 4°C. The ethanol was then removed, and the pellet allowed to air-dry for 10 minutes.

The RNA pellet was then either stored at -80°C or resuspended in 50μl of DEPC-treated water for further purification and quantification steps.

4.10.2 RNA purification

4.10.2.1 Removal of contaminating genomic DNA

Before the RNA samples could be submitted for library preparation for RNAseq, contaminating genomic DNA had be removed. On the recommendations of the institution performing the RNAseq on our behalf, we elected to use the Turbo DNA-free kit by Ambion©. This comprises purified Turbo DNase, 10x DNase buffer solution, and an inactivation agent to inactivate the DNase and chelate the divalent cations in the DNase buffer, and is certified RNase-free. The protocol supplied with the kit for its use is as follows:

Add 0.1 volumes of 10x DNase buffer to the RNA solution, and 1μl of DNase

Incubate at 20-30 minutes at 37°C

Add 0.1 volumes of the inactivation agent

Incubate at room temperature for 5 minutes

Centrifuge at 10000G for 90 seconds and remove the RNA solution from the inactivation agent- DNAse- buffer precipitate at the bottom of the tube

We found that the small starting volume of 50μl of RNA solution, and hence the small final volume of the reaction mixture meant that it was necessary to leave a significant proportion of the supernatant from step 5 behind to avoid contamination with the inactivation agent- DNase- DNase buffer precipitate. Even minor contamination of the RNA with divalent cations from the DNase buffer results in non-specific RNA cleavage in heating, necessary in later parts of library preparation.

Instead, following the protocol for the Turbo DNAse protocol, we substituted the addition of 0.5M EDTA solution to a final concentration of 15mMol EDTA at step 3, and then heating to 70°C for 10 minutes to inactivate the DNase. The EDTA was necessary to chelate the divalent cations in the DNase buffer and prevent them from causing non-specific RNA degradation on subsequent heating.

The resultant mixture of RNA, denatured DNase, and EDTA-DNase buffer was then run through a Ribominus concentration module. This is a system consisting of:

A silicate binding column that binds RNA, including <200nt

A binding buffer

A wash buffer, requiring the addition 6ml of 100% ethanol

The protocol supplied with the Ribominus columns for its use is as follows:

Mix the RNA solution with 1 volume of Binding buffer and 3 volumes of 100% ethanol to give a final ethanol concentration of 60%, allowing binding of the RNA <200nt to the silicate column

Load the mixture into the column, and place the column in a supplied collection tube

Centrifuge at room temperature for 1 minute at 12,000G

Discard the run-off from the collection tube

Wash the column with 200μl Wash buffer, made up with 6ml of 100% ethanol

Centrifuge at room temperature for 1 minute at 12,000G

Transfer the column to a fresh collection tube

Centrifuge at room temperature for 3 minutes at maximum speed to remove all Wash buffer, and to dry the column of any ethanol

Transfer the column to a fresh collection tube

Add 30μl of DEPC-treated water and incubate at room temperature for 1 minute

Centrifuge at room temperature for 1 minute at maximum speed

The RNA solution in the collection tube can then be used for down-stream analysis

4.10.3 RNA quality-control and quantification

The concentration of the RNA was determined using the Nanodrop 6000 spectrophotometer, and the Qbit spectrophotometer, the latter having the advantage of being less susceptible to erroneous readings in the presence of contaminants such as phenol, which is present in the RNA extraction protocol being used. The quality of the RNA, measured as a function of its level of degradation was measured initially using the Agilent Bioanalyser, and subsequently using the Agilent Tapestation. These returned a reading of 0-10 based upon the relative areas of the 28 and 18 subunits of the ribosome and the total RNA of the electrophrenogram. The greater the proportion of the electrophrenogram accounted for by the ribosomal RNA peaks, the higher the Ribosomal Integrity Number (RIN) returned by the Agilent 2100 Bioanalyser, or the RIN equivalent (RINe) returned by the Agilent Tapestation.

The Bioanalyser is a bench-top unit with an attached computer that uses a plastic “chip” consisting of 16 wells that are interconnected by system of channels linking to an optical chamber in the centre of the chip. The wells are loaded with a gel-dye mix that is then pressurised through the channels to create an electrical circuit. The RNA samples, and a ladder of RNA fragments of pre-determined size are loaded into the wells and mixed by vortexing. The chip is then loaded into the Bioanalyser and a series of electrodes lower into the wells in the chip. Sequential electrophoresis of the ladder and then each of the 12 sample wells, through the optical chamber at the centre of the

chip takes place, and the electrophrenogram of the ladder is used to calculate the RIN of each of the samples.

The Tapestation is the technical successor to the Bioanalyser. It consists of a bench-top unit and laptop computer, and uses “Screentape”- a ready-to-use plastic strip of 16 gel-filled chambers to carry out electrophoresis of the RNA. There is an RNA ladder, as with the Bioanalyser, and a buffer that is mixed with the RNA ladder and RNA samples: 1μl RNA or RNA ladder, 5μl buffer. The Tapestation automatically loads the samples from the 0.5ml tubes into the Screentape and carries out the electrophoresis. The RNA ladder is not essential to the calculation the RINe.

Although the Bioanalyser was used at the start, the Tapestation was adopted later on for the following reasons

Less wasteful

Tapestation uses the Screentape chambers in multiples of 2, and the remaining chambers remain usable for 2 weeks after this point

Superior reliability

Bioanalyser relies upon a “priming station” to pressurise the gel through the channels in the chip, and this in turn relies upon the seal in the syringe plunger and O-ring of the syringe. Any defect in these, and the chip will not establish an electrical circuit for electrophoresis. Failure of the RNA ladder electrophoresis at the very start nullifies the rest of the assay. While the user’s manual for the 2100 Bioanalyser states that the syringe and O-ring need replacement after 25 uses, the experience was that they failed more frequently than this, with subsequent wastage of samples and other reagents. There were no such instances of gels failing to run with Tapestation

Reproducibility

The Bioanalyser could return significantly variable RIN values for the same sample in the same run, while Tapestation was more consistent.

The importance of obtaining reliable, consistent results in the optimisation of the RNA extraction and purification protocol made Tapestation by far the better option.

4.11 Avoiding RNA degradation

Once quality control had been optimised- see 4.10.3- we could assess the effectiveness of the DNase treatment of the RNA samples, in particular for any RNA degradation, as reflected in the RINe value.

Our first Turbo DNase kit, used as set out in the protocol, caused very significant degradation of the RNA, as reflected by a very significant fall in RINe value.

All reagents- 0.5M EDTA solution, DEPC-treated water, 100% ethanol- were changed, and new, sealed boxes of pipette tips and Eppendorf tubes opened, and RNA extracted from different samples were used with similar results.

The RNA degradation persisted.

Having eliminated RNase-contamination from the reagents, pipette tips, and Eppendorf tubes, we ordered a new Turbo DNase kit. We used it in line with the same protocol as before, and had the same problems with RNA degradation.

The next step was to test each component of the process individually as a possible cause of the degradation. The RNA degradation, as reflected by falling RINe could be being caused by:

The Turbo DNase causing collateral damage to the RNA

The DNase buffer causing RNA degradation

The Ribominus Concentration module, either degrading the RNA, or removing the Ribosomal RNA peaks, and hence reducing the RINe value for the sample

The heating of RNA samples to 72°C for 2 minutes necessary as part of the preparation of samples for the Tapestation

While it was unlikely that proprietary RNA-specific kits would have such a detrimental effect upon RNA, the likely sources of exogenous RNase-contamination had been eliminated. It was necessary to circumvent the RNA degradation because the RNAseq analysis of the samples required:

Elimination of DNA contamination prior to library preparation

Library preparation from the RNA samples would be in the presence of buffers containing divalent cations

Library preparation for RNAseq and qPCR would require heating of the RNA without degradation

The problem of RNA degradation was solved through the sequence of experiments set out in Figure 19.

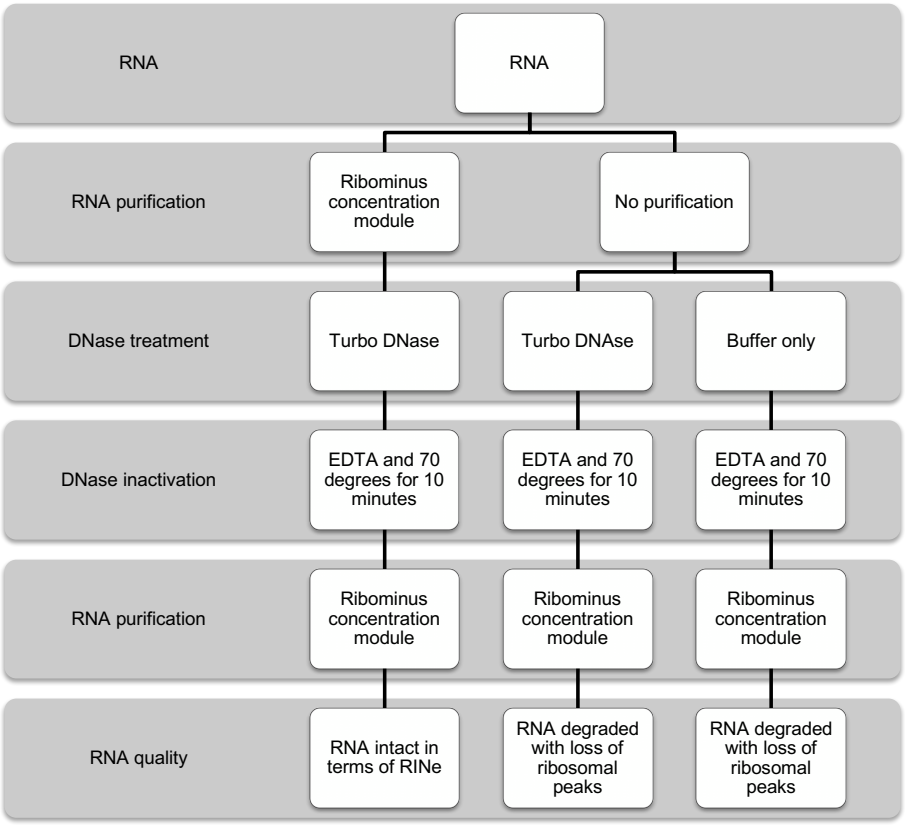


Figure 19: optimisation of RNA purification without degradation

4.12 Sequencing of the RNA

4.12.1 Preparation of cDNA libraries for sequencing

Using the left-hand sequence in the Figure 19 algorithm, the RNA was prepared and purified for sequencing. Five patients each giving 4 samples, one from each condition (cooled and untreated burns and controls), had 2µg of RNA extracted from each sample and submitted to the Wellcome Trust Centre of Human Genetics, Oxford.

Ribodepletion to remove ribosomal RNA and library preparation and the sequencing itself was performed at the WTCHG, and cDNA libraries were prepared for sequencing using the HiSeq4000 platform. Each library was run through 4 lanes giving 4 technical replicates of each library, 100bp paired end reads, with an expectation of generating 50 million reads per sample.

4.12.2 Analysis of the mRNA sequencing data

The sequence files were downloaded from the WTCHG onto the Computational Biology Research Group (CBRG) servers at the Weatherall Institute of Molecular Medicine who were involved throughout the analysis of the data.

First, the data was mapped to the Human Genome using Spliced Transcripts Alignment to a Reference (STAR) software. The resultant Fastq files were then converted to Binary Alignment Map (BAM) format, and then to BigWig format. BigWig files were then uploaded to the UCSC Genome browser to visualise how the transcripts map to the intron/exon boundaries to give an indication of the quality of the sequencing and the level of genomic DNA contamination. Sequence Alignment Map (SAM) files were also created and the featureCounts function was used to count how many transcripts mapped to each gene using EdgeR. EdgeR was used to create a

DGEList of the data and plot the biological coefficients of variability (BCVs) of each of the 4 technical replicates of each of the 20 libraries to determine if they could be pooled to increase the number of reads per sample. Having passed this test, the 80 files were merged to 20 files, and compared using the generalised linear model (GLM) function to examine the effects of the factors “burning” on the transcriptome of normal skin, and the effect of the factor “cooling” specifically on the transcriptomic changes caused by burning, with adjustment for multiple testing on the p-value for each gene giving the False Discovery Rate (FDR) for each test, and the fold-change for each gene induced by the factor(s) being tested. Analysis was carried out as per the “EdgeR” manual from “Bioconductor”. Significant differences were analysed with “Metacore” for pathway analysis, and with EdgeR to plot the significantly altered genes as a heatmap using hierarchical gene clustering.

4.13 Validation with quantitative polymerase chain reaction (qPCR)

4.13.1 cDNA library preparation

Samples of RNA left over from the five subjects sent for sequencing, and biological replicate samples extracted from a further 5 different subjects, using the same extraction, purification, and quantification protocols were then prepared for qPCR, taking equal amounts of each RNA sample used for each reverse transcriptase (RT) reaction using the Thermo Fischer High Capacity cDNA kit to make a 20µl reaction as per their protocol using the recommended thermal cycler program: 10 min at 25˚C, 120 min at 37˚C, 5 min at 85˚C, then hold at 4˚C, giving a 1:1 RNA:DNA ratio.

4.13.2 qPCR analysis of the cDNA libraries

The real-time qPCR was carried out using Sensimix SYBR No-ROX kit. Three housekeeping genes were selected from among accepted housekeeping genes, but

were checked for consistent levels of expression in the RNAseq datasets, and were run in each 384-well qPCR plate across all of the cDNA libraries, with each gene run in triplicate. A robot plating station was used to ensure accurate, consistent allocation of samples to wells.

Intron-spanning primers for genes of interest identified in the RNAseq data were designed using the Roche primer designer, and were tested for amplification against samples of cDNA to be tested to ensure amplification and to check the melt-curve.

All plates were run for 40 cycles with a dissociation cycle at the end to check the melt-curve and for specific primer-binding. The manual threshold function was used to obtain CT values in the exponential phase of amplification, and ensure that non-amplifying traces were not included. The data was exported in Excel format and the mean dCT for each gene relative to each housekeeping gene calculated. Statistical analysis was carried out with Prism 7 software and the 1-way ANOVA test to look for significant differences between levels of gene-expression between burns and controls and the effect of cooling on gene expression, with a view to validate the RNAseq findings.

4.14 Pre-fractionated tandem mass-tagged (TMT) proteomics

4.14.1 Sample preparation

The precipitated protein fractions in the organic layer of the Trizol RNA extraction that had been previously frozen were defrosted on ice. Allowing for approximately 10% of tissue being protein, there was approximately 10mg of precipitated protein in each sample, which represented a huge excess for the purposes.

Resuspension of the sample was achieved as follows:

400µl of methanol to abolish phase separation

add a further 1ml of methanol to precipitate the protein

Centrifuge at full speed for 5 minutes

Remove supernatant

Add 200µl water

Add 200µl chloroform

Add 800µl methanol

Add 600µl water

Centrifuge for 1 minute at full speed

Remove supernatant

Add 1ml of methanol to wash

Spin down and remove methanol

Add 1500µl of 6M urea

Shake on the bead-beater at full speed to break up protein pellet

Add DTT to final concentration of 10mMol to reduce proteins, incubate at RT for 1 hour

Add iodoacetamide to alkylate to a final concentration of 20mMol, incubate at RT 1 hour in dark

Dilute to a final urea concentration of 1M

Add 10µg of trypsin and incubate overnight at 37˚C

Inactivate the trypsin with trifluoroacetic acid (TFA)

The peptides were then desalted with SEP-PAK C18 columns and the vacuum manifold before being quantified with the Pierce quantitative colorimetric Peptide Assay (Thermo Scientific, 23275).

Equal quantities of each peptide were labelled with one of 10 isobaric tags from the TMT 10plex Mass Tag Labelling Kit (Thermo scientific, 90110) with an excess of tag, and equal amounts of peptide from each of the 20 samples were taken to make a 100% and 50% pool of samples to be run in each of the 3 runs as shown in Table 5.

Run	Isobaric TMT 10-plex tags									
	126	127C	127N	128C	128N	129C	129N	130C	130N	131
1	Pool of all 20 samples 100%	10BC	10BNC	10CC	10CNC	11BC	11BNC	11CC	12BC	Pool of all 20 samples 50%
2		11CNC	12BNC		12CC	12CNC	13BC	13BNC		
3		13CC	13CNC		25BNC	25CC	25CC	25BC		

Table 5: allocation of TMT tags to peptides from each sample, and reference pools of peptides from all 20 samples

The allocation of isobaric tags allowed 20 samples to be identified using 10 different tags. The two most abundant samples of peptide were analysed in all three runs to allow direct comparisons between runs, and the pools of all 20 samples at 100% and

50% concentrations served as standards for the mean concentration of each peptide across all 20 samples, and established a dynamic range for quantification.

Each of the 10 samples in each run was then combined to form three pools of 10 different samples, with each individual sample identifiable within the pool by their different isobaric tag. Each of the 3 pools was then desalted as before, and then pre-fractionated into 8 fractions according to hydrophobicity using Pierce High pH reversed-phase peptide pre-fractionation columns as shown in Figure 20.

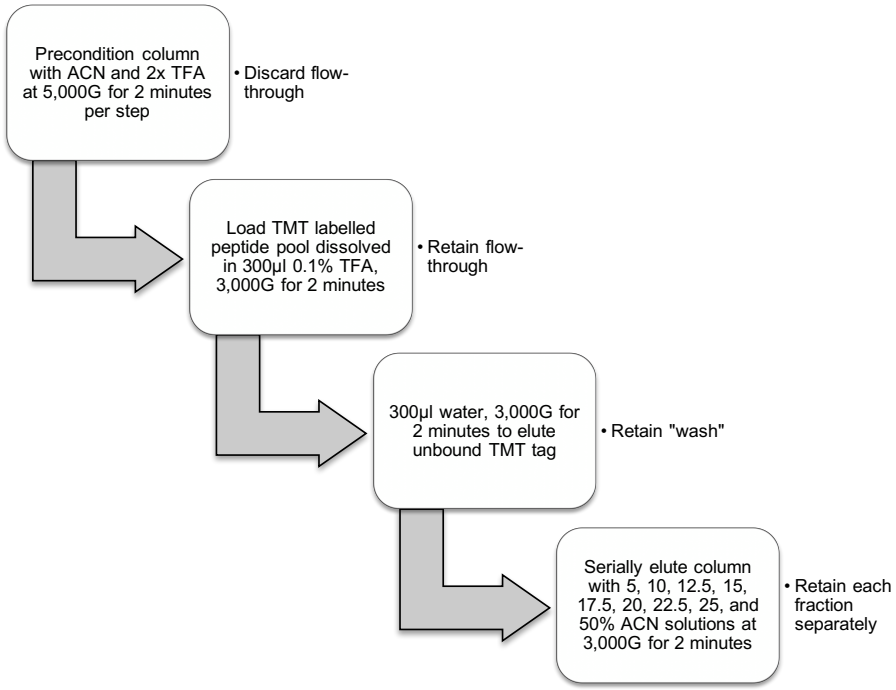


Figure 20: pre-fractionation of peptide samples prior to LC/MS3 analysis

Each of the 24 samples was desalted as described previously, dried in the SpeedVac overnight, and resuspended in 0.1% formic acid prior to LC/MS3 analysis as summarised in Figure 21.

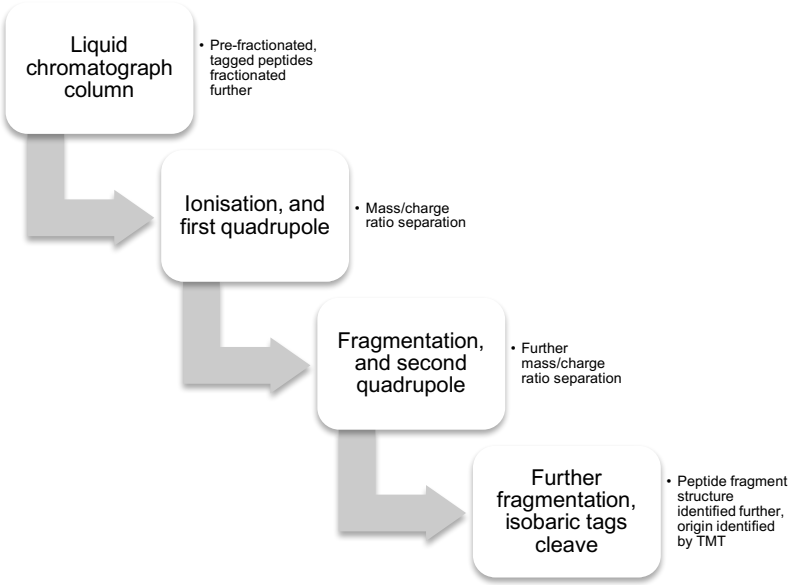


Figure 21: schematic of TMT LCMS3 analysis of peptides

The origin of the fragments was identified by the unique identifying signal from the isobaric tag, and the peptide was matched using “Protein Discoverer” software. The level of each peptide in the 100% and 50% pools was used to give a dynamic range to their abundance, and the abundance of each peptide in each individual sample was calculated as a ratio of the average across all 20 samples in the pooled peptide samples. Statistical analysis was performed with “Perseus” software, and adjusted p-values (FDRs) calculated. Pairwise comparisons were made as shown in Figure 22.

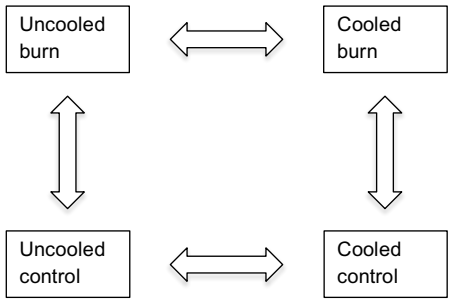


Figure 22: comparisons to be made between the four groups of samples

This series of comparisons allows the effects of greatest interest, namely:

The effects of burning on normal skin

The effects of cooling on normal skin

The effects of cooling on burned skin

Pathway analysis was also performed to identify patterns within the proteome of burns and interactions between pathways using “Metacore®”, an online resource that allows proteomic and transcriptomic data to be uploaded for analysis and extraction of ontological pathways and quantification of the likelihood of a particular pattern of results arising through pure chance.

4.15 Summary of methodology chapter

The literature review highlighted the considerable lack of published experimental work with experimental human burns. As a result, much of the experimental protocol development had to begin from first principles and undergo refinement as initial results from the pilot work became available.

The design of the apparatus for burn creation and cooling was particularly important as the success of the entire project depended upon the safe and consistent burn creation and cooling. Similarly, the quantification of burn severity was adapted from previous published work, but had to be proven under a new set of circumstances.

The adaptation of RNA extraction methods to burned human skin had to overcome the mechanical resilience of skin, its low RNA yield and high levels of RNase activity.

The immunohistochemistry protocols were adapted to the individual characteristics of the antibodies and antigens, particularly the very high background non-specific binding by the anti-Mast cell tryptase and anti-fibrinogen antibodies, requiring modification of

antigen retrieval, protein blockade, reduced antibody concentration, incubation time and DAB exposure to achieve optimal results.

The time and effort expended on this work will allow the analysis and interpretation of the results with confidence.

5 Results Chapter 1: Creation and validation of standardised human burns

5.1 Establishing the relationship between contact-time and standardised burn-depth

In the initial phase of the project, the priority was the establishment of a predictable thermal injury using novel apparatus, and a previously untested skin substrate- human abdominal skin. Burn-depth is contingent upon many variables, including temperature of the heat-source, pressure and duration of contact, volume of underlying tissue, and the thickness of the epidermis and dermis at the point of injury. Burns were created using an identical temperature as set on the control console of the apparatus, and with a consistent pressure as measured by the displacement of the spring in the hand-piece holding the heated copper rod. The anatomical site was symmetrical within individuals, and consistent between individuals- the lower abdomen. All the patients had been selected for an adequacy of excess skin and subcutaneous fat in the lower abdomen, but with a body mass index of <30, the volume of tissue underlying the burn areas could be described as broadly similar between and within individuals. With these variables controlled as far as could be reasonably achieved within the constraints of the model, the remaining variable was duration of contact.

It was established early in the pilot-work that Masson's Trichrome stain could identify occluded vessels within the dermis and subcutaneous fat, depending upon the depth of the burn, in burn samples excised at 3 hours after burning. Drawing on the work done in clinical burns, and at later time-points[2], the depth of the deepest occluded

dermal vessel as a proportion of the dermal depth at that precise point was measured at 1mm intervals across the burn.

5.2 Initial calibration phase

In the initial calibration phase of the study 8 patients were recruited, and had burns of the following durations of contact created bilaterally in the triangles of skin due to be discarded as shown in Table 6:

Patient	Contact-time/ seconds					
	5	7.5	10	15	30	60
1				2	2	2
2				2	2	2
3				2	2	2
4	2		2	2		
5	2	2	2			
6	2	2	2			
7	2	2	2			
Totals	8	6	8	8	6	6

Table 6: contact-time used for burn-creation in each patient

One patient (not included) had technical issues with the harvest of the flap that compromised the model by delaying the collection of the biopsy samples by nearly an

hour, rendering them incompatible with the other data points. The rationale for this will be demonstrated in the next part of this results chapter.

5.2.1 The clinical appearance of burns created with different contact-times

Burns were assessed according to their clinic appearances in terms of colour and consistency of the skin, presence or absence of blistering, blanching to pressure and capillary refill.

5.2.1.1 Burns created with 15, 30 and 60 seconds of contact-time

In the first 3 patients recruited, burns were created at identical pressure of application, and at 70˚C, and with one burn per side created with each of 15, 30 and 60 seconds of contact-time. Burns were harvested 3 hours post-injury. The clinical appearances of all the burns were those of a full-thickness thermal injury, with little by way of blister-formation, white colouring, and a leathery texture on palpation, and on excision. These changes were well-established at 3 hours after creation, as shown in Figure 23 and Figure 24.

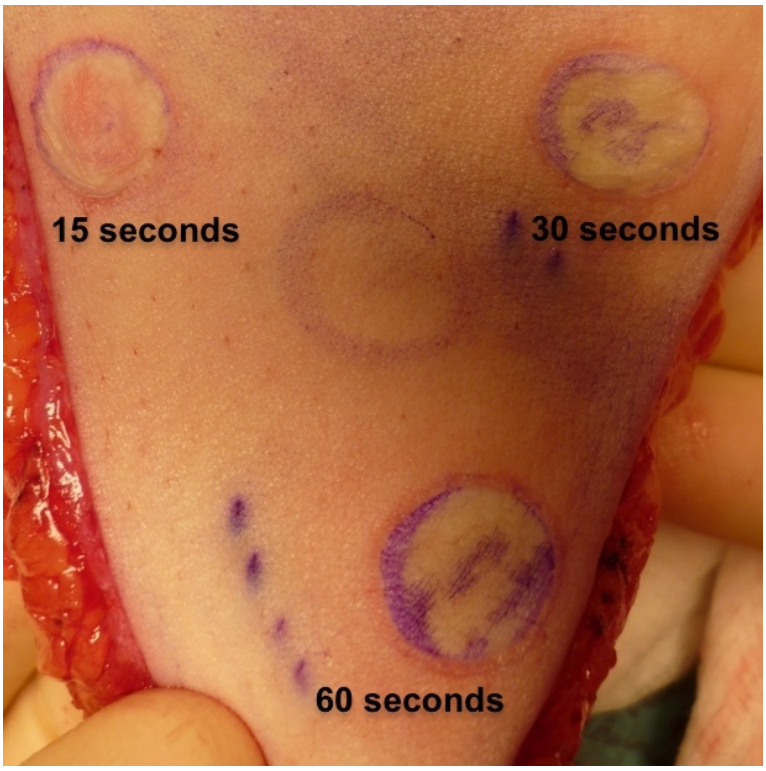


Figure 23: burns created with 15, 30, and 60 seconds of contact-time

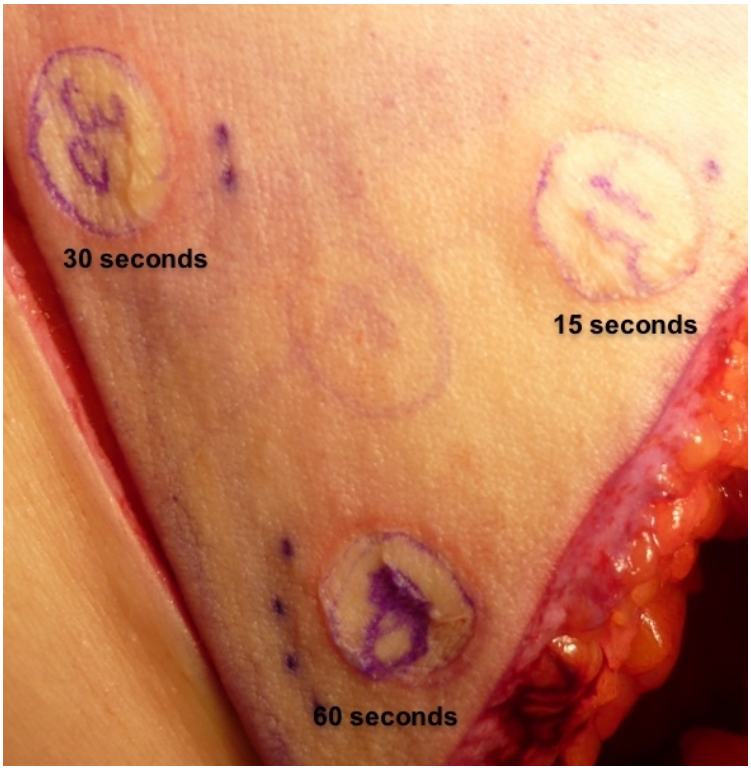


Figure 24: a second set of burns created with 15, 30, and 60 seconds of contact-time

5.2.1.2 Burns created with 5, 10 and 15 seconds of contact-time

The first three patients had provided a total of six biological replicates for each duration of contact, and all had the clinical appearance of full-thickness burns. Hence it was decided to reduce the contact time for the next patient, instead creating burns with 5, 10, and 15 seconds to each side, and again harvesting at 3 hours. The burns created with 5 seconds of contact-time formed large blisters with pale, blanching blister-bases, while those created with 10 seconds of contact-time had a deep, “salmon-red” blister base consistent with a deep-dermal injury, and those created with 15 seconds again displayed all the features of full-thickness burns.

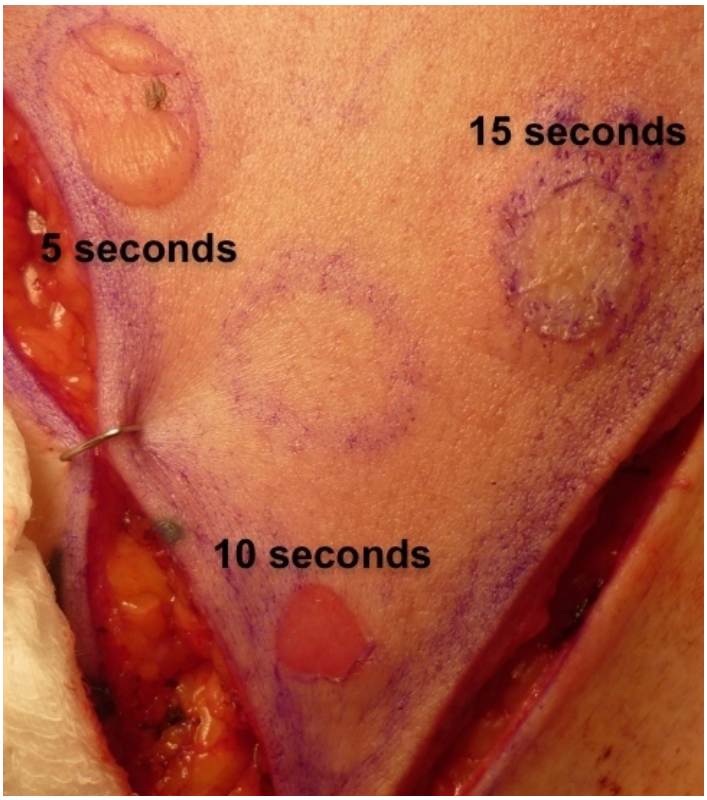


Figure 25: burns created with 5, 10, and 15 seconds of contact time

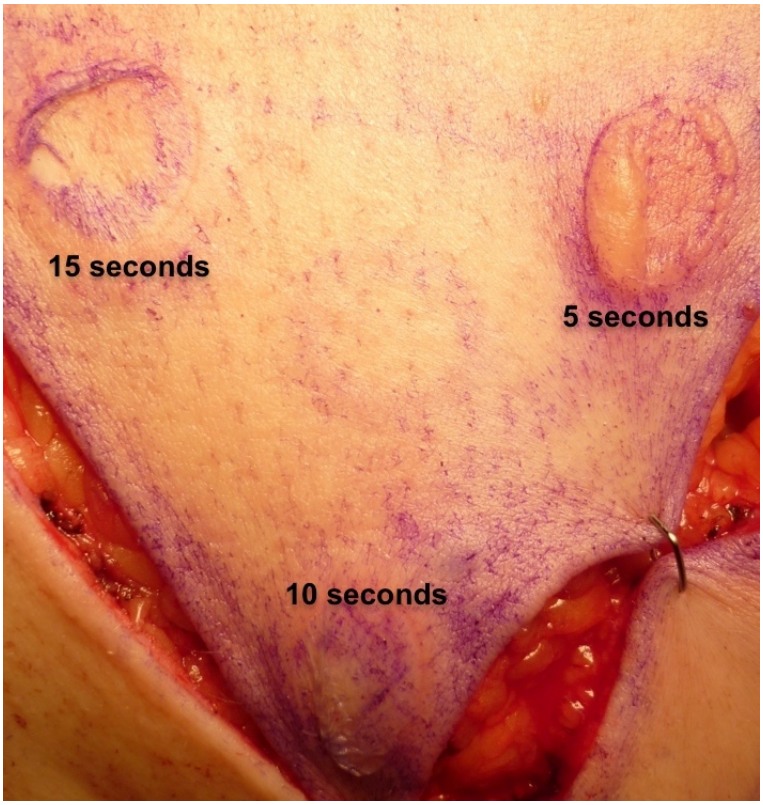


Figure 26: a second set of burns created with 5, 10, and 15 seconds of contact-time

5.2.1.3 Burns created with 5, 7.5 and 10 seconds of contact-time

Having confirmed that 15 seconds of contact-time would produce a consistently full-thickness burn, the focus was shifted to the interval between 5 and 10 seconds of contact time. A further 4 patients were recruited to have burns created with 5, 7.5 and 10 seconds of contact-time to each side, and be harvested at 3 hours post-burning. Again, the burns created with 5 seconds of contact-time produced burns with large, fluid-filled blisters and a pale, blanching blister-base, and those created with 10 seconds of contact-time produced blisters containing very little fluid, although the epidermis did loosen, and when inadvertently removed during the course of the surgery revealed a dark red or white blister-base indicating a deep-dermal or full-thickness burn. The burns created with 7.5 seconds of contact-time produced blisters containing less fluid than those created with 5 seconds of contact-time, and a slightly pinker centre to the blister-base suggestive of a mid-dermal injury.

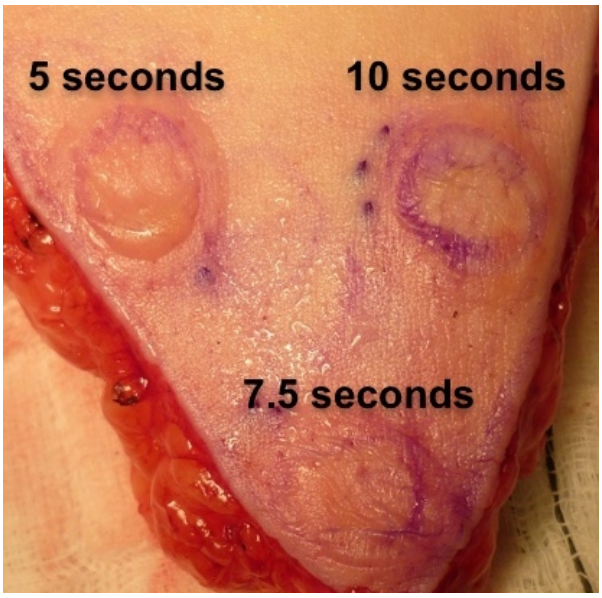


Figure 27: burns created with 5, 7.5 and 10 seconds of contact-time

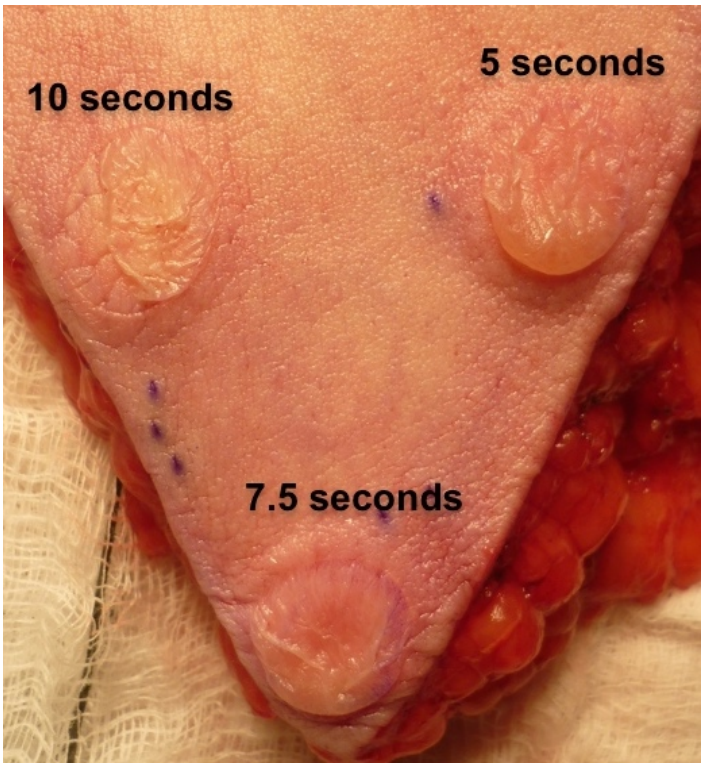


Figure 28: a second set of burns created with 5, 7.5 and 10 seconds of contact-time

The clinical appearance of the burns created with 5-60 seconds showed a clear relationship to contact-time. While it is very difficult to accurately assess very small burns of 15mm diameter, they can be assessed in comparison to other adjacent burns of identical size within the same area of skin, and a graduated response within the individual can be seen. By overlapping the ranges of contact times- 5-10, 5-15, and 15-60 seconds- it is also possible to make indirect comparisons between individuals, and consistent appearances are seen when burns created with 10 and 15 seconds of contact time are compared within the three groupings of contact-times.

Burns created with 5 seconds of contact-time had a consistent appearance of superficial, partial-thickness burns across all individuals in which they were created. The burns all resulted in blisters containing a large amount of fluid. Where these blisters were accidentally de-roofed during surgery, they revealed pale pink dermis consistent with a superficial, partial-thickness burn.

Burns created with 7.5 seconds of contact-time also produced blisters, but with slightly less fluid, and a slightly deeper pink centre to the blister-base, indicating a mid-dermal injury.

Burns created with 10 seconds of contact-time produced very little blistering, and had either a dark red or white, leathery blister-base indicating a deep-dermal or full-thickness injury.

Burns created with ≥15 seconds of contact-time invariably displayed features of full-thickness injury- white, leathery, non-blanching, and without blisters.

There is a significant limitation to the accuracy of assessment and photography of 15mm diameter burns in a surgical setting, as can be seen from the photographs: lighting, distance from the objective and angle of the specimen to the camera all contribute to inconsistencies in the imaging, and variations in skin texture, blood-staining and smearing of surgical marking ink all interfere with image quality. The texture of the skin, and blanching under pressure cannot be appreciated through photography, and cannot be quantified.

5.3 The histological appearances of burns created with 5-60 seconds of contact-time

It was desirable to establish a quantitative method of measuring burn-severity such that burns could be compared within and between individuals. In order to quantify the severity of the burns created, sections of thermally-injured and normal skin were cut and stained, initially with haematoxylin and Eosin, and then with Masson's trichrome stain.

5.3.1 Haematoxylin and eosin stain of normal skin

Figure 29 shows a section of normal abdominal skin from one of the patients recruited into the study. The epidermis is seen to be adherent to the papillary dermis, and it is also possible to see the superficial dermal plexus demarcating the boundary between the reticular and papillary dermis. The epidermal appendages- hair shafts and sweat glands- can be seen, as can the fat invaginating into the dermis around the epidermal appendages.

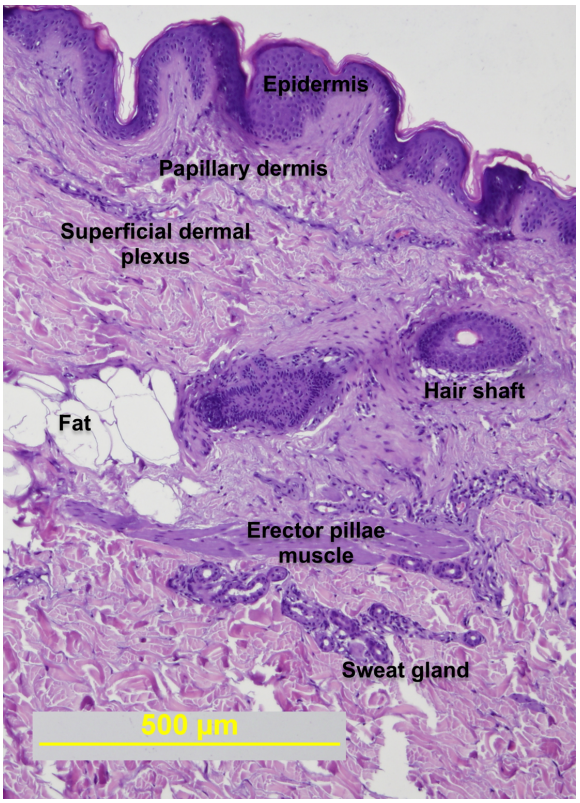


Figure 29: Haematoxylin and eosin stain of normal skin

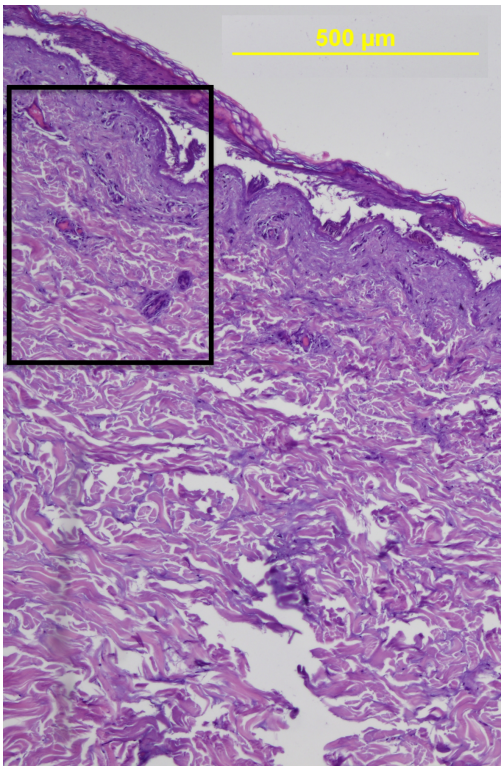


Figure 30: H&E stain of skin 3 hours after creation of a burn with a contact-time of 15 seconds

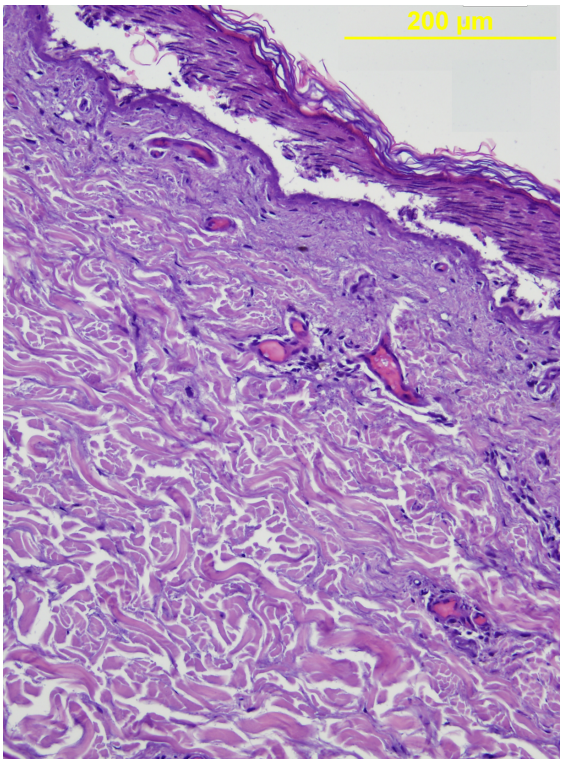


Figure 31: higher magnification of papillary dermis and blistered epidermis from rectangle in Figure 30

The sections shown in Figure 29- Figure 31 demonstrate several of the features by which the burns differ when compared to the normal skin. The epidermis has separated from the papillary dermis, which seem to have flattened when compared to the papillary dermis of normal skin, and the collagen fibres are more indistinct from one another. The nuclei of the epidermal keratinocytes have become elongated when compared to the round nuclei of the epidermal keratinocytes of normal skin. The superficial dermal plexus has become dilated and occluded with erythrocytes when compared to the normal skin in the previous section. These findings are in consistent with the blistering of the epidermis and the fixed staining of the dermis seen in the clinically deeper burns created with this contact-time.

5.3.2 Masson's trichrome staining of normal skin

Masson's trichrome stain has been used frequently in histological staining of burned skin and can distinguish keratin in the epidermis that stains red from collagen in the dermis that stains blue, the epidermal appendages also stain red as demonstrated in Figure 32.

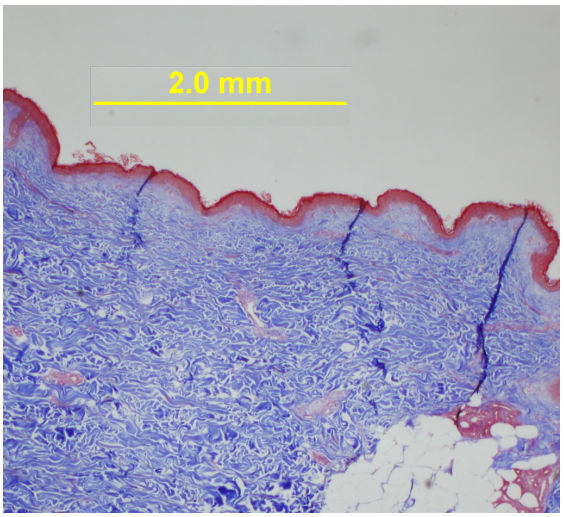


Figure 32: normal skin stained with Masson's trichrome stain

5.3.3 Masson's trichrome staining of burns

It has also been noted that collagen denatured by heat does not take up the blue stain of the aniline blue, and so the underlying red stain of the Fuschin comes through instead[77]. The mechanism for this is uncertain, but may relate to changes in the charge of the collagen fibres preventing the aniline blue stain from binding. This was found only sporadically in two patients in this series, and so was not used as a marker of burn-depth, but Figure 33 has been included below to illustrate the effect. What is interesting about this effect is that the papers originally describing this effect were using a brass burning-block heated to 375˚-400˚F applied for 10-45 seconds depending upon the model used[78]. In our samples, it was reproducibly demonstrated in 2 different patients burned with a 70˚C device for 5, 10, and 30 seconds, but could

not be demonstrated in any other burn samples of similar, or longer durations of contact-time.

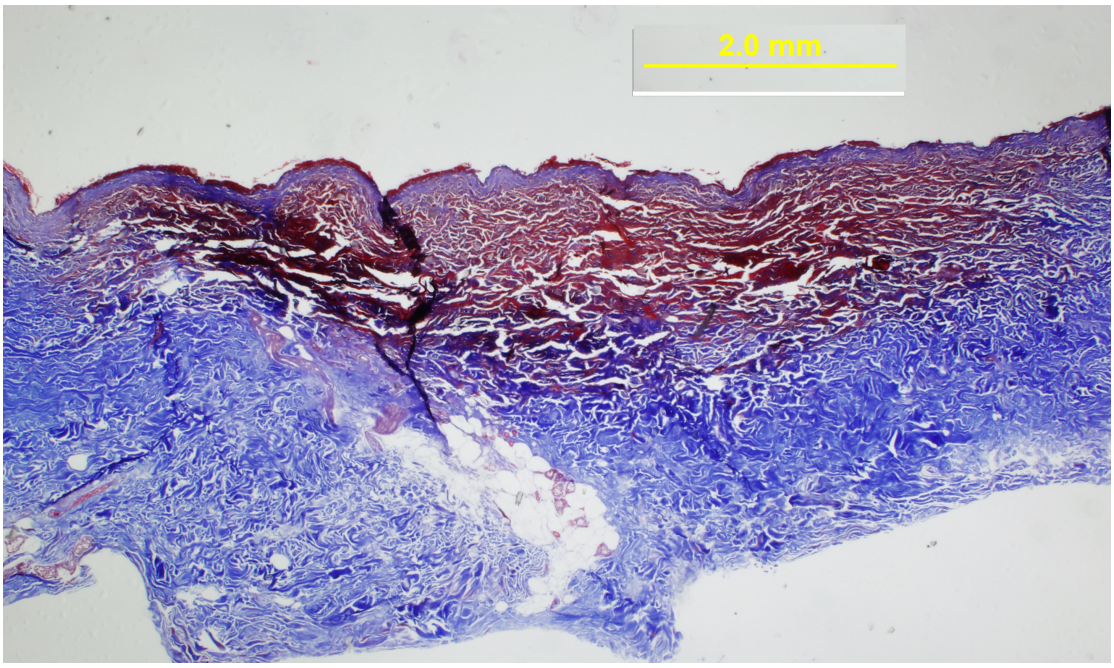


Figure 33: experimental burn created with contact-time of 30 seconds, Masson's trichrome stain

This burn was created with a contact-time of 30 seconds and harvested three hours later. The loss of uptake of the aniline blue stain has a sauceriform distribution across the area of the burn, and can be seen extending to the layer of the mid-dermis.

When the burns are examined under higher magnification other features become apparent. It is possible to see the separation of the epidermis from the dermis in the formation of the blister, and the change in nuclear morphology of the epidermal keratinocytes. It is also possible to visualise the dilation and occlusion of the microvasculature of the dermis. This is more prominent than with haematoxylin and eosin as the red of the occluded vessels contrasts sharply with the blue of dermal collagen.

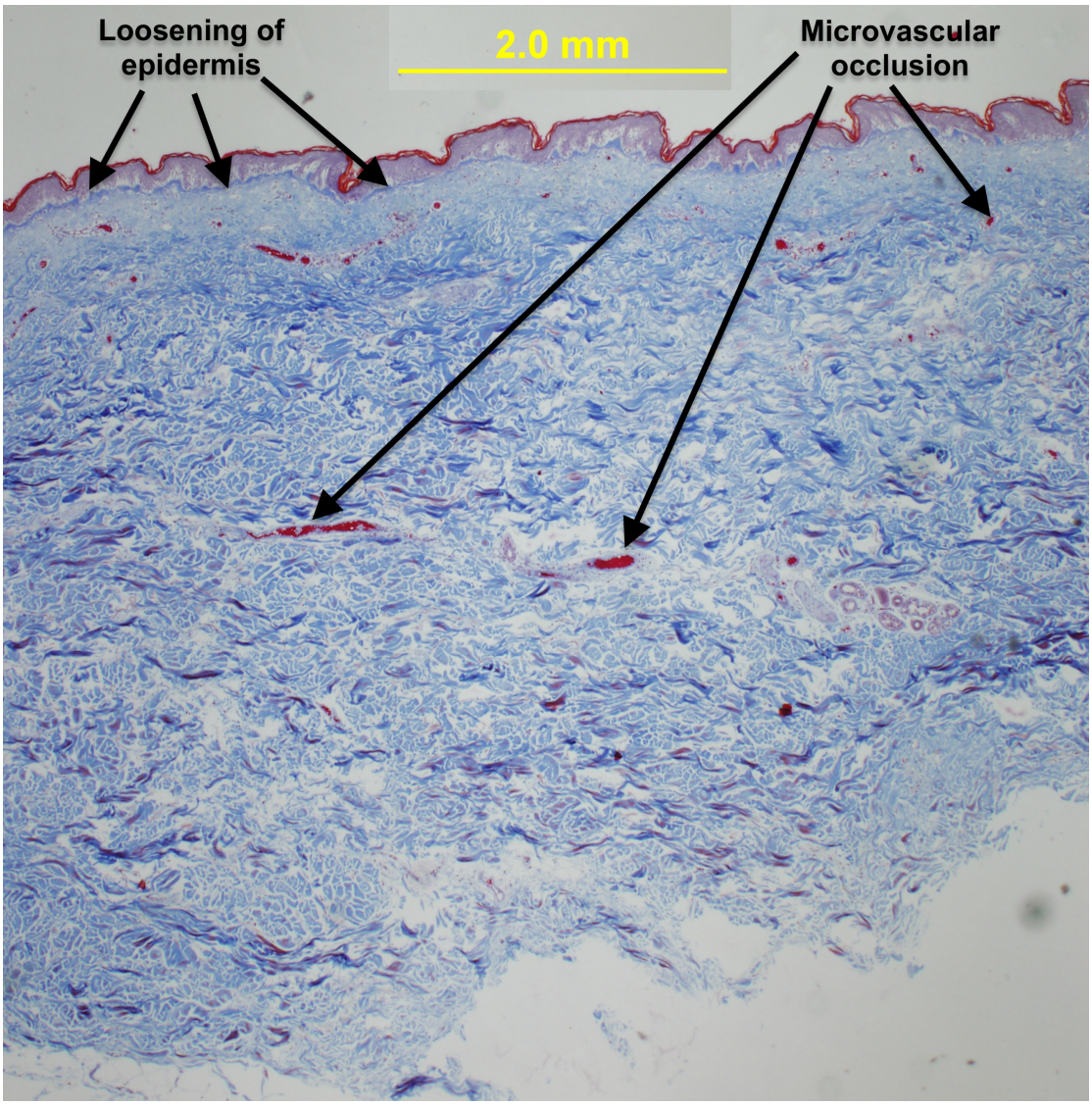


Figure 34: experimental burn created with contact-time of 7.5 seconds, Masson's trichrome stain

The burn shown in Figure 34 was created with 7.5 seconds of contact-time and shows microvascular occlusion to a mid-dermal level, in line with the clinical appearance. It is possible to see the early loosening of the dermo-epidermal junction, and the formation of the blister, although a large blister has not yet formed. The variation in dermal thickness across the area that measures only approximately 5mm across is also seen here, and underlines the importance of assessing the proportion of the dermal depth that has been damaged, rather than just the distance to which the damage extends within the dermis.

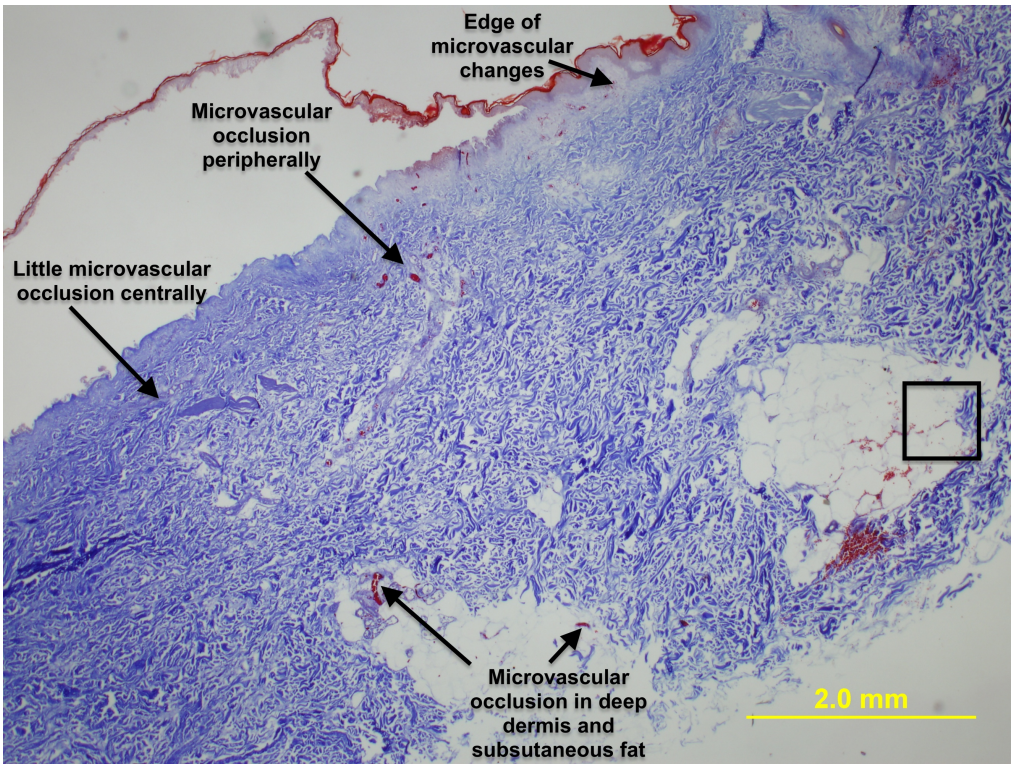


Figure 35: experimental burn created with a contact-time of 60 seconds, indicating distribution of microvascular occlusion and extensive blistering, Masson's trichrome stain

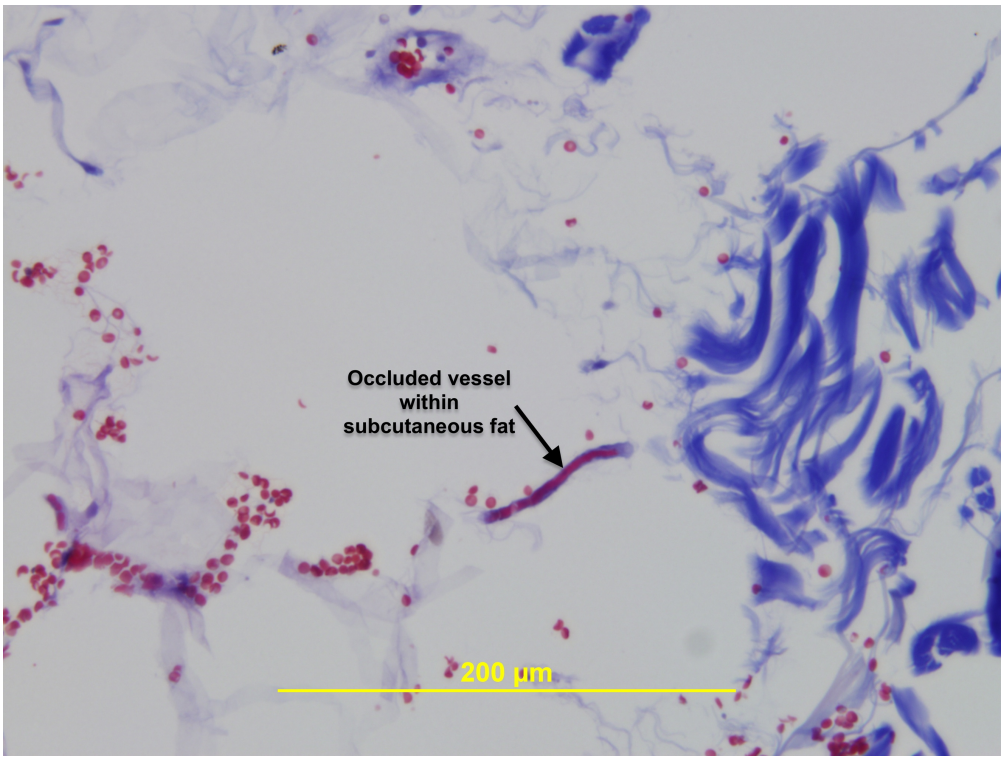


Figure 36: higher magnification of section from Figure 35 showing microvascular occlusion within subcutaneous fat

The experimental burn shown in Figure 35 and Figure 36 was created with 60 seconds of contact-time, and excised at 3 hours after creation. The epidermis can be seen to have blistered away from the dermis, and it is possible to see the occluded microvasculature staining red within the blue dermis. What is interesting is that the vessels in the superficial dermis of the central area of the burn show no staining, while vessels in the deep dermis and subcutaneous fat show occlusion. This correlates to the white, fixed appearance of the burns created with this contact-time. It is also worth noting that the vascular occlusion does not extend far laterally beyond the point at which the epidermis becomes adherent to the dermis.

Our hypothesis is that the pressure of the heated rod pushes the blood out of the dermal microvasculature and as it is applied for 60 seconds, is able to heat the skin to such a temperature that the occlusion with coagulation factors and platelets takes place at the deepest part of the dermis, and in the subcutaneous fat. When the

pressure is released, there is no longer a patent dermal microvasculature, and therefore no clotting factors or platelets can be delivered to the more superficial layers of the dermis, hence its relatively normal histological appearance.

5.4 Quantification of burn-depth

Having examined burns across the spectrum of clinical depth, and durations of contact-time, and seen the variation in depth of microvascular occlusion across the width of the burn, we decided to attempt to quantify the depth of thermal injury as evidenced by the perpendicular depth of microvascular occlusion expressed as a proportion of the dermal thickness at that precise point in the burn. We will refer to this as standardised burn-depth.

5.4.1 Measurement of standardised burn depth

Standardised burn-depth attempts to make allowance for the variations in dermal thickness across a burn biopsy, between different biopsies within the same individuals, and between individuals to make burns directly comparable to one another, and remove subjective judgement from the assessment as much as possible.

It is calculated as shown in the equation below:

$$\frac{\text{Distance to deepest occluded dermal vessel}}{\text{Dermal thickness at that point}} \times 100$$

Repeated measurements were taken across the burn at 1mm intervals and the mean was then calculated for the burn as a whole.

Figure 37 shows the measurement of standardised burn-depth across the width of a burn.

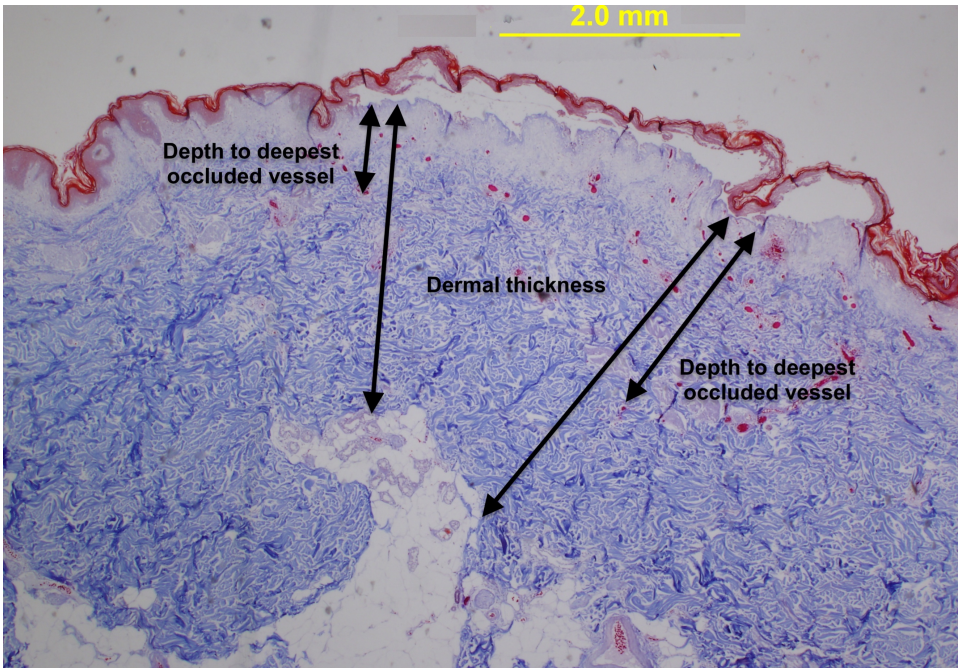


Figure 37: experimental burn, Masson's trichrome stain, showing the measurements made in the calculation of standardised burn-depth

5.4.2 The relationship between contact-time and standardised burn-depth

When standardised burn-depth was plotted for each contact-time, there was an increase in standardised burn-depth with increasing contact-time as shown in the Figure 38.

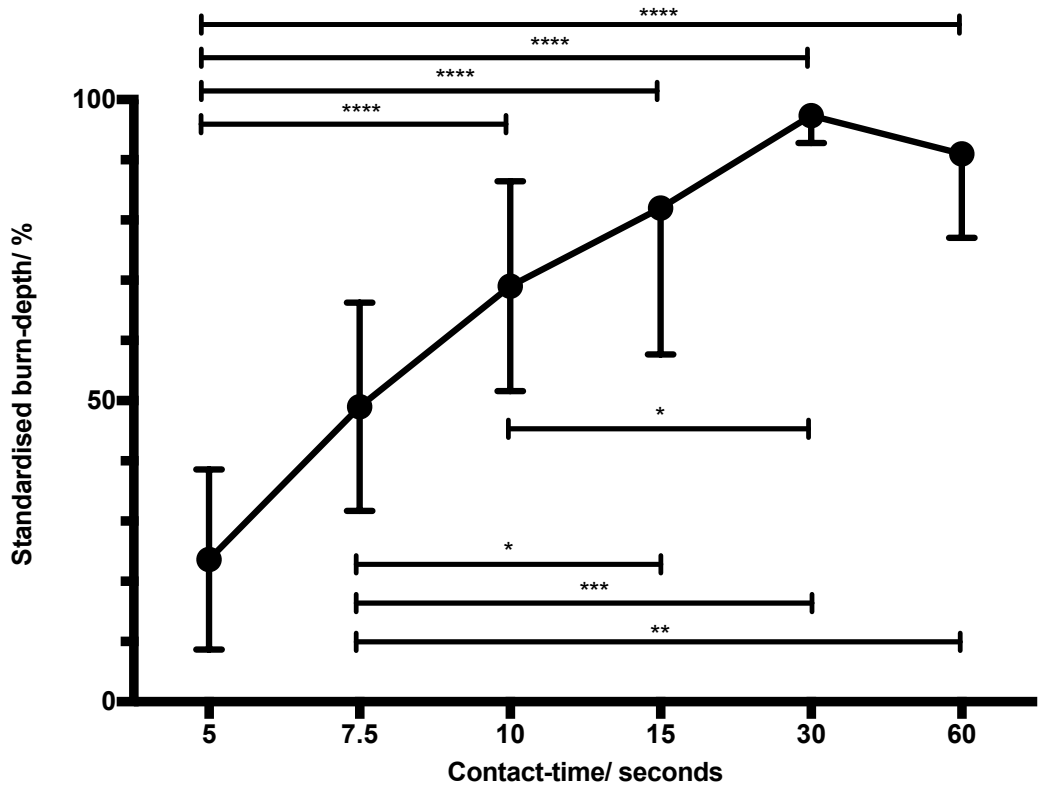


Figure 38: graph showing relationship between contact-time and standardised burn-depth during the initial calibration work, * $p<0.05$, ** $p<0.005$, *** $p<0.0005$, **** $p<0.0001$

Mean standardised burn-depth increased rapidly from between 5 and 15 seconds of contact time, and then saturated at a near full-thickness injury thereafter. The significant differences between the standardised burn-depths created by each contact-time contact time are summarised in Table 7 as p-values and 95% confidence intervals.

Time/ seconds	5	7.5	10	15	30	60
5		NS	<0.0001	<0.0001	<0.0001	<0.0001
7.5	-53 - +2		NS	0.001	0.0002	0.0016
10	-70 - -21	-46 - +6		NS	0.029	NS
15	-84 - -33	-61 - -5	-37 - +11		NS	NS
30	-101- -46	-78 - -19	-55 - -2	-43 - +12		NS
60	-95 - -40	-71 - -13	-48- +4.3	-37 - +19	-23 - +36	

Table 7: summary of statistically significant differences between the standardised burn depths of experimental burns created with different contact-times

Table 7 summarises the p-values to the right of the diagonal line of blacked-out cells, and 95% confidence intervals of the difference between the shorter and longer contact-time burns to the left of that line. Statistically significant differences existed between burns created with 5 seconds' contact and all burn groups beyond 7.5 seconds, and are highlighted. Similar differences existed between 7.5 second burns and all burn groups beyond 10 seconds. At 10 seconds and beyond, there was only a statistically significant difference between 10 and 30 seconds of contact time, and so all burns created with at least 10 seconds of contact time might be described as very deep-dermal or full-thickness burns and a statistically homogenous group.

5.5 Selection of the duration of contact-time

The selection of the duration of contact in burn creation was crucial- if the burn was too superficial, cooling might not have an appreciable, or statistically significantly beneficial effect of the severity of the burn, and conversely a very deep dermal or full-thickness burn might be too deep for cooling to have any appreciable effect, either. This has been a problem identified in previous burn models investigating the effects of cooling[9,18,32]. Given that the samples were to be submitted for RNAseq analysis and the aim was to maximise the beneficial effects of the cooling, the ideal burn had to be sufficiently deep for there to be room for clinical and histological improvement, but also still salvageable, with untreated burn samples still containing sufficient viable elements to allow mRNA extraction.

Considering the relationship between standardised burn-depth and contact-time, 7.5 seconds' contact was selected for all subsequent experiments. Some of the 5 second burns showed very little histological evidence of damage, while some of the 10 second burns were close to full-thickness on both clinical and histological appearance. In contrast, the 7.5 second burns were all in the mid-dermal range of injury on both clinical and histological assessment, and there was the least risk of some samples showing insufficient or excessive damage to allow meaningful interpretation.

5.6 Cooling of standardised burns

Following the adoption of 7.5 seconds' contact time for all burn-creation, a total of ten patients were recruited into the study, and had cooling administered to one of the triangular areas of skin forming the basis for the model after the burns had been created. In five, all three burns and control areas from each side were harvested at three hours, and in the remaining five the cooled and untreated burns and controls were harvested at 1, 2, and 3 hours after burning, and processed as before, and as described in the methodology. The numbers and types of samples at each time-point are summarised in Table 8.

	1 hour post-burn		2 hours post-burn		3 hours post-burn	
Sample type	Samples	Subjects	Samples	Subjects	Samples	Subjects
Cooled burn	5	5	5	5	20	10
Untreated burn	5	5	5	5	20	10
Cooled control	5	5	5	5	20	10
Untreated control	5	5	5	5	20	10

Table 8:the number of patients and samples harvested at each time-point in the cooling experiments

5.6.1 The effect of cooling on the clinical appearances of burns created with a 7.5 second contact time

Cooling resulted in a visible reduction in the amount of oedema and blistering seen in burns created with 7.5 seconds of contact-time when compared within the patient. This is well-illustrated in the two sides of the same patient shown below, shown both at the end of cooling, so 20-30 minutes after burn-creation, and at 3 hours after burn creation, just prior to harvest:

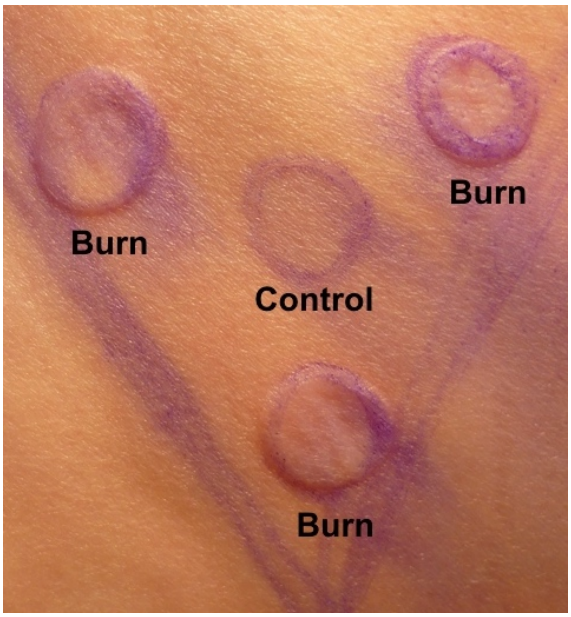


Figure 39: three uncooled experimental burns and central control area



Figure 40: three cooled experimental burns and central control area from the same patient as Figure 39

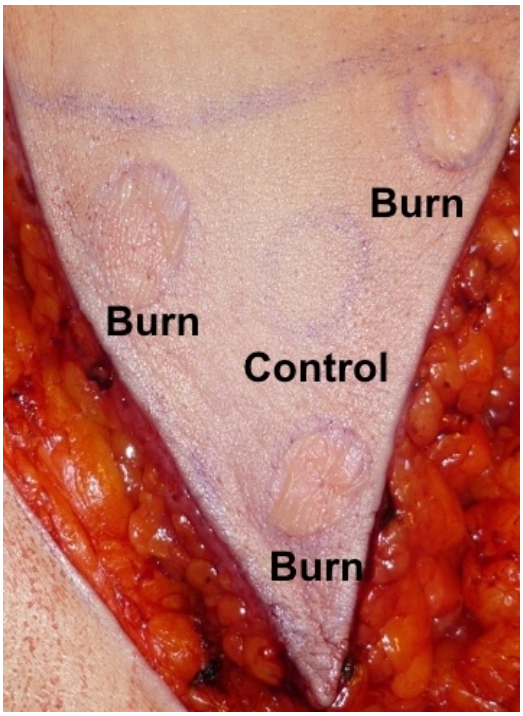


Figure 41: different patient, uncooled experimental burns just prior to harvest at 3 hours after creation

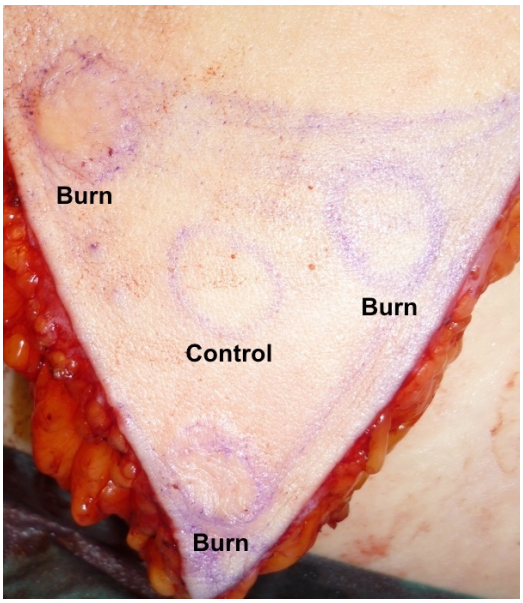


Figure 42: cooled experimental burns just prior to harvest at 3 hours after creation, from the same patient as Figure 41.

5.6.2 The effect of cooling upon the standardised burn-depth of experimental burns three hours after injury

Burn samples from ten different patients, harvested 3 hours after injury were compared. Five of the patients gave samples in triplicate, and five gave single samples, giving a total of 40 burns, from 10 different patients, 20 of which were treated with cooling and 20 left untreated. The mean standardised burn-depth was calculated for each triplicate set of burns, and then a paired t-test was performed comparing cooled and untreated burns within individuals. Figure 43 shows the standardised burn-depth of cooled and untreated burns created with 7.5 seconds' contact-time.

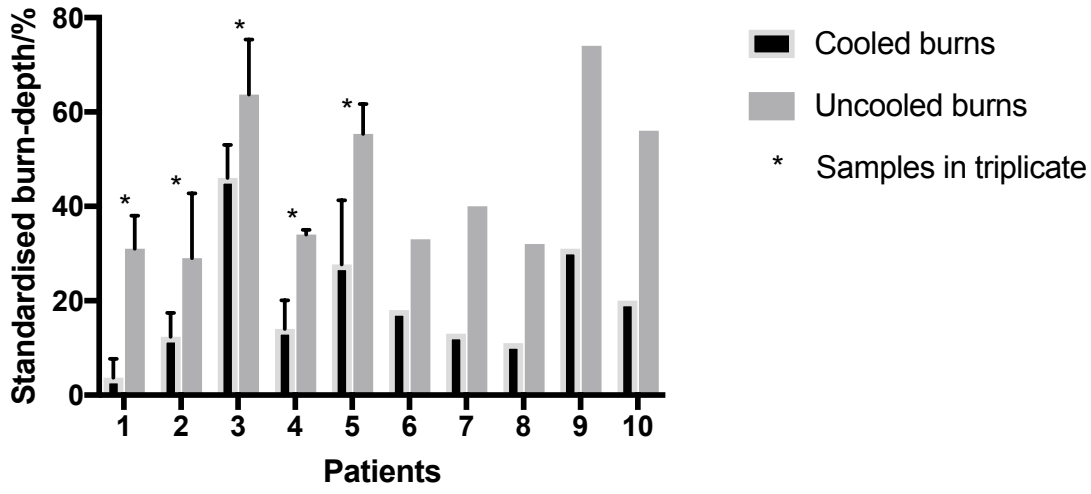


Figure 43: the effect of standardised cooling on the standardised burn-depth of experimental burns created with a contact-time of 7.5 seconds, three hours after burn-creation

The mean standardised burn-depth of the uncooled burns was 45%, consistent with the value achieved with 7.5 seconds' contact-time in the calibration phase (see Figure 38), while the mean standardised burn-depth was 21% for the cooled burns. The patients showed a reduction in standardised burn-depth in the cooled compared to the non-cooled burns in nine of the ten cases. When compared with a paired t-test, this difference was statistically significant with $p<0.0001$. The repeatability of the burn-

creation process was demonstrated, and the responsiveness of the model, and the measurement of depth of thermal injury to cooling was confirmed.

Five of the patients had provided samples at 1, 2 and 3 hours after burn-creation. The cooled and untreated burns from these patients were compared in a pair-wise manner at each time-point, and between the different time-points, again using the paired t-test. The graph below shows the individual data-points for each time-point, and significant differences between individual groups are bracketed.

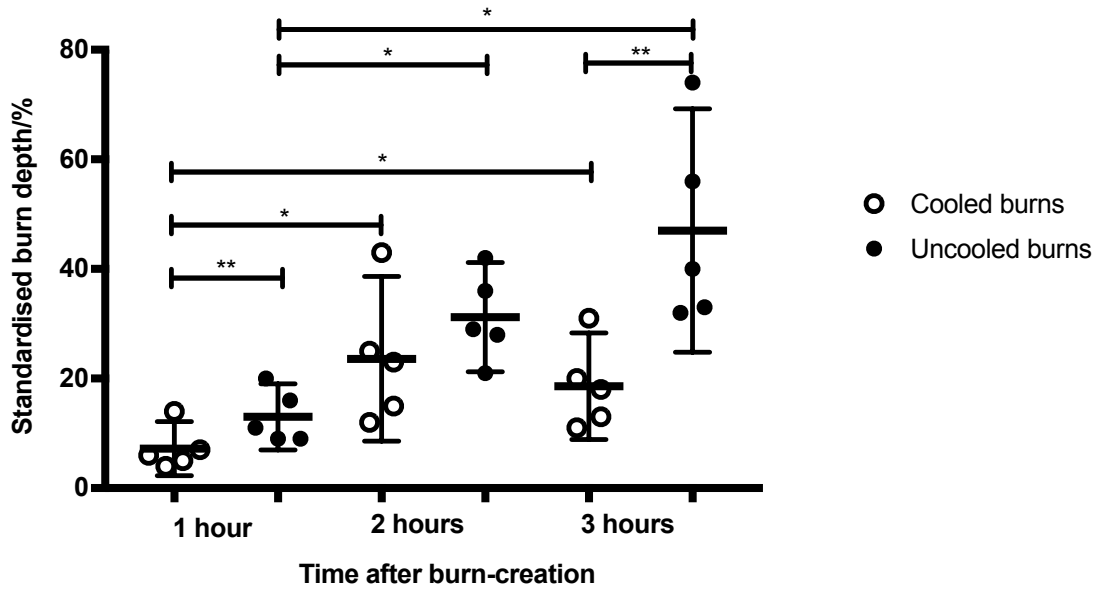


Figure 44: the progression of the standardised burn-depth of experimental burns with time, and the effect of standardised cooling

	1 hour cooled	2 hours cooled	2 hours uncooled	3 hours cooled	3 hours uncooled
1 hour uncooled	0.0056 (**)		0.02 (*)		0.02 (*)
2 hours cooled	0.013 (*)		NS	NS	
3 hours cooled	0.04 (*)	NS			0.005 (*)

Table 9: summary of significant differences in standardised burn depth of experimental burns between different time-points, and the effect of standardised cooling

There was a significant progression in standardised burn-depth from 1-2, and 1-3 hours after injury in both cooled and untreated burns. There was also a significant reduction in standardised burn-depth in cooled compared to untreated burns at 1 and 3 hours after injury. The progression of standardised burn-depth shows that the model is biologically active, and that the microvasculature of the dermis remains patent and perfused after injury, and that coagulation factors and platelets continue to be deposited within the zone of injury. Cooling significantly attenuated the progression of microvascular occlusion in thermally-injured skin.

5.6.3 Analysis of all untreated standardised burn-depth data

All untreated burns of all durations of contact-time were analysed together. The selection of 7.5 seconds' contact-time for the cooling experiments added a further 20 untreated burns for this duration Table 10.

	5 seconds	7.5 seconds	10 seconds	15 seconds	30 seconds	60 seconds
Samples	8	26	10	8	6	6
Patients	4	13	5	4	3	3

Table 10: summary of total number of standardised experimental burns created with each contact-duration and number of different sample-donors per duration

This increase in the number of biological and technical replicates at the 7.5-second point resulted in a considerable reduction in the 95% confidence interval of that data set, and had a considerable effect on the statistical significance of differences between the data points between 5 and 10 seconds of contact-time Figure 45. Only the comparisons involving the 7.5-second burns are bracketed as these are the only ones affected by the inclusion of the untreated burns from the cooling experiments in this analysis. The other significant differences between the other groups remain unchanged from Figure 38.

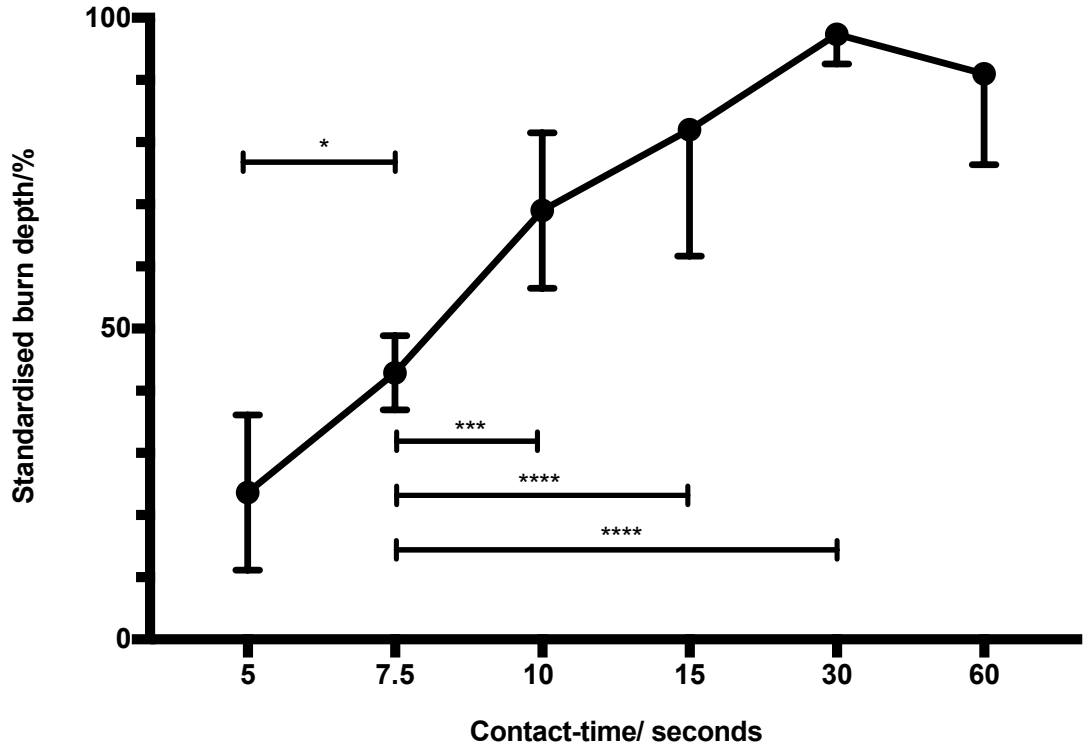


Figure 45: the standardised burn-depth of all uncooled experimental burns, created with all contact-durations

The p-values of the ANOVA comparisons of the time-points in Figure 45 are summarised in Table 11.

Contact-time	5 seconds	7.5 seconds	10 seconds	15 seconds	30 seconds	60 seconds
7.5 seconds	p=0.048 (*)		p=0.0007 (***)	p<0.0001 (****)	p<0.0001 (****)	p<0.0001 (****)
10 seconds	p<0.0001 (****)			NS	p=0.014 (*)	NS

Table 11: summary of significant differences between the standardised burn-depths of the experimental burns in Figure 45.

The inclusion of all 7.5-second burns reduced the 95% confidence interval of that data set significantly, and allowed the mean standardised burn-depth of the 7.5-second burns to be distinguished statistically from that of the 5 and 10-second burns lying either side of it. It also underlines the reproducibility of the model, and the reliability of its component parts, namely the choice of skin, the design of the burn-creation apparatus and its operating temperature, the application of the probe, both in terms of time and pressure, and the measurement of the standardised burn-depth as described previously.

5.7 Summary of the model

The standardisation of the model was accomplished from a starting-point of little previous published data regarding the temperature and duration of contact needed to create a consistent mid-dermal injury in normal human skin in vivo. The novel nature of the apparatus further complicated the process, as the pressure of application as a product of the mechanical properties of the spring, and the specific thermal properties of the heated copper rod were unique to the device.

The clinical appearance of the burns changed to that of a deeper burn with increased contact-time with the burn-creation device. The lateral extent of the changes was limited to a narrow rim around each burn, well outside the limit of the control areas of skin within each half of the model. The clinical appearance of cooled and untreated burns also differed when compared side-to-side within the same patient.

The adoption of a technique previously described in a small series of burns that were biopsied over a much longer time-course after injury[2] has been justified by these results. It has been demonstrated that this method of measuring the depth of thermal injury relative to dermal thickness at that point is responsive to differences in duration

of contact-time, and that this difference is statistically significant, even over differences of 2.5 seconds. The transition from partial-thickness to full-thickness injury at around the 10-second time-point correlates to the graph produced by Bull from experimental burn work[10]. Furthermore, the biological progression of burns seen clinically in patients, was demonstrated to a statistically significant level in a group of five patients over the course of 1-3 hours after burning using this same histological technique. This same histological technique also demonstrated the very limited lateral extent of the microvascular changes relative to the edge of the clinical and histological extent of the blister, placing the control areas of each side of the model out of the zone of thermally-induced microvascular changes.

In summary, the apparatus was shown to be reliable and safe, the model to be consistent and biologically active over the course of the experiment, and the method of quantification of thermal injury-severity to be sensitive and responsive to the biological progression of the injury.

The validation of the model is important for the following reasons:

We have demonstrated the relative stability of the burn model, even in within the field of a major reconstructive operation.

We have shown the dose-response relationship between contact-time and subjective clinical severity of burning

We have linked point 2 (above) to objective, histological changes seen in samples, and shown a robust relationship between the two features of the experimental burns

We can compare burns that are of very similar depths to one another between patients, reducing the variability inherent in a complex injury model

We have shown the dynamic evolution of the histological appearance of the burns with time, underlining the viability of thermally-injured skin

We have shown the clinical and histological changes induced by burning are attenuated by cooling, and that this also has a significant effect on the temporal evolution of the injury

We can submit samples from these burns and controls for transcriptomic and proteomic analysis, confident that there are significant, fundamental differences between burned and uninjured skin, and between cooled and untreated burns, and hence optimistic about finding changes in the transcriptome and proteome of skin following both burning and subsequent cooling when compared to normal, untreated skin.

6 Results Chapter 2: RNA sequencing and qPCR validation of findings

6.1 RNA extraction from the samples

Following optimisation of the extraction and purification of the RNA from the skin samples, and protection from degradation during this process, as set out in Figure 19, some initial observations were possible on the effects of thermal injury to normal human skin in vivo.

6.1.1 The yield and quality of RNA extracted from human skin

The yield of RNA from skin did not differ significantly between the four conditions in the study on ANOVA testing as shown in Table 12, and Figure 46.

Condition	Mean RNA yield (µg/g)	ANOVA test p-values
Uncooled burn (BNC)	30	BNC vs CNC p=0.46 BC vs BNC p=0.88 BC vs CC p=0.32 CC vs CNC p=0.99
Cooled burn (BC)	34	
Uncooled control (CNC)	83	
Cooled control (CC)	70	

Table 12: mean RNA yield for each condition and ANOVA testing

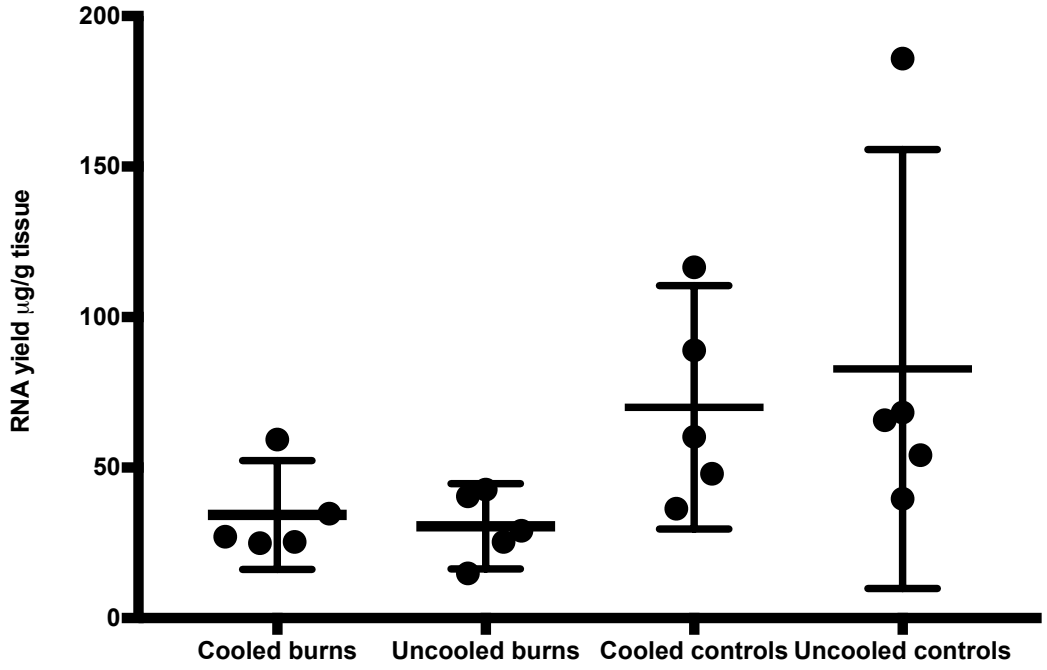


Figure 46: the RNA yield for samples from each condition

6.1.2 The effect of thermal injury on the integrity of RNA

Thermal injury had a significant detrimental effect upon the quality of the RNA extracted from burned skin samples as measured by the Ribosomal Integrity Number equivalent (RINe) on the TapeStation when compared to samples of RNA extracted from unburned skin. This difference existed between both the cooled and uncooled burns and their respective controls. The images in Figure 47 to Figure 50 are representative electrophrenograms of RNA samples from each of the four groups. The ribosomal RNA peaks are smaller in the thermally-injured samples when compared to the unburned skin samples, indicating degradation from thermal injury, and there is therefore a lower ratio between the areas of the ribosomal peaks and the rest of the RNA species in the electrophrenogram.

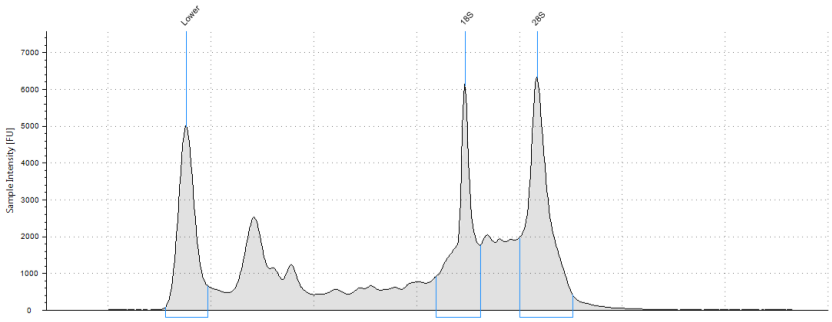


Figure 47: electrophrenogram of RNA extracted from an uncooled burn

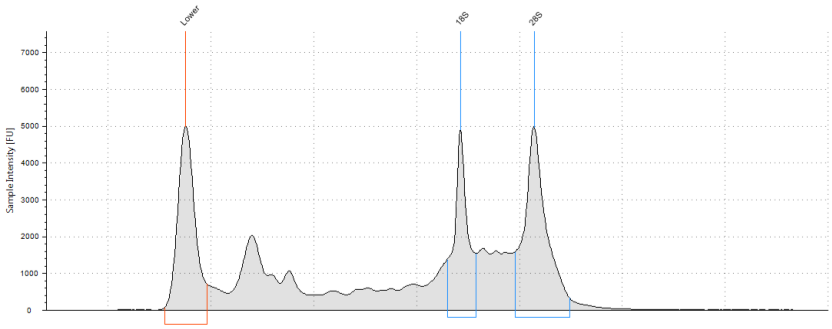


Figure 48: electrophrenogram of RNA extracted from a cooled burn

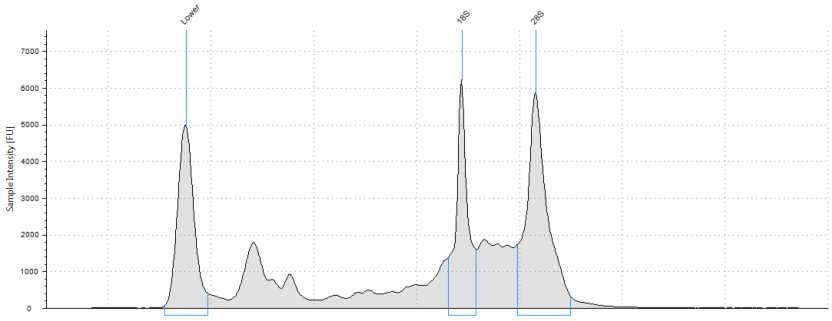


Figure 49: electrophrenogram of RNA extracted from an uncooled control

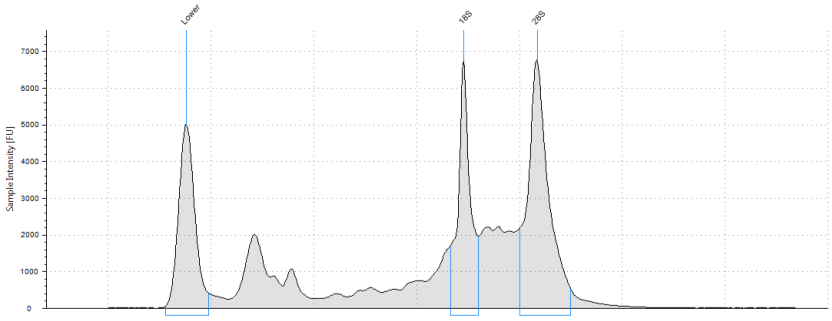


Figure 50: electrophrenogram of RNA extracted from a cooled control

6.1.3 The effect of cooling on the yield and quality of RNA extracted from thermally-injured human skin

While there was no statistically significant difference between the yields of RNA in µg/g tissue, there was a statistically significant difference in the quality of the RNA yielded by the burned and unburned samples of skin as measured by its RINe. The RINe of normal skin was statistically significantly higher than that of burned skin.

Cooling had no statistically significant effect upon the quality of RNA extracted from either burned or unburned skin, as shown in Figure 51.This is an important finding as the thermal degradation of RNA could be postulated as a mechanism involved in burn pathophysiology, and that cooling might have some effect in reducing its severity. Were this the case, we might reasonably expect to see higher RINe values in RNA samples extracted from cooled burns when compared to uncooled burns.

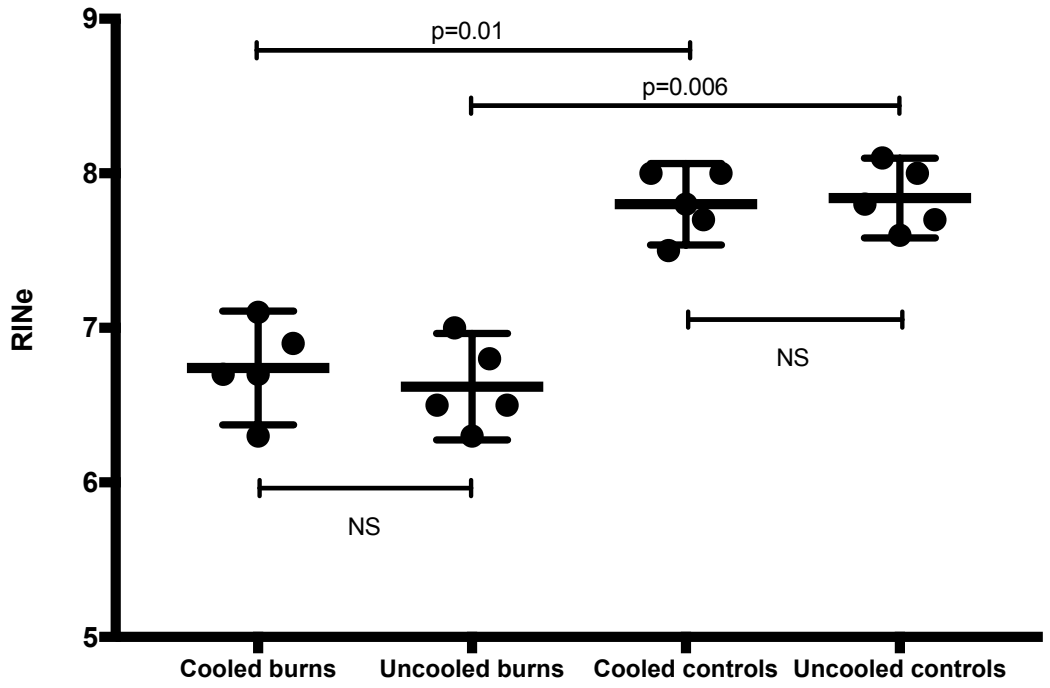


Figure 51: comparison of RINe values of samples from the four conditions, brackets indicate comparisons, significant p-values are stated, “NS” indicates "not significant"

6.2 Sequencing of the RNA extracted from the samples

Each of the 5 patients provided 4 different types of skin sample: a cooled and an uncooled burn and control, from which RNA was extracted. A 2.2µg sample of purified RNA from each sample was submitted for library preparation prior to sequencing. Each library was multiplexed to make it identifiable, pooled together, and run on 4 flow cells. This provided 5 biological replicates of each condition, and 4 technical replicates of each library.

6.2.1 The quality and consistency of the sequencing data

Following alignment of the RNAseq data to the human genome using the *featureCounts* function in edgeR, a DGEList of the data was generated. All genes not returning at least 1 count per million (CPM) in at least one condition were eliminated, and a multidimensional scaling (MDS) plot was generated for the 4 technical replicates of each of the 20 libraries, as shown in Figure 52.

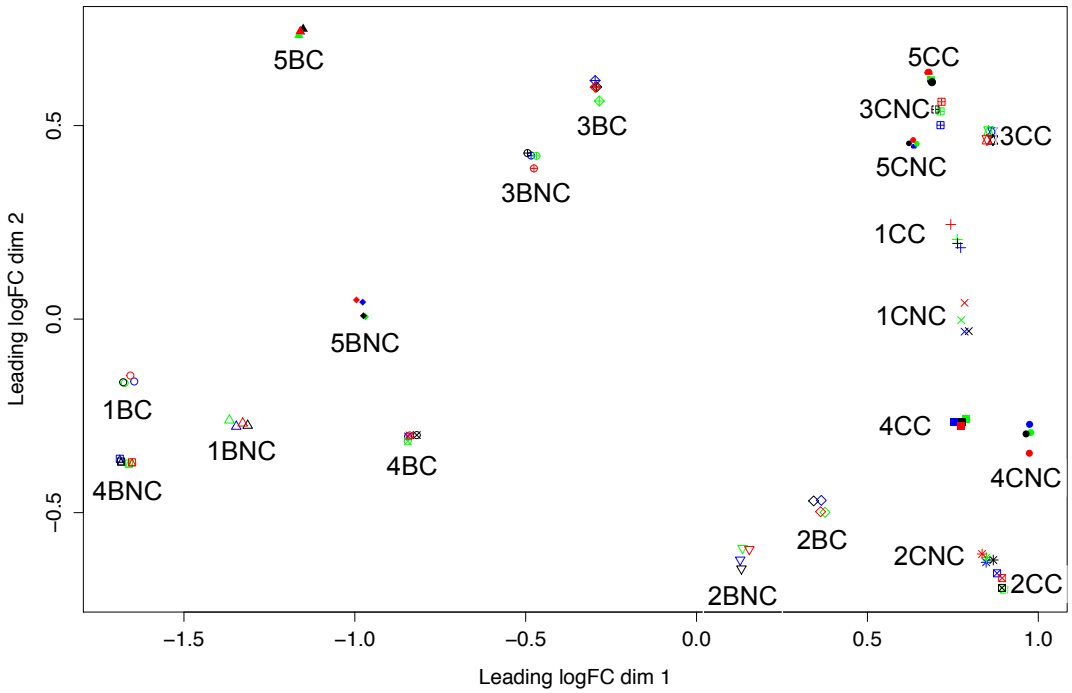


Figure 52: MDS plot of all 20 samples submitted for sequencing, showing the close correlation each of the 4 technical replicates of each library

The patients are numbered 1-5, and the conditions have been abbreviated to “burn, cooled” (BC), “burn, not cooled” (BNC), “control, cooled” (CC), and “control, not cooled” (CNC). The 4 different colours of each icon represent each of the 4 technical replicates of each library.

Each library has been expressed as a single data point with its position determined by the expression of each transcriptome as expressed by their biological coefficient of variability (BCV). Each of the technical replicates of each library map very closely to one another compared to other libraries, and can be considered sufficiently similar as to allow pooling and so increase the number of reads per sample.

These 5 sets of samples have been extracted from five different individuals, undergoing major, prolonged surgery, with the burn-creation experiments spread over a period of weeks, and the extractions spread over a period of days, so it is not surprising that the individual biological replicates do not map particularly closely to one another, given the inherent biological variability likely to exist between the five subjects.

The process of burning does seem to have had a major effect on the transcriptome of the skin. The four conditions themselves broadly separate into burned skin samples in the left side of the plot, and unburned skin samples in the right side of the plot. Cooled and untreated burns are separated from one another by a greater distance than the cooled and untreated controls of the same patients, suggesting that the effect of cooling on the transcriptome of thermally injured skin is greater than the effect on that of normal skin.

Of interest is “case 2”, where the burn samples map very closely to the control samples and away from the other burn samples. This patient had the deepest of the

experimental burns in terms of standardised burn-depth and shown in (figure reference) in the previous chapter. Cooling still reduced the standardised depth of the burns in this patient, but to a depth still greater than some of the uncooled burns from other patients. While we did not have a starting hypothesis as to how the samples might distribute on MDS plot, it is interesting that the deepest burns lie very close to the control samples, rather than furthest away. It is possible that, as the standardised depth of burn is inversely proportionally to the volume of undamaged tissue, the deepest burns have the fewest transcriptionally active elements and hence can mount a smaller transcriptomic response than deeper burns.

6.3 The transcriptome of human skin

After filtering for transcripts mapping to genes not expressed in at least one of the four conditions (cooled burn, uncooled burn, cooled control or uncooled control), a total of 17,261 genes were identified as expressed to some extent in the transcriptome of the skin samples submitted for sequencing. Following initial analysis of all 5 patient samples on Figure 52, it was decided to eliminate patient 2 from analysis as the burn samples from this patient were significant outliers relative to the other burns, as they mapped closest to the control areas on the MDS plot.

6.3.1 The effect of thermal injury on the transcriptome of normal human skin

When the transcriptomes of uncooled burns and uncooled controls were compared in a pair-wise manner within individuals, it was found that thermal injury resulted in up-regulation of 2,266 genes and down-regulation of a further 1,527 genes, with significance taken as a Log2 FC of ≥0.58 or ≤-0.58 (corresponding to a ≥50% increase or decrease in expression), and a false discovery rate (FDR) ≤0.05. This represents 22% of the identified transcriptome of normal skin being significantly up or down-regulated by burning within 3 hours of injury.

The analysis was checked by the bioinformaticians in the Computational Biology Research Group at the Weatherall Institute of Molecular Medicine, with similar results.

6.4 Examination of gene ontologies affected by thermal injury

With so many genes affected by thermal injury, and without a starting hypothesis as to which genes are most important, it was decided to examine the broader effects of thermal injury on groups of genes related to specific events or effects within cells and tissues, in particular those related to skin function- known to be compromised by

thermal injury-, and processes related to injury, heat-shock, and microvascular damage- empirically evident in our model.

6.4.1 Ontological analysis with GOPlot 1.0.2

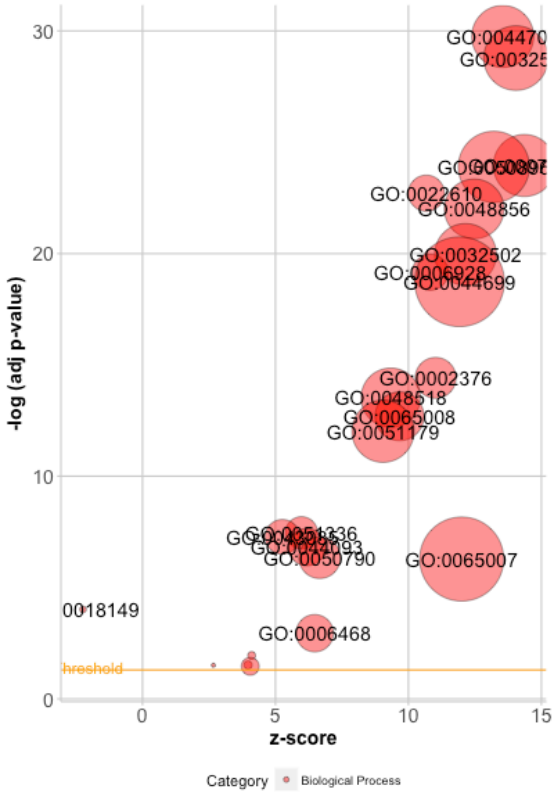
The enrichment of gene ontologies was analysed using GOPlot, a software package available for use in “R”. Briefly, GOPlot software ascribes the list of differentially expressed (DE) genes to known ontologies in terms of molecular function (MF), biological process (BP) and cellular component (CC). The z-score can be calculated as an indicator of net up or downregulation as shown in Equation 2.

$$\frac{(\text{number upregulated- number downregulated})}{\sqrt{\text{count}}}=\text{z-score}$$

Equation 2: calculation of z-score, "count" refers to the number of genes in the dataset ascribed to the ontology

While this does not take into account the magnitude of the respective changes with an ontology, or the relative importance of each gene within the ontology, it allows the general trend to be assessed.

Given the large overlap between ontologies with many genes belonging to multiple ontologies, the “reduce_overlap” function in GOPlot was used to eliminate ontologies with a >99% overlap, retaining 1 per group. This produced the following Bubble plots. Bubble plots plot the z-score of the ontology for that dataset against the $-\text{Log}_{10}$ adjusted p-value, and the diameter of the “bubble” reflects the number of genes in that ontology.



ID	Description
GO:0044707	single-multicellular organism process
GO:0032501	multicellular organismal process
GO:0007154	cell communication
GO:0050896	response to stimulus
GO:0022610	biological adhesion
GO:0048856	anatomical structure development
GO:0032502	developmental process
GO:0006928	movement of cell or subcellular component
GO:0044699	single-organism process
GO:0002376	immune system process
GO:0048518	positive regulation of biological process
GO:0065008	regulation of biological quality
GO:0051179	localization
GO:0051336	regulation of hydrolase activity
GO:0043085	positive regulation of catalytic activity
GO:0044093	positive regulation of molecular function
GO:0050790	regulation of catalytic activity
GO:0065007	biological regulation
GO:0018149	peptide cross-linking
GO:0006468	protein phosphorylation

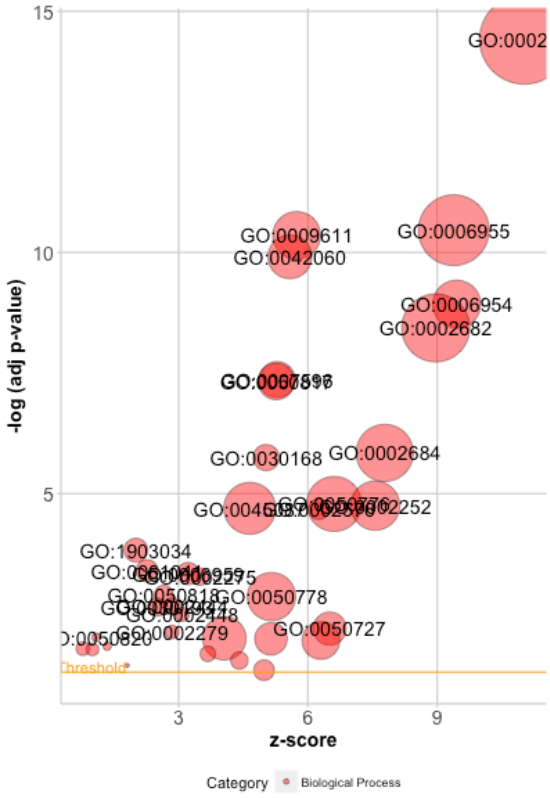
Figure 53: Bubble plot of biological processes with <99% overlap, and significant up or downregulation following burning

Figure 53 shows a manageable number of biological processes left after overlapping ontologies have been removed. With the exception of “peptide cross-linking GO:0018149”, they all have positive z-scores indicating general up-regulation. There are signs of response to a stimulus with “cell communication”, “response to stimulus”, “biological adhesion”, “protein phosphorylation” and “immune system process” all significantly upregulated, both in terms of z-scores and p-values. The biological processes are all fairly generic, and do not inform much in terms of transcriptional events following thermal injury.

6.4.2 Gene ontologies upregulated by burning

6.4.2.1 Wounding, inflammation, immune response, angiogenesis, and healing

The ontology descriptions were filtered for those associated with “wound”, “inflammation”, “immune”, “angiogenesis” and “healing”, using the “subset” function in GOPlot. This produced a Bubble plot of all ontologies for which there was enrichment in the list of DE genes, as shown in Figure 54.



ID	Description
GO:0002376	immune system process
GO:0006955	immune response
GO:0009611	response to wounding
GO:0042060	wound healing
GO:0006954	inflammatory response
GO:0002682	regulation of immune system process
GO:0007596	blood coagulation
GO:0050817	coagulation
GO:0002684	positive regulation of immune system process
GO:0030168	platelet activation
GO:0050776	regulation of immune response
GO:0002252	immune effector process
GO:0045087	innate immune response
GO:0002576	platelet degranulation
GO:1903034	regulation of response to wounding
GO:0061041	regulation of wound healing
GO:0006959	humoral immune response
GO:0002275	myeloid cell activation involved in immune response
GO:0050818	regulation of coagulation
GO:0050778	positive regulation of immune response
GO:0002444	myeloid leukocyte mediated immunity
GO:0030193	regulation of blood coagulation
GO:0002448	mast cell mediated immunity
GO:0050727	regulation of inflammatory response
GO:0002279	mast cell activation involved in immune response
GO:0050820	positive regulation of coagulation

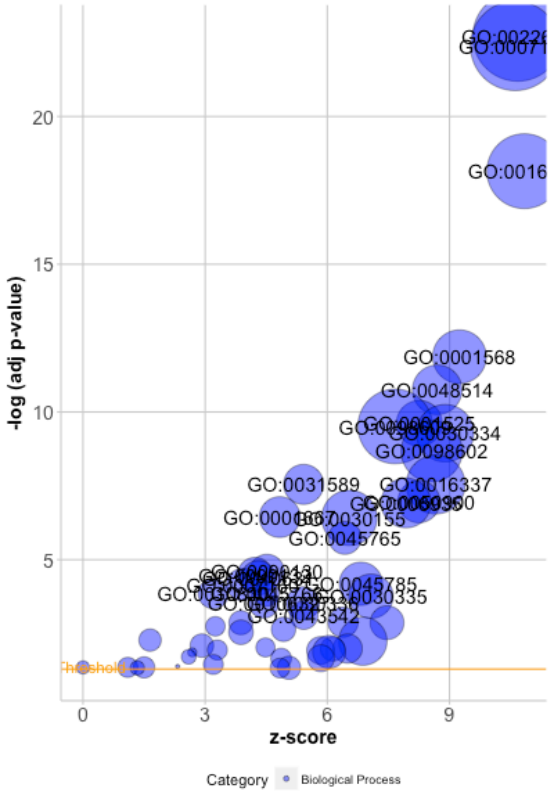
Figure 54: Bubble plot of ontologies related to "wound", "inflammation", "immunity", and "healing" significantly enriched in the list of DE genes

Figure 54 shows that there was a global upregulation of all ontologies related to these terms, as shown by their positive z-scores. Both the humoral and cellular elements, including Mast cells, of the immune system show positive enrichment. There is already published evidence of the innate immune system and Mast-cell-related peptidases playing a key role in the progression of burn wounds, and there is transcriptional

evidence of this in the list of DE genes. The wound healing ontologies show that the healing process has already begun at a transcriptional level within 3 hours of injury.

6.4.2.2 Haemostasis, platelet activation, and coagulation

Ontology descriptions were filtered for “blood”, “coagulation”, “haemostasis”, “platelet”, and “angiogenesis” and produced the Bubble plot Figure 55.



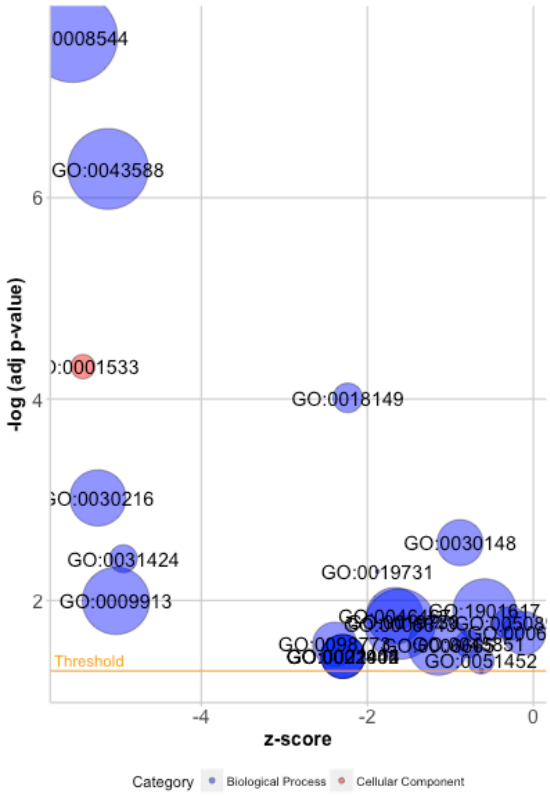
ID	Description
GO:0022610	biological adhesion
GO:0007155	cell adhesion
GO:0016477	cell migration
GO:0001568	blood vessel development
GO:0048514	blood vessel morphogenesis
GO:0001525	angiogenesis
GO:0098609	cell-cell adhesion
GO:0030334	regulation of cell migration
GO:0098602	single organism cell adhesion
GO:0031589	cell-substrate adhesion
GO:0016337	single organismal cell-cell adhesion
GO:0050900	leukocyte migration
GO:0006935	chemotaxis
GO:0001667	ameboidal-type cell migration
GO:0030155	regulation of cell adhesion
GO:0045765	regulation of angiogenesis
GO:0090130	tissue migration
GO:0090132	epithelium migration
GO:0010631	epithelial cell migration
GO:0045785	positive regulation of cell adhesion
GO:0007160	cell-matrix adhesion
GO:0010810	regulation of cell-substrate adhesion
GO:0045766	positive regulation of angiogenesis
GO:0030335	positive regulation of cell migration
GO:0010632	regulation of epithelial cell migration
GO:0030336	negative regulation of cell migration
GO:0043542	endothelial cell migration

Figure 55: Bubble plot of haemostasis, coagulation, and angiogenesis-related ontologies.

The effects of burning are to increase expression of genes related to haemostasis, coagulation, platelet activation and degranulation, and the response to VEGFR stimulation. Some of these changes correlate to the histological changes seen in the previous results chapter where there a was clear evidence of coagulation and microvascular occlusion.

6.4.2.3 Gene ontologies downregulated by thermal injury

Thermal injury also downregulated genes belonging to key ontologies. As a reflection of the relatively smaller number of such ontologies, it was possible to filter simply for a z-score <0 and plot this as a Bubble plot without producing a confusingly complicated plot. The resultant Bubble plot is shown in Figure 56.



ID	Description
GO:0008544	epidermis development
GO:0043588	skin development
GO:0001533	cornified envelope
GO:0018149	peptide cross-linking
GO:0030216	keratinocyte differentiation
GO:0030148	sphingolipid biosynthetic process
GO:0031424	keratinization
GO:0019731	antibacterial humoral response
GO:0009913	epidermal cell differentiation
GO:1901617	organic hydroxy compound biosynthetic process
GO:0046467	membrane lipid biosynthetic process
GO:0019730	antimicrobial humoral response
GO:0050891	multicellular organismal water homeostasis
GO:0006643	membrane lipid metabolic process
GO:0006721	terpenoid metabolic process
GO:0045851	pH reduction
GO:0098773	skin epidermis development
GO:0006665	sphingolipid metabolic process
GO:0001942	hair follicle development
GO:0022404	molting cycle process
GO:0022405	hair cycle process
GO:0051452	intracellular pH reduction

Figure 56: Bubble plot of ontologies downregulated by thermal injury

This Bubble plot outlines all the ontologies that were significantly downregulated by burning, and in doing so summarises many of the clinical features of a thermal injury. There is a loss of keratinisation, epidermal development, hair follicle differentiation, cornified envelope, and of the ability to reduce intracellular pH. There is also loss of water homeostasis and antimicrobial activity. These changes reflect the changes seen in the burned sections of skin where the epidermal keratinocytes showed elongation of the nuclei and loss of adherence to the basement membrane and underlying dermis.

They also reflect the formation of blisters, and the loss of antibacterial barrier seen clinically in burns.

6.4.2.4 Summary of the preliminary enrichment analysis

The preliminary analysis shows that the transcriptomic data correlates to features that would be expected from the clinical appearance of burns, and the natural time-course of a burn injury. There are transcriptional changes consistent with upregulation of coagulation, platelet activation, inflammation, cellular and humoral immune response associated with the injury to the microvasculature and occlusion seen histologically. There are also changes consistent with increased angiogenesis and migration of endothelial, and epithelial cells, as well as of leukocytes with increased adhesion and chemotaxis.

Those ontologies with negative z-scores indicating a net downregulation correspond to loss of epidermal and epidermal appendage function, including hair follicle differentiation, but it is interesting that there are already signs of transcriptional changes consistent with reepithelialisation and healing even at this early point.

6.4.3 Metacore analysis of the data

More in-depth analysis of the data is necessary to identify specific pathways and genes from within the data. Metacore is an online platform that allows the uploading and analysis of lists of DE genes. The data can be fitted to known pathways and disease processes and can also generate diagrams including the relative Log2 FCs between pairs of conditions. The legend for Metacore figures has been included as Figure 57.

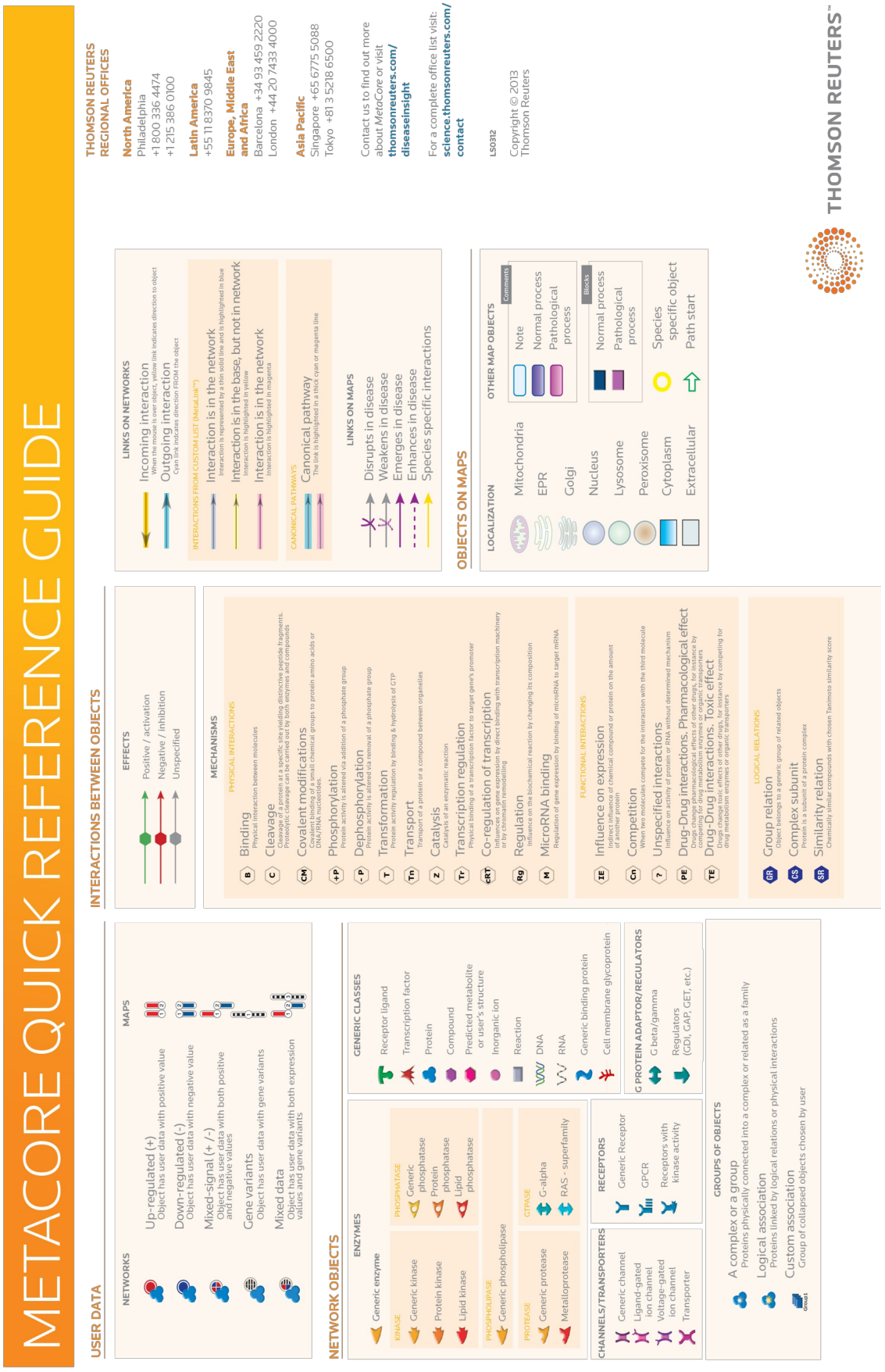


Figure 57: Metacore-generated figure legend

Key processes identified from the GOplot analysis were investigated in more detail using Metacore analytical tools. The processes and pathways of particular interest belong to the themes of inflammation, haemostasis, neutrophil and epithelial migration, and keratinocyte differentiation.

6.4.3.1 Inflammation

Inflammatory pathways identified from the data

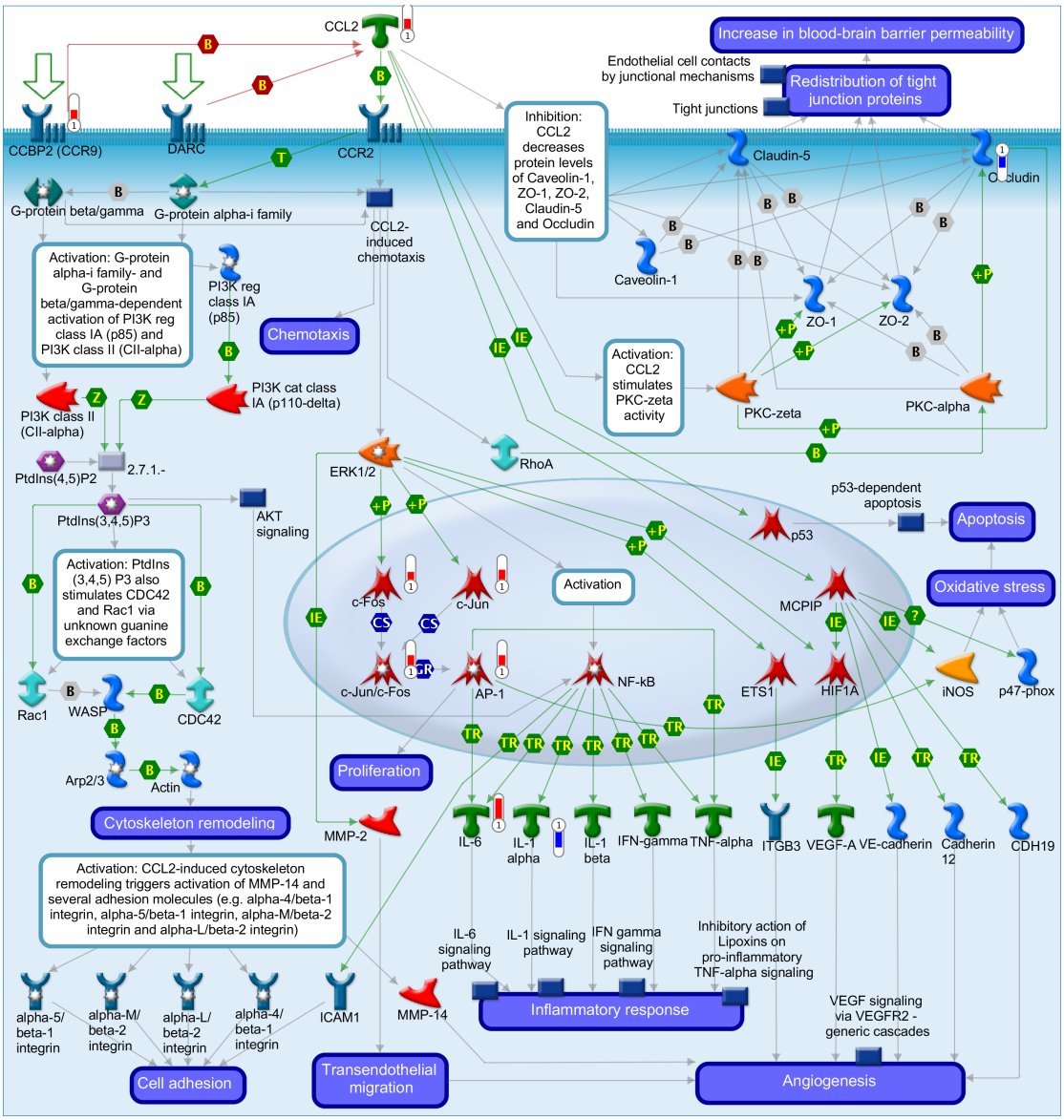


Figure 58: CCL2 signalling pathways showing Log2 FCs for BNC:CNC analysis

Figure 58 shows the effect of the 1.3 Log2 FC increase in CCL2 expression. Its effects include reduced expression of Occludin (a cytokine-regulated protein responsible for tight junction formation) by -1.3 Log2 FC (top right)-. This would contribute to the general increase in vascular permeability seen after thermal injury, and allow the migration of leukocytes. It also influences proliferation, cytoskeletal remodelling, cell adhesion, and inflammation via activation of NF-kB, identified as a key effector of burn pathophysiology via binding of GPCRs by such ligands as C3a and C5a[79,80], SP[81], and thrombin[82], all of which have been shown to have a role in burn pathology.

The transcriptional effect upon tight junction formation are further demonstrated in Figure 59.

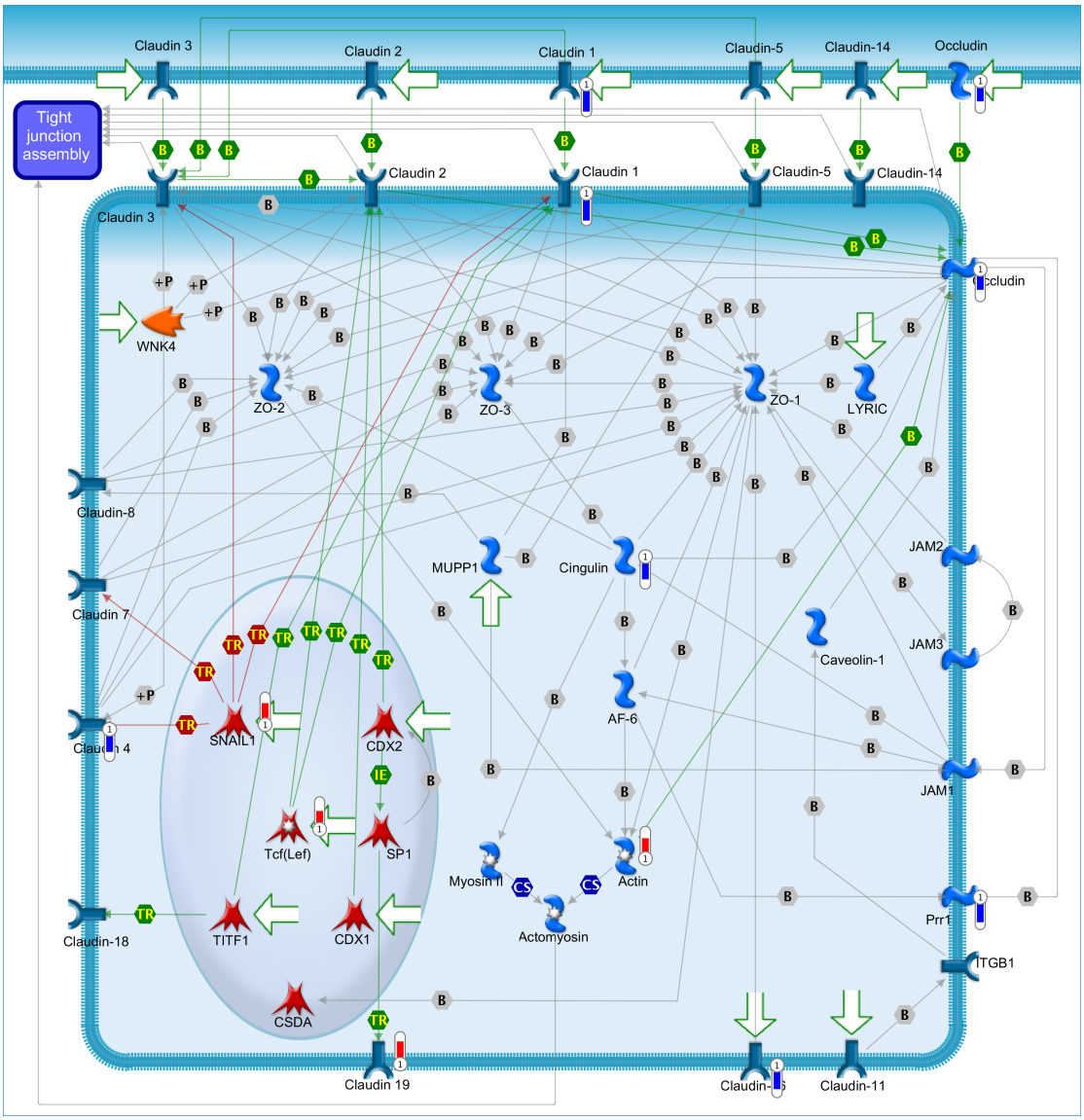


Figure 59: formation of tight junctions with the Log2 FCs from the BNC:CNC comparison.

With the exception of Claudin 19- responsible for the obliteration of the intercellular dead-space that was upregulated 1.6 fold- the other Claudins (1, 4 and 16) and Occludin were all down-regulated -1.5-2 fold. This reflects a loss of tight-junction formation between epithelial cells, and the resultant loss of fluid from burned skin, and also allowing the migration of epithelial cells.

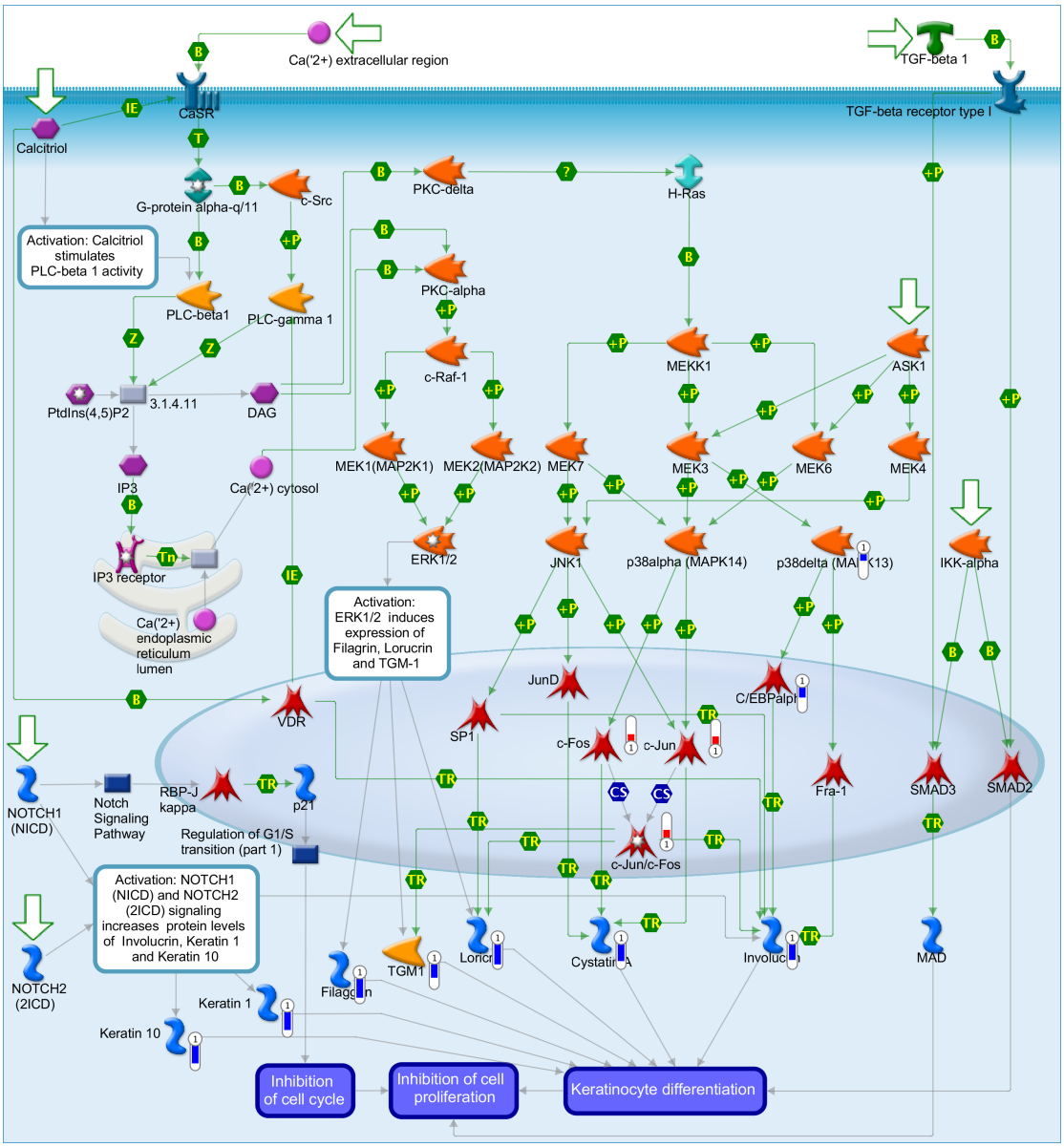


Figure 60: Keratinocyte differentiation with Log2 FCs from BNC:CNC comparison

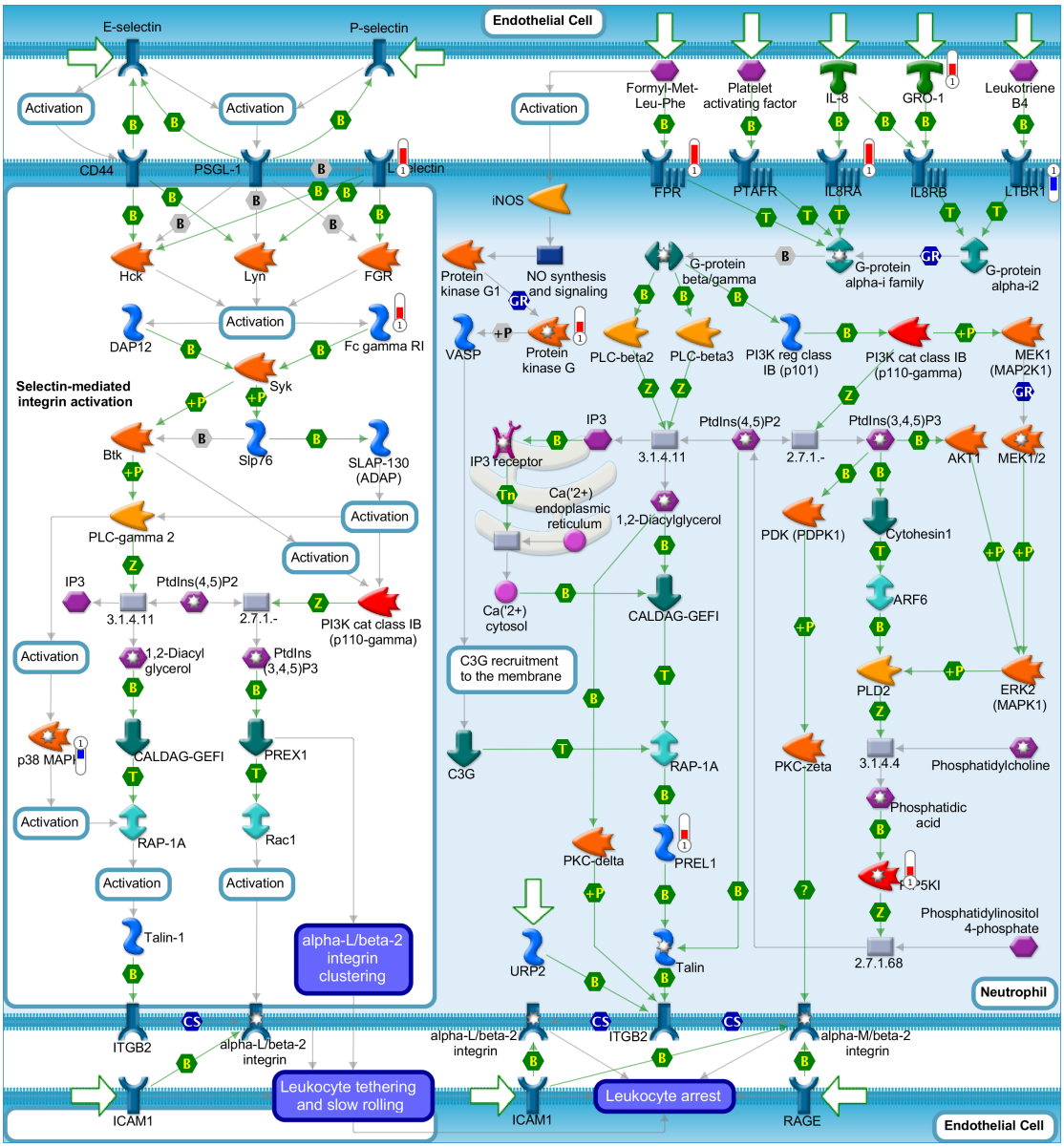


Figure 61: inside-out leukocyte arrest

Comparisons between the transcriptomes of the untreated burns and normal skin showed significant changes in the transcription of genes related to neutrophil adhesion to the vascular endothelium, as shown in Figure 61. There is increased expression of L-selectin- the initiator of neutrophil adhesion and rolling-, Formyl protein receptor (FPR)- an initiator of superoxide release via increases in intracellular calcium, interleukin 8 receptor alpha (IL8RA)- a potent activator of neutrophils- which if expressed on neutrophil plasma membranes, would result in increased adhesion and rolling. There is increased expression of growth-related protein 1, which if this were on

the vascular endothelium would act as a chemoattractant to neutrophils. Leukotriene B4 receptor (LTBR1)- was down-regulated by thermal injury.

Increases in the expression of Fc gamma RA- high-affinity immunoglobulin gamma Fc receptor 1- would result in more binding of the constant fragment of IgG, and is important in both the innate and adaptive immune responses.

The increased expression of protein kinase G followed by the increase in expression of PREL1 (amyloid beta precursor protein binding family B member 1 interacting protein) is a precursor to cytoskeletal remodelling- a requirement for invasion and migration after adhesion to the vascular endothelium. PIP5KI (phosphatidylinositol-4-phosphate 5-kinase type 1 gamma) is associated with cell migration, and is also upregulated in thermally injured skin.

The effect of these changes is to an overall trend is towards both endothelium and neutrophils to have higher number of transcripts for genes associated with adhesion between the two, and those associated with cytoskeletal remodelling that might be associated with neutrophil invasion following adhesion.

It cannot be determined from this data if this reflects a greater level of expression of these transcripts within the skin, or simply a larger number of neutrophils being present in thermally injured skin, with a resultant increase in the number of these transcripts.

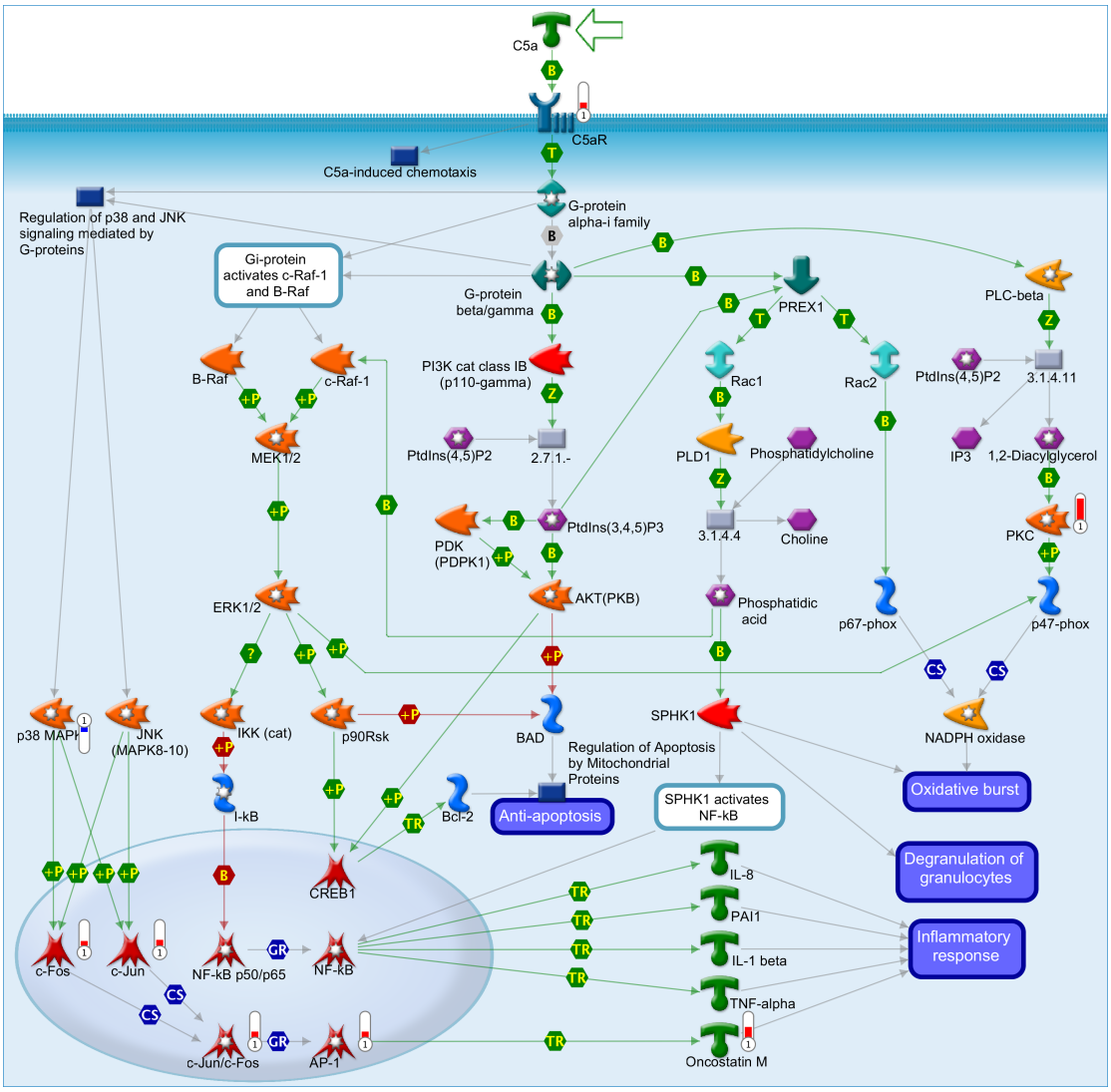


Figure 62: C5a mediated mediation of oxidative burst, inflammation and degranulation

Figure 62 illustrates the effects of C5a (the anaphylactotoxin released by the activation of complement factor 5) binding the C5a receptor on the cell membrane. The expression of C5aR I increased 1.2 fold, and initiates an inflammatory response via p38 MAPK (a stress-induced protein kinase 3 involved in myoblast differentiation), c-Jun/c-Fos (a dimer of Fos and Jun family proteins associated with differentiation, proliferation, and sometimes apoptosis) and Oncostatin M (in endothelial cells this regulates the production of IL6, GCSF, GMCSF). C5AR binding of C5a also initiates oxidative burst via PKC (4.8 fold increase), and activation of p47-phox (neutrophil

cytosolic factor 1) that is required in the generation of superoxide in conjunction with NADPH oxidase.

The enrichment of these transcripts may reflect their increased abundance within the neutrophil population, or the increased number of neutrophils present in thermally-injured skin.

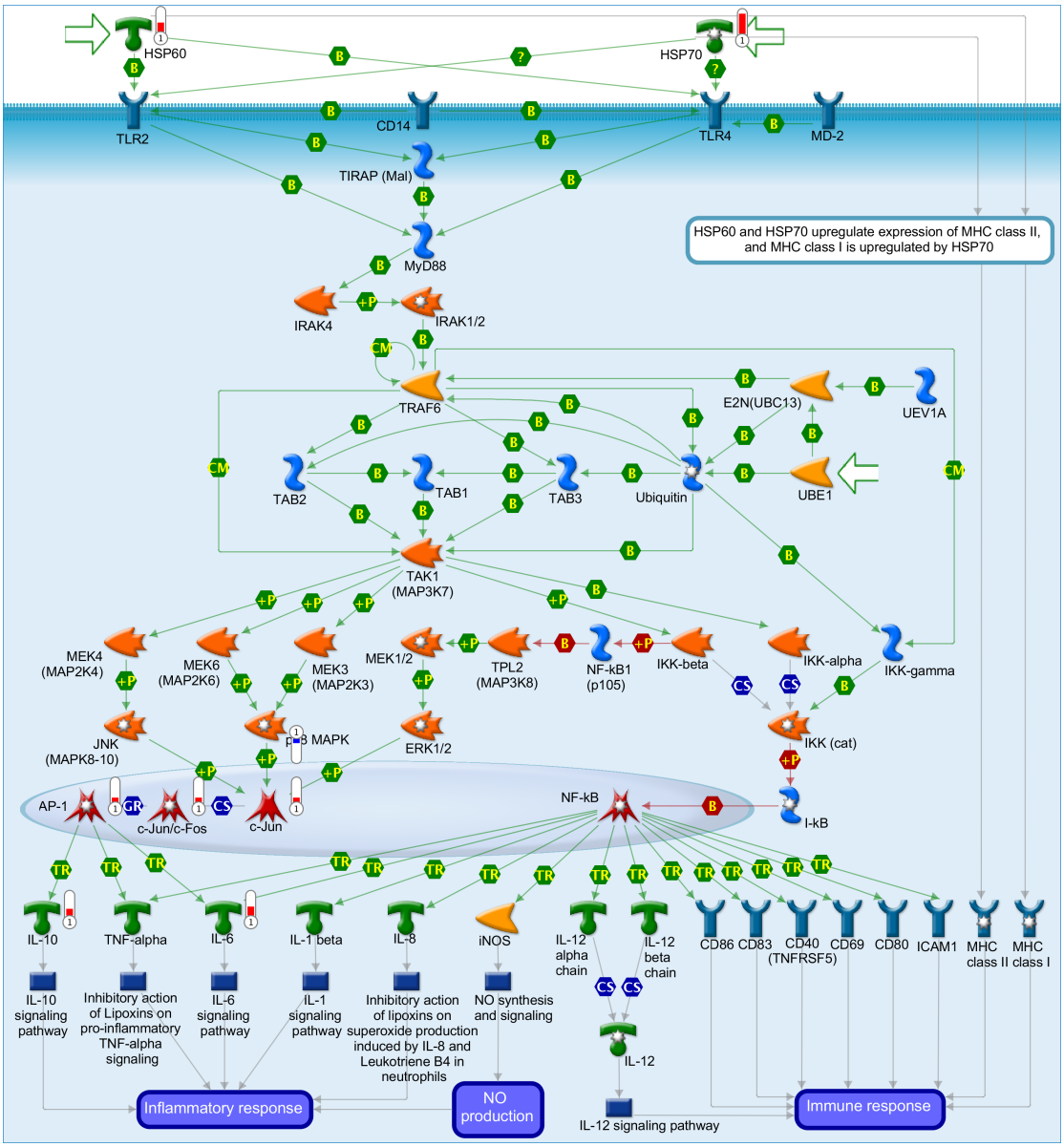


Figure 63: HSP60 and HSP70 mediation of inflammation in burns

This pathway shows the effect of the binding of HSP60 (+2.5FC) and HSP70 (+5.5FC) to toll like receptor (TLR) 2 and 4 respectively. The pattern of gene upregulation shows

that inflammatory response is dominant via the IL6 and IL10 signalling pathway with these cytokines showing increased expression compared to MHC classes 1 and 2 and the membrane receptors on the right side of the diagram with no significant change in expression.

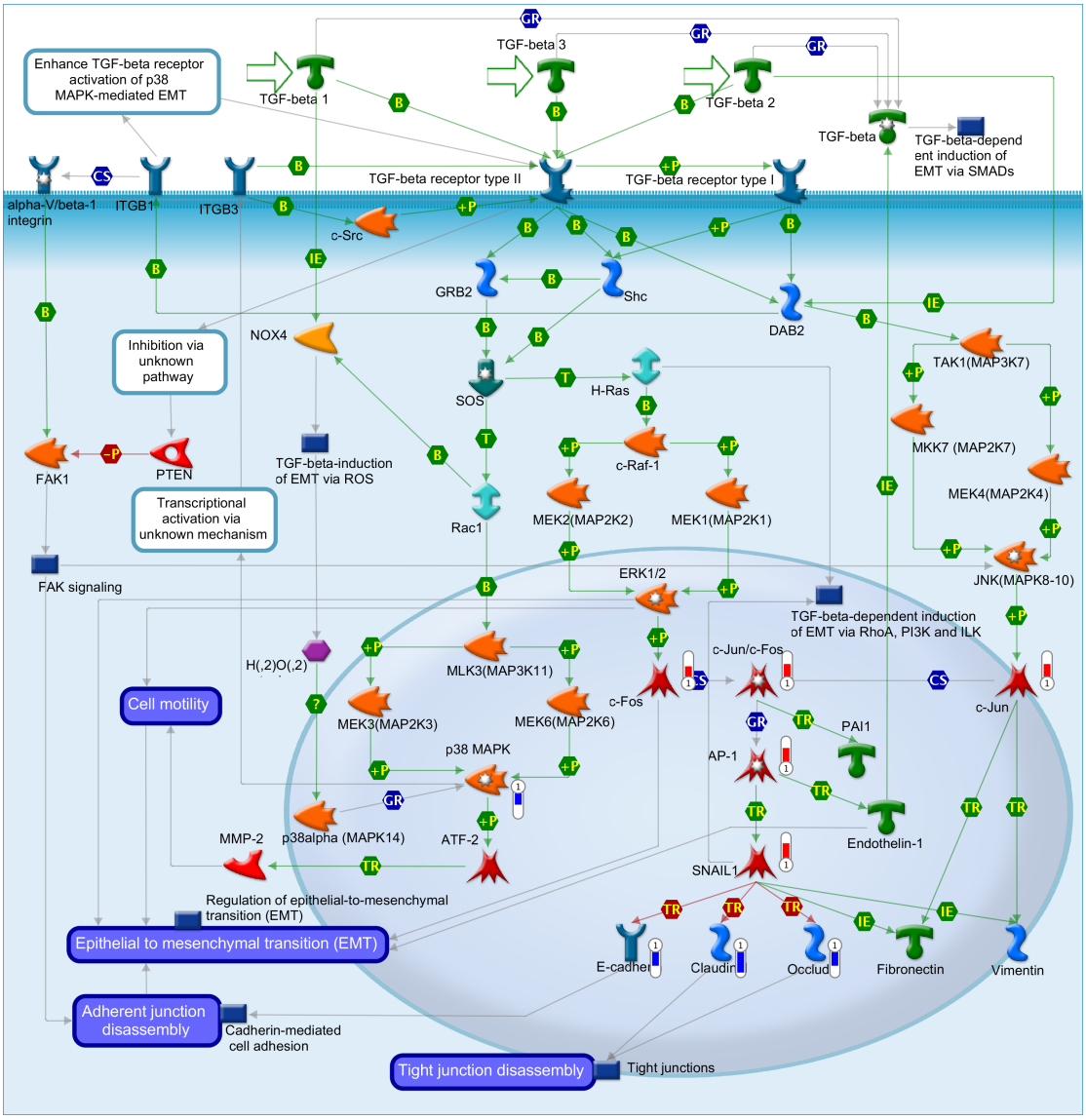


Figure 64: TGF beta induced epithelial to mesenchymal transition in burns
This diagram shows the process by which epithelium loses its tight junctions and becomes mesenchymal. The key step is the inhibition by SNAIL1 (Zinc finger protein SNAI1, represses ectodermal genes, and critical in embryonic mesodermal formation) of E-cadherin, Claudin, and Occludin, as shown above. The result is that there is

disassembly of tight junctions and adherent junctions, and epidermal dedifferentiation (epithelial to mesenchymal transition- EMT). It is striking that these changes are seen within 3 hours of injury, and represent both upregulation and downregulation of genes.

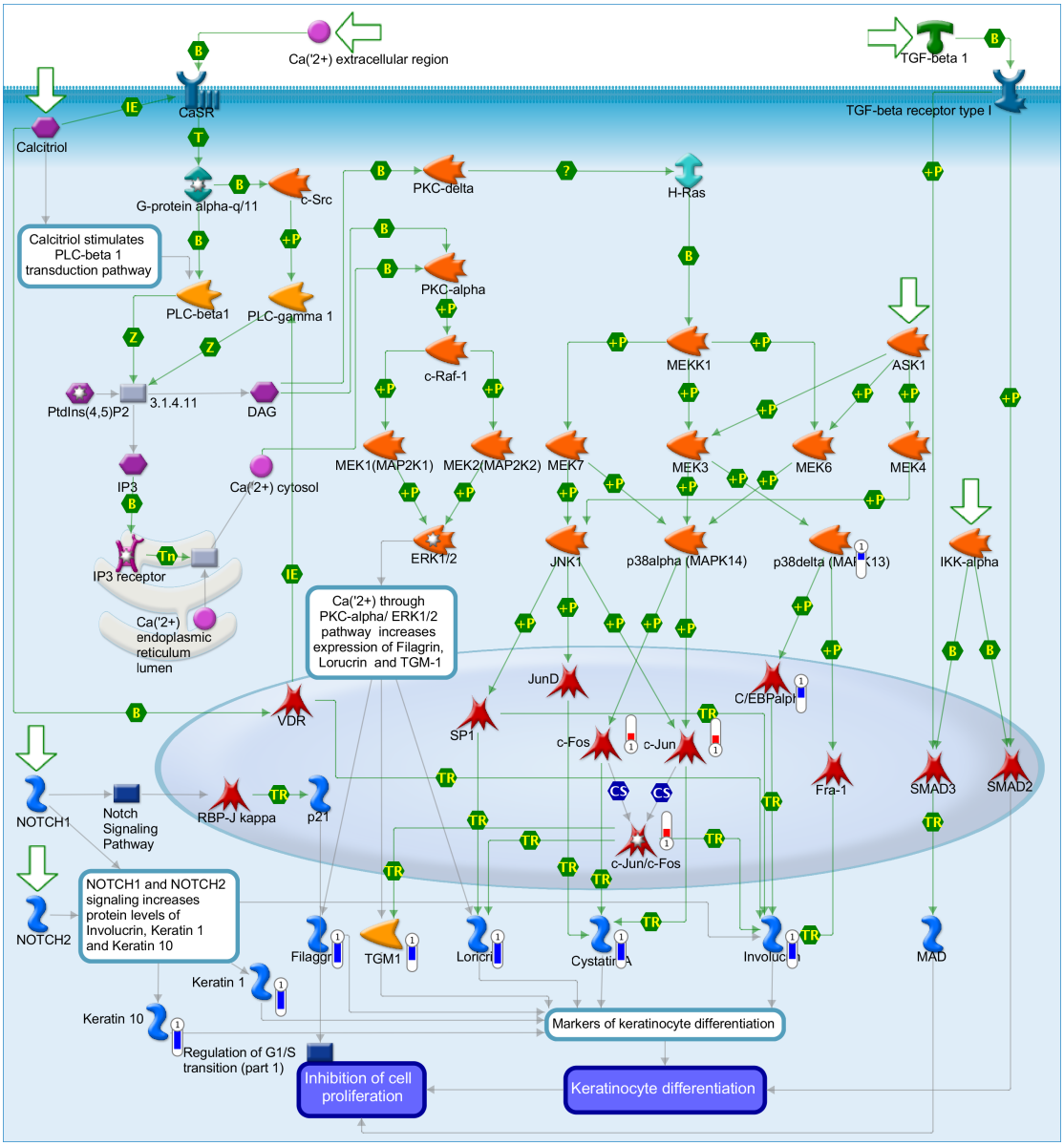


Figure 65: loss of keratinocyte differentiation

Figure 65 shows a global downregulation of keratins responsible for keratinocyte differentiation. The process is controlled via C/EBPalpha (CCAAT enhance binding protein, a regulator of differentiation during embryogenesis) that alongside the c-Jun/c-Fos complex, and NOTCH signalling controls the expression of:

Keratin 10: Forms the cytoskeleton on epithelial cells (-2.9 FC)

Keratin 1: Expressed in spinous and granular layers of the epidermis (-2.8 FC)

Filaggrin: associates with intermediate filament, in mammalian epidermis. Derives from profilaggrin, consisting of multiple units of filaggrin that are stored in keratohyalin granules, and proteolytically cleaved into individual filaggrin (-3.0 FC)

TGM1 (Transglutaminase 1): alkylates glutamine residues, causing cross-linking of proteins (-2.2 FC)

Loricrin: component of the cornified envelope of terminally differentiated epidermal cells (-3.1 FC)

Cystatin A: a cysteine protease inhibitor that forms complexes with cathepsins, and is a precursor protein for the cornified envelope of keratinocytes (-2.7 FC)

Involucrin: cytoplasmic protein crosslinked to membrane proteins of keratinocytes by transglutaminase (-2.4 FC)

The above markers of keratinocyte differentiation have all shown downregulation by >2 FC, or to 25% or less than their resting level of expression. Coupled with the increase in EMT, and loss of hair-follicle differentiation markers, it can be shown that the dedifferentiation of thermally-injured skin begins, and is well-established within 3 hours of injury.

6.4.4 Summary of the effects of thermal injury on the transcriptome of human skin

The comparison between the transcriptomes of burned and unburned skin has shown that there are significant changes in the transcription of genes upregulation of genes related to inflammation, coagulation, proliferation, and response to misfolding of protein, while genes related to differentiation of tissues, adhesion to the basement membrane, adjacent cells, and the extracellular matrix are downregulated indicating dedifferentiation in response to thermal injury, and a change towards a dedifferentiated, migratory phenotype. It also reflects the loss of skin functions both as a physical barrier, and as a barrier to water loss and infection. The changes are coherent, falling into canonical pathways, and indicating an integrated transcriptomic response to burning establishing itself within 3 hours of injury.

It is of great interest that inflammation and microvascular occlusion featured so prominently in the ontologies affected by thermal injury. The effects mediated by cooling were seen in terms of a visible reduction in oedema and blistering- possible clinical surrogate markers for inflammation- and a reduction of the depth of microvascular injury and occlusion.

6.4.5 The effect of cooling on the transcriptome of thermally-injured human skin

A comparison was made between the cooled and untreated burns in a pairwise manner within individuals using EdgeR software. This yielded a list of genes significantly affected by burning and this change, in turn, was significantly altered cooling.

When plotted in an Figure 52, the difference between the cooled and untreated burn transcriptomes was much less than that between uncooled burns and normal, uncooled skin. This was also apparent in the pairwise comparison between cooled and untreated burns. The FDR threshold was lowered to 0.2 from 0.05 to increase the number of candidate genes.

Below is a table of the genes with the greatest change in their expression levels mediated by cooling when cooled burns were compared to uncooled burns (BC BNC). The effect of burning upon these genes, i.e. the fold-change between uncooled skin and uncooled burn, is also shown for the genes where there was a significant difference (BNC CNC). Genes that were upregulated in the test sample compared to the baseline are in red, while those downregulated in that context are in blue.

	logFC BNC CNC	FDR	logFC BC BNC	FDR
SPRR2G	-4.1	5.4E-10	2.34	3.2E-07
PDE4C	3.0	1.8E-44	-0.80	1.5E-02
NAALAD2	1.3	7.7E-32	-0.44	3.6E-02
HSPA6	5.5	6.2E-113	-0.72	3.7E-02
MIR5087	4.5	5.9E-46	-0.82	3.7E-02
HBB	2.5	1.5E-06	-1.53	3.7E-02
KRT82			3.86	8.6E-02
ADAMTS16			0.65	1.5E-01
DNAJB1	3.8	2.5E-86	-0.55	1.8E-01
LRP1B	0.6	1.5E-07	-0.37	1.8E-01
TCHH			2.52	1.8E-01
PRKCG	4.8	2.5E-20	-1.36	1.8E-01
HORMAD1	0.8	1.7E-01	-0.90	1.8E-01
PRR9	-1.2	8.9E-02	2.52	2.0E-01
GDA	-1.4	1.7E-03	1.32	2.0E-01
TCHHL1			2.33	2.0E-01
AZGP1			0.41	2.0E-01

Table 13: genes showing differential expression in cooled burns compared to uncooled burns

1.1.1.1.1 Genes upregulated by cooling in the context of burning

Taking an FDR of 0.2 as the threshold, 8 genes were upregulated by cooling. In three (SPRR2G, PRR9, and GDA), there was a significant downregulation in the context of burning, when compared to normal, unburned skin.

Those genes that were upregulated by cooling in the context of burning have following functions:

Small proline-rich protein 2G (SPRR2G) is found in the envelope of keratinocytes where it is cross-linked by transglutaminase.

Keratin 82 (KRT82) is a type II hair keratin, and forms heterodimers with type I keratins in hair and nails, and is hair cuticle-specific.

ADAM Metallopeptidase with Thromospondin Type 1 Motif 16 (ADAMTS16) has several distinct regions, including a disintegrin-like domain, a metalloprotease domain, and a thrombospondin type I region. It has been implicated in inhibition of chondrosarcoma metastasis, and may regulate blood pressure.

Trichohyalin (TCHH) is found in the inner root sheath of hair follicles and contributes to mechanical strength. It is covalently modified by TGM3, which is itself downregulated in burned skin.

Proline rich 9 (PRR9) is found at an RNA level predominately in skin, and is involved in keratinocyte differentiation.

Guanine deaminase (GDA) deaminates guanine and may play a role in microtubule assembly.

Trichohyalin-like 1 (TCHHL1), also known as S100A17, is restricted to the distal inner root sheath of the hair follicle, and plays a role in hair morphogenesis.

Alpha-2-glycoprotein 1, zinc-binding (AZGP1) increases lipolysis in adipocytes, and may have a role in fat loss seen in advanced cancer.

1.1.1.1.2 Genes downregulated by cooling in the context of burning

With the same FDR threshold, the following genes were down-regulated by cooling in the context of burning:

Phosphodiesterase 4C (PCE4C) regulates levels of cAMP and thereby the response to this second messenger.

N-acetylated alpha-linked acidic pipeptidase 2 (NAALAD2) is a member of the prostate-specific antigen family. It cleaves N-acetyl-L-aspartate-L-glutamate (NAAG), a neuropeptide in the central and peripheral nervous system.

Heat-shock protein A6 (HSPA6) is expressed in response to misfolded protein, as follows thermal injury, and is associated with the cellular response and acclimatisation to heat.

MicroRNA 5087 (mir5087) is a non-coding RNA molecule that modifies the expression of other genes through missense matching with mRNAs.

Haemoglobin beta (HBB) encodes for the beta chain of adult haemoglobin. The downregulation of this may simply reflect a smaller volume of coagulated vasculature and hence fewer trapped reticulocytes containing the RNA species, as evidenced by the significantly reduced vascular occlusion in the cooled burns, see previous chapter.

DnaJ heat shock protein family (HSP40), member B1 (DNAJB1) is a molecular chaperone that ensures correct folding of newly-synthesised proteins, assembles complexes of different proteins, and enhances the ATPase activity of HSP70 in order to improve its protein-folding activity.

Low-density lipoprotein receptor 1B (LRP1B) effects receptor-mediated endocytosis in response to ligand-binding.

Protein kinase C gamma (PRKCG) is activated by DAG and intracellular calcium. Found within neurones, it plays a role in long-term potentiation and long-term depression in neural tissues. It may also have a role in neuropathic pain.

HORMA domain containing 1 (HORMAD1) is involved in the formation of gametes through its role in meiosis in both sexes. Unlikely to be significant in this scenario, and its downregulation was not significant in the context of burning.

1.1.1.1.3 Heat map of the first 17 genes affected by cooling in the context of burns

When plotted as a heatmap with EdgeR software, with hierarchical gene clustering, the groups of samples clustered as shown in Figure 66.

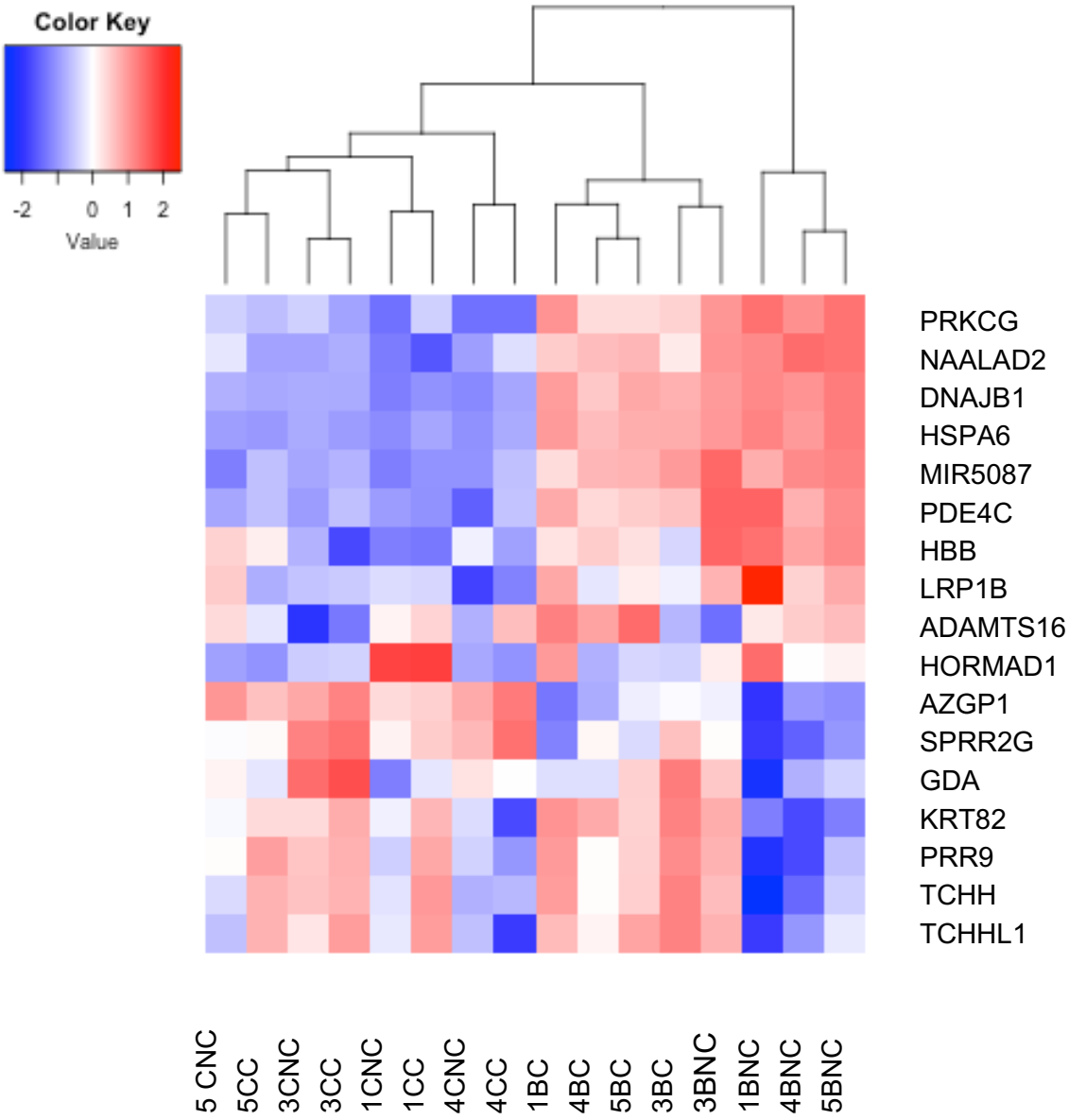


Figure 66: heat map plotting the 16 samples from 4 patients with respect to the 17 genes identified as significantly altered when BN was compared to BNC

In Figure 66, the relative up regulation and downregulation of the genes identified in the comparison of the cooled and untreated burns have clustered the samples more closely by condition (cooled or uncooled burn) than by individual, even though on the MDS plot they were more widely separated by individual. The controls have grouped by individual rather than according to their relative expression levels of these genes, showing that these genes are important in the context of cooling with burning, but not in cooling alone in normal skin. Cooling also seems to move the expression levels of the genes in question in the direction of that seen in normal skin, i.e. reducing the

expression of genes upregulated by burning, and increasing the expression of genes downregulated by burning.

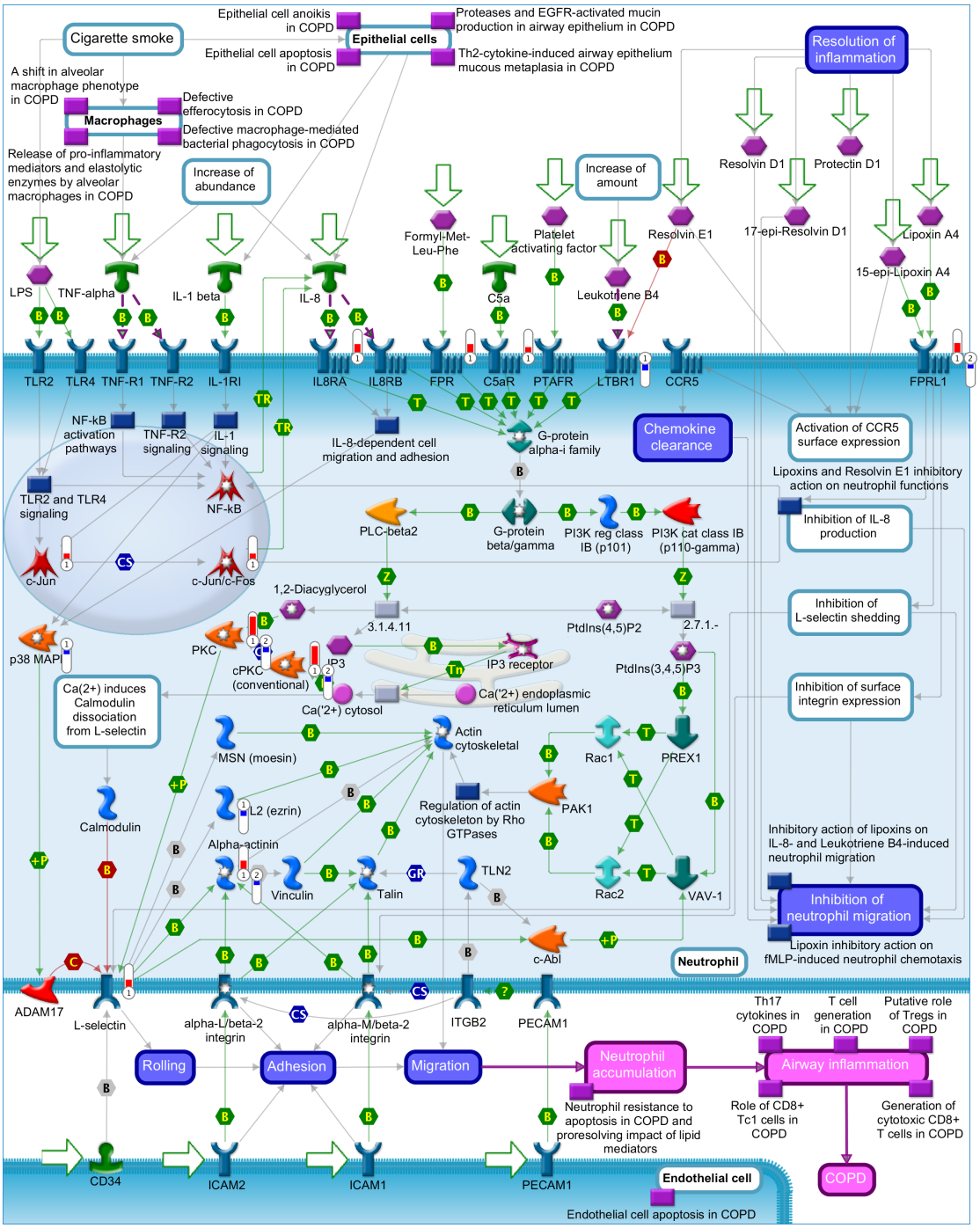
6.4.5.1 The effect of cooling burns on pathway analysis in Metacore

1.1.1.1.4 ADAMTS16 and PRKCG

This diagram shows the interaction of genes identified in both the comparison of untreated burns and normal skin, and cooled and untreated burns. ADAMTS16 (circled in blue, upregulated 0.65FC in cooled compared to untreated burns) cleaves Aggrecan (large aggregating proteoglycan), thereby inactivating it. Aggrecan binds CD44 (involved in cell adhesion and migration) and activates it, in turn activating L-selectin (binding and rolling of leukocytes on endothelium, upregulated 1.7FC in burned compared to normal skin). It can hence be seen that an increase in expression of ADAMTS16 might result in less expression of L-selectin, and less neutrophil adhesion and migration as a result.

Cooling also reduces (-1.4FC) the expression of PRKCG (upregulated in burning 4.8FC), and PRKCG phosphorylates and activates L-selectin, making it possible that the reduction of PRKCG expression might have an inhibitory effect on neutrophil binding on endothelium. The combined effect of an upregulation of ADAMTS16 and a downregulation of PRKCG might be sufficient to reduce neutrophil adhesion vial L-selectin sufficiently to have a beneficial effect on the burn.

The diagram from Metacore below puts this in the context of neutrophil adhesion (in the lung affected by COPD), but never the less shows the integration of these mechanisms.



The thermometer icons labelled “1” are the expression change seen between untreated burns and normal skin, while the “2” denotes the comparison between cooled and untreated burns. The position of conventional protein kinase C (cPKC) in the activation of the L-selectin receptor, and the subsequent binding of alpha-actin to drive migration are both depressed (blue thermometer icon) in cooled, compared to untreated burns. It can also be seen that burning reduces the expression of p38 MAPK

which in turn phosphorylates and activates ADAM17 to inactivate L-selectin through cleavage, hence burning reduces the inhibition of L-selectin, and increases endothelial adhesion.

1.1.1.1.5 Protein kinase C in complement pathway disruption in thrombotic microangiopathy

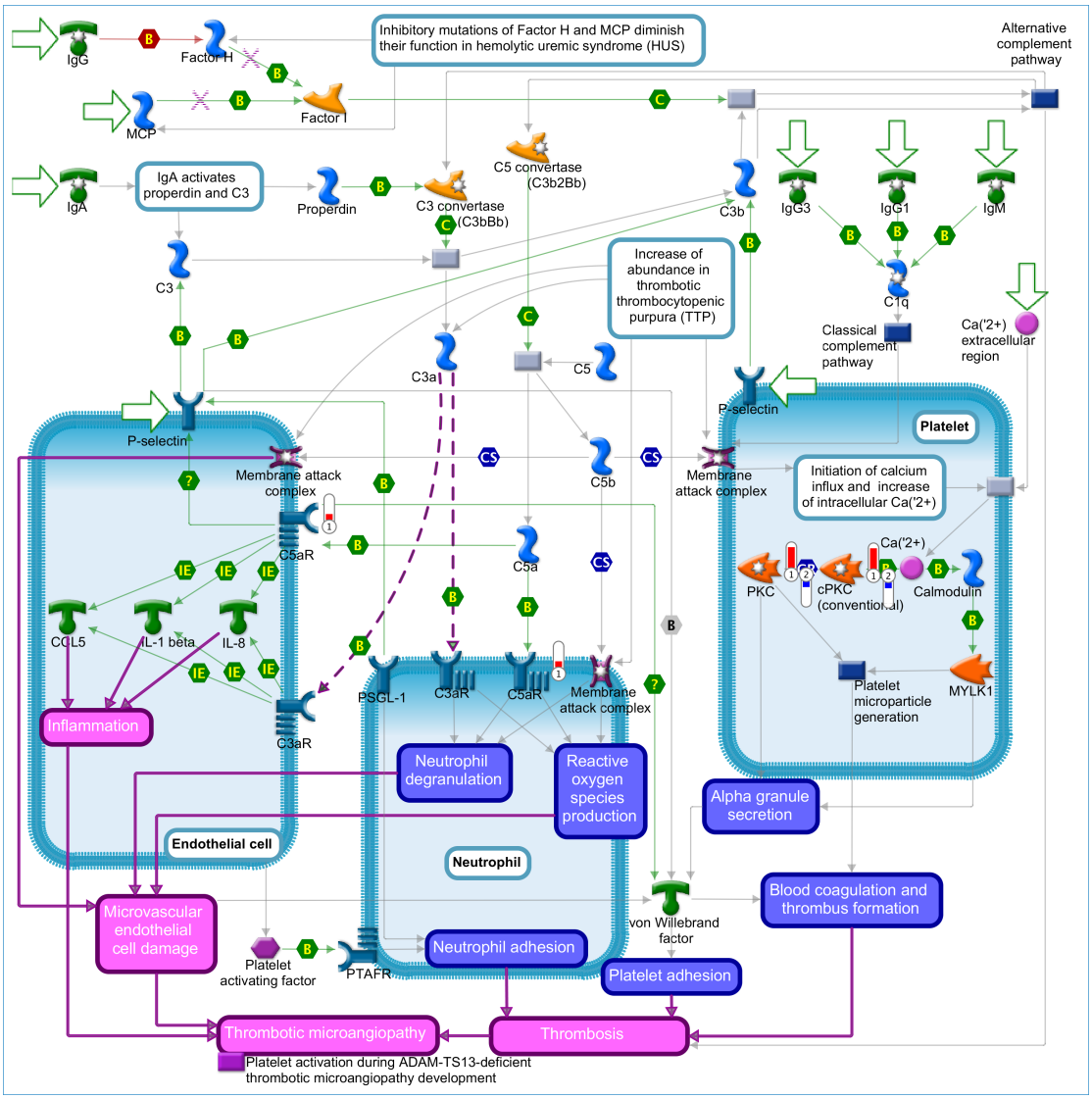


Figure 67: PRKCG and its possible role in complement pathway disruption in thrombotic microangiopathy.

While not purpose-built for the burn model, Figure 67 shows the interaction between effectors known to be active and regulated in the burn model. The C5aR is upregulated by burning, and activation by C5a causes release of platelet activating factor. The

same binding of C5a to C5aR in neutrophils results in generation of reactive oxygen species via NADPH oxidase. The action of PKC in platelets causes the release of alpha granules, and the generation of platelet microparticles, leading to microvascular occlusion. There was reduction of PKC in cooled burns, where there was also reduced vascular occlusion, indicating a possible interaction between PKC and platelet microparticle formation and vascular occlusion. A more detailed diagram of platelet microparticle formation is shown in Figure 68.

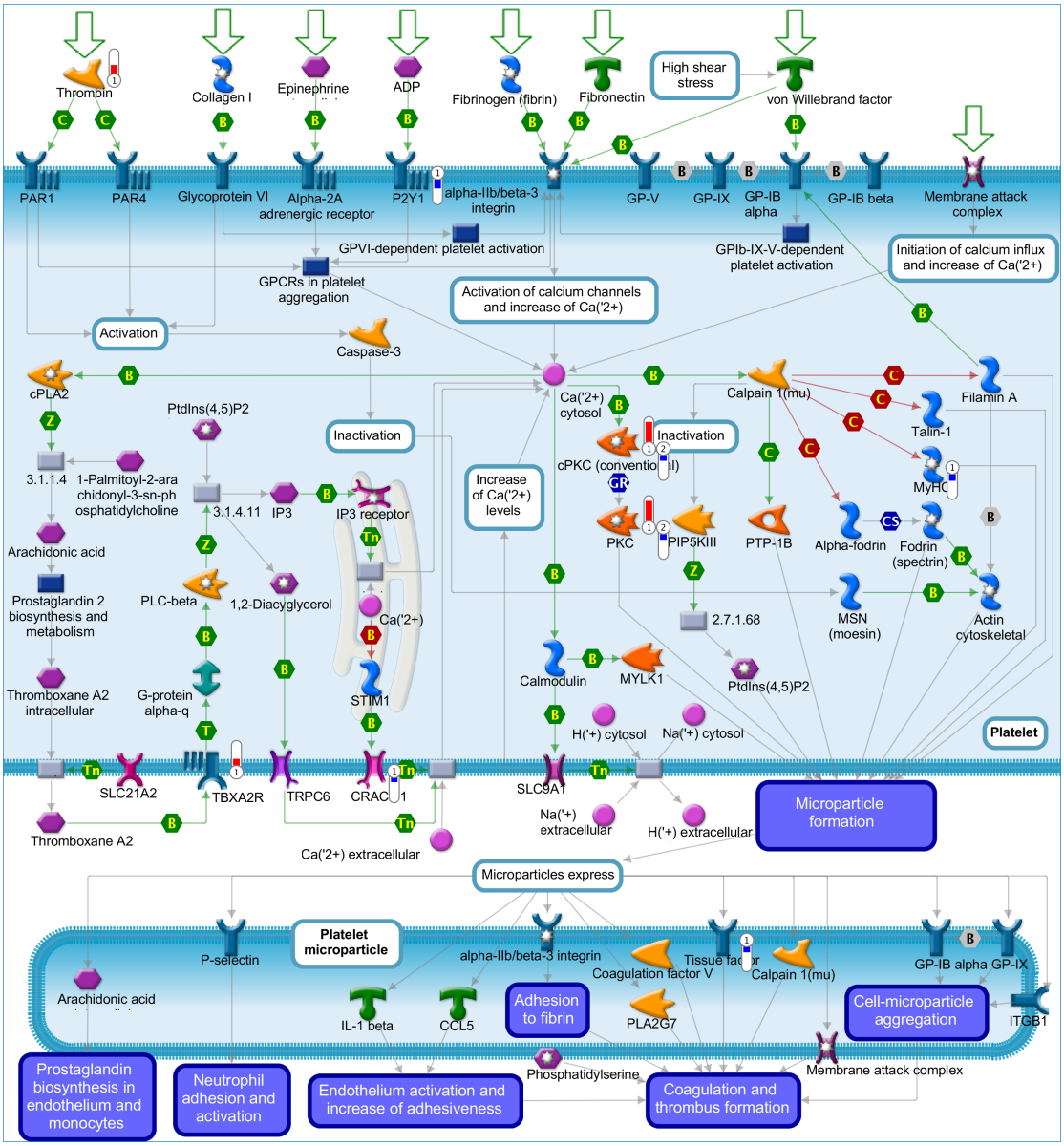


Figure 68: platelet microparticle formation, and the possible effect of reduced PRKCG expression in cooled burns.

The “1” by the thermometer icon indicates comparison between uncooled burns and uncooled controls, while “2” denotes the comparison between cooled and uncooled burns.

The increase in both thrombin and TBXA2R expression results in an increase in intracellular calcium, and activation of PKC, in turn driving the formation of microparticles and vascular occlusion through a combination of platelet and neutrophil adhesion, and activation of clotting factors.

1.1.1.1.6 The effects of cooling on epidermal differentiation

Taken together, the genes upregulated by cooling in a burn represent aspects of epidermal differentiation.

The upregulation of KRT82, TCHH and TCHHL1 all reflect either an increase in the transcription of these RNA species within the burned tissues, or an increase in the number of viable cells that express them. The localisation of TCHHL1 to the distal hair follicle, i.e. a more superficial part of it, would make it more vulnerable to thermal injury, and so the increase in the expression of this RNA species in cooled burns may reflect the salvage of this very specific part of the hair follicle through cooling.

The upregulation of PRR9 and SPRR2G suggests a retention of keratinocyte and epidermal differentiation, either by relative upregulation within individual keratinocytes, or a greater number of viable keratinocytes expressing these genes.

Taken in context with findings from the comparisons of untreated burns and normal skin, where it was found that there was widespread downregulation of genes associated with epidermal and keratinocyte differentiation, in can be argued that cooling reversed some of these changes and effects.

6.5 Validation of findings with qPCR

The findings from the RNAseq data regarding the effects of burning and cooling upon the transcriptome of human skin. Given the limited amounts of RNA available for this part of the project, the genes of greatest interest were those that were differentially expressed in cooled and untreated burns, and this was a relatively short list of genes to validate.

The RNA was taken from the same samples as those submitted for RNAseq, and from a further 5 patients in the study with cooled and uncooled burns and controls harvested at 3 hours after burning. This provided a total of 10 biological replicates of the experiment.

The list of genes was compiled from analysis of all five patients as well as analysis of the four with patient 2 excluded as a relative outlier in terms of transcriptional response to burning as shown in Figure 52. These genes showed significant alteration in expression in cooled compared to uncooled burns.

The RNAseq data had shown that there was a wide variation in expression of these genes in terms of CPM in Table 14: Counts per million (CPM) of each gene

Geneid	Counts per million (CPM)																			
	1BC	1BNC	1CC	1CNC	2BC	2BNC	2CC	2CNC	3BC	3BNC	3CC	3CNC	4BC	4BNC	4CC	4CNC	5BC	5BNC	5CC	5CNC
HSPA6	123.3	164.5	3.9	2.7	42.2	119.5	1.6	3.7	82.6	104.6	3.0	4.2	63.3	109.8	3.2	3.4	79.1	193.2	2.6	2.7
HSPH1	655.9	728.9	53.8	46.5	221.1	377.2	48.8	47.2	445.5	565.6	45.4	55.4	393.6	725.8	37.0	43.7	621.0	910.6	47.8	40.4
PDE4C	5.8	10.6	1.0	1.2	4.5	6.1	1.6	1.1	4.4	9.1	1.3	1.0	3.5	5.3	1.3	0.5	3.8	7.6	1.2	0.9
PTGER1	2.5	2.9	0.1	0.2	0.7	1.6	0.1	0.1	1.3	2.6	0.0	0.1	1.1	4.5	0.1	0.1	2.7	5.9	0.0	0.1
CHORDC1	118.6	156.0	38.5	43.3	66.9	85.4	47.9	39.7	108.4	118.1	46.5	51.7	85.8	127.9	42.8	50.8	119.6	162.3	40.7	38.1
PRKCG	2.1	3.5	0.1	0.0	0.8	0.9	0.2	0.2	0.9	1.9	0.1	0.1	0.6	1.9	0.0	0.0	0.8	3.4	0.1	0.2
RAB3B	10.3	7.1	37.4	34.2	41.0	27.8	52.4	44.7	23.2	15.7	45.5	44.4	8.0	7.3	27.7	37.9	19.1	11.5	38.6	38.1
AZGP1	82.4	55.6	180.9	187.1	161.7	131.9	188.7	189.6	132.8	114.4	209.9	204.1	95.5	83.0	191.3	245.1	120.1	85.2	176.9	178.0
PALMD	86.8	75.4	127.8	111.6	123.1	90.6	131.5	96.0	117.5	92.2	143.7	135.7	103.4	82.4	146.2	130.7	112.7	93.7	143.1	147.4
KRT25	46.1	0.1	44.4	11.2	0.1	0.0	0.0	0.2	60.1	34.8	40.1	34.7	22.1	4.1	6.4	10.3	13.7	3.4	29.9	8.4
KRT27	20.2	0.0	19.6	4.9	0.1	0.1	0.1	0.2	21.9	10.0	14.9	13.8	7.3	1.7	2.0	4.2	9.7	2.1	14.3	3.5
PRR9	13.6	0.1	11.3	2.6	0.1	0.1	0.2	0.2	14.3	8.5	9.3	7.4	4.6	0.3	0.4	2.7	5.2	2.0	10.5	3.1
EHF	170.6	97.8	184.6	155.0	202.4	138.1	183.6	171.0	177.9	152.5	184.6	161.2	124.5	121.1	135.7	130.8	211.1	157.7	164.8	163.6
TCHH	85.8	1.7	90.3	24.7	1.4	1.2	0.9	0.7	109.6	49.7	59.1	55.8	28.9	5.0	10.5	14.7	46.2	15.7	62.5	15.9
KRT82	2.5	0.1	1.7	0.5	0.0	0.1	0.1	0.1	3.2	1.6	1.7	1.0	1.7	0.0	0.0	0.4	1.0	0.1	1.1	0.4
KRT34	1.9	0.1	1.8	1.1	0.4	0.1	0.1	0.0	7.0	3.5	1.7	1.7	0.1	0.1	3.4	1.3	2.8	1.4	1.5	0.5
KRTAP3-1	1.3	0.0	0.9	0.3	0.0	0.0	0.0	0.0	3.5	1.2	0.5	0.9	0.3	0.0	1.9	0.1	1.2	0.7	0.6	0.1
TCHHL1	1.3	0.0	1.7	0.5	0.0	0.0	0.0	0.0	2.6	1.1	1.2	0.5	0.3	0.0	0.0	0.2	1.5	0.3	1.2	0.0

Table 14: Counts per million (CPM) of each gene

The red columns represent the four samples from patient 2, who's samples grouped closer together in Figure 52 than the other samples. There is a wide range of expression levels, from the very abundant (HSPA6, HSPH1, CHORDC1), to those expressed at very low levels (TCHHL1, KRT34, KRT82, KTRTAP3-1).

A review of the literature on housekeeping gene choice in a wound model highlighted the importance of selecting housekeeping genes[83] that have a stable expression across all 4 groups in all 4 patients in the study.

A dataset of all genes expressed as CPM was used, and the Log2 of each count was calculated. The standard deviation of the log2 value for each gene for each sample was then calculated and sorted to establish the genes with the lowest variability for this precise dataset, and for this model. Known housekeeping genes were selected from the genes showing the least variability

Housekeeping gene	Mean Log2 CPM	SD
GAPDH	6.4	0.09
Succinate dehydrogenase	9.2	0.11
Actin R2	8.1	0.01

Table 15: Log2 counts per million (CPM) and SD CPM for housekeeping genes in the burns dataset

6.5.1 Primer sequences

Primer	Direction	Sequence 5'-3'	Direction	Sequence 5'-3'
ACT2R	F	GCGGTCGCTGTAGGTTGT	R	GCCTGCATATCCACACTTCAC
AZGP1	F	CCCCAGGAGAACCAAGATG	R	CGGGGACGTCTTCAACAT
CHORDC1	F	GCCAGTAGAAGCAATAAAAAGACC	R	TGATGACAGTTTAAGTTTATCAAGTGC
EHF	F	GCAACAACCTCCTTCACCAG	R	TTGGTCCAGTACTGAGGATGAAT
HSPA6	F	GGATAAAAAGCCCGTGGAA	R	GCTCTCCCTGCGGTTTCT
HSPH1	F	AAATCCCAGATGCTGACAAAG	R	CCACCTTTATTTTGGGCTTTTTA
KRT25	F	ACCTCAAAAAGAACCATAAAGAGG	R	CTGCGTTCATCTCCACGTT
KRT27	F	CTCAAGAAGAATCATGAGGAGGA	R	GCGTTCATCTCCACGTTCA
KRT34	F	GGAGAGTGAGGACTGCAAGC	R	CCACAGGAGTTGCCACTAGC
KRT82	F	CGAAGCAGAGGCCTGGTA	R	CGGAGGTTGTCACAGTGGT
KRTAP3_1	F	GCTGCAAGCCTGATACCTATG	R	GGAGTCGGGTGACAGTTGTT
PALMD	F	TGAGGATCCATCCTTAACAGC	R	GGTGGTACAACTCTTAGATCACCTT
PDE4C	F	ATGCCTAGGAGCAGCCAAG	R	GCTCGTCTAGCGTCTCCAAT
PRKCG	F	CTGTATGAGATGTTGGCAGGAC	R	GTTCCATGATGGCCTGAAA
PRR9	F	CCCCTGCCAAGATAAGTGTC	R	TTGATTCCTGGCACTGAGAA
PTGER1	F	ATGGTGGTGTCGTGCATCT	R	CGCTGCAGGGAGGTAGAG
RAB3B	F	TGACATCACCAATGAAGAGTCC	R	TGTCCCAGGAGTAGGTCTTGA
SDHA	F	TCCACTACATGACGGAGCAG	R	CCATCTTCAGTTCTGCTAAACG
TCHHL1	F	ACCTGCCTCGCTTGTGAAC	R	TGGAATGTCTCAATTACACAGAGG
TCHH	F	TGCAGTTCGTGATAACCAAGGTT	R	AACTGCCGGAACTGTTCATT

Table 16: primer sequences for QPCR

The primers in Table 16 were designed with the Roche primer design web tool and made intron-spanning to prevent amplification of genomic DNA.

6.5.2 Primer validation

The primers were all tested on a DNA library prepared from the most abundant sample. All primers amplified except for KRT34, KRT82, KRTAP3-1, and TCHHL1, reflecting their low abundance in the sample.

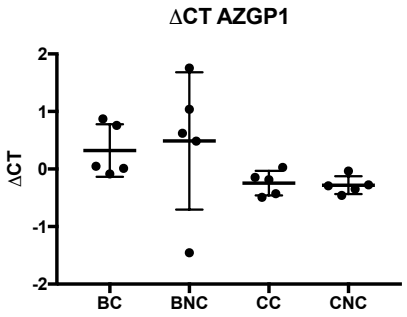
6.5.3 Validation of the genes altered by cooling in burns

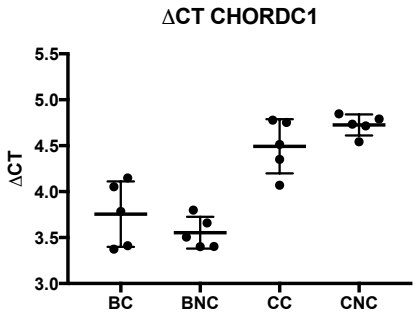
Each gene was run in triplicate against all genes identified, with all 3 house-keeping genes tested on all samples in triplicate on each plate used.

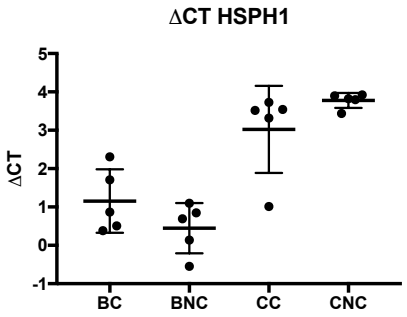
The scatter plots with 95% confidence intervals for each gene follow, with each gene's expression level (ΔCT) expressed in relation to the house-keeping gene Actin R2.

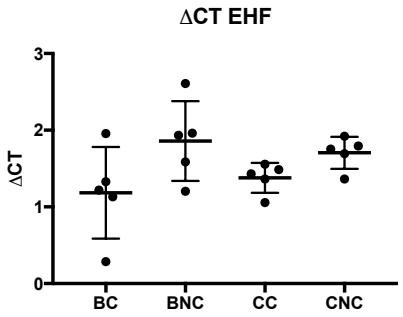
6.5.3.1 Scatter plots of qPCR data

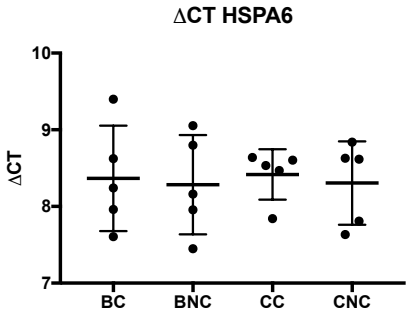
The following scatter plots show the ΔCT of each gene relative to the housekeeping gene Actin R2. All three housekeeping genes showed very uniform amplification and consistent CT values across all samples tested.

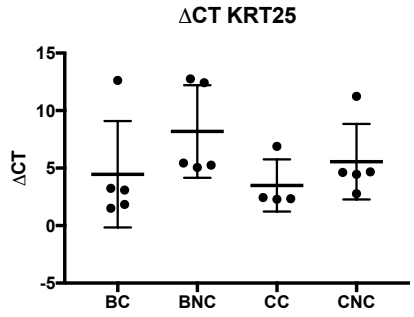


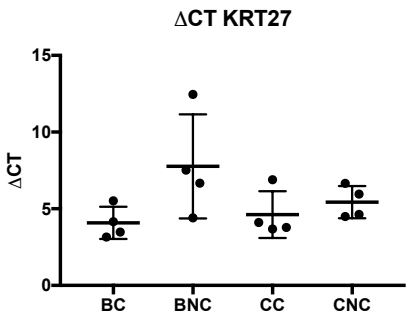


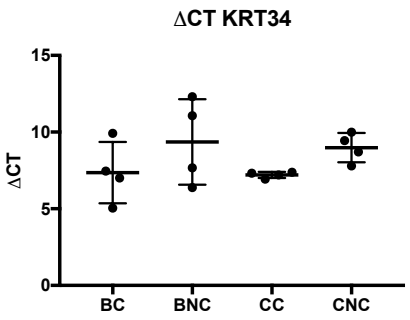


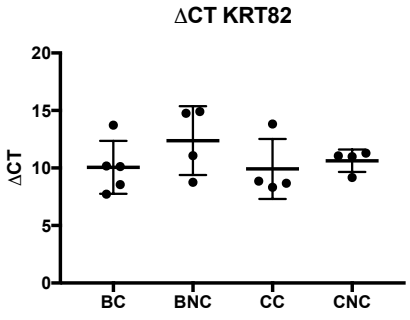


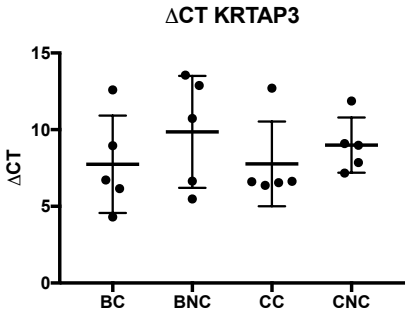


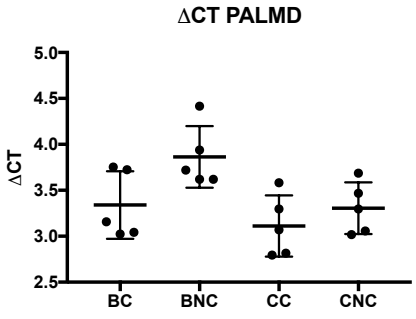


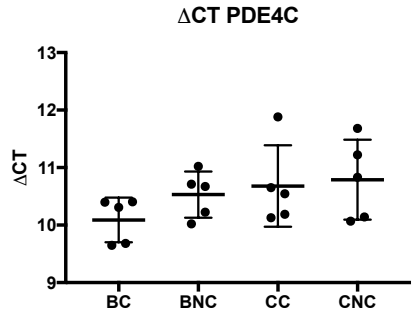

ΔCT KRT27
ΔCT
15
10
5
0
BC
BNC
CC
CNC

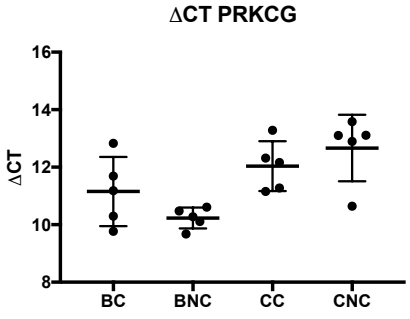

ΔCT KRT34
ΔCT
15
10
5
0
BC
BNC
CC
CNC

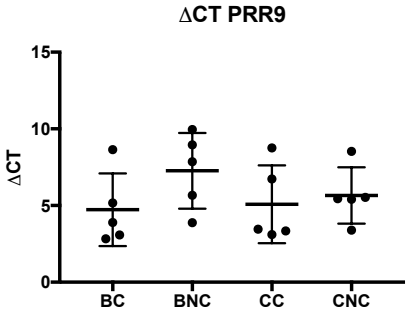

ΔCT KRT82
ΔCT
20
15
10
5
0
BC
BNC
CC
CNC

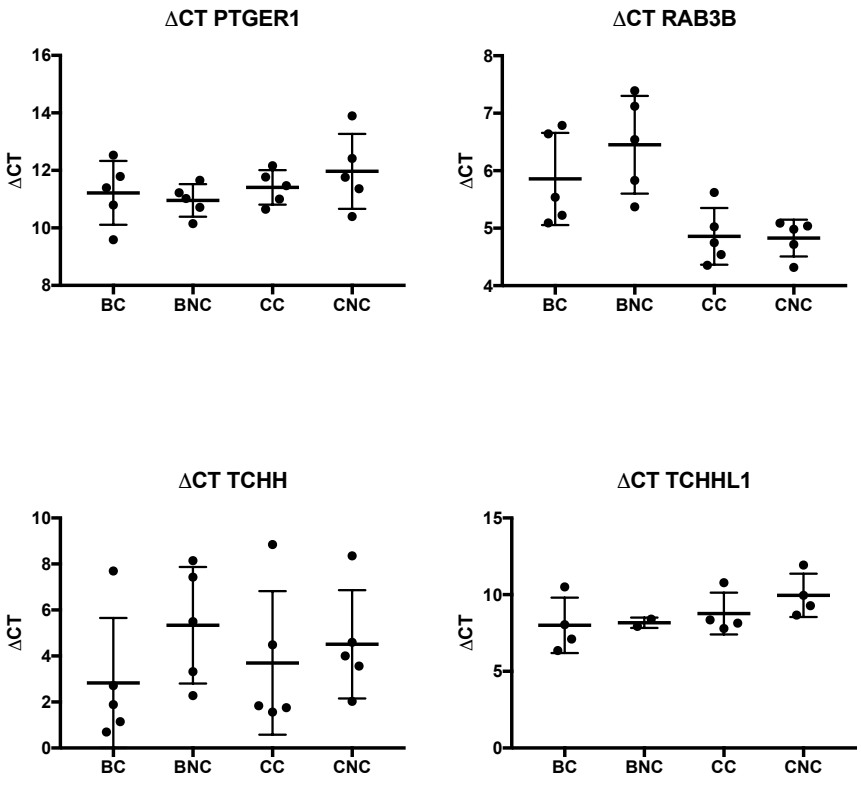

ΔCT KRTAP3
ΔCT
15
10
5
0
BC
BNC
CC
CNC


ΔCT PALMD
ΔCT
5.0
4.5
4.0
3.5
3.0
2.5
BC
BNC
CC
CNC


ΔCT PDE4C
ΔCT
13
12
11
10
9
BC
BNC
CC
CNC


ΔCT PRKCG
ΔCT
16
14
12
10
8
BC
BNC
CC
CNC


ΔCT PRR9
ΔCT
15
10
5
0
BC
BNC
CC
CNC



6.5.3.2 Summary of qPCR and RNAseq data

The scatter-plots show a generally more consistent level of expression of the gene in the two control samples compared to the burned samples. There is a tendency for the cooled group of burn samples to have a level of expression for the given gene between that of the uncooled burns and the controls, while the level of expression between the cooled and uncooled control samples is broadly similar.

Table 17 below summarises the mean fold-changes for each gene when pairs of conditions- uncooled burn (BNC) and uncooled control (CNC), cooled burn (BC) and cooled control (CC), and cooled burn (BC) and uncooled burn (BNC)- are compared, and shows the fold-changes obtained from the RNAseq data.

Gene	BNC vs CNC		BC vs CC		BC vs BNC	
	RNAseq	qPCR	RNAseq	qPCR	RNAseq	qPCR
AZGP1	-1.1	-0.8	-0.7	-0.6 (0.05)	0.4	0.2
CHORDC1	1.5	1.2 (0.0008)	1.17	0.7	-0.4	0.2
HSPH1	3.8	3.3 (0.002)	3.2	1.9	-0.5	-0.7
EHF	-0.2	-0.5	0.04	0.2	0.4	0.7
HSPA6	5.3	0.02	4.7	0.05	-0.9	0.08
KRT25	-1.8	-3.0	0.4	1.1	2.8	4.7
KRT27	-1.6	-2.3	0.4	0.5	2.6	3.7
KRT34	-0.6	-0.4	0.3	-0.1	1.5	2.0
KRT82	-1.2	-1.2	1.0	-0.2	2.9	2.8
KRTAP3-1	0.3	-0.9	0.5	0.02	1.9	2.1
PALMD	-0.5	-0.6	-0.4	-0.2	0.3	0.5 (0.02)
PDE4C	3.0	0.3	1.8	0.6	-0.8	0.4
PRKCG	4.4	2.4 (0.03)	3.2	0.88	-1.2	-0.9
PRR9	-1.6	-1.6	0.6	0.4	2.7	2.5

Gene	BNC vs CNC		BC vs CC		BC vs BNC	
	RNAseq	qPCR	RNAseq	qPCR	RNAseq	qPCR
PTGER1	4.9	1.0	4.8	0.2	-1.1	-0.3
RAB3B	-1.7	-1.6 (0.02)	-1.2	-1.0 (0.06)	0.5	0.6
TCHH	-0.9	-0.8	0.5	0.9	2.1	2.5
TCHHL1	0.01	-	0.6	0.8	2.3	-

Table 17: summary and comparison of qPCR and RNAseq data, with p-values given in parentheses where significant

1.1.1.1.7 Correlation of RNAseq and qPCR results in fold-changes in cooled and untreated burn comparisons

There seems to be a reasonable correlation between the fold-changes in gene-expression between RNAseq and qPCR, despite the differing mechanisms of the two experiments: RNAseq can match partially-degraded transcripts to a gene, while qPCR requires an exact match to the primer for it to amplify. The comparison that had been used to identify the genes of interest was that of cooled burns to uncooled burns. Furthermore, there was significant RNA degradation when burned skin RNA samples were compared to unburned RNA samples, but not a significant difference between the RNA integrity of cooled and uncooled burn-derived RNA samples.

The correlation of the RNAseq and qPCR fold-changes for BNC/CNC, BC/CC and BC/BNC has been calculated.

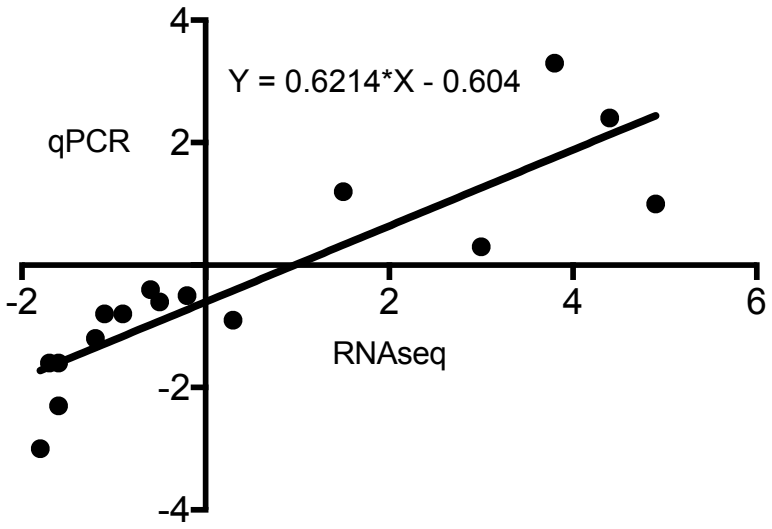


Figure 69: RNAseq qPCR correlation for the comparison of Log2 FC of the genes of interest in uncooled burns and controls

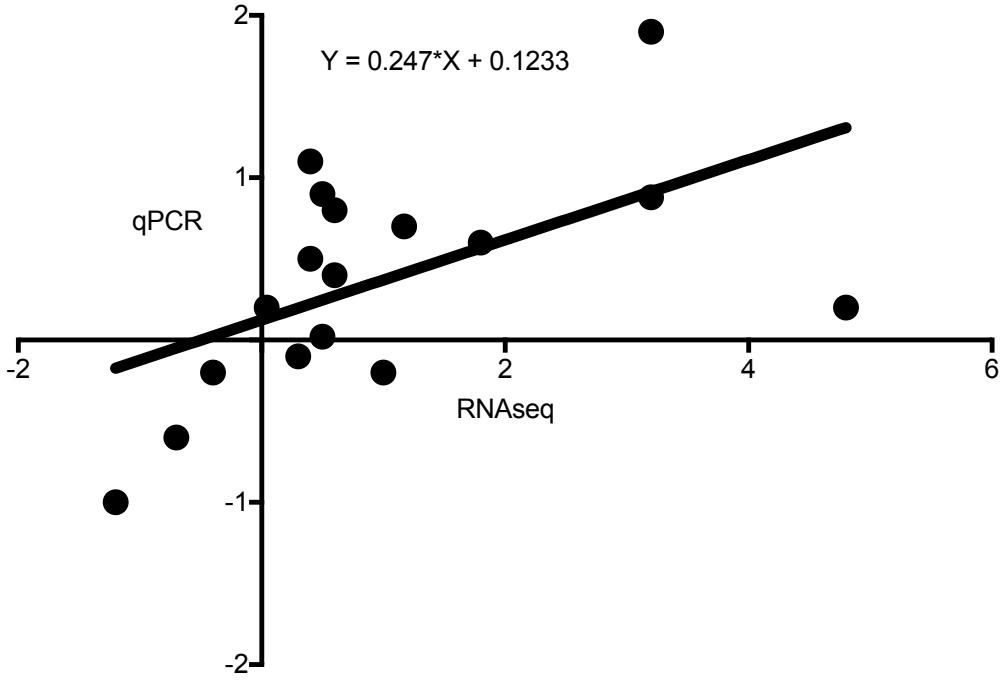


Figure 70: RNAseq qPCR correlation for the comparison of Log2 FC of the genes of interest in cooled burns and controls

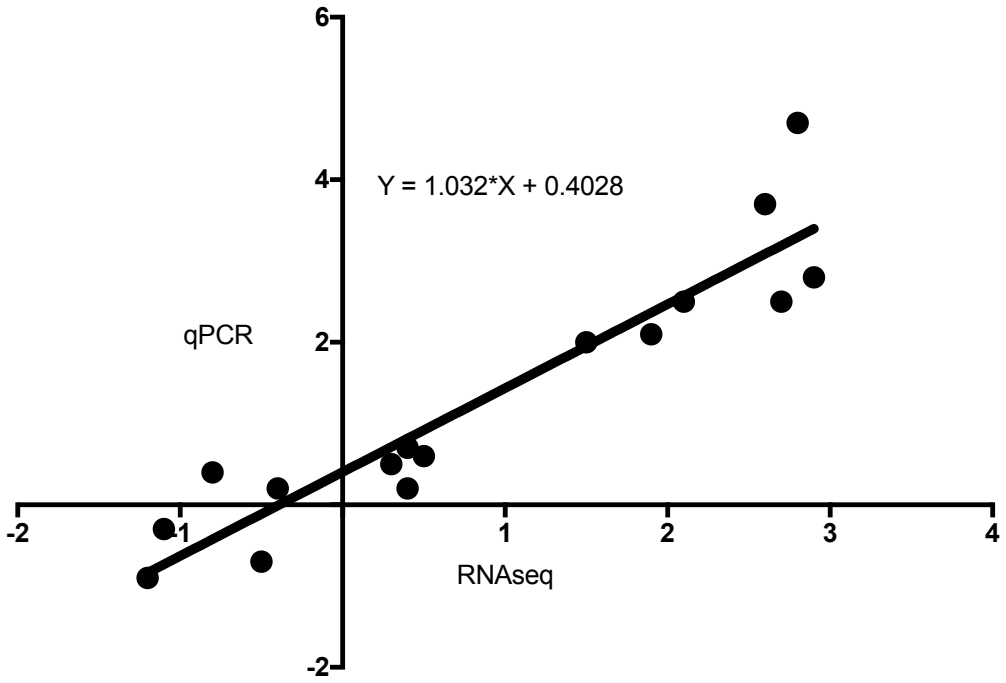


Figure 71: RNAseq qPCR correlation for the comparison of Log2 FC of the genes of interest in cooled burns and uncooled burns

Figure 69- Figure 71 show that the best correlation of RNAseq and qPCR fold-changes was seen in the comparison of cooled and untreated burns, where there was a near 1:1 correlation. This may reflect the neutralisation of the RNA degradation artefact by the comparison of 2 sets of RNA that were not statistically significantly different in terms of quality. There is a strong correlation between the fold-changes caused by cooling between the RNAseq data and qPCR, despite the actual fold-changes being relatively small when these two groups were compared to one another.

6.5.4 Confirmation of qPCR with samples from a further 5 patients

A second set of samples from a different group of 5 patients, again harvested at 3 hours after burning were also analysed in the same way, the only difference being the amount of cDNA was 5ng per reaction instead of 10ng because of RNA availability from this set of samples. The results for this experiment are summarised in the table below.

The less abundant transcripts- TCHHL1, and the keratins- amplified unreliably in these experiments. These genes were also downregulated by burning, making them even scarcer in the burn samples. Furthermore, they are anatomically localised in the superficial papillary dermis and epidermis, so were in the tissue closest to the burning device, and so most likely to be destroyed, or even rubbed away as part of the blister during the surgery as happened in some cases.

Gene	BNC vs CNC	BC vs CC	BC vs BNC
AZGP1	-0.9 (0.002)	1.2 (0.07)	-0.4
CHORDC1	0.9 (0.004)	0.6	-0.3
HSPH1	2.4 (0.006)	1.6	-0.8
EHF	-0.2	-0.3	-0.1
HSPA6	0.6	0.004	-0.3
KRT25	0.8	-0.05	-1.6
KRT27	0.6	-1.5	-2.6
KRT34	-0.5	-2.3	-1.6
KRT82	0.8	-1.3	-3.1
KRTAP3-1	-0.1	-2.9	-2.2
PALMD	-0.5 (0.01)	-0.7	-0.2

Gene	BNC vs CNC	BC vs CC	BC vs BNC
PDE4C	0.7	1.3 (<0.0001)	0.05
PRKCG	2.4	2.0 (0.03)	-1.2
PRR9	-0.1	-1.6	-2.2
PTGER1	0.9	1.0 (0.04)	-0.3
RAB3B	-1.6 (0.01)	-1.7 (0.05)	-0.4
TCHH	0.5	-1.1	-2.1
TCHHL1	-1.2	-1.5	-0.9

Table 18: qPCR Log2 FC for second set of 5 biological replicates with the same 4 conditions harvested at 3 hours after burning.

These results in Table 17 and Table 18 were then combined into Table 19. The genes are summarised below, with their fold-changes and p-values.

Gene	BNC vs CNC	BC vs CC	BC vs BNC
AZGP1	-0.9 (0.03)	-0.9 (0.005)	-0.1
CHORDC1	1.0 (<0.0001)	0.7 (0.005)	-0.2
HSPH1	2.9 (<0.0001)	1.7 (0.01)	-0.7
PALMD	-0.5 (0.0003)	-0.5 (0.03)	0.1
PDE4C	0.5	1.0 (0.002)	0.2
PRKCG	2.4 (0.0006)	1.5 (0.03)	-1.1 (0.07)
PTGER1	1.0 (0.006)	0.6	-0.3
RAB3B	-1.6 (<0.0001)	-1.3 (0.0014)	0.1

Table 19: combined qPCR results from 10 different patients, harvested at 3 hours after burning, showing genes with significant results only

Not all the genes identified in the RNAseq as significantly altered by cooling in burned skin were confirmed to a significant extent in the confirmatory analysis. The fold-changes that the RNAseq analysis demonstrated were <1 in the more highly expressed mRNAs and higher in the mRNA species that were expressed at levels ≤1 CPM, or in the epidermis- the area most severely damaged in the burn model. In general, the fold-change direction, and magnitude of change in the RNAseq data correlated to that of the qPCR, and there was a near 1:1 correlation between the RNAseq and qPCR fold-changes.

6.6 Conclusions from the RNAseq and qPCR validation experiments

6.6.1 The RNA extraction, purification, yield and quality

The extraction of RNA from skin was consistent, and yielded sufficient RNA for the purposes of library preparation for RNAseq, with sufficient remaining for validation with qPCR. The RNA was stable enough for cDNA synthesis without degradation. There was no significant difference between the RNA yields per gram of tissue between any of the groups.

The RNA showed significant degradation from the process of burning, but this was not significantly altered by cooling. The effects of thermal injury would not, therefore, seem likely to be purely a reflection of RNA degradation, and there were significant differences between cooled and untreated burns in terms of microvascular occlusion, but this was not reflected in the levels of degradation seen in their respective RNA samples.

6.6.2 The RNAseq data quality

The RNAseq data identified over 17,000 genes expressed to some extent in the samples submitted for sequencing. Each library was run 4 times, and the technical replicates mapped very closely to each other on the MDS plot, allowing them to be pooled into one dataset. This significantly increased the number of reads obtained for each sample.

While the process of burning had significantly degraded the quality of the RNA, the overall findings of the RNAseq were that 2,266 genes were significantly upregulated and 1,527 genes significantly downregulated by burning, within 3 hours of injury. Gene upregulation, either within the constituent cells of the skin, or in cells trafficking into the

area of trauma, points towards the evolution of burn pathophysiology as an active transcriptomic process.

6.6.3 The transcriptomic effects of burning

The transcriptomics of burn injuries have not been published before so soon after injury, so there is little to which one can compare this data. However, the data we obtained fitted into logical ontological groups of genes, and processes.

6.6.3.1 Upregulated ontologies and processes

Ontologies and processes showing significant up-regulation related to inflammation, chemotaxis and migration, response to misfolded proteins, thrombosis and haemostasis and a response to wounding and ectoderm-to-mesoderm transformation. This is logical in the light of the changes seen clinically in burns, and histologically in the same samples as those from which the RNA was extracted.

6.6.3.2 Downregulated ontologies and processes

Ontologies and processes that were downregulated by burning related to keratinocyte differentiation, tight junction formation, adhesion to the basement membrane by epithelial cells, hair follicle differentiation, and the maintenance of the skin as a barrier to water loss and pathogens. There was also down-regulation of genes associated with blistering skin disorders.

6.6.3.3 The effects of cooling on the transcriptome of burned human skin

When cooled and untreated burns were compared, there were several genes that showed significant alteration in expression in response to cooling. Those that were downregulated in cooled burns relative to untreated burns related to the inflammatory response, and inflammatory second messenger systems. Those that were

upregulated in response to cooling compared to in untreated burns were involved in epidermal differentiation, hair follicle differentiation, and the function of the skin as a barrier.

While the fold-changes were relatively small, they were confirmed by qPCR, in both direction, and magnitude of change, in both the samples from which the RNA was extracted, and biological replicates from different patients, created at different times and extracted with identical methods, but on different days.

There was a correlation between the segregation of the 20 libraries in Figure 52, and the segregation of the 16 libraries in Figure 66 after patient 2 was removed from analysis in view of its anomalous placement in the MDS plot.

6.7 Conclusions from transcriptomics

Within 3 hours of injury, transcriptional changes are seen in burns that reflect the effects of burning and loss of skin function seen in burned skin as shown in Figure 54-Figure 56. It is not possible to tell in the setting of such a diverse organ as the skin where the transcriptional changes are taking place, and it is highly likely that downregulation of epidermal genes and those related to skin function reflects in part at least the destruction of the cells responsible for their transcription under normal conditions, rather than the loss of transcription of those genes within viable keratinocytes.

Cooling the burn in the acute setting has effects on the transcriptomic changes caused by burning that reflect the clinical and histological changes seen in the cooled burns when compared to those that were left uncooled. In part, the transcriptional changes may be the result of reduction of the damage to the skin, particularly to the epidermal appendages, and retention of viable cells transcribing epidermal-related genes.

Although the number of individual patients is small, the experiments have robustly demonstrated the effects of burning on the transcriptome of human skin, and to a lesser extent shown that there are significant effects on these changes mediated by cooling. These findings have partially validated with qPCR and in a separate group of individuals.

7 Results chapter 3: Proteomics of thermally-injured skin, and the effects of cooling

7.1 Introduction

The protein precipitates from the Trizol extraction process used for RNA extraction had been stored, and it was decided to analyse these samples with the following aims:

Characterisation the effects of burning on the proteome of normal human skin, and the effects of cooling on these changes

Characterisation of the involvement and roles of proteins synthesised distally to the skin, but activated or deposited within the burn injury

Identification of known pathological processes involving the same transcriptomic changes or pathways

7.2 Proteomic analysis of protein pellets from Trizol extraction process

A full description of the proteomic analysis can be found in the “Patients and Methods” chapter. Briefly, pellets of precipitated protein from each Trizol extraction of RNA for sequencing (see Results chapter 2) were successfully resuspended, digested with trypsin, quantified and labelled with TMT 10-plex tags as in Table 20.

Run	Isobaric TMT 10-plex tags									
	126	127C	127N	128C	128N	129C	129N	130C	130N	131
1	Pool of all 20 samples 100%	1BC	1BNC	1CC	1CNC	2BC	2BNC	2CC	3BC	Pool of all 20 samples 50%
2		2CNC	3BNC		3CC	3CNC	4BC	4BNC		
3		4CC	4CNC		5BNC	5CC	5CC	5BC		

Table 20: the allocation of TMT tags to peptide samples from the 5 patients

7.3 The effect of burning on the proteome of normal skin

A total of 211 proteins were found to have a significantly altered level of expression (adjusted p-value <0.05) when untreated burns and untreated controls were compared. When the Log2 FC of each protein relative to its concentration in the pooled sample of all 20 samples was plotted as a heat map using “gplots” software in “R”, with hierarchical clustering of proteins and samples according to similarities in expression profile, the

Figure 72 was obtained.

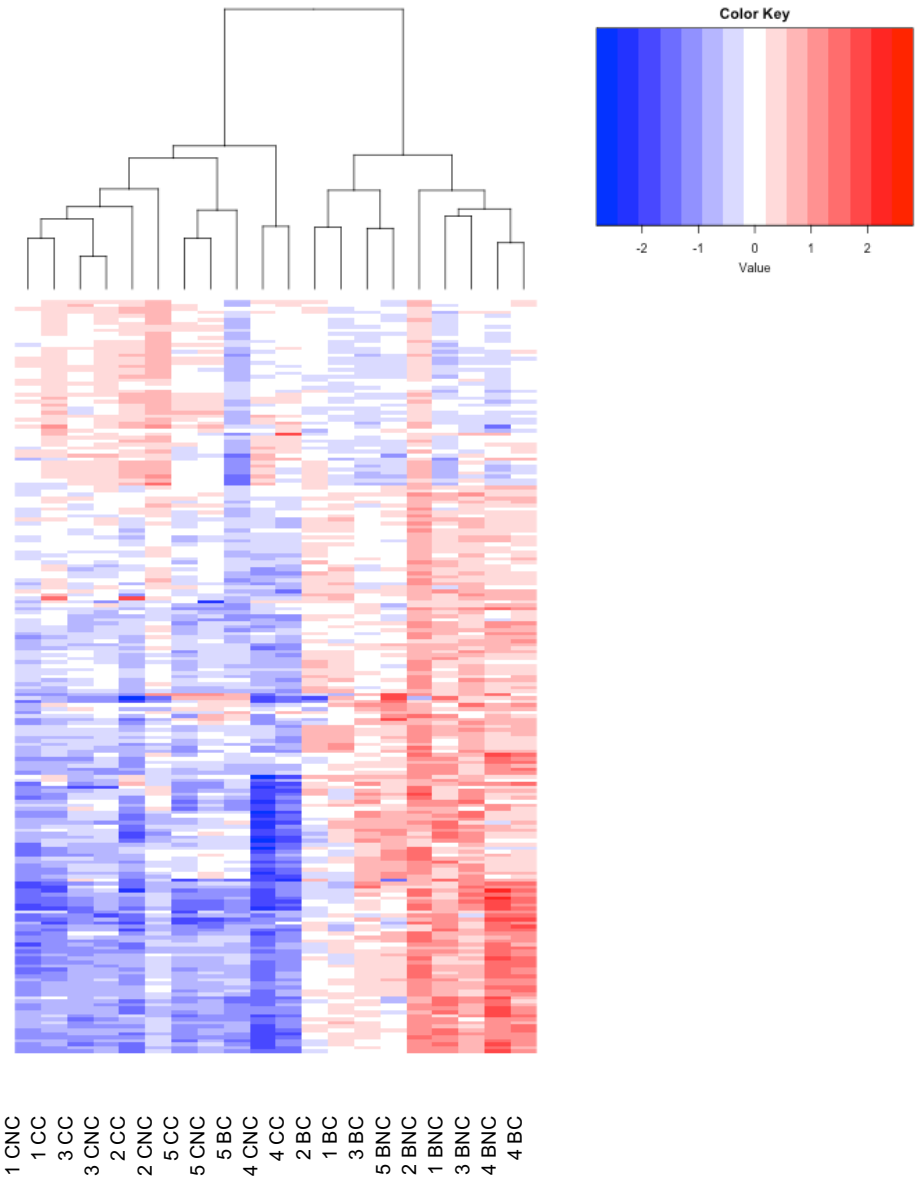


Figure 72: heatmap of all proteins found to be differentially expressed when paired uncooled burns and uncooled controls were compared within the 20 samples analysed The names of the individual proteins have been omitted from

Figure 72 as there is insufficient space, and the aim was to establish an overall pattern of the effect of burning on the proteome of human skin. There is clustering of 9 burned samples- 5 uncooled and 4 cooled burns- to the right of the heat map, and 10 controls and one cooled burn cluster together on the left side. This shows an overall difference between the proteomes of burned and unburned skin when all proteins with significantly differing expressions between the conditions BNC and CNC are

compared. The grouping of CC and CNC samples by patient on the left side of the heat map in

Figure 72 indicates that the unburned skin samples from either side of the same patient had more in common with one another, irrespective of cooling, than they did with unburned skin samples from another patient.

The 5 cooled burn samples group together, between the untreated burn samples and the controls with 2 outliers- the cooled burn sample from Patient 4 on the far right of

Figure 72, and the cooled burn from patient 5 lying amongst the control samples. With the single exception of Patient 4, all the BC samples lie to the left- and hence towards the proteomes of uninjured controls- of their respective BNC samples, including Patient 5. Cooling may therefore be said to have the effect of opposing the changes to the proteome caused by the burning of skin and bringing it back towards that of normal skin, much as it was shown to do at a transcriptomic level in the (Reference to results 2).

7.4 Overview of the effect of cooling on the proteome of burned skin

When a pairwise comparison between cooled and uncooled burns from the same patient was made, 109 proteins were found to have their expression significantly altered when cooled and uncooled burns were compared. Again, the Log2 function of each protein's expression as a proportion of the reference 100% pooled sample was plotted with hierarchical clustering, and is shown in Figure 73.

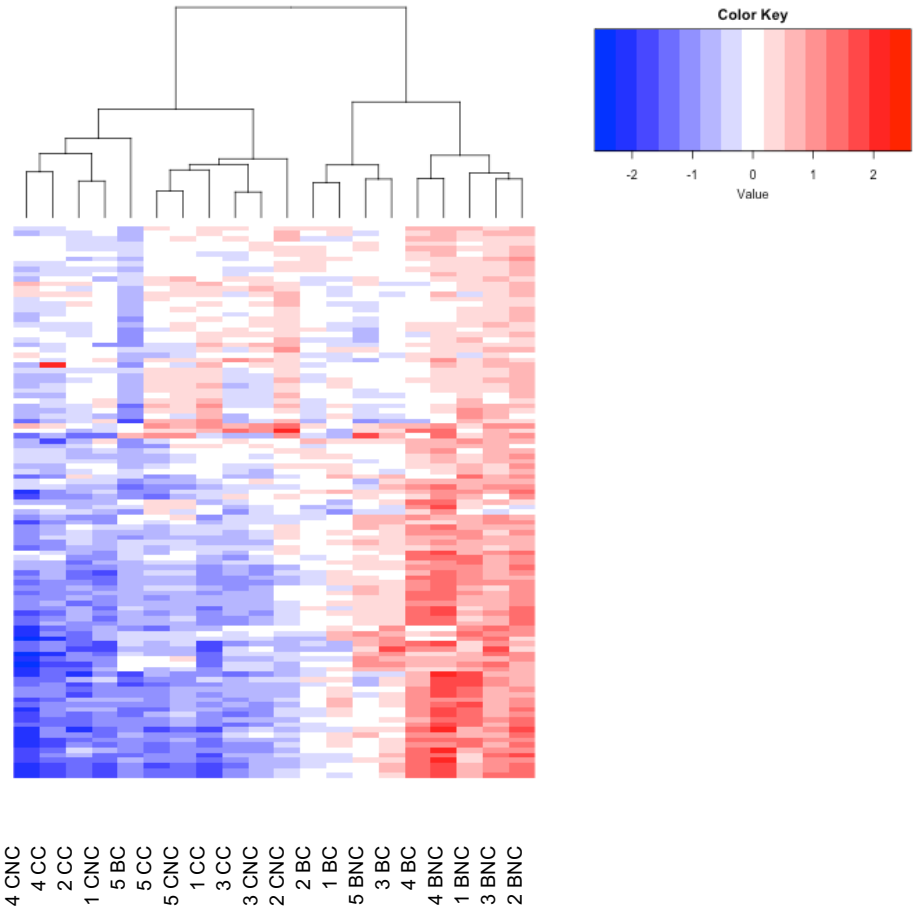


Figure 73: heatmap of proteins significantly altered when cooled and uncooled burns were compared

Again, the names of the proteins have been omitted from the rows as there is insufficient space. There is still the grouping of the untreated burns to the right side of the heat map with the cooled burns lying to the left of that, and the controls lying to the

left of that, again. There is some overlap between the cooled and untreated burns and the controls, with the uncooled burn from patient 5 interspersed with the cooled burns, and the cooled burn from patient 5 interspersed with the controls.

The ordering of the samples has changed, and there is now a consistent relationship between the cooled burns and the corresponding untreated burns from each patient, with each cooled burn lying to the left of the untreated counterpart, in the direction of the control samples, and hence of the proteome of uninjured skin.

It can also be seen that there are no proteins with reduced expression in burns compared to controls that had their level of expression increased significantly by cooling. This indicates that the significant effects of cooling upon the proteomic changes seen in burned skin are the attenuation of proteins with significant increases in expression caused by burning.

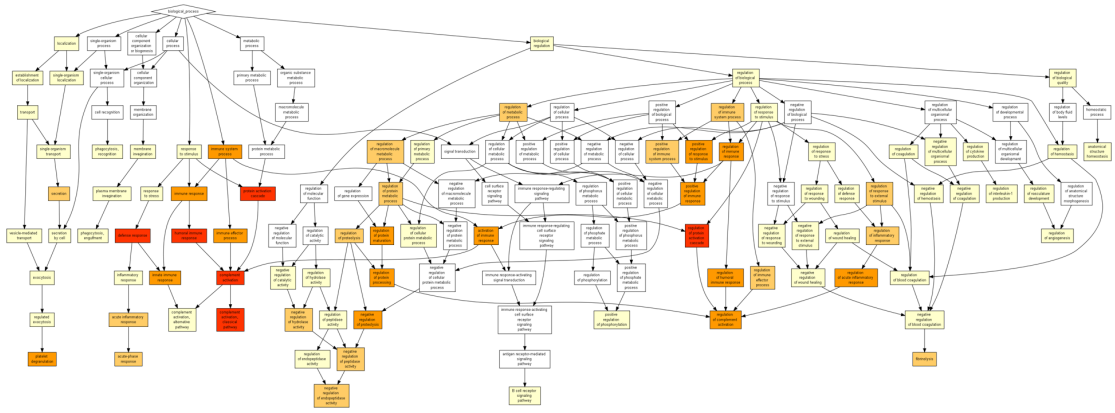
In summary of the initial analysis of the proteome of normal, uninjured skin and comparison to that of burned human skin, thermal injury causes significant alteration in the expression of proteins within the proteome of human skin. When plotted as a heat map of the Log2 fold-changes, the samples group by condition- burn and control- and then by treatment in the case of the burns- cooled and untreated- and by individual in the case of the control samples.

7.5 Detailed analysis of the effect of burning on the proteome of human skin

The Uniprot IDs for the proteins identified were analysed with Metacore software to assess enrichment for specific cellular, biological and disease processes, and pathways.

7.5.1 Enrichment in the proteome of thermally-injured human skin

7.5.1.1 Biological process enrichment in burned skin (GOrilla analysis)



$>10^{-3}$	10^{-3}-10^{-5}	10^{-5}-10^{-7}	10^{-7}-10^{-9}	$<10^{-9}$

Figure 74: enrichment analysis of the proteomic data for differentially-expressed proteins in uncooled burns compared to uncooled controls

Pathways of particular interest are those associated with the red and orange boxes in the biological process map above.

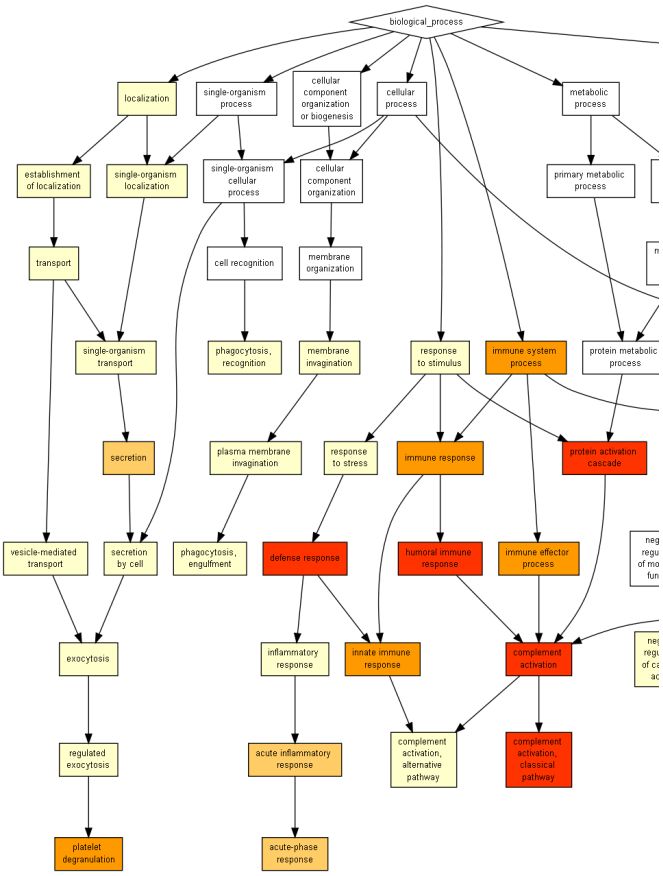


Figure 75: closer detail of the left side of Figure 74

A more detailed view of the left-hand side of the biological process map above shows enrichment of the biological processes related ultimately to complement activation via the classical pathway, and platelet degranulation.

On the right side of the overall view of the biological processes, it can be seen that there is some, less significant enrichment of processes related to haemostasis and inflammatory response and ultimately fibrinolysis.

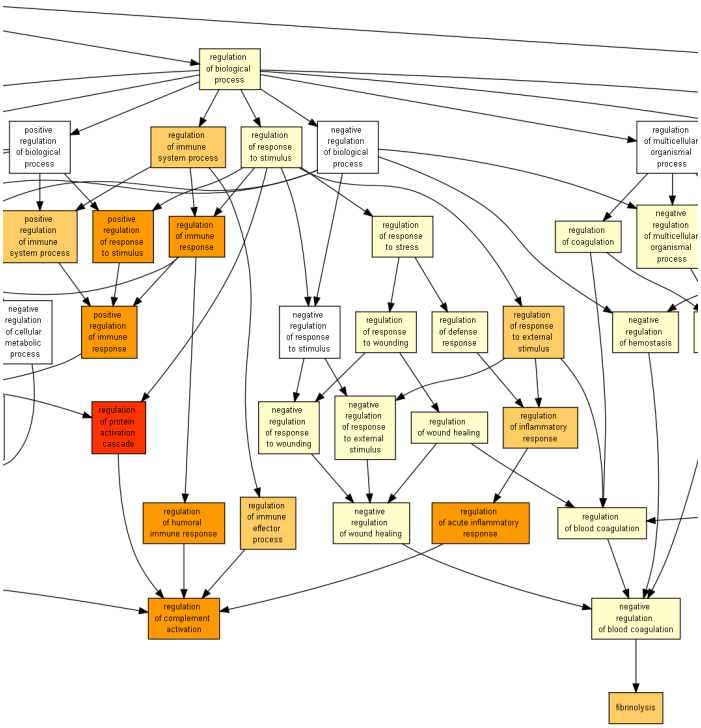


Figure 76: the right side of Figure 74 in greater detail

The pathways that were significantly affected by thermal injury fall into the categories of immune response, blood coagulation, protein folding, cell adhesion and cytoskeletal remodelling, response to DNA damage, and apoptosis. Three pathways related to pathological processes involving either complement activation (thrombotic microangiopathy, age-related macular degeneration) or coagulation (high shear stress-induced platelet activation).

7.6 The effects of burning upon the clotting cascade

The original work by Jackson described a central zone of coagulation and necrosis[1], and thrombosed vessels are seen during debridement of non-viable dermis. The prominence of the coagulation pathway on enrichment analysis correlates to microvascular occlusion seen in the thermally-injured specimens from the model itself. The mean Log2 fold-changes and p-values of the clotting factors with significantly altered expression within the burn proteome are summarised in Table 21.

Factor	Log2 fold-change BNC:CNC (p-value)	Log2 fold-change BC:BNC (p-value)
Alpha-2 antiplasmin	2.43 (0.03)	-1.04 (0.01)
Fibrinogen beta chain	2.41 (0.018)	-0.87 (0.008)
Fibrinogen alpha chain	2.3 (0.01)	-0.83 (0.003)
Antithrombin III	2.06 (0.01)	-0.88 (0.007)
Heparin cofactor 2	2.00 (0.02)	-0.99 (0.005)
Alpha-2 macroglobulin	1.89 (0.02)	-0.55 (0.02)
Alpha-1 antitrypsin	1.86 (0.04)	-0.76 (0.03)
Serine protease inhibitor	1.80 (0.01)	-0.83 (0.001)
Plasminogen	1.78 (0.007)	-0.75 (0.04)

Factor	Log2 fold-change BNC:CNC (p-value)	Log2 fold-change BC:BNC (p-value)
Prothrombin	1.77 (0.01)	-0.65 (0.04)
LMW Kininogen	1.50 (0.01)	-0.42 (0.13)*
Vitamin-K dependent protein S	1.00 (0.02)	-0.72 (0.03)
Factor X	1.00 (0.018)	-0.71 (0.05)
Von Willebrand factor	0.57 (0.02)	-0.16 (0.32)*

Table 21: coagulation factors with Log2 FC and p-values, * signifies non-significant p-value

The abundances of each of the factors relative to the pooled reference sample shows a statistically significant increase in the levels factor X- the point at which the intrinsic and extrinsic pathways converge into the common pathway- and of the alpha and beta chains of fibrinogen- the end-product of the clotting cascade responsible for haemostasis. Alpha-2 antiplasmin inhibits the actions of plasmin on fibrin, hence a 2.4 fold increase in its level would significantly inhibit fibrinolysis of newly deposited fibrin, hence stabilising the thrombus.

The components of the clotting cascade with abundances significantly altered by burning as summarised in the heat map in

Figure 77.

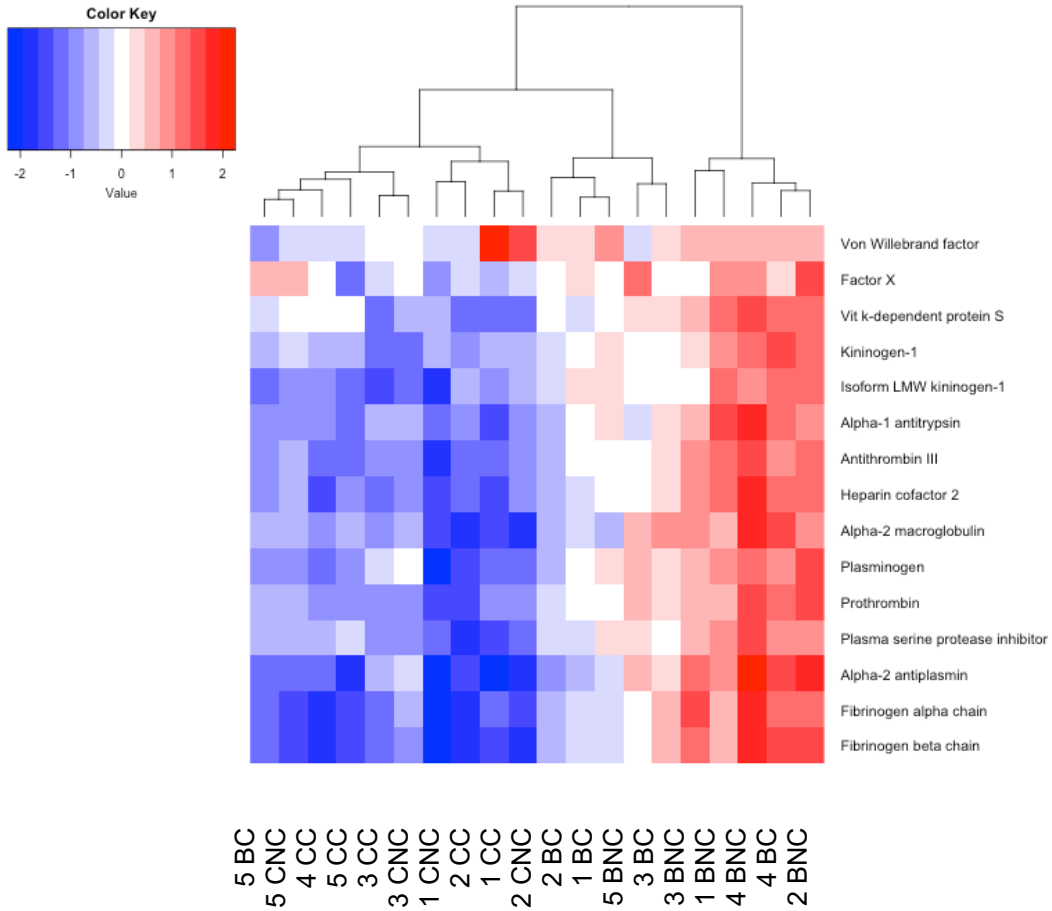


Figure 77: heatmap of coagulation cascade proteins with expression levels significantly altered by cooling in the context of burning

There is a general grouping of the burns to the right side of the heatmap and controls to the left side, with the cooled burns generally lying to the left of the uncooled burn from the same patient.

Figure 77 with the exception of “5BC”- the cooled burn from patient 5. The cooled burns lie to the left of the uncooled burns with the exception of patient 4, indicating that their clotting component elements of their proteomes have been elevated to a lesser extent than in the uncooled burns.

For the final step of the cascade- the deposition of fibrinogen - the fibrinogen alpha and beta chains are present in higher concentrations in uncooled burns when

compared to cooled burns, including in patient 4 where the overall clustering of the clotting components places the cooled burn sample to the right of the uncooled sample.

Analysis of the relative abundances of clotting factors and comparisons between untreated burns and untreated controls, and cooled and untreated burns using Metacore software yielded the following diagram. The thermometer icons suffixed with "1" are comparisons between uncooled burns and controls, and the thermometer icons suffixed "2" are comparisons between cooled and uncooled burns.

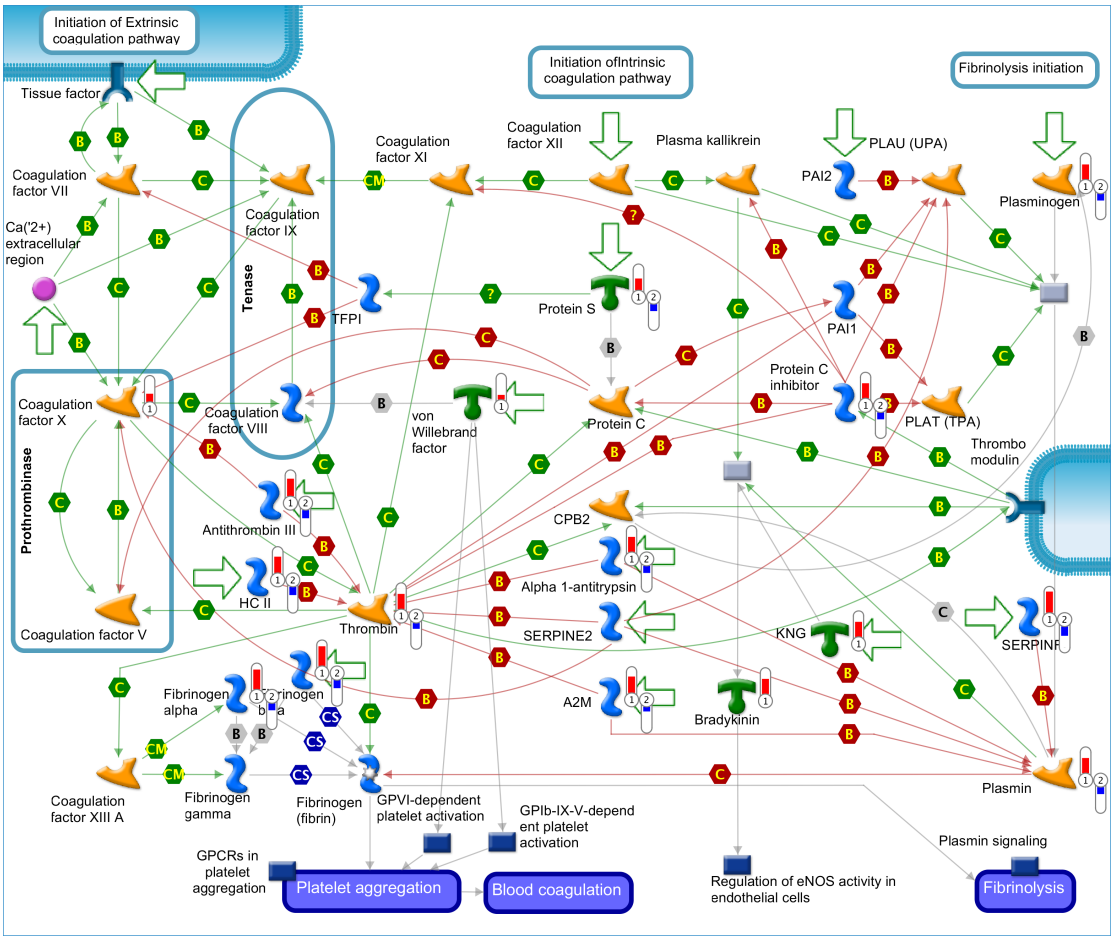


Figure 78: coagulation cascade proteomic results as a pathway diagram from Metacore. "1" compares BNC:CNC, "2" compares BC:BNC

7.7 The effects of thermal injury on the complement system

Factor	BNC:CNC Log2 FC (p-value)	BC:BNC Log2 FC (p-value)
C1q subunit A	1.2 (0.002)	-0.55 (0.005)
C1q subunit C	0.98 (0.02)	-0.48 (0.05)
C1r	1.2 (0.01)	-0.53 (0.1)
C1s	1.27 (0.02)	-0.64 (0.03)
C2	1.97 (0.01)	-0.57 (0.04)
C3	2.1 (0.007)	-0.68 (0.05)
C4a	1.67 (0.005)	-0.54 (0.05)
C4b	1.44 (0.003)	-0.52 (0.12)
C5	1.77 (0.01)	-0.63 (0.05)
C6	1.8 (0.01)	-0.66 (0.06)
C7	1.35 (0.004)	-0.44 (0.06)
C8 alpha chain	1.54 (0.002)	-0.53 (0.02)
C8 beta chain	1.04 (0.05)	-0.78 (0.01)
C9	1.38 (0.009)	-0.68 (0.007)

Factor	BNC:CNC Log2 FC (p-value)	BC:BNC Log2 FC (p-value)
Complement factor H	1.23 (0.01)	-0.58 (0.03)
Complement factor I light chain	1.66 (0.004)	-0.66 (0.03)

The significant Log2 fold-changes in complement cascade components are summarised in Table 22.

Table 22: complement proteins with Log2 FC and P-values

The data from Table 22 is plotted as a heatmap in Figure 79 below.

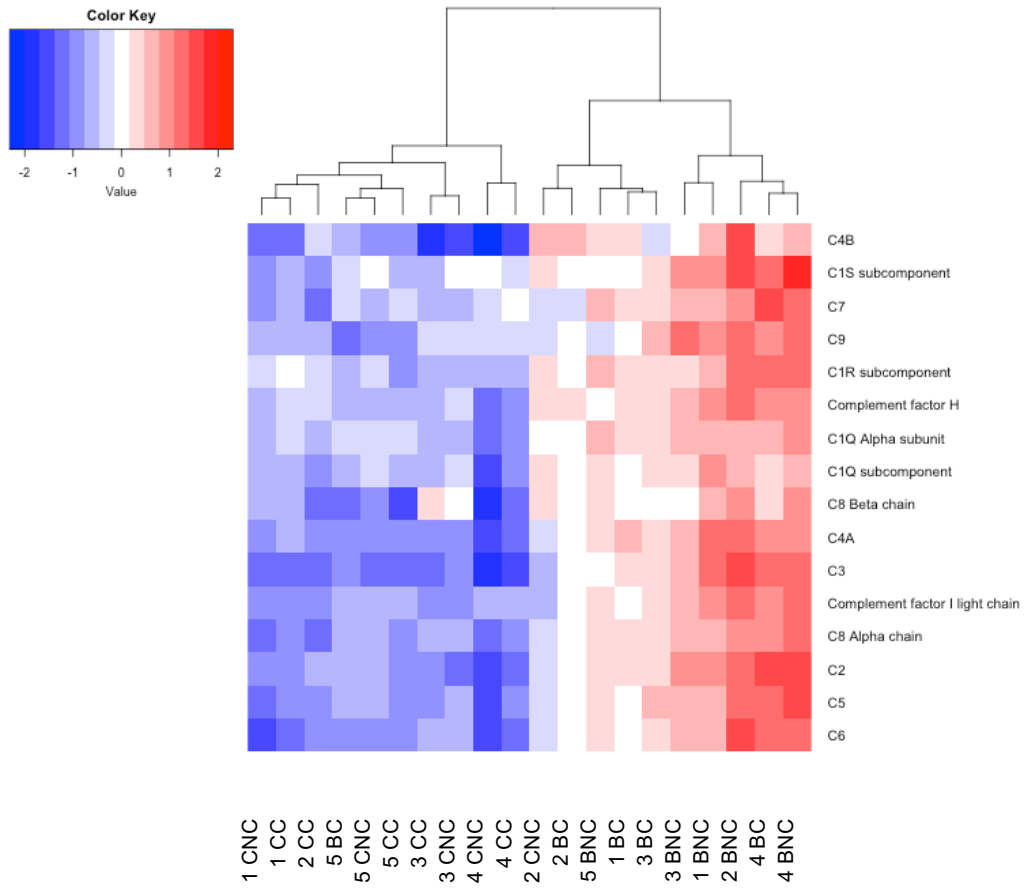


Figure 79: heatmap of complement proteins and the effects of burning and cooling

There is a segregation of burns from controls, with the exception of the 5BC (cooled burn) sample that lies amongst the controls, interestingly next to 2 other samples- the cooled and uncooled controls- also from patient 5. This is seen again with the cooled burn from patient 2 that lies next to 2CNC. In each case, the cooled burn sample lies to the left, albeit to a varying degree, of the uncooled burn from the same patient. This hierarchical clustering indicates that the change in the proteome of the skin, as related to the complement cascade, is partially reversed by cooling.

The attenuation of the activation of complement by cooling is well-demonstrated in the diagram below, generated from the experimental data on Metacore, showing not just the enrichment of the activation of the classical complement pathway, but also the increased levels of the “a” fragments of the cleaved complement components, that in turn act as chemotactic anaphylactotoxins.

The first comparison made was between uncooled burns and uncooled controls (thermometer icon number “1”), and shows the increased abundance of complement components from the first stages of activation through the classical activation pathway of antigen-antibody complex formation to the formation of the membrane attack complex (MAC).

The second comparison was made between cooled and uncooled burns and the changes in the abundances of the complement peptides are indicated by thermometer icons with the suffix “2”. The diagram shows that for every complement component that has its abundance increased by burning, cooling has an antagonistic effect, and results in a reduction of the increase when cooled and untreated burns are compared.

In the previous chapter, it had already been demonstrated that there is a significant upregulation of C5aR- the receptor for C5a- induced by thermal injury, and together

with the activation of the complement cascade and the generation of anaphyactotoxins this would result in both an increased chemotactic stimulus, and increased sensitivity and response to in in the burned tissue compared to the control skin.

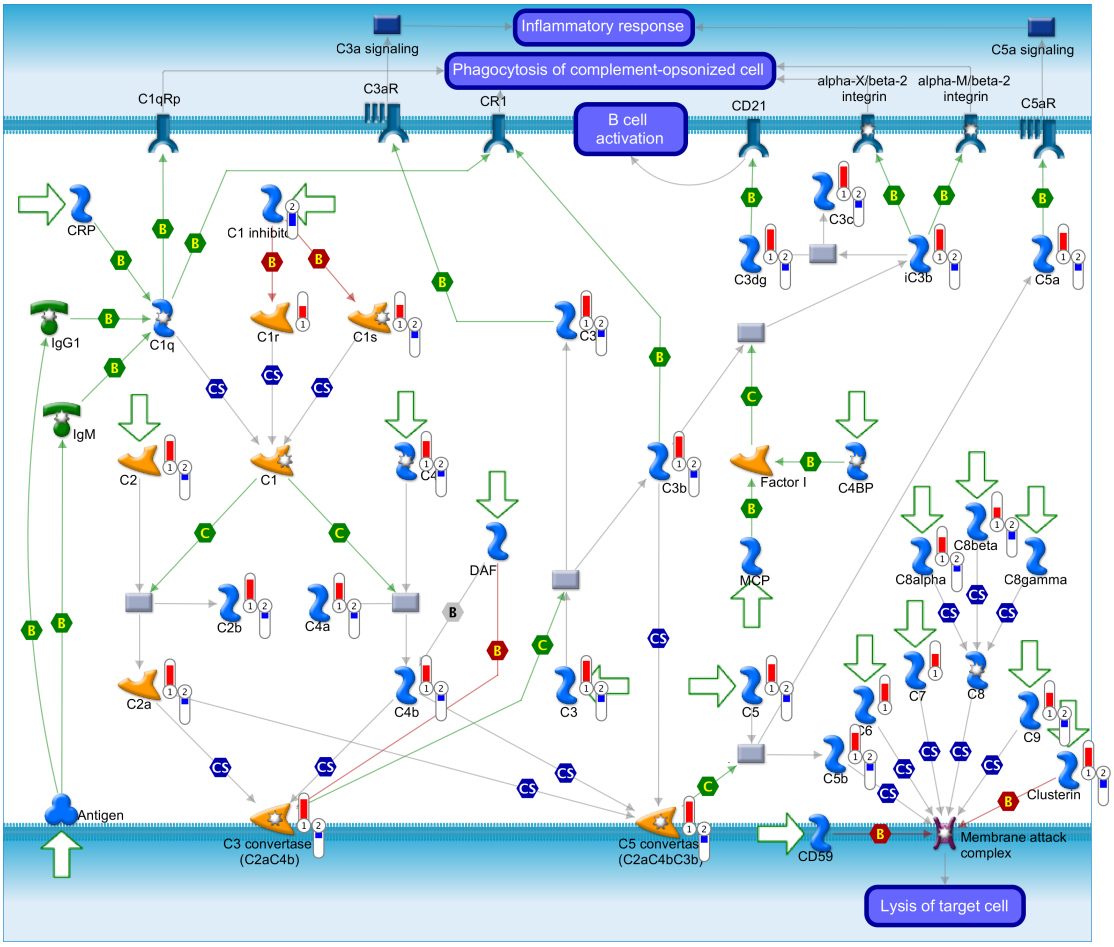


Figure 80: complement cascade pathway with "1" indicating BNC vs CNC and "2" indicating BC vs BNC

The significant increase in “C1qrs” at the start of the classical complement activation pathway (with 47% of the proteins significantly upregulated and an FDR of 7.2E-30) would indicate that the activation of complement is initiated by antigen/antibody complex formation. This is demonstrated in Figure 81.

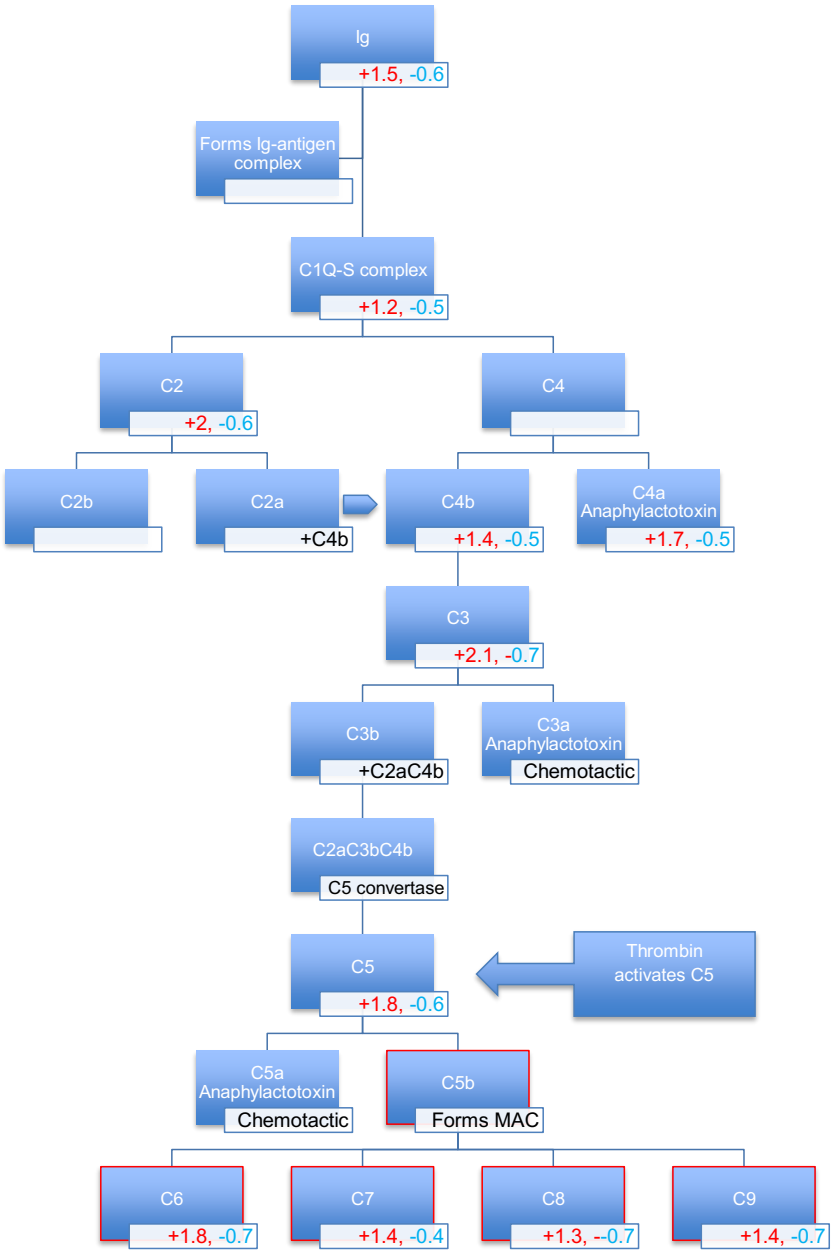


Figure 81: the complement cascade with the Log2 FC effects of burning in red and cooling in blue

7.8 Immunoglobulin deposition in thermally-injured skin

The classical activation of the complement cascade requires the formation of antigen-antibody complexes. The role of classical activation of the complement cascade in thermal injury evolution may be supported by the levels of immunoglobulin elements within the burn proteome being increased significantly compared to the proteome of control skin, as shown in the heat map of immunoglobulin peptides identified in the TMT LC-MS-MS below:

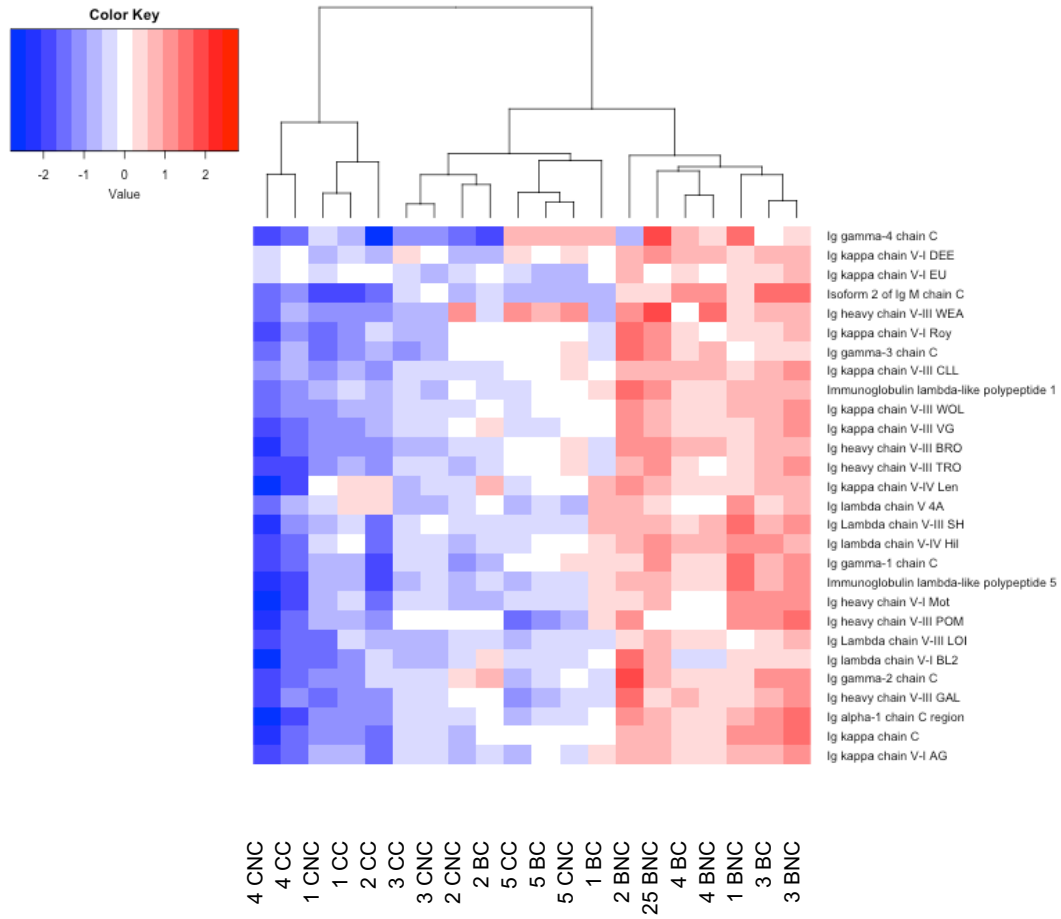


Figure 82: heatmap of immunoglobulin protein Log2 fold-changes

The significant finding of this analysis is that peptides derived from antibody subunits are found at increased levels in thermally-injured skin. The effect of burns on circulating immunoglobulins has been established[58–60], and this confirms the

sequestration of immunoglobulins into the burn. The burns all lie to the right of the heat map and in each case, the cooled burn lies to the left of its respective uncooled counterpart from the same patient.

The control samples group in pairs, or close to one another, indicating that cooling has had little effect on the levels of these antibody peptides in normal skin. The immunoglobulin peptides identified as having significantly altered expression in the untreated burns compared to the untreated controls are summarised in the table below, with their mean Log2 fold-changes between the conditions of untreated burn and untreated control, and cooled burn and untreated burn.

Peptide	Log2 FC BNC/CNC (p-value)	Log2 FC BC/BNC (p-value)
Ig Kappa V-I AG	1.41 (0.0002)	-0.52 (0.02)
Ig Kappa V-III WOL	1.35 (6.1E-5)	-0.51 (0.04)
Ig Lambda V-IV Hil	1.43 (0.0003)	-0.46 (0.08)
IG Kappa V-III CLL	1.26 (0.001)	-0.48 (0.04)
Ig heavy chain V-III BRO	1.49 (0.0001)	-0.69 (0.05)
Ig Kappa V-III VG	1.42 (0.0002)	-0.57 (0.05)
Isoform 2 IgM chain C	1.74 (0.01)	-0.39 (0.04)
Ig alpha-1 chain C	1.73 (0.001)	-0.63 (0.02)

Peptide	Log2 FC BNC/CNC (p-value)	Log2 FC BC/BNC (p-value)
Ig Kappa chain C	1.52 (0.002)	-0.58 (0.02)
Ig Lambda V-III LOI	1.18 (0.007)	-0.55 (0.07)
Ig heavy chain V-III TRO	1.25 (0.001)	-0.60 (0.07)
Ig Lambda-2 chain C	1.50 (0.005)	-0.71 (0.09)
Ig Lambda chain V 4A	1.33 (0.004)	-0.47 (0.03)
Ig Kappa V-I Roy	1.28 (0.002)	-0.67 (0.14)
Ig Lambda V-III SH	1.44 (0.002)	-0.72 (0.01)
IgG-1 chain C	1.48 (0.003)	-0.68 (0.05)
Ig heavy chain V-I BL2	1.4 (0.005)	-0.57 (0.02)
Ig Lambda V-I Len	1.3 (0.006)	-0.3 (0.2)
IgG-2 chain C	1.46 (0.01)	-0.62 (0.09)
Ig heavy chain V-III WEA	1.04 (0.04)	-1.05 (0.02)
Ig Kappa V-I DEE	0.84 (0.003)	-0.47 (0.14)
Ig heavy chain V-III GAL	1.44 (0.007)	-0.60 (0.14)
IgG-3 chain C	1.38 (0.007)	-0.70 (0.12)

Peptide	Log2 FC BNC/CNC (p-value)	Log2 FC BC/BNC (p-value)
Ig heavy chain V-III POM	1.38 (0.01)	-0.72 (0.04)
IgG-4 chain C	1.43 (0.03)	-0.63 (0.14)
IG Kappa V-I EU	0.84 (0.02)	-0.28 (0.11)

Table 23: immunoglobulin Log2 FC and p-values

In total, 27 immunoglobulin-related peptides were significantly (p-value<0.05) altered when uncooled burns and controls were compared, and 12 of these changes were significantly altered when cooled and uncooled burns were compared. The statistically significant changes caused by burning were all positive Log2 fold-changes, while those caused by cooling were all negative Log2 fold-changes.

The immunoglobulin classes increased significantly by burning are immunoglobulin A as evidenced by alpha heavy chains, immunoglobulin G, as evidenced by the gamma heavy chain peptides, and immunoglobulin M and evidenced by the μ heavy chain peptides, with IgM heavy chains showing the largest increase in Log2 fold-change with burning. A mix of variable and constant regions of the heavy and light chains are also identified.

Only one immunoglobulin- Ig kappa variable chain I EU was affected significantly by cooling in isolation when cooled and untreated controls were compared, with a Log2 fold-change of 0.29 and a p-value of 0.009. This change is in the opposite direction to the statistically insignificant change caused by cooling in the context of burning and is of questionable significance.

The significantly elevated levels of immunoglobulin peptides in burns compared to controls, and the significant reduction of the levels of some of the same peptides in cooled burns when compared to untreated burns indicates that the binding of antibody is a causative agent in, or significant result of thermal injury.

Combined with the significantly elevated levels of complement cascade components in the classical complement activation pathway, upstream of the point at which plasminogen and thrombin activate the complement cascade indicate the role of the formation of antigen-antibody complexes between thermally-altered or exposed native proteins and circulating antibodies.

7.8.1 Possible antigens in burns

Published work examining the role of IgM-mediated inflammation in burn wound progression showed that blockade of IgM from binding the neo-antigen non-muscle myosin with peptide N2 in pigs reduced burn severity at 4 hours after burning and resulted in significantly faster healing when compared to administration of a non-blocking control peptide or administration of intravenous saline treatment[57].

When our proteomic data was searched, non-muscle myosin was identified within the proteome (Uniprot ID P35579), but there was a statistically significant (p-value= 0.03) -0.3 Log2 fold-change in its levels in uncooled burns when compared to uncooled controls, but no significant difference in the levels found on comparison of cooled and uncooled burns. This finding indicates that the non-muscle myosin is relatively depleted by the burning process, possibly from lysis of damaged cells in burned tissues. Cooling fails to alter this significantly.

The above finding might indicate that if there is a similar mechanism in humans compared to pigs responsible for the reduction in burn depth- namely inhibition of the

formation of autoantigen-antibody complexes and their activation of the classical complement cascade- by which cooling reduces the progression of thermal injury, it is either through alteration of the binding kinetics of this interaction resulting in less IgM being retained in the tissues, or there is some sort of segregation of the non-muscle myosin from the immune system following thermal injury that is mediated by cooling.

Having demonstrated that the depth of thermal injury caused by our burning device is very reproducible, the amount of initial damage as a direct result of heating is similar between burned samples. The relative abundance of non-muscle myosin in the samples was reduced by a similar fold-change by the process of burning, regardless of cooling, indicating that the abundance of the non-muscle myosin is not the key factor in the interaction with IgM, if this is a mechanism responsible for classical complement activation and burn wound progression. What may be more likely is that the response to an identical thermal insult to the tissues, and resultant release of antigens and their interaction with circulating antibodies is altered by cooling, resulting in less activation of the complement and clotting cascades, and hence less damage to the microvasculature and tissue.

Previous work showed that C4 deficient mice heal without scarring from partial-thickness thermal injury and that administering sCR1 (a complement inhibitor) reproduces this effect in mice with a normal complement system[56].

7.9 The interaction of complement and coagulation cascades within the experimental data

The prominence of complement system components in the proteome of thermally-injured skin indicates an acute-phase response to tissue injury, and the role of complement activation in acute injury and its role in chemotaxis and increase in vascular permeability has been recognised. In fact, the clotting and complement systems have a synergistic relationship[84,85], as shown in Figure 83.

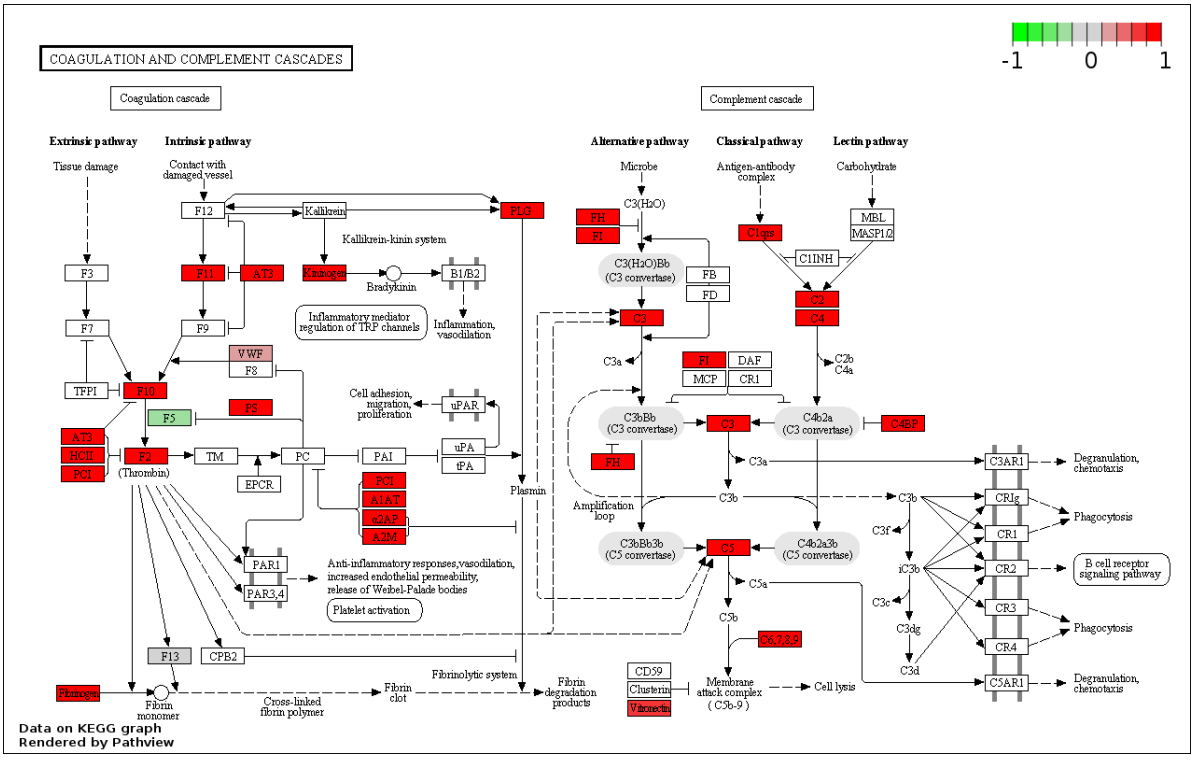


Figure 83: Pathview analysis of the proteomic data and Log2 fold-changes in complement and coagulation pathway proteins when uncooled burns and controls are compared

The enrichment leans towards the intrinsic clotting pathway, as there is no significant increase in the clotting factors of the extrinsic pathway (Factors III and VII), compared to those of the intrinsic pathway (Factor XI, Plasminogen). The intrinsic and extrinsic pathways converge via Factor X, that activates Factor II, in turn activating fibrinogen.

Plasmin and Thrombin[55,86] both have the effect of activating C3 and C5 of the complement system, by cleaving them to their respective “a” and “b” fragments. In both cases, the smaller “a” fragments act as anaphylactotoxins, causing increased vascular permeability, degranulation and chemotaxis. From this point C5b binds and activates components C6-9, with variable numbers of the C9 components forming the membrane attack complex (MAC)- a permeable pore in the cell membrane that causes osmotic lysis.

Plotting the clotting and complement data together in a single heat map produces Figure 84.

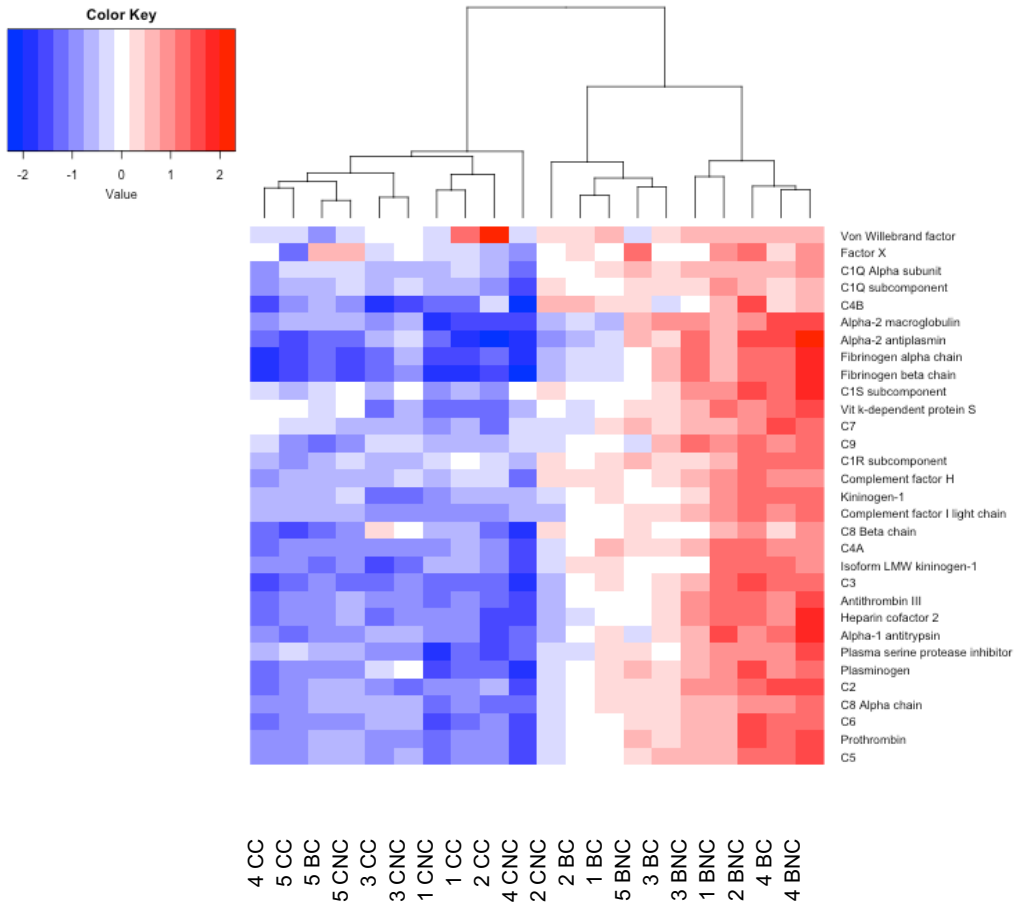


Figure 84: heatmap of coagulation and clotting factor protein Log2 FC

An important observation is that this is a very similar clustering and ranking of samples to the complement and coagulation cascade proteins when analysed in isolation of

one another. The relative positions of the cooled and untreated burns to one another is maintained.

7.10 The validation of the proteomics data

The proteomic findings were confirmed and localised within the burn and control samples with commercially-available antibodies, as set out in Table 4.

Samples from a minimum of four different patients were stained with each antibody, with representative sections of anatomical structures and boundaries between blistered and unblistered epidermis used to illustrate findings.

7.10.1 The localisation of C4a within the burn injury

The identification of C4a- the anaphylactotoxin[87] released by the activation of C4 through cleavage into a membrane-bound C4b and the soluble C4a- in the proteomic data as being significantly increased by burning and this change significantly reduced in size by cooling is of great interest in view of its chemotactic effects, and the role of complement in burn pathology. C4a has been isolated from the CSF of subarachnoid haemorrhage patients and may have a correlation to delayed neurological deficits caused by vasospasm, with C4a having a proven vasoconstrictive effect[88].

Paired sections from tissue blocks from the same burn samples as those from which the RNA and protein extractions were prepared were stained for C4a using the commercially-available monoclonal antibody to C4a from Abcam.

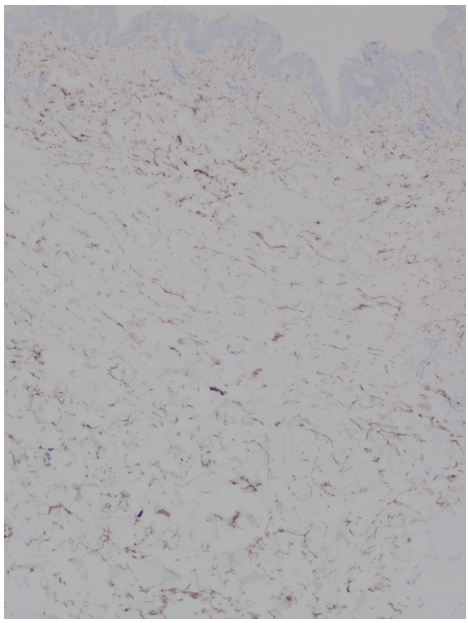


Figure 85: unburned control skin stained for C4a

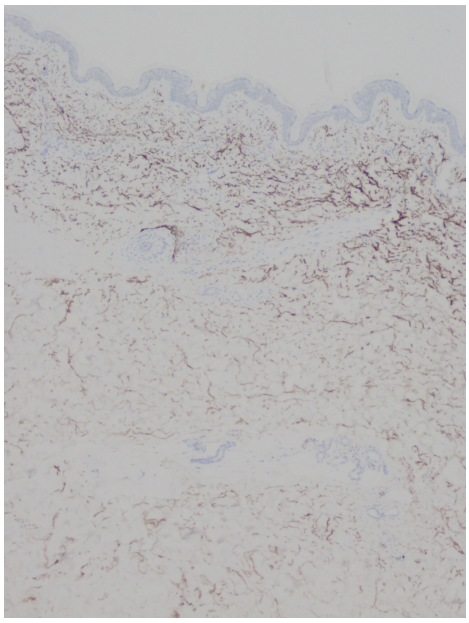


Figure 86: unburned control skin from second patient stained for C4a

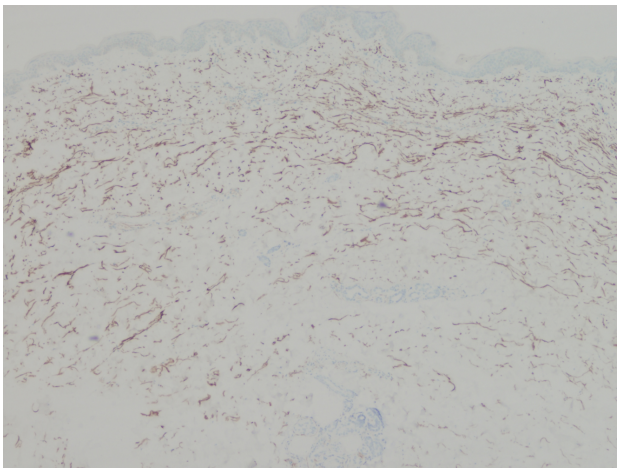


Figure 87: unburned control skin form third patient stained for C4a

Figure 85- Figure 87 above show unburned skin from 3 different patients stained for C4a. While there is staining of the collagen fibres, and around hair follicles and sebaceous glands, there is no staining in the dermal-epidermal junction. By way of comparison, sections from two of the same patients are shown below, this time from uncooled burns.

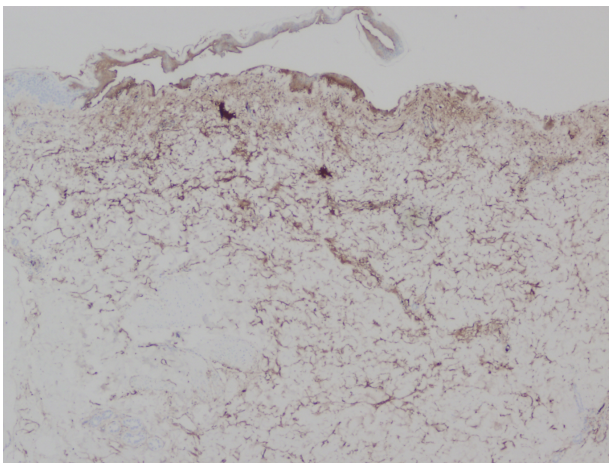


Figure 88: burned skin stained for C4a showing C4a localising to the blister

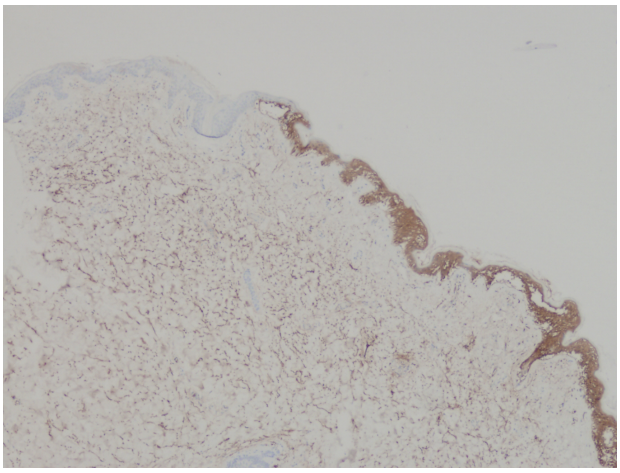


Figure 89: second sample of skin stained for C4a, showing concentration within the blister base

There is a clear increase in staining at the dermal-epidermal junction, and within the blister between the epidermis and dermis. There is a clear transition from no staining to strong positive stain at the edge of the blister. These biopsies are taken from entirely within the burn, so the entire width of the section has been exposed to the same temperature and pressure for the same duration of exposure. The formation of the blister is therefore closely associated with the deposition of C4a within the skin at that precise point.

7.10.2 The localisation of C5b-9 in the burn injury

The enrichment of complement proteins within burned tissues is of clear statistical significance, with 47% of proteins upregulated- well above the level of chance. This is reflected in the FDR of 7.2E-30. However, the functions of the complement cascade: opsonisation, chemotaxis, activation and degranulation, and lysis via the MAC cannot all be taken for granted. In particular the insertion of the MAC into the cell membrane requires the polymerisation of multiple C9s. To distinguish this from the trapping of C9 in its native, unpolymerised form in, for example, occluded vessels, monoclonal anti-C5b-9 antibody (Abcam, Rabbit polyclonal C5b-9, ab55811) was used to stain tissue sections from the same samples as those from which the proteomics results were

generated. The antibody is generated to the polymerised C9 neoantigen and will stain the MAC in tissue.

7.10.3 Staining normal skin for C5b-9

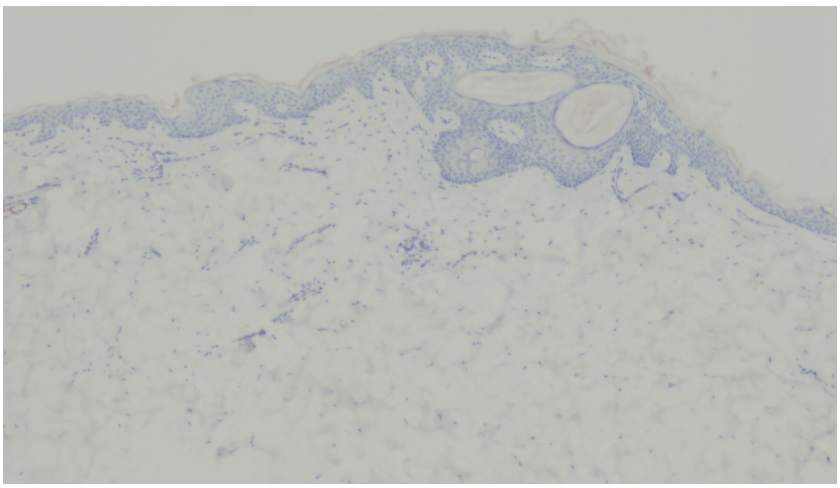


Figure 90: unburned skin stained for C5b-9

There is little by way of background staining in unburned skin in Figure 90, and the nuclei of the epidermis are clearly visible. The epidermis is adherent to the dermis.

7.10.4 Staining an untreated burn for C5b-9

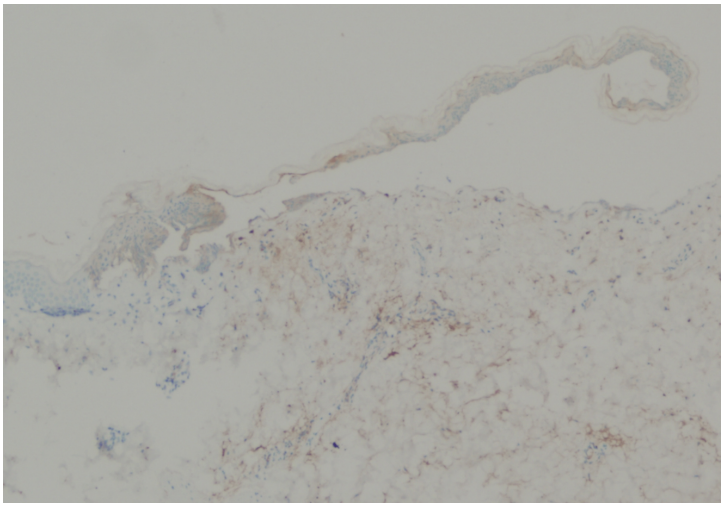


Figure 91: uncooled burned skin stained for C5b-9 showing localisation of C5b-9 within the blister.

Figure 91 shows increased staining in the dermis, and where the dermo-epidermal junction has separated to form a blister. This is particularly prominent within the basal layer of the epidermis, as shown in Figure 92.

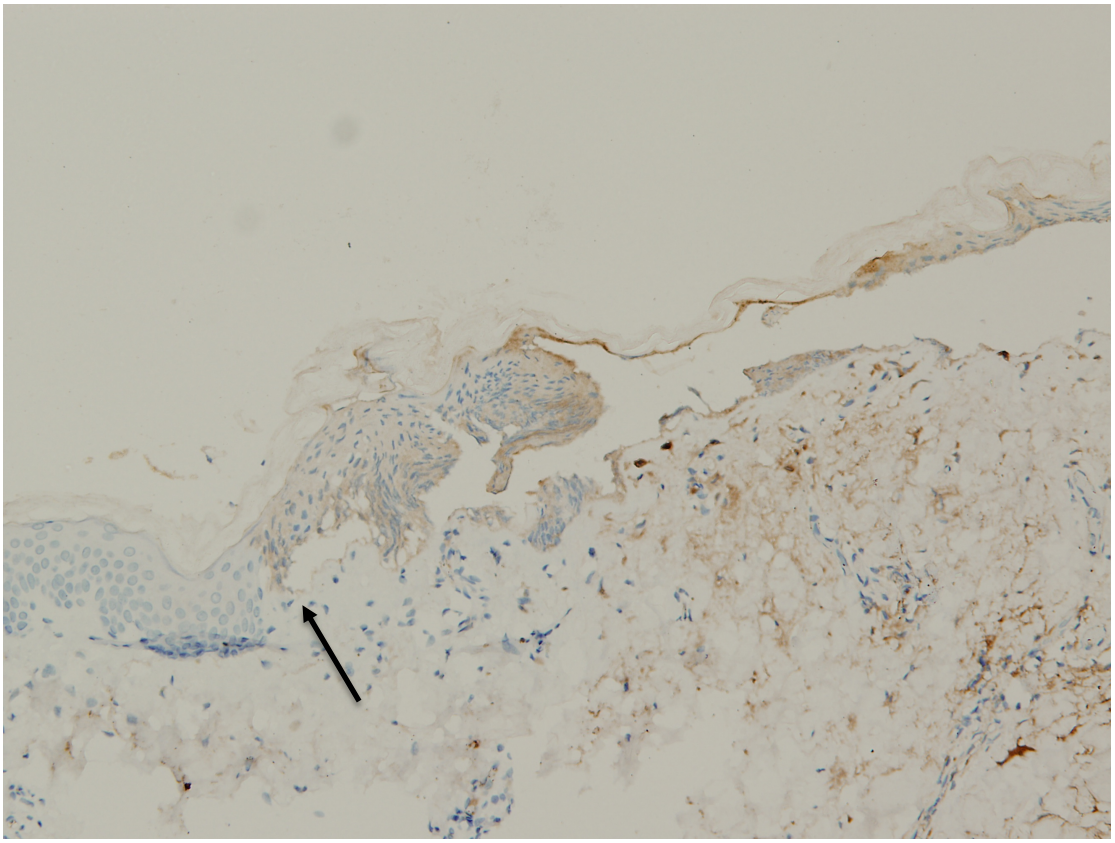


Figure 92: higher magnification from the same section as Figure 91 showing the localisation of C5b-9 to the blister

There is a sharp transition from negative to positive staining (arrowed) in Figure 92, and a corresponding increase in staining of the dermis underlying the blister. C5b-9 staining correlates to the epidermal nuclei taking on an elongated appearance, as previously described in the first results chapter.

The MAC (C5b-9) has been localised within the blisters of pemphigoid vulgaris and foliaceus[89], as have IgG molecules, although blistering was only seen where there was also MAC neoantigen. Our immunohistochemistry shows the same close relationship between blister formation and the deposition of the MAC.

7.10.5 Neutrophil adhesion and migration within burned tissues

The role anaphylactotoxins- including C4a- in increased vascular permeability, chemotaxis and Mast cell degranulation has been implicated in systemic inflammatory response syndrome (SIRS) in response to trauma. Sections of the same burns and controls were stained for neutrophil elastase to identify the presence of neutrophils within sections.

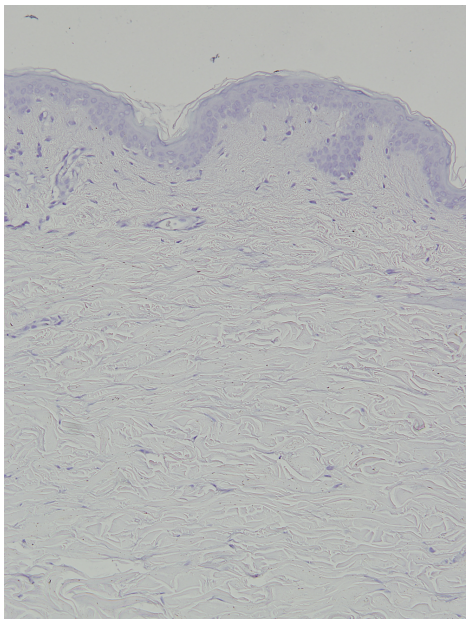


Figure 93: unburned skin stained for neutrophil elastase

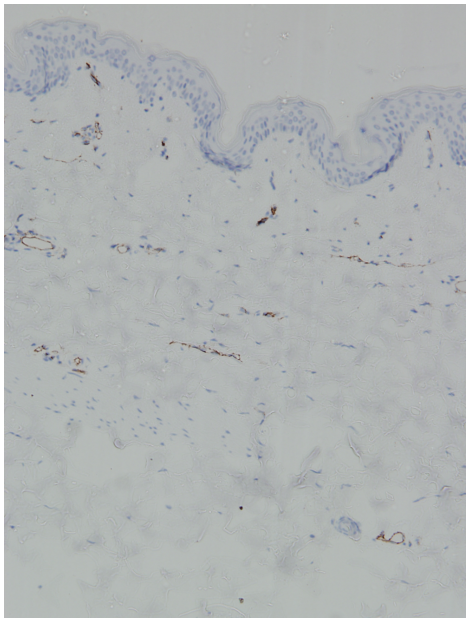


Figure 94: unburned skin stained for CD31 identifying vascular endothelium

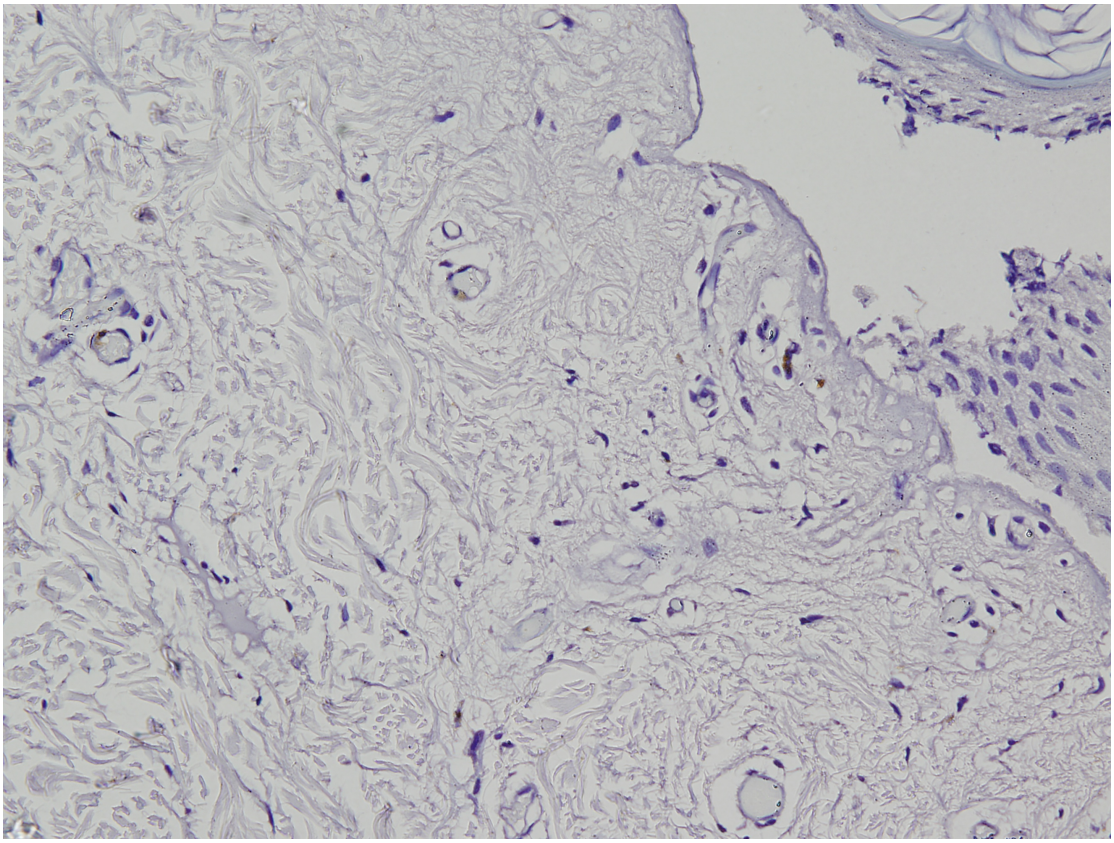


Figure 95: burned skin stained for neutrophil elastase, showing a few intravascular neutrophils

Figure 95 dilated vessels within the superficial dermal plexus and neutrophils adherent

to the endothelium. The epidermis has blistered away from the papillary dermis.

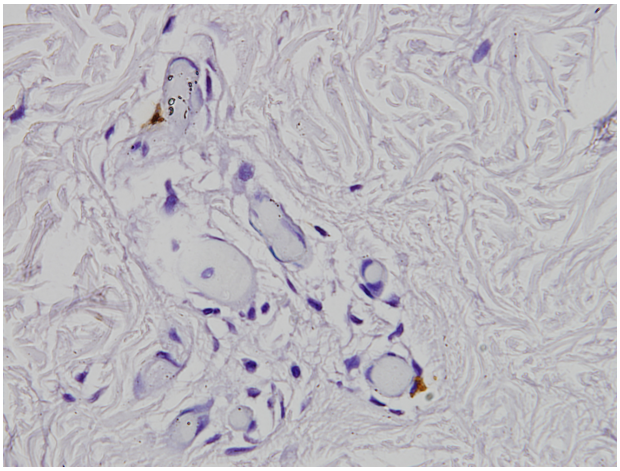


Figure 96: higher magnification of burned skin stained for neutrophil elastase, showing intravascular neutrophils top left, and a neutrophil migrating between endothelial cells bottom centre

The anaphylactotoxins produced during complement activation act as chemo-attractants to neutrophils, and cause endothelial cells to upregulate the expression of P-selectin[90]. These sections have shown that in the same area as the blistering is seen, C4a is also localised, and neutrophils are adherent to vessel endothelium and are migrating through it. They are, however, not particularly numerous, and this indicates that initial burn-injury evolution is independent of them.

7.10.6 The effect of de-roofing of the blister on the proteome of the burn

A conspicuous outlier of the proteomics data when visualised as a heat map is patient 25, in whom the cooled burn- “5BC”- grouped most closely among the control samples “5CC” and “5CNC”, and the untreated burn “5BNC” grouped to the left of several of the cooled burns from other patients. Examination of the sections of the 5BC and 5BNC samples shows that the blisters were “de-roofed”- the loosened epidermis was removed- inadvertently during surgery. Figure 97 and Figure 98 show sections from 5BC and 5BNC stained for C5b-9.

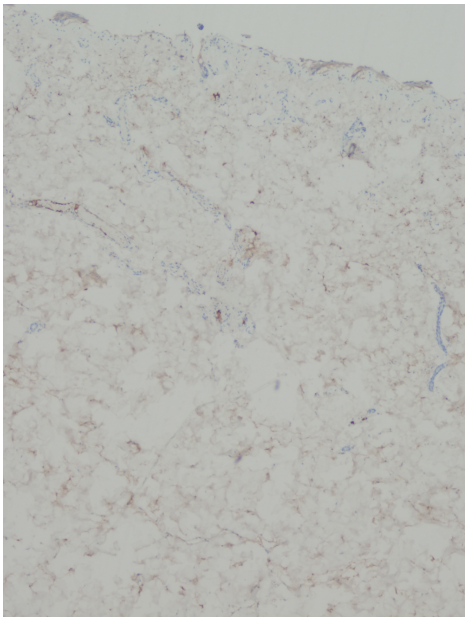


Figure 97: section 5BC stained for C5b-9

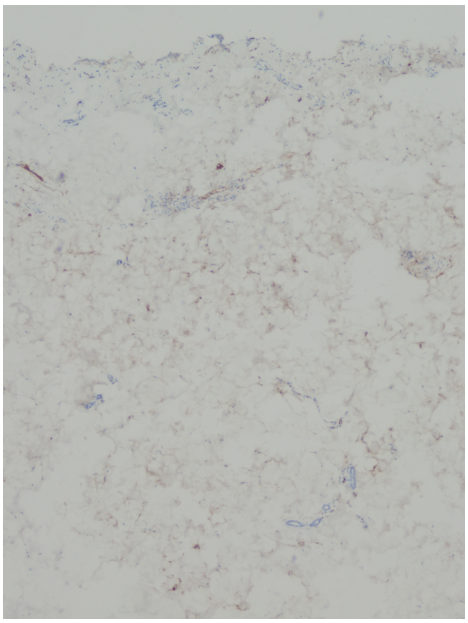


Figure 98: section 5BNC stained for C5b-9

In both sections burns the epidermis is completely removed and with it the layer of C5b-9-positive tissue/ exudate. This correlates to the low expression of complement proteins within these samples when they are compared to the other burn samples from different patients.

7.10.7 The clinical context of the proteomic findings

Complement activation in the contexts of burns[91], severe trauma[92], traumatic brain injury[51,54,93], ischaemia-reperfusion injury[94–97], sepsis[85,98–101], and dermatological blistering conditions[102,103] has been demonstrated to have an aggravating effect on the injured tissues themselves, and upon the subject at a systemic level. A model using a deep scald burn in dogs showed an increase in pulmonary arterial resistance following burning[104], and C4a (significantly elevated in the burned samples) is a potent vasoconstrictor, with a correlation to vasospasm following subarachnoid haemorrhage[88]. The use of pharmacological blockade, or gene knock-out animals has shown reduction in the severity of ischaemia-reperfusion injuries in which there is an

active role played by the cellular and humoral immune system, or has prevented the passive transfer of bullous pemphigoid in animal models.

The role of debridement of burns, through the removal of non-viable skin including any blisters, is a mainstay of acute burn management, with proponents arguing that excision removes a significant proportion of the inflammatory stimulus derived from the thermally-injured tissue and alters the systemic and pulmonary response to antigens such as lipopolysaccharide (LPS) seen in animal models[105], as well as reducing the post-burn catabolism seen in large burns in human subjects with delayed surgical management[106]. Topical treatment to modify the inflammatory response within the burn injury in mice was shown to reduce pulmonary inflammation and improve pulmonary resistance to infection[107].

The topical burn agent “Flammacerium”- a 1% silver sulphadiazine cream with cerium nitrate- is antibacterial by virtue of the silver content, and has the effect of reducing post-burn immunosuppression in rats[108], prevents burn oedema during plasma transfer from burned to unburned animals when the donor animals are treated with topical cerium nitrate after injury[109], and prevents the TNF-alpha response in rats following standardised burning[110]. One of the functions of cerium salts is their ability to fix tissues and bind compounds and limit their systemic dissemination. It is possible that part of the benefit of Flammacerium treatment is the sequestration of complement and coagulation cascade activation byproducts, including the anaphylactotoxins C3-5a, from systemic circulation, and also sequestering neoantigens that otherwise bind and deplete circulating immunoglobulins, reflected in the attenuation of post-burn immunosuppression[108].

7.11 The localisation of fibrinogen within the burn injury

The end-point of the activation of the clotting cascade by thermal injury- the deposition of fibrinogen- was affected significantly by cooling.

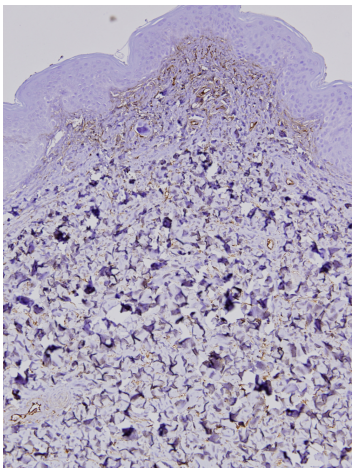


Figure 99: unburned skin stained for fibrinogen
There is some intravascular staining for fibrinogen, and background staining by the antibody, as reflected by the modifications of the protocol from that provided by the manufacturers (please see methods section). It is likely, too, that the use of skin very close to the wound edge in the context of major surgery resulted in a higher than normal background level of fibrinogen in the skin.

When consecutive sections to those used for the C5b-9 stained sections from untreated burn samples were stained for fibrinogen using an identical protocol:

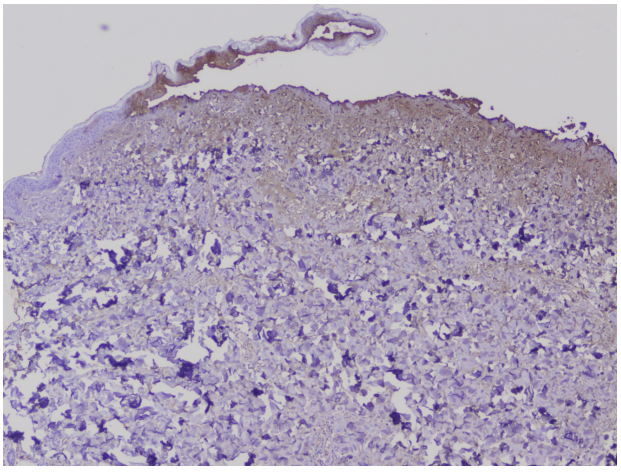


Figure 100: uncooled burn stained for fibrinogen

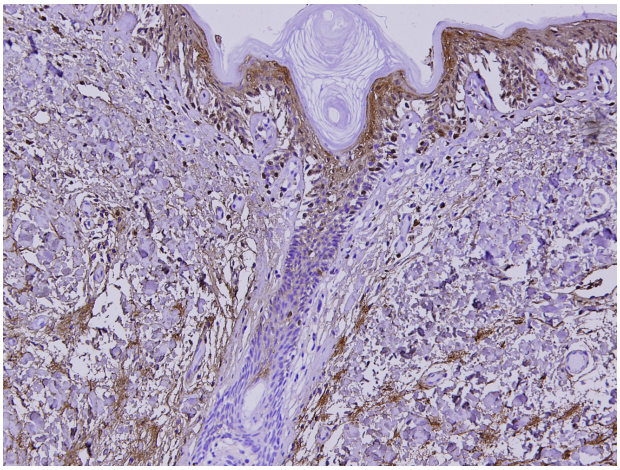


Figure 101: uncooled burn stained for fibrinogen at a higher magnification, and showing a hair follicle with fibrinogen deposition extending part-way down it

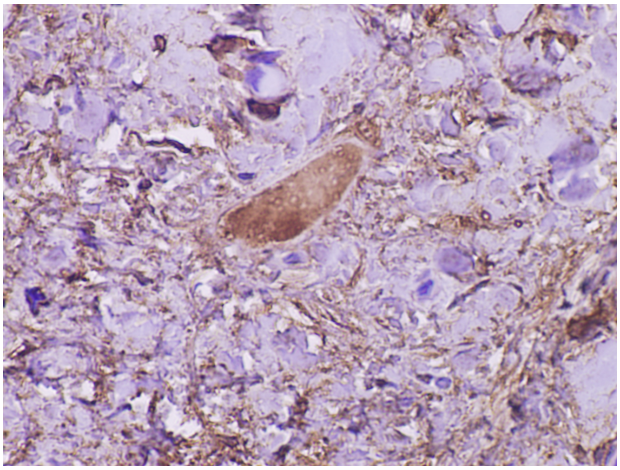


Figure 102: uncooled burn stained for fibrinogen showing intradermal vessel occluded by fibrinogen centrally

The relationship between cooling and depth of microvascular thrombosis, and the role of fibrinogen in thrombus formation demonstrated in this model makes it logical; that for a greater proportion of the proteome of a burn would consist of clotting factors compared to controls, and a cooled burn would contain proportionally less fibrinogen than an untreated burn. Cooling has been demonstrated to prolong both the prothrombin time (PT) and activated partial thromboplastin time (APTT) in vitro, with the lowest temperature used in the study of 28˚C producing a prolongation of the PT by 44% and the APTT by 59%[40]. Our experimental protocol involved cooling at a

temperature of 16˚C for 20 minutes, with a further period of sub-physiological temperature as the cooled area passively rewarmed.

Our experimental protocol did not allow the measurement of skin temperature after surgery had begun to establish the point at which normothermia of the skin resumed, but serial measurement of the author's skin temperature after 20 minutes of standardised cooling using the cooling device showed that the skin temperature remained hypothermic for at least a further 20 minutes. It is therefore logical that the coagulation cascade activation may have been subjected to cooling during the critical period after thermal injury, and deposited less fibrinogen.

The blisters stained strongly for fibrinogen, and the burns "5BC" and "5BNC" where the blisters had been de-roofed mapped towards the left side of the heat map, in the direction of the control samples. This indicates that a large proportion of the fibrinogen has been deposited within the blister itself, and within the extravascular space within the thermal injury. For this to happen, there needs to be a significant capillary leak for the fibrinogen and complement proteins to have gained access to the extravascular space. The anaphylactotoxins C3-5a released during complement activation would have this effect upon the microvasculature.

7.12 Platelet aggregation within the injured microvasculature

The role of thrombin (activated factor II) in platelet activation and the creation of a haemostatic plug is a key step in coagulation. Sections from normal and burned skin were stained with CD61 to identify platelets within the specimens.

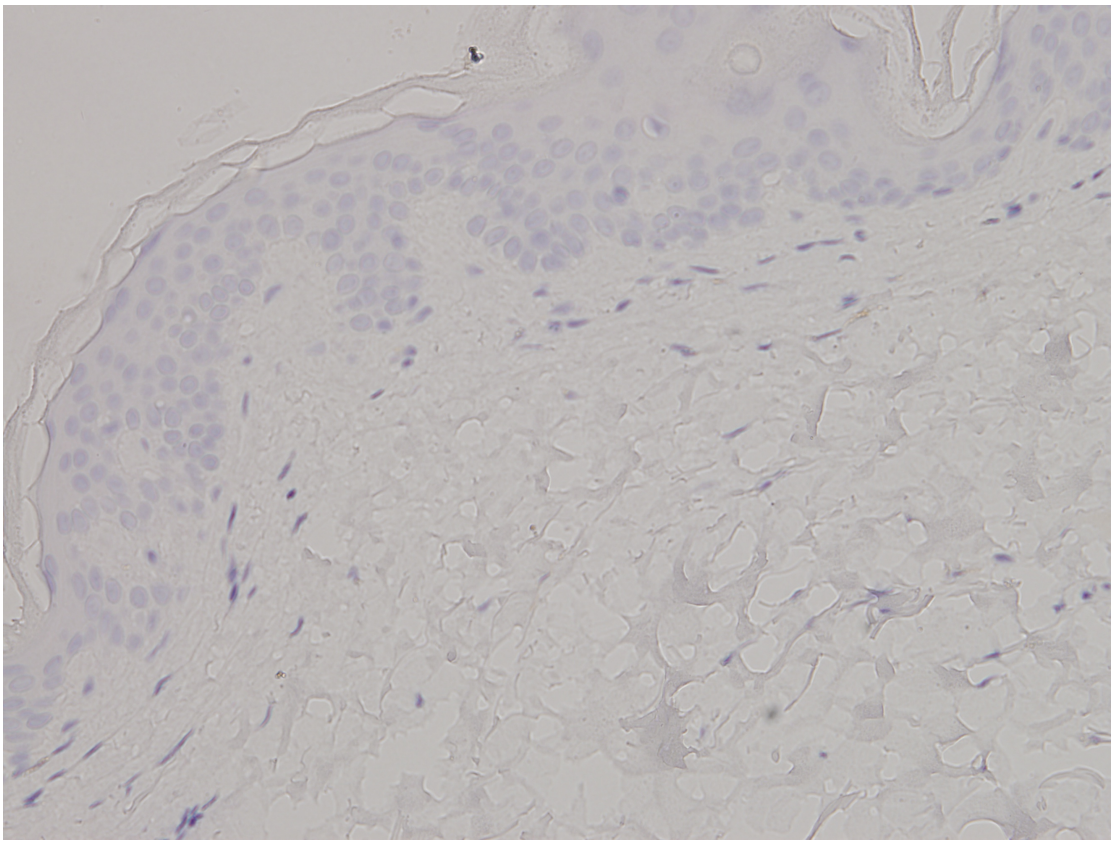


Figure 103: unburned skin stained for CD61, showing an absence of platelets

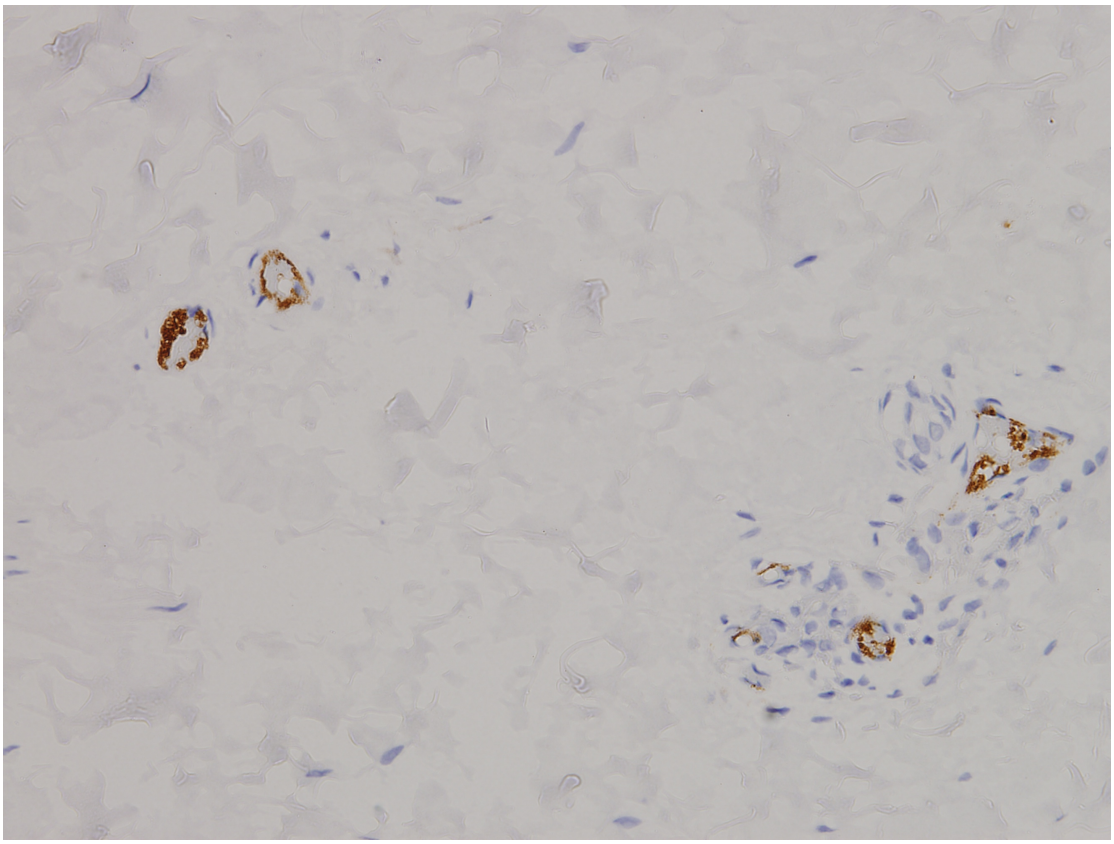


Figure 104: section of burned skin from the same patient stained for CD61, showing vascular endothelium outlined by adherent platelets

Activated platelets secrete alpha granules containing Von Willebrand factor, causing further platelet adhesion and activation, and form platelet microparticles that are shed from the phospholipid membrane of activated platelets and have a pro-thrombotic and pro-inflammatory effect.

7.12.1 Summary of the coagulation proteomics and immunohistochemistry

In summary of the coagulation factor proteomics and immunohistochemistry, there is objective quantification from the first chapter of results of the dose-response relationship between contact-time and standardised burn-depth using the burn-creation apparatus. The microvascular occlusion shows significant progression over the first three hours after burning, indicating an active process, and patent and

perfused microvasculature for the cellular and humoral clotting components to be delivered to the site of injury.

The extent and progression of the microvascular occlusion showed significant reduction in response to standardised cooling.

The proteome of burned skin shows significant increases in expression of clotting factor proteins and these changes are significantly reduced in amplitude by cooling, particularly with respect to fibrinogen- the end-product of the cascade.

Immunohistochemical staining for fibrinogen showed minimal staining in unburned skin, but burned skin showed significant staining within the microvasculature, the collagen of the dermis, and most strikingly in the blister itself. Staining for CD61 shows platelets forming a dense layer on the vascular endothelium, indicating that they are an active part of the evolving microvascular occlusion, and have accumulated after thermal injury, while the microvasculature was still patent and perfused. There were modest increases in VWF in burning, unaffected by cooling (Table 20). There was significant reduction in levels thrombin in cooled burns compared to uncooled burns.

Both thrombin and VWF bind to GPIb-IX[111] expressed on platelets and are responsible for the arrest of platelets at higher shear-stresses. Fibrinogen binds $\alpha_{IIb}\beta_3$ fibrinogen receptor- a member of the integrin family- on the platelet plasma membrane and causes platelet activation to allow platelet aggregation and stable thrombus formation. Hence a reduction in fibrinogen deposition will result in a reduction in platelet aggregation.

7.13 Summary of the proteomics data

The proteomic analysis of these 20 samples has shown several significant findings. Firstly, we identified over 900 proteins from thermally injured skin. Previous proteomic studies of skin injured with sodium dodecyl sulphate were able to identify 653 proteins with no statistically significant differences in expression[112]. In contrast, we identified 211 proteins significantly altered by burning and 109 of these were altered significantly by cooling of the burn injury. All those responding to cooling were up-regulated by burning and this up-regulation was reduced by cooling.

The two main themes of the proteomics data were complement activation and coagulation. Coagulation had already been demonstrated in the initial analysis of the burns in Results 1. Complement activation has been described previously in burn studies, but the quantifiable reduction of complement activation by cooling at three hours after injury has not been described. The significant reduction in immunoglobulin levels in cooled burns compared to their untreated counterparts and the elements of the complement cascade that were most increased point towards the classical complement activation by antibody-antigen complexes. It is not possible to discern from our data what the antigen might be, but the autoantigen non-muscle myosin has been described in ischaemia-reperfusion injury and indeed in burn injury progression, and it was identified in our proteomics data. Non-muscle myosin levels were reduced significantly by burning and were unaffected by subsequent cooling, meaning that- were it to be the autoantigen in this case, too- cooling may have affected the antibody-antigen interaction, rather than the abundance of the autoantigen.

The activation of C5 by thrombin is a further point at which the complement cascade can be activated, downstream of the classical and alternative pathways. Prothrombin

was present in statistically significantly higher levels in burns compared to controls, and was statistically significantly reduced by cooling, and this may also have had inhibitory effect on complement activation downstream of C5 and on the C5-9 protein levels.

Cooling has been shown on an in vitro level to prolong significantly both the prothrombin time and the activated partial thromboplastin time. Prolonging these measurements of clotting function would have the effect of reducing the levels of thrombin present and hence both the deposition of fibrin and the activation of complement, as well as reducing vascular occlusion.

The MAC has been shown to have a causal relationship to blister formation in pemphigoid skin conditions, and was identified as present focally at the points at which the epidermis separated from the dermis in our model, indicating a similar mechanism is responsible for blister formation after burning.

It is also likely that the formation of the MAC in endothelial cells will result in their lysis and the exposure of collagen, tissue factor and neoantigens, resulting in activation of the clotting and complement cascades respectively.

The close interaction of the clotting cascade and the complement cascades at multiple levels may help explain why the blockade of one process at one level was unsuccessful in halting burn progression, with the possible exception of C4 deficient mice, and the blockade of IgM-non-muscle myosin antibody antigen complex formation which did show significant attenuation of burn-progression.

This results section has further validated our model as it has quantified the microvascular occlusion at a proteomic level with significant reduction of the corresponding proteins and also concurred with the role of complement activation and

MAC formation in blistering skin disorders, and localised the MAC to the blistered points of the epidermis.

8 Discussion

8.1 Summary of the conception of the project

The starting point of the project was an appraisal of the published literature on the effects of burning on skin, comprising experimental animal models[4,15,17–20,46,113] and observational studies of human burn patients[8,9,13,65] presenting to burns surgeons for treatment. There are also a small number of mathematical models for thermal injury, although they concentrate on the effects of thermal injury to tissues and do not include cellular, proteomic or transcriptomic events[21,22].

Clinical cohort studies have demonstrated the effectiveness of timely appropriate cooling of burns in reducing the need for skin-grafting, and animal experimental models have supported this, although there are some issues around translating animal burn models to humans.

The few human experimental burn studies were several decades old, and had created burns that were probably too deep to benefit from cooling, or had used interventions that were ineffective in improving burn outcome[9]. There are more recent transcriptomic analyses of human burn specimens from burn debridement surgery. By definition, these samples are deeper burns and hence cannot give answers as to what is changed by cooling to reduce the severity of burns, and hence the need for skin-grafting surgery. It is difficult to justify ethically taking biopsies from a burn that has a high clinical likelihood of healing primarily in order to make a comparison to areas requiring excision and skin-grafting to heal in a timely manner. Even if cooling had been administered, it must have been ineffective for the burn to still require skin-grafting. Fundamentally, it is practically very difficult to select near-identical burns in

terms of depth, mechanism, anatomical site, patient demographics, and interval since injury that have not been cooled, and matched samples that have been treated with cooling to make a direct comparison.

8.1.1 Establishment of a human burn model for cooling of a partial-thickness burn

The model that we developed has overcome many of these obstacles. We have developed a methodology that utilises anatomically consistent and symmetrical areas of skin that are due to be discarded during the normal execution of the operation. This overcomes the ethical issue surrounding sampling burned skin that is likely to heal without surgery following the successful administration of cooling in a clinical scenario, as the entire area of skin is due to be discarded.

With our model the mechanism of burning is entirely consistent. We have demonstrated a dose-response relationship between duration of contact with the burning device and the depth of the burn created using the method described in the context of non-experimental human burns[2], and demonstrated a statistically significant difference between the depths of burns created with 5, 7.5, 10, and 15 seconds of contact. Beyond 15 seconds of contact the burn samples showed occlusion of vessels within the subdermal fat, corresponding to a full-thickness burn. These statistically significant differences corresponded to differing clinical appearances of burns created with these durations of contact time, with all burns created with >15 seconds of contact time having the clinical appearance of full-thickness burns.

The reproducibility of the depth of burning as measured by dividing the depth of the deepest occluded capillary divided by the dermal depth at that point (standardised burn depth) is very good, as can be seen when the untreated burns created with 7.5

seconds of contact time were plotted on the contact-time vs standardised burn-depth graph. This data point consists of 26 individual burns from 13 different patients with a mean standardised burn depth of 43% (37%-49% 95%CI).

The longitudinal study of burns from the same 5 patients taken at 1, 2, and 3 hours after injury shows significant progression in burn-depth from 1-2 and 1-3 hours, showing that the burned tissues remain perfused and that the thermal injury is actively evolving over the 3 hours following creation.

The cooling device is both compatible with the surgical environment and consistent in terms of temperature and duration of application. In contrast, cold running water has variables of temperature, flow rate, and inconsistencies in terms of how it runs across the skin surface. The burns are harvested at an identical time-point and stored and processed identically.

Cooling reduced burn-depth significantly in all cases, as measured by the depth of microvascular occlusion, and this response was seen in the time-course study of 5 patients with paired burns harvested at 1, 2, and 3 hours after creation.

The microvascular changes are seen within the dermis underlying the blistered areas of epidermis, and do not extend more than 1-2mm laterally from the edges of the blisters, which is significantly less that the distance between the burn and control samples.

8.1.2 Optimisation of mRNA extraction from burns

The high RNase activity, and the relatively low yield of RNA in skin was overcome, allowing good-quality RNA to be extracted from unburned skin. A major issue encountered with the RNA extracted from the burns was significant degradation as reflected by the significantly reduced RINe values obtained. This degradation was not

affected by cooling, and probably reflects the amount of thermal damage to the tissues and hence the volume of transcriptionally inactive or necrotic tissue containing increased amounts of thermally or enzymatically degraded RNA.

The degradation issues with RNA extracted from burned skin seen with these samples may make microarray and qPCR assays less reliable as it may not be possible to identify partially degraded transcripts if they are unable to bind predetermined probes or primers, respectively.

RNAseq can identify degraded transcripts so long as there is a sufficient length of recognisable transcript to match to a known gene, and as such may have advantages in the burn scenario with associated RNA degradation. In the absence of a starting hypothesis or list of candidate genes, a transcriptome-wide approach allowed a more unbiased evaluation of the transcriptome to be made.

8.1.3 Analysis of mRNA extracted from cooled and untreated burns and controls

The limitation of the histological extent of burn-associated microvascular and epidermal changes was reflected in the clear separation of the transcriptomes of burned and unburned skin, and to a lesser extent the separation of cooled and untreated burns, when plotted on an MDS plot. The burns with the greatest histological depth plotted closer to the respective controls from the same patient than to other burn samples, and as such were relative outliers on the diagram. The untreated and cooled burns for this patient had, on average, a standardised burn-depth of 66% and 54%, respectively, making each the deepest burn in their respective group. A possible explanation for this relative anomaly is that a deeper burn has fewer viable cells within it, and hence mounted a smaller transcriptomic response to thermal injury, and the

transcriptome of the remaining viable tissue to be like that of unburned skin. The relative outlier status of this patient's samples in terms of burn depth as reflected on the MDS plot in Figure 52 justifies its exclusion from the more detailed transcriptomic analysis.

The transcriptome of normal human skin was shown to undergo significant changes in response to thermal injury. There was significant upregulation of 2,266 and downregulation of 1,527 genes of the 17,261 expressed within the transcriptome. Analysis of individual genes is less useful than the functional ontological and pathway analysis for patterns in the changes in gene transcription.

The ontologies showing significant upregulation as measured by their z-scores and adjusted p-values relate to the processes of inflammation, cell adhesion and migration, haemostasis, and platelet activation, and extracellular matrix remodelling.

The ontologies showing significant downregulation related to epidermal differentiation- although there was a small positive z-score for epithelial migration GO:0090132- formation of the cornified envelope (GO:0001533) showed a more marked downregulation, as did keratinisation (GO:0031424), both with z-scores of -5. Hair follicle differentiation (GO:0001942) was also downregulated with a z-score of -2.3. Taken together, these results show a loss of viable keratinocytes and damage to hair follicles, but also enrichment for ontologies of epithelial proliferation and migration indicating that the initial phases of healing have already begun within 3 hours of injury.

The pathological picture of a cutaneous thermal injury is of cellular and humoral inflammation, Mast cell degranulation with histamine release causing increased vascular permeability, neutrophil adhesion and migration, microvascular occlusion, and denaturing of the dermis with realignment of the collagen fibre orientation. There

is also separation of the epidermis from the dermis, blister formation, and loss of skin-barrier formation with associated increased water-loss. Deeper burns will show loosening of hairs from the follicles and a relative lack of blister-fluid production as the necrotic dermis forms a relatively waterproof layer and the microvasculature of the superficial dermis is completely thrombosed.

More superficial burns re-epithelialise from the wound edges and through migration of surviving keratinocytes from within deeper parts of the epidermal appendages- the pilosebaceous units and sweat glands. Retention of these structures is a feature of healed superficial burns and has been reported as a feature of cooled burns in animal models.

Deeper burns that have lost their epidermal appendages lack this source of keratinocytes for wound re-epithelialisation. As a result, healing is achieved entirely through migration from the wound edges, and there is a characteristic lack of hair follicles and sebaceous glands in the healed wound as these structures cannot be regenerated.

There was no significant effect on the transcriptome of normal skin in response to cooling alone, refuting the possibility of a protective transcriptional response to cooling that is some way attenuated the response to thermal injury.

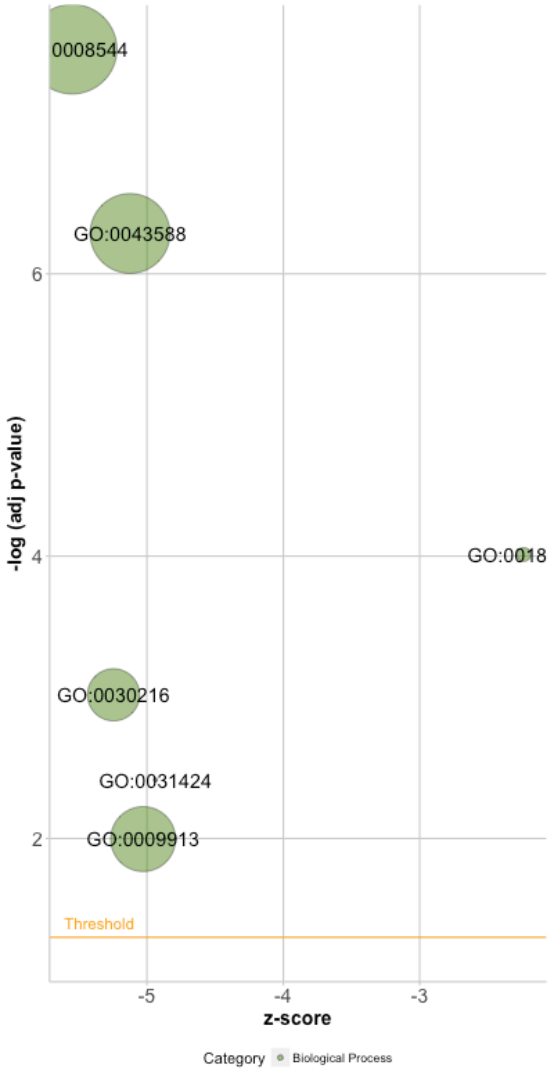
The effect of cooling on the transcriptome on thermally injured skin was relatively modest, given the scale of the response to burning. The effect was to attenuate the changes in transcription in response to thermal injury in the genes in question, through relative downregulation of genes transcribed at increased levels in response to thermal injury, and relative upregulation of genes transcribed at reduced levels in response to thermal injury.

The genes downregulated in cooled burns compared to untreated burns relate to platelet activation, wound healing, and response to misfolded proteins.

The genes upregulated in cooled burns compared to untreated burns that relate to the differentiation of the hair follicle (SPRR2G, KRT82, TCHH, TCHHL1, and PRR9) indicate that these structures are retaining their viability and are continuing to transcribe these RNA species at a higher level than they are in burned, untreated skin. These structures lie in the watershed area between the deeper untreated burns and the more superficial, cooled burns. A more superficial burn will have less damage to the deeper structures, including a greater proportion of the hair follicle. Through cooling, the viability of these structures has been preserved and they will form foci of re-epithelialisation during healing.

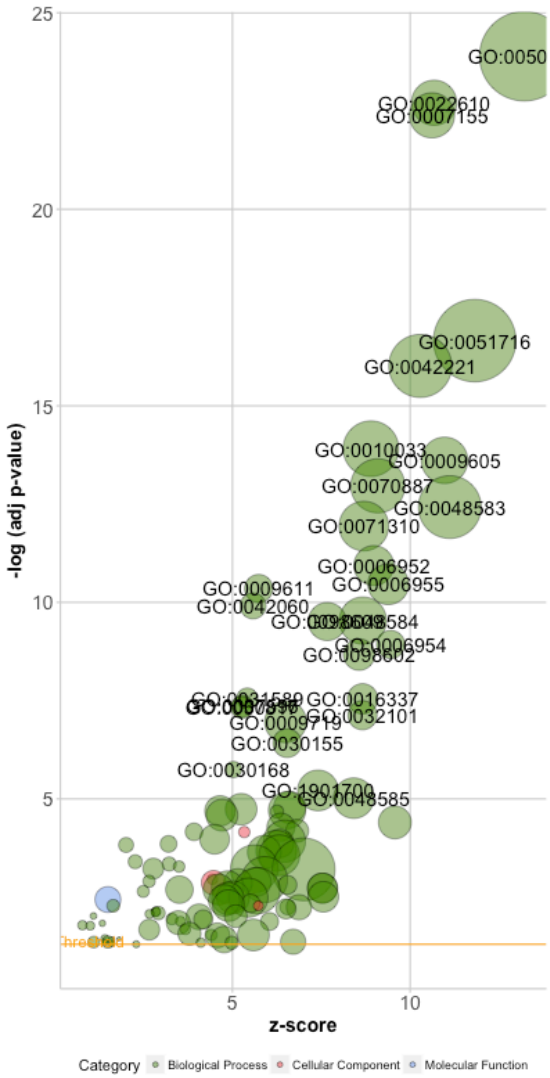
The use of z-scores to give an overall measure of whether an ontology is upregulated or downregulated has some limitations in that it does not make allowance for the extent to which the individual genes have been up or down regulated, or their respective interactions to one another. It does give an overall picture of the changes in the transcriptome of burned skin. The effects of cooling are too small, and too limited in terms of number of genes affected for there to be an appreciable effect on the z-scores.

A GOBubble plot of the ontologies to which the genes significantly upregulated by cooling in the context of burning belong was plotted, and illustrates that the genes that were upregulated significantly by cooling in the context of burning were related to ontologies essential to epidermal function and development, and negatively enriched by the process of burning, as evidenced by the negative z-scores.



ID	Description
GO:0008544	epidermis development
GO:0043588	skin development
GO:0018149	peptide cross-linking
GO:0030216	keratinocyte differentiation
GO:0031424	keratinization
GO:0009913	epidermal cell differentiation

A similar diagram was plotted for the ontologies of which genes significantly down-regulated by cooling in the context of burning were members. The most significantly (in terms of adjusted p-value) enriched ontologies, selected from the full list of ontologies showing significant enrichment in this data, of which the genes significantly downregulated by cooling were members pertain to defence response, response to wounding, coagulation, haemostasis, and platelet activation.



ID	Description
GO:0050896	response to stimulus
GO:0022610	biological adhesion
GO:0007155	cell adhesion
GO:0051716	cellular response to stimulus
GO:0042221	response to chemical
GO:0010033	response to organic substance
GO:0009605	response to external stimulus
GO:0070887	cellular response to chemical stimulus
GO:0048583	regulation of response to stimulus
GO:0071310	cellular response to organic substance
GO:0006952	defense response
GO:0006955	immune response
GO:0009611	response to wounding
GO:0042060	wound healing
GO:0048584	positive regulation of response to stimulus
GO:0098609	cell-cell adhesion
GO:0006954	inflammatory response
GO:0098602	single organism cell adhesion
GO:0031589	cell-substrate adhesion
GO:0016337	single organismal cell-cell adhesion
GO:0007596	blood coagulation
GO:0050817	coagulation
GO:0032101	regulation of response to external stimulus
GO:0009719	response to endogenous stimulus
GO:0030155	regulation of cell adhesion
GO:0030168	platelet activation
GO:1901700	response to oxygen-containing compound
GO:0048585	negative regulation of response to stimulus

It illustrates that the small number of genes affected by cooling in the context of burning are members of key ontologies including wound healing, programmed cell death, haemostasis, platelet activation, epidermal development, keratinisation, and hair follicle development. These are all relevant to thermal injury and wound healing.

8.1.4 Immunohistochemical validation of key transcriptomic findings

The tissue sections from the same samples as those from which the RNA had been extracted were stained with commercially-available antibodies as follows.

8.1.4.1 CD61: Platelets

The presence of platelets adherent to the lumen walls of thermally-injured vessels. This was consistent throughout the depth of the thrombosed microvasculature of thermally-injured dermis and demonstrates the role of platelets in microvascular occlusion following thermal injury. Just as the depth of microvascular occlusion was reduced by cooling, so the number of platelets is reduced by the reduction in volume of thrombosed microvasculature.

8.1.4.2 Neutrophil elastase: neutrophils

Neutrophils were not present consistently across the width of the blister bed, and although examples were found of neutrophils migrating between endothelial cells and into the interstitial space, most were still intraluminal, in association with thrombosis. It is likely that the 3-hour time point is too soon to see widespread infiltration of neutrophils into the burn area. Previous video microscopy studies found that although peak neutrophil adhesion takes place within 60-90 minutes, infiltration does not begin for 24-48 hours.

8.1.4.3 Mast cell tryptase

Ontologies associated with degranulation and vesicle Mast cell tryptase identified a similar number of mast cells in all four conditions- cooled burn, untreated burn, cooled control, untreated control- but the edge of the brown DAB staining was completely contained to the Mast cell in control skin, while in untreated burns, there was a leaking

of the DAB stain into the surrounding dermis, indicating degranulation had taken place. Where there was no blistering of the epidermis, the Mast cells retained a sharper outline and cooling may also have reduced the degranulation of the Mast cells as indicated by the staining for Mast cell tryptase.

Cooling has been shown to stabilise Mast cell granules and reduce the release of histamine following thermal injury. It is possible that this is demonstrated here- cooling has reduced degranulation and consequent release of tryptase as evidenced by less staining of the surrounding dermis.

8.1.4.4 BCL-2 oncoprotein

The loss of expression of BCL-2 oncoprotein is a key step in apoptosis. Ontologies related to apoptosis and programmed cell death were upregulated by burning. Staining of sections for BCL-2 showed strong baseline expression of BCL-2 in epidermis and epidermal appendages. This positive staining was lost following burning, and specifically where the epidermis blistered away from the underlying dermis, and where the nuclei take on an abnormal, elongated appearance. It is possible that even at 3 hours after injury there is loss of BCL-2 expression, and that the blistering process involves apoptosis of the epidermal keratinocytes. Previous studies have shown that BCl-2 is downregulated at a protein level in burns at 2-48 hours[70], and at an RNA level is upregulated in cooled burns compared to untreated burns at 2 and 24 hours[114], in both cases in rat models.

8.1.4.5 TCHH: Trichohyalin

Trichohyalin is has a Log fold-change of +2.5 in cooled compared to untreated burns, and is expressed in keratinocytes and melanocytes within the epidermis and related appendages. Immunohistochemistry confirmed this within tissue sections from the

same burns as those from which the RNA was extracted. Loss of keratinisation and pigmentation are seen following burning and loss of the epidermis, and it is a frequent clinical observation that the wound re-epithelialises and re-pigments from the hair follicles, provided that they remain viable. Preservation of viable basal epidermal keratinocytes and melanocytes, as indicated by the increased level of expression of TCHH mRNA in cooled compared to untreated burns would confer a healing advantage to the cooled burn compared to its untreated counterpart.

8.1.4.6 KRT82: Keratin 82

Keratin 82 showed a 3.9 Log2 fold change in cooled compared to untreated burns. It is a Type II hair keratin that forms heterodimers with Type I keratins in the hair. While it is reported as limited to the hair cuticle, our IHC identified it strongly within the epidermis and epidermal appendages, including within the hair follicle and pilosebaceous units. Again, the effect of cooling in reduction of the burn depth as a proportion of total dermal thickness will protect the deeper epidermal appendage structures and result in this relative increase in KRT 82 mRNA compared to the untreated burns.

8.1.4.7 HSPA6: Heat-shock protein 70B

Heat-shock protein (HSP)70B is a chaperone protein responsible for the correct folding of newly synthesised proteins, and the refolding or hydrolysis of misfolded proteins. Cooling reduced the expression of HSPA6 mRNA by -0.72 Log2 fold-change when cooled and untreated burns were compared. Our immunohistochemistry localised HSP70B expression to the basal epidermal cells and epidermal appendages. There was a slight loss of staining from blistered epidermis, but it was not possible to identify any areas of increased HSPA6 staining in the sections examined. This may

represent thermal denaturing of the protein and loss of the epitope that the antibody binds. The reduction in HSPA6 mRNA transcription in cooled burns compared to untreated burns may reflect less damage- thermal and inflammatory- to the epidermis and epidermal appendages, and hence reflect a reduction in the extent of the injury.

8.1.5 Proteomic analysis of paired samples from the same specimens

The proteomic data was in many ways more informative that the transcriptomics- while the number of proteins identified was smaller than the number of RNA transcripts, the proportion of the identified proteome that was altered significantly by burning, and most importantly by cooling was much higher. There is the potential for bias towards soluble plasma proteins as the Trizol extraction method formed a very insoluble precipitate of the protein fraction, and required prolonged resuspension and trypsin digestion before analysis. However, this is a constant factor across all 20 samples submitted for analysis and it does not detract from the findings.

Many of the proteomic changes in skin caused by burning, and modified by cooling can be categorised into two systems of acute phase proteins: the coagulation system and the complement system.

8.1.5.1 The coagulation system

The preservation of the microvasculature is a key goal of burn therapy, and conversely occlusion of the microvasculature is an indicator of increased burn severity as assessed both clinically- as assessed by blanching and capillary refill in the burn- and during surgery when the debrided wound is assessed for normal bleeding to indicate adequate debridement prior to skin grafting.

The initial sections from each burn showed microvascular occlusion in a dose-response relationship to the duration of contact with the burn-creation device. Cooling was found to reduce this significantly.

The proteome of the untreated burn was found to have significantly elevated levels of proteins from the coagulation pathway compared to that of normal, untreated control skin. Many of these proteins were expressed at significantly lower levels in cooled compared to untreated burns. Specifically, there was significant reduction in the levels of thrombin and both the alpha and beta subunits of fibrinogen. These three clotting factor proteins are of particular interest because thrombin has the ability to activate C5 in the complement cascade, while fibrinogen deposition results in the microvascular occlusion seen in the burn specimens.

Hypothermia is a recognised cause of coagulopathy, and cooling of normal human blood samples has been shown to prolong both the prothrombin time- a measure of the extrinsic pathway requiring tissue factor- and the partial thromboplastin time- a measure of the intrinsic pathway requiring contact activation[40]. Cooling at 16˚C for 20 minutes may have a similar effect on the activation of the coagulation cascade in vivo. It has also been shown that hypothermia increases shear-induced platelet activation, and hence platelet aggregation in vitro[42]. The temperatures studied in this paper were 24-34˚C, and our cooling treatment was 16˚C, although the intradermal temperature during treatment is unknown. This does illustrate the balance to be struck with cooling: while cooling reduces the activation of the clotting cascade proteins, and slows enzyme reactions in general, it increases the aggregation and activation of platelets, and may explain why ice-treatment has been shown to worsen burns compared to no treatment at all[19,26].

8.1.5.1.1 Staining for fibrinogen in burns

Immunohistochemical staining for fibrinogen showed that the fibrinogen was deposited within the lumen of the vessels, around the hair follicles and within the blister between the epidermis and dermis. The widespread staining indicates that there is an increase of vascular permeability allowing fibrinogen to pass into the interstitial spaces rather than simply form a haemostatic intravascular plug.

8.1.5.1.2 CD61: Platelet adhesion

As previously stated, there is immunohistochemical confirmation of platelets adhering to the endothelium of occluded vessels in burns, and are an integral part of the microvascular occlusion seen in response to burning.

8.1.5.2 The complement system

Complement cascade proteins were present at significantly higher levels in the untreated burns compared to control samples. Cooled burns contained significantly less of these complement proteins than the untreated burns from the same patients.

The specific pattern indicates activation via the classical pathway, through the formation of antigen-antibody complexes. This is further supported by the presence of IgM and IgG at increased levels in untreated burned skin compared to untreated controls and a significantly reduced level of some antibody subunits in cooled burns compared to untreated burns. In vitro work on antibody-induced complement activation- the classical pathway- has determined that in fact modest clinical hypothermia of 31˚C actually increased complement activation and cell lysis compared to 37˚C, but found that this change was reversed by temperatures below 19˚C, where there was significantly less complement activation through both the classical and alternative pathways[115]. This study acknowledged that the in vitro findings did not

explain the clinical benefit of cooling to neurological outcome following ischaemia-reperfusion injury, and that other mechanisms must be responsible. Our study used a temperature of 16˚C for cooling, and although we cannot know the corresponding intradermal temperature, this value is within the inhibitory temperature range for this experiment.

It is unlikely that the bacterial antigens necessary for the activation via the Lectin pathway would be present in an acute burn created under aseptic conditions. However, it is a common clinical observation that infection of a burn can cause it to progress to a deeper level of injury, and convert a partial-thickness burn that might heal primarily to a deep dermal or full-thickness injury that requires grafting. Mannose residues on bacterial cell walls provide an additional mechanism of complement activation via binding to Mannose-binding proteins and activation of C2 and C4 proteins to ultimately form the membrane attack complex and lyse the organism. It is possible that complement activation by this mechanism would result in collateral damage to viable elements of the epidermis and dermis, resulting in progression of the burn.

The presence of increased levels of thrombin in burns, and their significant reduction in cooled burns offers a further mechanism for complement activation following thermal injury and its reduction through cooling. Thrombin has been shown to activate C5 to $C5b_T$- a variant of C5b that forms a more potent MAC than C5b with generation of a non-C5a fragment $C5_T$ in place of C5a[55,116]. The changes in thrombin levels caused by the processes of burning and of cooling following burning are reflected in the changes in complement proteins from C5 onwards. However, this does not account for the similar changes in C1-4 proteins in response to burning and cooling seen in our data. Furthermore, there is animal model work demonstrating that blockade of IgM-antigen binding and C4 protein knock-out both reduce the progression

of burns and subsequent scarring[56,57]. The activation of C5 by thrombin would provide a mechanism that would bypass both these interventions, were it a key mechanism in burn progression.

8.1.5.2.1 The immunohistochemistry of C4a

The only soluble “a” fragment of complement activation identified from the proteomics was C4a. Sections from the same samples as those used for the proteomic analysis, and samples from different patients, but representing the same 4 conditions of cooled and untreated burns and controls were stained for C4a.

Control skin had very little staining for C4a. By contrast, burned skin showed marked staining for C4a in the upper dermis, and particularly where the epidermis had blistered away from the dermis, with a sharp transition at the edge of the blister corresponding to the immunohistochemical changes seen with fibrinogen deposition, and the microvascular occlusion in the dermis.

8.1.5.2.2 The immunohistochemistry of C5b-9

The key final step of the complement cascade activation if the formation of a membrane-spanning pore consisting of C5b, C6, C7, C8 and multiple units of C9. This allows the passage of water, ions and small molecules and causes cell lysis. The antibody used was generated specifically for the neoantigen of multiple C9s produced through the activation of the human complement cascade with cobra venom, and will only bind to the multiple C9s in the assembled membrane attack complex.

Unburned skin had very little positive staining for C5b-9, but burned skin had strong staining for it, particularly at the precise points where the epidermis had blistered away from the dermis and the keratinocytes changed to an elongated appearance. There was a distinct transition at the edges of blisters to non-staining, adherent epidermis.

Where hair follicles were found in burns, the C5b-9 staining was found extending to a varying extent into the depths of the dermis, indicating deposition of the MAC in the epidermal appendages.

It is worth mentioning the relative paucity of neutrophils within the areas of the burn where C5b-9, and C4a were localised by their respective antibodies. Previous studies have postulated the role of neutrophils in the activation of complement, but their presence within the burns in this model is too sporadic for this to be a main mechanism for complement activation, at lease within the timeframe of this experimental model.

Complement activation has been shown to aggravate tissue damage, and the deposition of the MAC in the epidermis and along the underlying hair follicles indicates that it may have a role in the evolution of the burn injury in our model.

The inhibition of the deposition of MAC in the epidermis and epidermal appendages might explain the relative increase of hair follicle and epidermal-specific mRNA species (SPRR2G, TCHH, TCHHL1, KRT82, and PRR9) in cooled burns compared to untreated burns. It is possible, also, that the reduction of the secondary tissue injury may be reflected in the relative reduction of heat-shock protein mRNA transcription.

8.2 Integration of the results

Generating a unifying hypothesis from the results from the three modalities of experiment- transcriptomics, proteomics and immunohistochemistry and histology- must overcome some of the limitations of each.

The initial work established the correct duration of burning and the reliability of the method of burn-depth measurement. Histologically, there was a clear response to burning, and there was a dose-response relationship between the duration of contact and the depth to which these changes extended. These changes responded to cooling, paralleling the effect of cooling on the burn's clinical appearance.

The RNAseq experiments revealed a large transcriptomic shift in burned skin, with very significant fold-changes and FDR values. The upregulated ontologies included inflammation, wound response and healing, coagulation and platelet activation, and cell migration, while those downregulated included those related to epidermal differentiation and keratinisation, and corresponded to the clinical features of a burn, and to experimental work already done. Cooling had a very modest effect on the transcriptome compared to its effect upon the clinical and histological appearances of the burns. The genes that were significantly altered in their expression by cooling related to epidermal and epidermal appendage differentiation that were downregulated by burning, with this change partially reversed by cooling, and those related to platelet aggregation, protein misfolding and heat-shock response that were upregulated by burning, with this change partially reversed by cooling.

The proteomic findings showed a marked acute-phase protein response from the coagulation and complement systems, with both significantly activated by burning, and this activation significantly inhibited by cooling.

These changes, and the points at which cooling is has an effect in this data are set out in Figure 105

8.3 Proposed mechanism of thermal injury, the role of cooling, and the supporting experimental evidence from this work

The proposed mechanism for burning, and the modifications to this brought about by cooling are summarised in the diagram below. The thermal energy results in direct damage to the tissue and endothelium of the microvasculature. This activates two parallel, but interconnected cascades- complement and clotting. Cooling reduces the rate of antibody-induced complement activation, and both the intrinsic and extrinsic coagulation pathways. This results in, respectively, less complement-induced tissue damage and less microvascular occlusion. This in turn results in a larger number of viable epidermal cells expressing the genes identified as significantly upregulated by cooling, and reduces the transcriptomic response to damage as seen in the comparison between cooled and untreated burns.

The key point of intervention is blockade of the activation of C5 for assembly of the membrane-attack complex, and the lysis of injured, but possibly still viable cells expressing neoantigens that are subsequently bound by circulating IgM molecules. The associated generation of C5a damages vascular endothelium, with C5a increasing the expression of adhesion molecules by endothelial cells through binding of C5aR, including P-selectin, increasing neutrophil adhesion, and Von Willeband factor, increasing the activation of the clotting cascade[90].

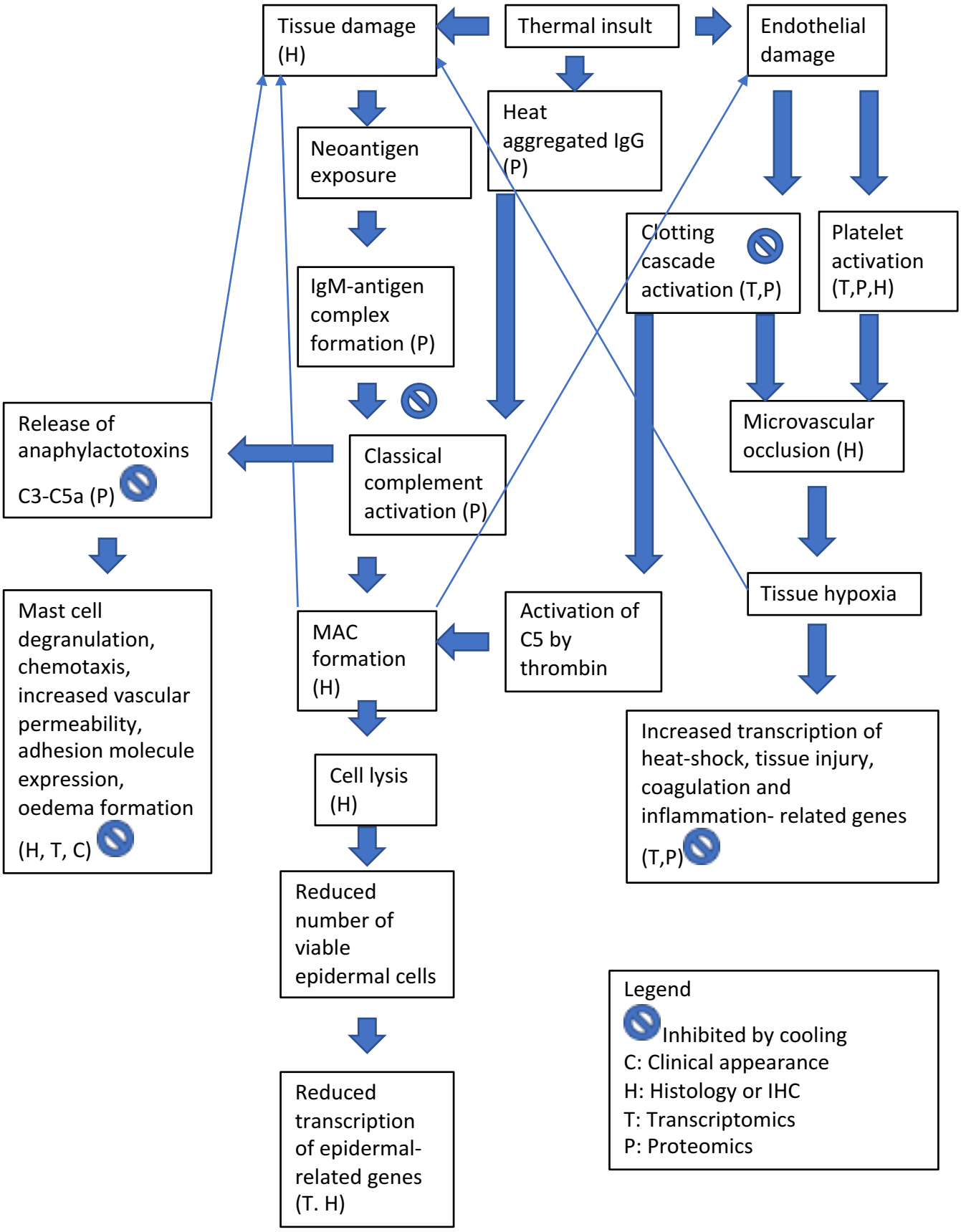


Figure 105: Summary of post-burn transcriptomic, proteomic and histological changes as described in this thesis.

8.4 Summary

In summary, the key findings of this project are:

There is a dose-response relationship between the amount of thermal energy delivered during the burning process and the severity of microvascular damage at even one hour after injury

Cooling, delivered in line with the best current clinical evidence, reduces this damage significantly

There is a consistent transcriptomic and proteomic response to burning consistent with the clinical and histological appearance of the burns

Cooling has a significant on both the transcriptome and the proteome of burns within 3 hours of injury, again with changes in line with the clinical and histological features of the burns

The proteomic findings are more widespread within the identified proteome of the burns in this study, and represent the activation of pre-synthesised proteins and migration of circulating cellular effectors. The transcriptomic changes indicate the longer-term response to thermal injury.

The complement and coagulation cascades have established roles in damage amplification and in ischaemia-reperfusion injury models. Pharmacological agents to block the activation of complement already exist, and may have a role in burn management in the future.

9 Future directions

9.1 Laboratory phase

9.1.1 Stain existing sections for IgM and IgG Fc

9.1.1.1 Aim

To prove that the IgM is present within the area of the burn and complement activation at higher levels than within controls. Proving that IgM-antigen interaction and formation of heat-induced IgG aggregation are key parts of the complement activation mechanism in burning.

9.1.1.2 Materials and methods

Sections of burned and control skin would be stained for IgM and heat-induced IgG aggregates using anti-human-IgM Fc and IgG aggregate antibodies to localise these to the area of the burn and to characterise which cells were staining the strongest for IgM. Demonstrating a difference between cooled and untreated burns might not be possible on IHC, but it would confirm the presence of IgM in the immediate zone of complement activation.

9.1.2 Identification of burn-induced neoantigen binding the IgM

9.1.2.1 Aim

The aim would be the identification of the neoantigen(s) expressed by thermally injured tissues that binds to the IgM and causes classical complement activation.

9.1.2.2 Materials and methods

Protein samples extracted from cooled and untreated burned and unburned skin would be treated with anti-human IgM and IgG antibody-coated magnetic beads to precipitate the antigen-antibody complexes. These would then be processed in the normal way for LC/MS/MS proteomic analysis to identify the peptides and hence proteins that were present within this fraction of the proteome. Candidate proteins would have monoclonal antibodies made to them and these antibodies would then be used to confirm the presence and location of these proteins within the skin sections. Confirmation of their presence within the area of burn injury, and complement activation would confirm their potential role in thermal-injury induced classical complement activation. Transcriptomic data already analysed in this project could then be analysed for any changes in transcription of the genes related to these antigens in burning, and any changes caused by cooling.

9.1.3 Mathematical model of burn based on data from initial calibration of thermal injury depth

9.1.3.1 Aim

The aim is to establish a mathematical model for thermal injury that models highly standardised burning and cooling.

9.1.3.2 Materials and methods

Burn-depth data and the very precise characteristics of both burning and cooling from this study would be used to create a finite-element mathematical model that would predict the characteristics of burning and cooling. The results of this would allow the magnitude and duration of temperature rise in the watershed area of tissue between the limit of damage in cooled and untreated burns during burning and subsequent

cooling to be calculated. This data would allow the accurate planning of heat-shocking experiments in future to reproduce the burning conditions as accurately as possible.

9.1.4 Cell culture, heat-shock, and cooling, and the effects on the transcriptome and the proteome

9.1.4.1 Aim

These experiments aim to identify the transcriptomic and proteomic effects of heat-shocking and cooling individual cell populations.

9.1.4.2 Vascular endothelial cells and keratinocytes

Vascular endothelial cells and keratinocytes would be cultured under standard conditions, and then treated according to 4 sets of conditions: heat-shocked as determined from the mathematical model and no cooling, heat-shocked and then cooled, normothermia and not cooled, and normothermial and cooled. Cells would then be stained with the monoclonal antibodies to the putative neoantigens identified from previous experiments, and Western blotting would be performed to quantify the expression of these neoantigens with radiolabelled antibodies.

Complement activation assays would be carried out on cell lines grown under the 4 conditions described above to examine the activation of complement and cell lysis in conjunction with the monoclonal antibodies to the neoantigens. This would confirm the role of the neoantigen(s) and classical complement activation in burn injury pathology.

9.1.5 Small-molecule inhibitors

Once the identity of the neoantigen(s) is established, development or identification of competitive inhibitors of antigen-antibody complex formation could be used to produce a potential inhibitor of classical complement activation by burning.

9.2 Animal model

Following standardisation of the burning process for a rat or pig model, burns would be created in this model and either cooled or left untreated in one animal and in a different group half treated with the small-molecule inhibitor or placebo. The severity, progression, and healing of the burns could then be assessed and ultimately determine if the small-molecule inhibitor had matched the effect of cooling in terms of burn severity, burn progression, healing and the associated proteomic and transcriptomic changes.

If this were to be successful, we would have a potential therapeutic agent for the management of burns in conjunction with, or in place of cooling. The sequence of experiments is summarised in Figure 106.

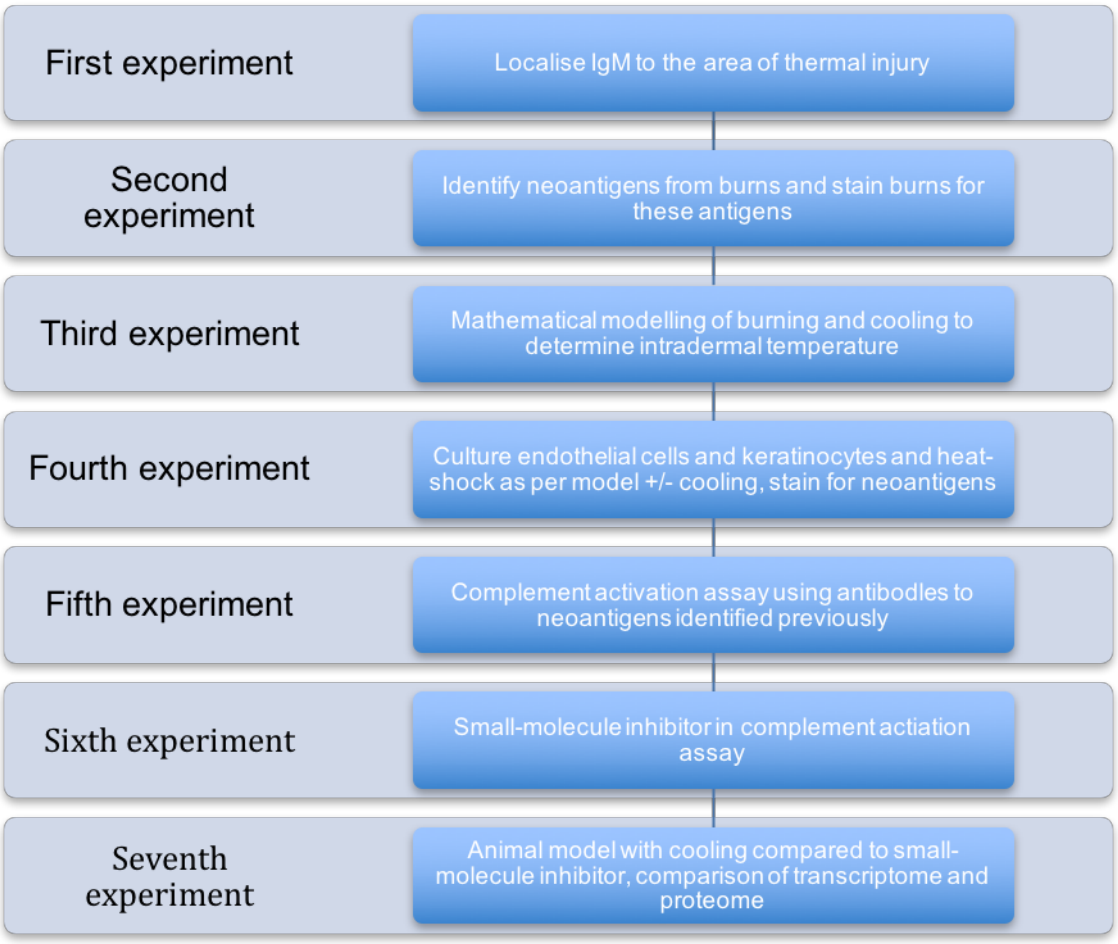


Figure 106: Sequence of proposed experiments for future work following on from this project

10 Bibliography

1. Jackson, D. M. The diagnosis of the depth of burning. *Br. J. Surg.* **40,** 588–96 (1953).

2. Watts, A M., Tyler, M. P., Perry, M. E., Roberts, A H. & McGrouther, D. a. Burn depth and its histological measurement. *Burns* **27,** 154–60 (2001).

3. Moserova, J., Behounkova, E. & Prouza, Z. Subcutaneous temperature measurements in a thermal injury. *Burns* **1,** 267–268 (1975).

4. Cuttle, L., Kempf, M., Liu, P.-Y., Kravchuk, O. & Kimble, R. M. The optimal duration and delay of first aid treatment for deep partial thickness burn injuries. *Burns* **36,** 673–9 (2010).

5. Moritz, A. R. Studies of thermal injury III. The pathology and pathogenesis of cutaneous burns an experimental study. *Am. J. Pathol.* **23,** 915–941 (1947).

6. Hodson, A. H. Treating burns by initial cooling. *J. R. Soc. Med.* **85,** 121 (1992).

7. Ofeigsson, O. J. Observations and experiments on the immediate cold-water treatment for burns and scalds. *Br. J. Plast. Surg.* **12,** 104–119 (1959).

8. Chiu, T. W., Ng, D. C. K. & Burd, a. Properties of matter matter in assessment of scald injuries. *Burns* **33,** 185–8 (2007).

9. Raghupati, N. First-aid treatment of burns: efficacy of water cooling. *Br. J. Plast. Surg.* **21,** 68–72 (1968).

10. Bull, J. P. Burns. *Postgrad. Med. J.* **39,** 717–724 (1963).

11. Moritz, A. . & Henriques, F. . Studies of thermal injury II. The relative importance of time and surface temperature in the causation of cutaneous burns. *Therm. Inj.* 695–720 (1946).

12. Shulman, A. G. Ice water as primary treatment of burns. *J.A.M.A* **173,** 1916–1919 (1960).

13. Nguyen, N. L., Gun, R. T., Sparnon, A. L. & Ryan, P. The importance of immediate cooling — a case series of childhood burns in Vietnam. *Burns* **28,** 173–176 (2002).

14. Cuttle, L., Pearn, J., McMillan, J. R. & Kimble, R. M. A review of first aid treatments for burn injuries. *Burns* **35,** 768–75 (2009).

15. Jandera, V., Hudson, D. A, de Wet, P. M., Innes, P. M. & Rode, H. Cooling the burn wound: evaluation of different modalites. *Burns* **26,** 265–70 (2000).

16. Venter, T. H. J., Karpelowsky, J. S. & Rode, H. Cooling of the burn wound: the ideal temperature of the coolant. *Burns* **33,** 917–22 (2007).

17. Yuan, J. *et al.* Assessment of cooling on an acute scald burn injury in a porcine model. *J. Burn Care Res.* **28,** 514–20 (2007).

18. Bartlett, N. *et al.* Optimal duration of cooling for an acute scald contact burn injury in a porcine model. *J. Burn Care Res.* **29,** 828–34 (2008).

19. Cuttle, L. *et al.* The optimal temperature of first aid treatment for partial thickness burn injuries. *Wound Repair Regen.* **16,** 626–34 (2008).

20. Rajan, V. *et al.* Delayed cooling of an acute scald contact burn injury in a porcine model: is it worthwhile? *J. Burn Care Res.* **30,** 729–34

21. Van de Sompel, D., Kong, T. Y. & Ventikos, Y. Modelling of experimentally created partial-thickness human skin burns and subsequent therapeutic cooling: a new measure for cooling effectiveness. *Med. Eng. Phys.* **31,** 624–31 (2009).

22. Ng, E. Y. K. & Chua, L. T. Comparison of one- and two-dimensional programmes for predicting the state of skin burns. *Burns* **28,** 27–34 (2002).

23. Arturson, G. & Jakobsson, O. P. Oedema measurements in a standard burn model. *Burns. Incl. Therm. Inj.* **12,** 1–7 (1985).

24. Blomgren, I., Eriksson, E. & Bagge, U. Effect of cold water immersion on oedema formation in the scalded mouse ear. *Burns. Incl. Therm. Inj.* **9,** 17–20 (1982).

25. Demling, R. H., Mazess, R. B. & Wolberg, W. The effect of immediate and delayed cold immersion on burn edema formation and resorption. *J. Trauma* **19,** 56–60 (1979).

26. Blomgren, I., Eriksson, E. & Bagge, U. The effect of different cooling temperatures and immersion fluids on post-burn oedema and survival of the partially scalded hairy mouse ear. *Burns. Incl. Therm. Inj.* **11,** 161–5 (1985).

27. Jakobsson, O. P. & Arturson, G. The effect of prompt local cooling on oedema formation in scalded rat paws. *Burns. Incl. Therm. Inj.* **12,** 8–15 (1985).

28. Boykin, J. V, Eriksson, E., Sholley, M., Pittman, R. N. & Scholley, M. M. Cold-Water Treatment of Scald Injury and Inhibition of histamine-mediated Burn Edema. *J. Surg. Res.* **31,** 111–123 (1981).

29. Boykin, J. V & Crute, S. L. Mechanisms of burn shock prevention after severe scald injury by cold-water treatment. *J. Trauma* **22,** 859–866 (1982).

30. Björk, J. & Arturson, G. Effect of cimetidine, hydrocortisone superoxide dismutase and catalase on the development of oedema after thermal injury. *Burns. Incl. Therm. Inj.* **9,** 249–56 (1983).

31. Searcy, R. M., Cone, J. B., Bowser, B. H. & Caldwell, F. T. The deleterious effects of high dose cimetidine in acute thermal injury. *Burns. Incl. Therm. Inj.* **9,** 62–5 (1982).

32. Sevitt, S., Bull, J., Cruickshank, C., Jackson, D. & Lowbury, E. Failure of an antihistamine drug to influence the course of experimental human burns. *Br. Med. J.* **12,** 57–62 (1952).

33. Nanney, L. B. Changes in the microvasculature of skin subjected to thermal injury. *Burns. Incl. Therm. Inj.* **8,** 321–7 (1982).

34. Wiedeman, M. P. & Prince Brigham, M. The effects of cooling on the microcasculature after thermal injury. *Microvasc. Res.* **3,** 154–161 (1971).

35. Eriksson, E., Boykin, J. V & Pittman, R. N. Method for in Viva Microscopy of the Cutaneous Microcirculation of the Hairless Mouse Ear. *Microvasc. Res.* **19,** 374–379 (1980).

36. Boykin, J. V, Eriksson, E. & Pittman, R. N. Microcirculation of a scald burn: an in vivo experimental study of the hairless mouse ear. *Burns* **7,** 335–338 (1981).

37. Eriksson, E. & Robson, M. C. New pathophysiological mechanism explaining post-burn oedema *. *Burns* **4,** 153–156 (1977).

38. Saranto, J. R., Rubayi, S. & Zawacki, B. E. Blisters, cooling, antithromboxanes, and healing in experimental zone-of-stasis burns. *J. Trauma* **23,** 927–933 (1983).

39. Raine, T. J., Heggers, J. P., Robson, M. C., London, M. D. & Johns, L. Cooling the burn wound to maintain microcirculation. *J. Trauma* **21,** 394–397 (1981).

40. Rohrer, M. J. & Natale, A. M. Effect of hypothermia on the coagulation cascade. *Crit. Care Med.* **20,** 1402–1405 (1992).

41. Straub, A. *et al.* Critical temperature ranges of hypothermia-induced platelet activation: Possible implications for cooling patients in cardiac surgery. *Thromb. Haemost.* **96,** 756–66 (2006).

42. Zhang, J. *et al.* Effects of low temperature on shear-induced platelet aggregation and activation. *J. Trauma* **57,** 216–223 (2004).

43. Robson, M. C., Kucan, J., Paik, K. & Heggers, J. P. The effect of heparin on dermal ischaemia after burning *. *Burns* **5,** 260–264 (1977).

44. Robson, M. C., DelBeccaro, E. J., Heggers, J. P. & Loy, G. L. Increasing dermal perfusion after burning by decreasing thromboxane production. *J. Trauma* **20,** 722–725 (1980).

45. Wang, S. L. *et al.* The effect of the thromboxane synthetase inhibitor Dazmegrel (UK-38,485) on wound healing, dermal ink perfusion and skin blood flow measurements in deep partial thickness burns. *Burns. Incl. Therm. Inj.* **12,** 312–7 (1986).

46. Jakobsson, O. P., Benediktsson, G. & Arturson, G. Early post-burn oedema in leucocyte-free rats. *Burns* **12,** 18–21 (1985).

47. Mileski, W. *et al.* Inhibition of leukocyte-endothelial adherence following thermal injury. *J. Surg. Res.* **52,** 334–9 (1992).

48. Melikian, V., Laverson, S. & Zawacki, B. Oxygen-derived free radical inhibition in the healing of experimental zone-of-stasis burns. *J. Trauma* **27,** 151–154 (1987).

49. Oldham, K. T., Guice, K. S., Till, G. O. & Ward, P. A. Activation of complement by hydroxyl radical in thermal injury. *Surgery* **104,** 272–279 (1988).

50. Younan, G. *et al.* The inflammatory response following an epidermal burn depends on teh activities of mouse mast cell proteases 4 and 5. *J. Immunol.* **185,** 7681–7690 (2010).

51. Sewell, D. L. *et al.* Complement C3 and C5 play critical roles in traumatic brain cryoinjury: Blocking effects on neutrophil extravasation by C5a receptor antagonist. *J. Neuroimmunol.* **155,** 55–63 (2004).

52. Neher, M. D., Weckbach, S., Flierl, M. A., Huber-Lang, M. S. & Stahel, P. F. Molecular mechanisms of inflammation and tissue injury after major trauma-is complement the 'bad guy'? *J. Biomed. Sci.* **18,** 90 (2011).

53. Oikonomopoulou, K., Ricklin, D., Ward, P. A. & Lambris, J. D. Interactions between coagulation and complement--their role in inflammation. *Semin Immunopathol* **34,** 151–165 (2012).

54. Bellander, B. M. *et al.* Secondary insults following traumatic brain injury enhance complement activation in the human brain and release of the tissue damage marker S100B. *Acta Neurochir. (Wien).* **153,** 90–100 (2011).

55. Huber-Lang, M. *et al.* Generation of C5a in the absence of C3: a new complement activation pathway. *Nat. Med.* **12,** 682–687 (2006).

56. Suber, F., Carroll, M. C. & Moore, F. D. Innate response to self-antigen significantly exacerbates burn wound depth. *Proc. Natl. Acad. Sci. U. S. A.* **104,** 3973–7 (2007).

57. Sadeghipour, H. *et al.* Blockade of IgM-Mediated Inflammation Alters Wound Progression in a Swine Model of Partial-Thickness Burn. *J. Burn Care Res.* 2017 MAy/Jun;38(3):523-528

58. Arturson, G., Hogman, C. F., Johnasson, S. G. O. & Killander, J. Changes in immunoglobulin levels in severely burned patients. *Lancet* **1,** 546–548 (1969).

59. Bjornson, A. B., Altemeier, W. A. & Bjornson, H. S. Changes in Humoural Components of Host Defense Following Burn Trauma. *Ann Surg* **186,** 88–96 (1977).

60. Sobouti, B., Fallah, S., Ghavami, Y. & Moradi, M. Serum immunoglobulin levels in pediatric burn patients. *Burns* **39,** 473–476 (2013).

61. Pintér, E., Brown, B., Hoult, J. R. S. & Brain, S. D. Lack of evidence for tachykinin NK1 receptor-mediated neutrophil accumulation in the rat cutaneous microvasculature by thermal injury. *Eur. J. Pharmacol.* **369,** 91–98 (1999).

62. Rawlingson, A., Gerard, N. P. & Brain, S. D. Interactive contribution of NK(1) and kinin receptors to the acute inflammatory oedema observed in response to noxious heat stimulation: studies in NK(1) receptor knockout mice. *Br. J. Pharmacol.* **134,** 1805–1813 (2001).

63. Rizzo, J. A, Burgess, P., Cartie, R. J. & Prasad, B. M. Moderate systemic hypothermia decreases burn depth progression. *Burns* **39,** 436–44 (2013).

64. Greco, J. A, Pollins, A C., Boone, B. E., Levy, S. E. & Nanney, L. B. A microarray analysis of temporal gene expression profiles in thermally injured human skin. *Burns* **36,** 192–204 (2010).

65. Liang, P. *et al.* MicroRNA profiling in denatured dermis of deep burn patients. *Burns* **38,** 534–40 (2012).

66. Brown, S. a *et al.* Heat shock proteins 47 and 70 expression in rodent skin model as a function of contact cooling temperature: Are we overcooling our target? *Lasers Surg. Med.* **39,** 504–12 (2007).

67. Zhang, Y. *et al.* Role for heat shock protein 90α in the proliferation and migration of HaCaT cells and in the deep second-degree burn wound healing in mice. *PLoS One* **9,** (2014).

68. Ashcroft, G. S. *et al.* Secretory leukocyte protease inhibitor mediates non-redundant functions necessary for normal wound healing. *Nat. Med.* **6,** 1147–53 (2000).

69. Pollins, A. C., Friedman, D. B. & Nanney, L. B. Proteomic investigation of human burn wounds by 2D-difference gel electrophoresis and mass spectrometry. *J. Surg. Res.* **142,** 143–52 (2007).

70. Tan, J.-Q. *et al.* The roles of autophagy and apoptosis in burn wound progression in rats. *Burns* **39,** 1551–6 (2013).

71. Cuttle, L., Kravchuk, O., Wallis, B. & Kimble, R. M. An Audit of First-Aid Treatment of Pediatric Burns Patients and Their Clinical Outcome. *J. Burn Care Res.* **30,** 1028–1034 (2009).

72. Friedl, H. P., Till, G. O., Trentz, O. & Ward, P. a. Roles of histamine, complement and xanthine oxidase in thermal injury of skin. *Am. J. Pathol.* **135,** 203–17 (1989).

73. Moritz, A. R. & Henriques, F. C. Studies of thermal injury: the relative importance of time and surface temperature in the causation of cutaneous burns. *Am. J. Pathol.* **23,** 695–720 (1947).

74. Sevitt, S. The failure of anti-histamine drugs to influence the local vascular changes in experimental burns. *Br. J. Exp. Pathol.* **30,** 540–547 (1949).

75. Chvapil, M., Speer, D. P., Owen, J. A. & Chvapil, T. A. Identification of the Depth of Burn Injury by Collagen Stainability. *Plast. Reconstr. Surg.* **73,** 438–441 (1984).

76. Younan, G. *et al.* The Inflammatory Response after an Epidermal Burn Depends on the Activities of Mouse Mast Cell Proteases 4 and 5. *J. Immunol.* **185,** 7681–7690 (2010).

77. Chvapil, M., Speer, D. P., Owen, J. A. & Chvapil, T. A. Identification of the depth of burn injury by collagen stainability. *Plast. Reconstr. Surg.* **73,** 438–441 (1984).

78. Chvapil, M. *et al.* Identification of the depth of burn injury by collagen stainability. *Plast. Reconstr. Surg.* **73,** 438–441 (1984).

79. Ember, J. A., Sanderson, S. D., Hugli, T. E. & Morgan, E. L. Induction of interleukin-8 synthesis from monocytes by human C5a anaphylatoxin. *Am. J. Pathol.* **144,** 393–403 (1994).

80. Hsu, M. H., Wang, M., Browning, D. D., Mukaida, N. & Ye, R. D. NF-kappaB activation is required for C5a-induced interleukin-8 gene expression in mononuclear cells. *Blood* **93,** 3241–9 (1999).

81. Lieb, K., Fiebich, B., Berger, M. & Bauer, J. The neuropeptide substance P activates transcription factor NF-kappa B and kappa B-dependent gene expression in human astrocytoma cells. *J. Immunol.* **159,** 4952–4958 (1997).

82. Rahman, A, Anwar, K. N., True, A L. & Malik, a B. Thrombin-induced p65 homodimer binding to downstream NF-kappa B site of the promoter mediates endothelial ICAM-1 expression and neutrophil adhesion. *J. Immunol.* **162,** 5466–76 (1999).

83. Anna Turabelidze, B.S.; Shujuan Guo, Ph.D.; Luisa A. DiPietro, DDS, P. . Importance of Housekeeping gene selection for accurate RT- qPCR in a wound healing model. *Wound Repair Regen* **18,** 460–466 (2010).

84. Amara, U. *et al.* Interaction between the coagulation and complement system. *Adv. Exp. Med. Biol.* **632,** 71–79 (2008).

85. Lupu, F., Keshari, R. S., Lambris, J. D. & Mark Coggeshall, K. Crosstalk between the coagulation and complement systems in sepsis. *Thromb. Res.* **133,** (2014).

86. Krisinger, M. J. *et al.* Thrombin generates previously unidentified C5 products that support the terminal complement activation pathway Thrombin generates previously unidentified C5 products that support the terminal complement activation pathway. *Thromb. Hemost.* **120,** 1717–1725 (2012).

87. Gorski, J. P., Hugli, T. E. & Müller-Eberhard, H. J. C4a: the third anaphylatoxin of the human complement system. *Proc. Natl. Acad. Sci. U. S. A.* **76,** 5299–5302 (1979).

88. Kasuya, H. & Shimizu, T. Activated complement components C3a and C4a in cerebrospinal fluid and plasma following subarachnoid hemorrhage. *J. Neurosurg.* **71,** 741–746 (1989).

89. Kawana, S., Geoghegan, W. D., Jordon, R. E. & Nishiyama, S. Deposition of the membrane attack complex of complement in pemphigus vulgaris and pemphigus foliaceus skin. *J. Invest. Dermatol.* **92,** 588–592 (1989).

90. Foreman, K. E. *et al.* C5a-induced expression of P-selectin in endothelial cells. *J. Clin. Invest.* **94,** 1147–1155 (1994).

91. van de Goot, F. *et al.* Acute Inflammation is Persistent Locally in Burn Wounds: A Pivotal Role for Complement and C-Reactive Protein. *J. Burn Care Res.* **30,** 274–280 (2009).

92. Flierl, M. a *et al.* The role of C5a in the innate immune response after experimental blunt chest trauma. *Shock* **29,** 25–31 (2008).

93. Stahel, P. F., Morganti-Kossmann, M. C. & Kossmann, T. The role of the complement system in traumatic brain injury. *Brain Research Reviews* **27,** 243–256 (1998).

94. Arumugam, T. V. *et al.* Protective effect of a human C5a receptor antagonist against hepatic ischaemia-reperfusion injury in rats. *J. Hepatol.* **40,** 934–941 (2004).

95. Proctor, L. M. *et al.* Comparative anti-inflammatory activities of antagonists to C3a and C5a receptors in a rat model of intestinal ischaemia/reperfusion injury. *Br. J. Pharmacol.* **142,** 756–64 (2004).

96. de Vries, B. *et al.* Complement Factor C5a Mediates Renal Ischemia-Reperfusion Injury Independent from Neutrophils. *J. Immunol.* **170,** 3883–3889 (2003).

97. Kawle, A. P. *et al.* Comparative evaluation of risk factors, outcome and biomarker levels in young and old acute ischemic stroke patients. *Ann. Neurosci.* **22,** 70–77 (2015).

98. Riedemann, N. C., Guo, R.-F. & Ward, P. A. A key role of C5a/C5aR activation for the development of sepsis. *J. Leukoc. Biol.* **74,** 966–970 (2003).

99. Bosmann, M. & Ward, P. A. Role of C3, C5 and anaphylatoxin receptors in acute lung injury and in sepsis. *Adv. Exp. Med. Biol.* **946,** 147–159 (2012).

100. Kang, H. J. *et al.* Change of complement system predicts the outcome of patients with severe thermal injury. *J. Burn Care Rehabil.* **24,** 148–153 (2003).

101. Markiewski, M. M., DeAngelis, R. A. & Lambris, J. D. Complexity of complement activation in sepsis. *J. Cell. Mol. Med.* **12,** 2245–2254 (2008).

102. Heimbach, L. *et al.* The C5a receptor on mast cells is critical for the autoimmune skin-blistering disease bullous pemphigoid. *J. Biol. Chem.* **286,** 15003–15009 (2011).

103. Liu, Z. *et al.* The role of complement in experimental bullous pemphigoid. *J. Clin. Invest.* **95,** 1539–1544 (1995).

104. Asch, M. J. *et al.* Systemic and pulmonary hemodynamic changes accompanying thermal injury. *Ann. Surg.* **178,** 218–221 (1973).

105. Demling, R. H., LaLonde, C., R.H., D. & C., L. Early burn excision attenuates the postburn lung and systemic response to endotoxin. *Surgery* **108,** 28–35 (1990).

106. Hart, D. W. *et al.* Effects of Early Excision and Aggressive Enteral Feeding on Hypermetabolism, Catabolism, and Sepsis after Severe Burn. *J. Trauma Inj. Infect. Crit. Care* **54,** 755–764 (2003).

107. Ipaktchi, K. *et al.* Attenuating burn wound inflammatory signaling reduces systemic inflammation and acute lung injury. *J. Immunol.* **177,** 8065–8071 (2006).

108. Peterson, V. M., Hansbrough, J. F., Wang, X. W., Zapata-Sirvent, R. & Boswick, J. A. J. Topical cerium nitrate prevents postburn immunosuppression. *J. Trauma* **25,** 1039–1044 (1985).

109. Kremer, T. *et al.* Topical application of cerium nitrate prevents burn edema after burn plasma transfer. *Microvasc. Res.* **78,** 425–431 (2009).

110. Deveci, M., Eski, M., Sengezer, M. & Kisa, U. Effects of cerium nitrate bathing and prompt burn wound excision on IL-6 and TNF-alpha levels in burned rats. *Burns* **26,** 41–45 (2000).

111. Savage, B., Saldívar, E. & Ruggeri, Z. M. Initiation of platelet adhesion by arrest onto fibrinogen or translocation on von Willebrand factor. *Cell* **84,** 289–297 (1996).

112. Parkinson, E. *et al.* Proteomic analysis of the human skin proteome after in vivo treatment with sodium dodecyl sulphate. *PLoS One* **9,** e97772 (2014).

113. Feezor, R. J. *et al.* Temporal patterns of gene expression in murine cutaneous burn wound healing. *Physiol. Genomics* **16,** 341–8 (2004).

114. Neutelings, T., Lambert, C. a, Nusgens, B. V & Colige, A. C. Effects of mild cold shock (25°C) followed by warming up at 37°C on the cellular stress response. *PLoS One* **8,** e69687 (2013).

115. Shah, T. A *et al.* Clinical hypothermia temperatures increase complement activation and cell destruction via the classical pathway. *J. Transl. Med.* **12,** 181 (2014).

116. Krisinger, M. J. *et al.* Thrombin generates previously unidentified C5 products that support the terminal complement activation pathway. *Blood* **120,** 1717–1725 (2012).

11 Appendices

11.1 Appendix 1: The initial ethical approval for the study

NHS
Health Research Authority

NRES Committee South Central - Berkshire
Bristol REC Centre
Whitefriars
Level 3, Block B
Lewins Mead
Bristol
BS1 2NT

Telephone: 0117 342 1333
Facsimile: 0117 342 0445

06 December 2013

Mr Edmund Hugh Wright
Duke of Kent Research Fellow Restore Foundation
Weatherall Institute of Molecular Medicine
John Radcliffe Hospital
Headley Way
Oxford
OX39DS

Dear Mr Wright

Study title: **Investigating the molecular effects of cooling human burns**
REC reference: **13/SC/0518**
IRAS project ID: **119975**

Thank you for your letter of 5th December 2013. I can confirm the REC has received the documents listed below and that these comply with the approval conditions detailed in our letter dated 29 October 2013

Documents received

The documents received were as follows:

Document	*Version*	*Date*
Covering Letter		05 December 2013
Other: Flowchart	1	05 December 2013
Participant Consent Form	2	21 February 2013
Participant Information Sheet	2	30 October 2013

Approved documents

The final list of approved documentation for the study is therefore as follows:

Document	*Version*	*Date*
Covering Letter		19 September 2013
Covering Letter		05 December 2013

11.2 Appendix 2: First substantial amendment

Health Research Authority

NRES Committee South Central - Berkshire
Bristol REC Centre
Whitefriars
Level 3, Block B
Lewins Mead
Bristol
BS1 2NT

Tel: 0117 3421391

26 August 2014

Mr Edmund Hugh Wright
Duke of Kent Research Fellow Restore Foundation
Weatherall Institute of Molecular Medicine
John Radcliffe Hospital
Headley Way
Oxford
OX39DS

Dear Mr Wright

Study title: **Investigating the molecular effects of cooling human burns**
REC reference: **13/SC/0518**
Amendment number: **1**
Amendment date: **03 April 2014**
IRAS project ID: **119975**

The above amendment was reviewed by the Sub-Committee in correspondence.

Ethical opinion

The committee approved:

1. Reduction in exposure time.
2. Inclusion of a thermoelectric cooling device.

The members of the Committee taking part in the review gave a favourable ethical opinion of the amendment on the basis described in the notice of amendment form and supporting documentation.

Approved documents

The documents reviewed and approved at the meeting were:

Document	*Version*	*Date*
Covering letter on headed paper		23 July 2014
Notice of Substantial Amendment (non-CTIMP)	1	03 April 2014
Other [Skin Cooling Manual]	1	10 June 2014
Participant consent form	3	26 April 2014
Participant information sheet (PIS)	3	26 April 2014
Research protocol or project proposal	2	26 April 2014
Summary, synopsis or diagram (flowchart) of protocol in non technical language	2	27 April 2014

11.3 Appendix 3: Second substantial amendment

NHS
Health Research Authority

NRES Committee South Central - Berkshire

Bristol REC Centre
Whitefriars
Level 3, Block B
Lewins Mead
Bristol
BS1 2NT

Tel: 0117 3421389

11 November 2014

Mr Edmund Hugh Wright
Duke of Kent Research Fellow Restore Foundation
Weatherall Institute of Molecular Medicine
John Radcliffe Hospital
Headley Way
Oxford
OX39DS

Dear Mr Wright,

Study title: **Investigating the molecular effects of cooling human burns**
REC reference: **13/SC/0518**
Amendment number: **2**
Amendment date: **14 October 2014**
IRAS project ID: **119975**

The above amendment was reviewed on 08 November 2014 by the Sub-Committee in correspondence.

Ethical opinion

The members of the Committee taking part in the review gave a favourable ethical opinion of the amendment on the basis described in the notice of amendment form and supporting documentation.

Approved documents

The documents reviewed and approved at the meeting were:

Document	*Version*	*Date*
Covering letter on headed paper	2	24 October 2014
Notice of Substantial Amendment (non-CTIMP)		14 October 2014
Research protocol or project proposal	3	24 October 2014

Membership of the Committee

The members of the Committee who took part in the review are listed on the attached sheet.

R&D approval

11.4 Appendix 4: Patient information sheet





Investigating the molecular effects of cooling human burns

Chief Investigator: Mr Hugh Wright

Research Ethics Committee: South Central- Berkshire

Research Ethics Committee Reference Number: 13/SC/0518

Funding Sources: Restore Burn and Wound Research

Research Sponsor: University of Oxford

UNIVERSITY OF OXFORD

restore
Burn and Wound Research

Part 1 – Introduction

We would like to invite you to take part in our study. The purpose of this leaflet is to provide you with information to enable you to make an informed choice as to whether you wish to participate or not, and it is essential that you read this, understand what is involved, and are happy to proceed before you sign the consent form. Your treatment will not be affected by your participation in this study. The first part outlines the purpose of the study, and the second part sets out the steps involved, if you agree to participate. Please feel free to ask any questions that you may have in order to help you reach your decision.

Burns

Almost everyone has had a burn of some sort during the course of their life, and in the vast majority of cases the burns are small, superficial, and heal without any surgery, hospitalisation, or long-term problems. In their more severe forms, burns can cause pain, severe illness, scarring, psychological harm, disability, and in some cases death. Treatment of severe burns is complex, painful, prolonged, expensive, and still far from perfect.

What are the aims of the study?

Burns develop over the 24-48 hours after initial injury until they reach the limit of their severity, before beginning to heal. Depending upon the depth, they may heal in 5-7 days for the very superficial burns with very little scarring, or over the course of months in the case of deep burns. The longer a burn takes to heal, the worse the scarring and functional outcome, the greater the trauma to the patient, and the greater the cost to the patient and society in terms of treatment costs, loss of earnings and long-term disability.
First-aid recommends the cooling burns under cool running water for at least 20 minutes, as soon as possible after injury, and this has the proven effect of reducing the severity of the burn. However, it is not clear how this works, as the heat of the burn disperses before the cooling starts if there is more than a couple of minutes delay, and yet the benefit of cooling persists even after the heat has dispersed. Hence, complex chains of events in the cells that make up the skin must be taking place, and these are modified by cooling, reducing the severity of the burn. All events taking place in cells are ultimately controlled by "genes" which act as templates for making proteins, which in turn dictate cell behaviour and function. Genes are switched "on" or "off" to change cell behaviour in response to certain events. We want to understand the genes that are switched on and off by burning, and by cooling the burn in order to better understand the mechanism of cooling, and improve the management of burns in the future. Further down the line, it may allow the development of drugs that reduce the severity of burns and improve healing without surgery.

UNIVERSITY OF OXFORD

restore
Burn and Wound Research

Why have I been selected to participate?

Human skin is unique, compared to other mammals' skin. It has less hair, more sweat and oil glands and a different structure of blood vessels and muscle. Humans are also unique in forming problem scars after injury, particularly burns, referred to as hypertrophic or keloid scars. Hence, human skin is the ideal skin for research into human burns.
You have elected to undergo breast reconstruction using skin and tissue from your abdomen- the DIEP flap that you have been told about. During the course of your surgery, areas of skin that are not needed for the reconstruction have to be removed to give a neat scar along the abdomen, areas at either end of the scar near the hip areas. Usually, these are discarded at the end of the operation. We would like to ask you for your permission to use these pieces of excess skin for our experiment. This experiment involves the creation of a number of 1.5cm diameter burns on these areas of excess skin early in the operation, while they are still attached to you, but after you are anaesthetised, so that you experience no pain, and are in fact unaware of the whole process.

What would I have to do if I agreed to participate?

If you agree to participate in the study, you will be asked to sign a consent form to this effect, and will be enrolled in the study. If you change your mind, you can withdraw from the study at any point before your operation. On the day of surgery, the Consultant will mark the DIEP flap on your abdomen before you have your anaesthetic, and you will then go to the anaesthetic room as normal for the operation. The anaesthetist will anaesthetise you, and once you are asleep we will use a specially designed piece of apparatus to create a number of very small burns in the skin on the abdomen that is due to be removed, but not used to make the new breast, and would in other cases be discarded. Cooling may be administered at some point using another piece of purpose-built apparatus, and the burned areas of skin removed and sent for processing and analysis. The operation will proceed as normal while this is going on, and you will wake up in the recovery area of theatres when the operation is finished. The process of the experiments will make no change to your operation, or recovery, and your end result will look no different to those of women who have not participated in the study.

UNIVERSITY OF OXFORD

restore
Burn and Wound Research

What will happen to the sample I provide?

The skin samples will be assigned a unique identification number to allow their identification, but prevent them being linked to the patient. They are then processed in a number of ways so that they can be examined under a microscope, or analysed to see which genes have been switched on or off. While we will extract genetic material from your skin, we will not be conducting any genetic tests on you for any diseases you might develop in the future. Samples will be kept in secure storage or freezers, and there will be no identifiable information attached to the samples. The results and data will be stored securely, but again there will be no identifiable information attached to these files.

What if I do not want to participate?

If you do not wish to participate, you simply say so and you will not be enrolled in the study. You will have your surgery as normal, but no experiments will be carried out. Not participating in the study will not change the clinical care you are given.

If the information in Part 1 has interested you and you are considering participation, please read the additional information in Part 2 before making any decision.

Part 2 – Further Information

What are the benefits of participating?

There are no benefits in participating in the study, but in the long term, the study may help improve the management and treatment of burns.

What are the risks of participation?

The apparatus has all been designed to the highest standards by medical engineers, and the project has been approved by an ethics committee who have carefully considered the risks to patients. The cooling device is thermostatically controlled, and cannot get cold enough to damage your skin. There is a very small risk of a very superficial burn being created accidentally in a place on the body that we did not plan. However, the apparatus has inbuilt safety features that limit the temperature and protect the hot part from accidental contact, and the area around where the burn will be created will be protected by a heat-proof template as can be seen in the attached photographs of the apparatus. Were such an event to occur, we would tell you, and the burn would almost certainly heal within a few days with dressings and leave no significant scar.

UNIVERSITY OF OXFORD

restore
Burn and Wound Research

Where will information I provide be stored?

The data will be anonymised, assigned a unique identification number, and transferred to a password protected database, access to which will be restricted to researchers working on the project, and responsible members of the University for monitoring and audit. Any data collected may also be used retrospectively for other ethically approved studies. At the end of the study, anonymous data and samples will be available to other researchers outside of the University of Oxford, performing studies looking into the molecular basis of burns, or other studies that have been given approval by the relevant ethical review body. Anonymised data collected during the course of the study may be passed on to other organisations that may include commercial organisations. Data may be sent to associated researchers to countries, either within or outside the European Economic Area where the laws don't protect your privacy to the same extent as the law in the UK. However, there will be no confidential personal information shared in this way.
Responsible members of the University of Oxford or the Buckinghamshire Healthcare NHS trust may be given access to data for monitoring and/ or audit of the study to ensure we are complying with regulations.

Can I withdraw from the study?

You may withdraw from the study at any point before your operation, even after signing the consent form, simply by telling us you do not want to participate, and your surgery will be conducted as normal. Your withdrawal will have no effect upon your treatment. If you decide that you do not want to participate after the surgery, however, it will not be possible to identify your samples and destroy them, as they will have been anonymised and cannot be traced to you.

How can I find out the results of the study?

Lay summaries of the study results will be posted at regular intervals on the website of the Restore Foundation - http://www.restore-research.org.uk/

Who has reviewed the study?

All research in the NHS is looked at by independent group of people, called a Research Ethics Committee to protect your safety, rights, wellbeing and dignity. This study has been reviewed and given favourable opinion by Research Ethics Committee Berkshire.

What if I come to harm by participating in the study?

Given the nature of this study, it is unlikely that you will suffer harm by taking part, however if you are harmed by participation in the study, you may have grounds for legal action for compensation against the University of Oxford.

The University has a specialist insurance policy in place which would operate in the event of any participant suffering harm as a result of their involvement in research: **Newline Underwriting Management Ltd, Lloyds's of London, policy number WD1200463.** NHS indemnity operates in respect of the clinical treatment provided.

If you wish to complain about any aspect of the way in which you have been approached or treated during the course of this study, you should contact Mr Hugh Wright on burncoolingproject@gmail.com or 07968826781 or you may contact the University of Oxford Clinical Trials and Research Governance (CTRG) office on 01865 572224 or the head of CTRG, email ctrg@admin.ox.ac.uk

Who can I contact for more information about the study?

If you require further information, are unsure whether or not to participate, in the study, please contact a member of the team in writing, by email, or by telephone using the contact details below.

Mr Hugh Wright
Duke of Kent Research Fellow with the Restore Burn and Wound Research Foundation
The Weatherall Institute of Molecular Medicine
University of Oxford
John Radcliffe Hospital
Headington
Oxford
OX39DS
burncoolingproject@gmail.com
Phone 07968826781

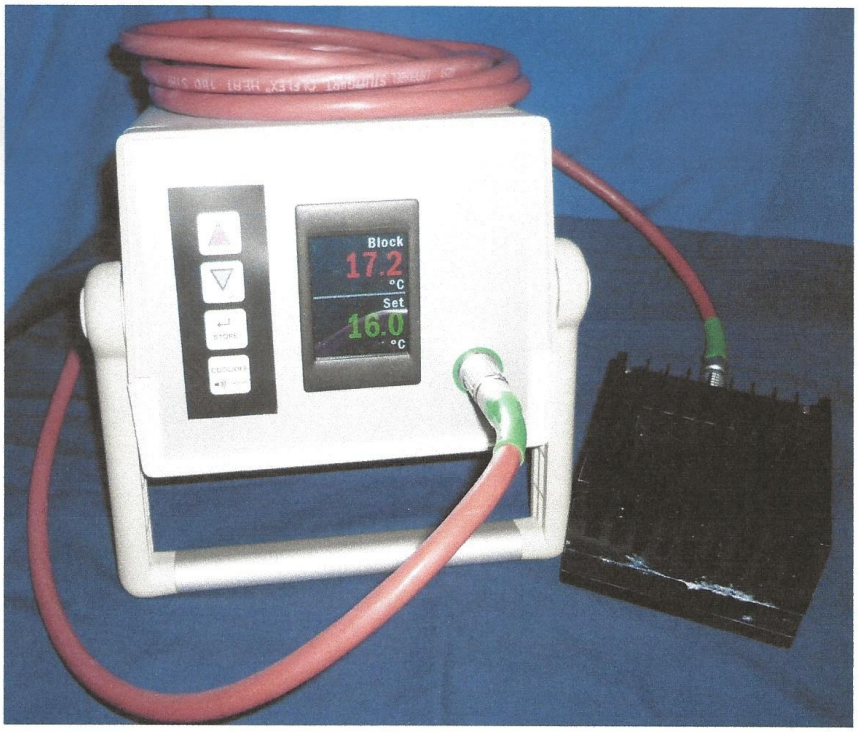
UNIVERSITY OF OXFORD

restore
Burn and Wound Research

The apparatus

The temperature control display on the control unit, the insulated sleeve on the probe, and the silicone template have all been specifically designed to maximise participant safety.





The cooling device is also thermostatically controlled and cannot get cold enough to damage your skin.

11.5 Appendix 5: Patient consent form

UNIVERSITY OF OXFORD

restore
Burn and Wound Research

Consent Form

Investigating the molecular effects of cooling human burns

Research Ethics Committee South Central- Berkshire 13/SC/0518
Name of Researcher: Mr Hugh Wright
Site: Stoke Mandeville Hospital, Buckinghamshire Healthcare NHS Trust

	Please Initial
1. I confirm that I have read and understand the information sheet dated 26/4/14 (version 3) for the above study. I have had the opportunity to consider the information, ask questions and have had these answered satisfactorily. I understand that I can contact a member of the research team to ask questions at any time.	☐
2. I understand that my participation is voluntary and that I am free to withdraw at any time without giving any reason, without my medical care or legal rights being affected.	☐
3. I agree to take part in the study, and for samples of my skin to be used for extraction and analysis of DNA, RNA, protein or other molecules, and samples of my skin may be stored in accordance with the Human Tissue Act in University of Oxford laboratory facilities.	☐
4. I understand that anonymised data and samples may be shared with other researchers and commercial organisations performing studies into burns, or used for future studies that have been given approval by the relevant ethical review body, either within or outside the European Economic Area.	☐
5. I understand that the relevant sections of my research notes and anonymised data collected during the study may be looked at by individuals from the University of Oxford, from regulatory authorities, or from Buckinghamshire Healthcare NHS trust, where it is relevant to my taking part in this research. I give permission for these individuals to have access to my research records.	☐
6. I agree to gift samples taken for the purpose of the research study to the University of Oxford. If a commercial product were developed as a result of this study, I will not profit financially from such a product.	☐
7. I consent to photography, video, and audio recordings of research procedures being taken and used in publications and presentations, after all reasonable steps have been taken to remove any identifying details and information.	☐

_____	_____	_____
Patient name- please print	Patient signature	Date
_____	_____	_____
Investigator name	Investigator signature	Date